B cell deficiency and anaemia caused by mutations in the murine *Atp11c* gene

Mehmet Yabas

B.Sc., M.Phil.

Australian National University

THE JOHN CURTIN
SCHOOL OF MEDICAL RESEARCH

A thesis submitted for the degree of Doctor of Philosophy of The Australian National University

July, 2014

Statement of Originality

The research presented in this thesis was performed in the Immunogenomics Laboratory, the John Curtin School of Medical Research, the Australian National University under the supervision of Dr. Anselm Enders and Professor Christopher C. Goodnow. The data is the result of original research, has not previously been submitted for a degree, and my own work, with all contributions from others explicitly stated.

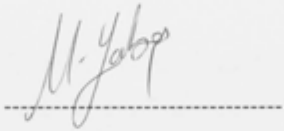

Mehmet Yabas

Dr. Anselm Enders

Supervisor

Professor Christopher C. Goodnow

Co-supervisor

Acknowledgements

Anselm Enders – I would like to express my deepest gratitude to my supervisor for his patience, guidance and support during my Ph.D. Thank you Anselm for being a great mentor.

Christopher C Goodnow – I also thank my co-supervisor Chris for his invaluable ideas and encouragement throughout my program. Thank you Chris for sharing your tremendous wealth of knowledge with me.

Supervisory panel members – Thank you very much Stefan Broer and Rob Brink for their feedback, constructive suggestions and discussions that we had during the panel meetings. Also a special thank to Stefan Broer for his help in the establishment of the flippase assay.

Carola Vinuesa, Katrina Randall, Keisuke Horikawa, Ian Parish, Rebecca Sweet – for helpful advice and discussions.

The members of Immunogenomics Laboratory, past and present – It has been a great privilege to be part of such a positive and simulative team. Thank you very much all the past and present members of the lab, especially lab manager Michelle Townsend, my PhD peers Hannes Bergmann (for long hours discussions and help in the lab), Charis Teh, Manu Singh, Zahra Sabouri, Yogesh Jeelall, James Wang and others, and great staff especially Debbie Howard (for her help in bone marrow chimera experiments), Nadine Barthel and Edyta Kucharska.

Collaborators – Jon Sprent, Narci Teoh, Geoff Farrell, Lucy Coupland, Chris Parish, Markus Winterberg, Kiaran Kirk, James D'Rozario, Deborah Cromer, Owen Siggs, Bruce Beutler for providing mouse, reagent, advice and helping with some experiments.

Gerard Hoyne – for kindly agreeing to proofread this thesis and his invaluable feedback.

Imaging and Cytology Facility – Harpreet Vohra, Mick Devoy, Cathy Gillespie and Anne Prins for their assistance in using the facility.

Australian Phenomics Facility Staff and Genotyping Team – Especially Holly Burke and Anthony Barker for the training, technical help and animal husbandry.

Anna Cowan and Wendy Riley – for their assistance throughout my PhD program.

The Ministry of National Education, Republic of Turkey – for the scholarship that made this thesis possible.

My friends in Australia – Especially Mehmet Fatih Saglam, Emrah Tumer, Sarp Kaya, Cemil Kurekci, Mustafa Ucgul for continual support and friendship.

My mom, dad, brothers and sisters, all my nephews and nieces, father-in-law, mother-in-law, brother-in-law, sister-in-law and all my friends back in Turkey – for their prayers, constant support and encouragement.

Last but not least, my lovely wife, ***Emine*** – thank you for being a great wife. Without your constant support and encouragement I would have not been successful! I love you!!!

Publications, Presentations and Awards arising from this study

Peer-reviewed Journals:

- **Mehmet Yabas**, Charis E. Teh, Sandra Frankenreiter, Dennis Lal, Carla M. Roots, Belinda Whittle, Daniel T. Andrews, Yafei Zhang, Narci C. Teoh, Jonathan Sprent, Lina E. Tze, Edyta M. Kucharska, Jennifer Kofler, Geoffrey C. Farell, Stefan Bröer, Christopher C. Goodnow & Anselm Enders (2011). "ATP11C is critical for the internalization of phosphatidylserine and differentiation B lymphocytes. ***Nature Immunology***, 12(5):441-449.

- **Mehmet Yabas**, Lucy A. Coupland, Deborah Cromer, Markus Winterberg, Narci C. Teoh, James D'Rozario, Kiaran Kirk, Stefan Bröer, Christopher R. Parish & Anselm Enders (2014). Mice deficient in the putative phospholipid flippase ATP11C exhibit altered erythrocyte shape, anemia and reduced erythrocyte lifespan. ***The Journal of Biological Chemistry***, 289(28):19531-19537.

Conference Presentations:

- "Ambrosius, a new X-linked B cell immunodeficiency" 2nd Annual Australasian Society for Immunology NSW/ACT Branch Retreat, Craigieburn Conference Centre and Resort, Bowral, NSW, Australia, 9-10 September 2010 (Oral presentation).

- "Regulation of B cell development by a putative lipid transporter in Ambrosius mouse strain" Australasian Society for Immunology 40th Annual Scientific Meeting, Perth, WA, Australia, 5-9 December 2010 (Poster presentation).

- "ATP11C is critical for phosphatidylserine internalization and B lymphocyte differentiation" 5th Australian B Cell Dialogue, Melbourne, Victoria, Australia, 26-27 May 2011 (Oral Presentation).

- "ATP11C is critical for phosphatidylserine internalization and B lymphocyte differentiation" Canberra Health Annual Research Meeting, Canberra, ACT, Australia, 6-8 June 2011 (Oral Presentation, awarded as a Merit Presentation).

- "ATP11C is critical for phosphatidylserine internalization and B lymphocyte differentiation" The Australian Society for Medical Research ACT Young

Investigators Forum, Canberra, ACT, Australia, 9 June 2011 (Oral Presentation).

- "ATP11C mutation causes X-linked B cell deficiency" 3rd Annual Australasian Society for Immunology NSW/ACT Branch Retreat, Craigieburn Conference Centre and Resort, Bowral, NSW, Australia, 25-26 August 2011 (Oral presentation).
- "ATP11C mutation causes X-linked B cell deficiency with diminished phosphatidylserine internalization" Australasian Society for Immunology 41st Annual Scientific Meeting, Adelaide, SA, Australia, 11-15 December 2011 (Poster presentation).
- "ATP11C mutation causes X-linked B cell deficiency with diminished phosphatidylserine internalization" IFReC-SIgN Winter School on Advanced Immunology, Awaji Island Hyogo, Japan, 16-20 January 2012 (Oral and Poster presentation).
- "Flipping of lipids by a putative transporter is essential for B-cell development and function" 3rd European Congress of Immunology, Glasgow, UK, 5-8 September 2012 (Poster presentation).
- "ATP11C controls early B-cell development but not their function" Keystone Symposia on B Cell Development and Function, Keystone Resort, Keystone, Colorado, USA, 10-15 February 2013 (Poster Presentation).
- "Mice deficient in the P4-type ATPase ATP11C exhibit stomatocyte formation and anaemia due to a shortened erythrocyte life span" Canberra Health Annual Research Meeting, Canberra, ACT, Australia, 20-23 August 2013 (Oral Presentation).
- "The putative aminophospholipid translocase ATP11C controls early B-cell development but not their function" Australasian Society for Immunology 43rd Annual Scientific Meeting, Wellington, New Zealand, 2-5 December 2013 (Poster presentation).

Awards:

- Travel and accommodation bursary to attend the first IFReC-SIgN Winter School on Advanced Immunology, Awaji Island Hyogo, Japan, 16-20 January 2012.
- American Association for the Advancement of Science (AAAS)/Science Program for Excellence in Science Award, 2012.
- The Australian National University Vice-Chancellor's Higher Degree Research Travel Award, 2012.
- European Federation of Immunological Societies (EFIS) Travel Award, 2012.
- Australasian Society for Immunology (ASI) Postgraduate International Travel Award, 2013.
- Australasian Society for Immunology (ASI) Postgraduate Travel Award, 2013.

Abbreviations

ABA	Azo-benzene-arsonate
ABC	ATP-binding cassette
ALT	Alanine aminotransferase
ANOVA	Analysis of variance
AST	Aspartate aminotransferase
ATP	Adenosine triphosphate
BAFF	B cell-activating factor
BCL-2	B-cell lymphoma 2
BCR	B cell receptor
BP	Bordetella pertussis
BSA	Bovine serum albumin
CD	Cluster of differentiation
CDC50	Cell divisional control 50
CFSE	Carboxyfluorescein succinimidyl ester
CGG	Chicken gamma globulin
CHCM	Corpuscular haemoglobin concentration mean
CLP	Common lymphoid progenitor
CMP	Common myeloid progenitor
C57BL/6	Wild-type strain
C_6-NBD-PS	1-palmitoyl-2-{6-[(7-nitro-2-1,3-benzoxadiazol-4-yl)amino]hexanoyl}-*sn*-glycero-3-phosphoserine
C_{12}-NBD-PS	1-palmitoyl-2-{12-[(7-nitro-2-1,3-benzoxadiazol-4yl)amino]dodecanoyl}-*sn* glycero-3-phosphoserine
D	Diversity gene segment
DN	Double negative
DP	Double positive
E	Erythroid lineage
EBF1	Early B-cell factor 1
ELISA	Enzyme-linked immunosorbent assay
ELP	Earliest lymphoid progenitor
ENU	*N*-ethyl-*N*-nitrosourea
FCS	Foetal calf serum
Flt3	Fms-like tyrosine kinase 3
FO B	Follicular B cells
FSC	Forward scatter
GC	Germinal centre

GFP	Green fluorescence protein
HBBS	Hanks' balanced salt solution
HCC	Hepatocellular carcinoma
HEL	Hen egg lysozyme
HPLC	High pressure liquid chromatography
HSC	Haematopoietic stem cell
H&E	Haematoxylin and eosin
Ig	Immunoglobulin
IL	Interleukin
IRF	Interferon regulator factors
ITAM	Immunoreceptor tyrosine-based activation motif
J	Joining gene segment
JAK	Janus associated kinase
LMPP	Lymphoid-primed multipotent progenitor
MCH	Mean corpuscular haemoglobin
MCV	Mean corpuscular volume
MAPK	Mitogen-activated protein kinase
MFI	Mean fluorescence intensity
Mk	Megakaryocyte lineage
MPP	Multipotent progenitor
MZ B	Marginal zone B cells
NK	Natural killer cell
NKT	Natural killer T cell
NP-Ficoll	Nitrophenyl-Ficoll
PA	Phosphatidic acid
PAX5	Paired box protein 5
PBS	Phosphate buffer saline
PE	Phosphatidylethanolamine
PC	Phosphatidylcholine
PI	Phosphatidylinositol
PI3K	Phosphatidylinositol-3-kinase
Pre-BCR	Precursor B cell receptor
PS	Phosphatidylserine
RAG1/2	Recombination activating gene 1/2
RBC	Red blood cell

SD	Standard deviation
SEM	Scanning electron microscope
SLC	Surrogate light chain
SM	Sphingomyelin
SNV	Single nucleotide variant
SRBC	Sheep red blood cell
SSC	Side scatter
STAT5	Signal transducer and activator transcription-5
SYK	Spleen tyrosine kinase
S.E.M	Standard error of the mean
TCR	T cell receptor
T_{FH}	T follicular helper cell
TSLP	Thymic stromal lymphopoietin
V	Variable gene segment
VCAM-1	Vascular cell adhesion molecule-1
7-AAD	7-Aminoactinomycin D

Abstract

Organization of the plasma membrane into specialised substructures in lymphocytes facilitates important biological functions including the initiation of crucial intracellular signalling cascades at the plasma membrane. The eukaryotic plasma membrane is a lipid bilayer that consists of asymmetrically distributed phospholipids. Membrane-bound lipid transporters are believed to generate and dynamically maintain the lipid asymmetry between the two leaflets of the cell membranes, but not much is known about the role of these transporters in a variety of biological systems in mammals.

This thesis examines the effect of two ENU-induced mutations of the murine *Atp11c* gene, which encodes a member of the P4-type ATPase family thought to serve as 'flippases' that mediate the translocation of specific aminophospholipids to the cytoplasmic leaflet of cell membranes. Loss of ATP11C in mice led to a severe B cell deficiency due to a developmental arrest at the pro-B cell stage during early B cell development in the bone marrow. The number of splenic follicular B cells and peritoneal B1 cells was also severely reduced in mutant mice. However, marginal zone B cells as well as other haematopoietic lineages including T, NK and myeloid cells appeared to accumulate normally in mutant mice. Moreover, the requirement for ATP11C in B cells was cell autonomous, and could not be corrected by the expression of pre-rearranged immunoglobulin transgenes or enforced expression of the pro-survival protein BCL-2 or by transgenic expression of IL-7. Further analysis of mutant mice revealed that while the IL-7R-mediated signalling pathway appears mostly intact, the ATP11C^{umb} mutation leads to a defect in the expression and/or signalling through the pre-BCR, which provides essential signals for the development of pre-B cells. In contrast, B cells from B cell receptor (BCR) transgenic ATP11C-deficient mice were able to form germinal centres upon immunisation when adoptively transferred into wild-type host, indicating an intact *in vivo* signalling through the mature BCR in mutant animals.

Functional analysis using fluorescently labelled phospholipid derivatives revealed that cells of the immune system from ATP11C-deficient mice exhibit impaired aminophospholipid flippase activity compared to those from control animals,

indicating for the first time that ATP11C functions as a phospholipid flippase in biological membranes.

Although the first phospholipid translocase activity was described in erythrocytes about 30 years ago, the characterisation of enzyme activity and its effect on the membrane asymmetry, development and survival of erythrocytes remains to be unveiled. Intriguingly, ATP11C-deficient mice developed anaemia due to a shortened erythrocyte lifespan, exhibited a large proportion of abnormal-shaped erythrocytes, and increased phosphatidylserine exposure on their surface due to impaired flippase activity. Thus, these findings identified ATP11C as a candidate for aminophospholipid translocation activity in erythrocytes.

In conclusion, the findings of this thesis provide novel insights into the role of the putative phospholipid transporter ATP11C in B cell development and erythrocyte survival, and suggest a new candidate for inherited B cell deficiency and anaemia in humans.

Table of Contest

List of Figures

List of Tables

CHAPTER 1: Literature Review

1.1 Overview of the Mammalian Immune System

The immune system provides the body with an effective defence mechanism against any potential infectious agents including bacteria, viruses, fungi and parasites that are readily found in our natural environment. There are two arms of the immune system to help fight off these infectious agents, namely innate and adaptive immune system.

1.1.1 The innate immune system

The innate immune system provides the first line defence by a range of different cell types (i.e. macrophages, granulocytes, dendritic cells, NK cells, polymorphonuclear leukocytes and platelets) and physical and chemical barriers that prevent pathogens from entering the body. The roles of the innate immune system also include the initial identification and removal of pathogens from the circulation by producing antibacterial enzymes and peptides, and alerting cells of the adaptive immune system to the presence of a pathogen (Janeway, 2001). However, the cells of the innate immune system have no specificity for any individual antigen and they do not generate a memory response, which is the hallmark of the adaptive immune response (Janeway, 2001).

1.1.2 The adaptive immune system

The adaptive immune system in vertebrates evolved approximately 500 million years ago (Pancer and Cooper, 2006). It is composed of a population of white blood cells termed lymphocytes. There are two main types of lymphocytes called B and T cells that are activated if the innate immune system is unable to rapidly eliminate the pathogen. Like other cells of the immune system, lymphocytes originate from the self-renewing haematopoietic stem cells (HSCs). Each individual T and B cells expresses a clonally restricted antigen receptor that is generated by somatic gene rearrangements during development within primary lymphoid tissues (Janeway, 2001). While the multipotent HSCs-derived B cell progenitors reside in the bone marrow and complete their development within the bone marrow, T cell progenitors must migrate from the bone marrow through the blood to the thymus to complete their development (Murphy, 2012).

B cells play a nonredundant role in the generation of humoral immunity through their ability to secrete a large amount of antibodies in response to recognition of a specific antigen (Hardy and Hayakawa, 2001). Antibodies can bind to antigens expressed by microbes to make them the main targets for phagocytes (Murphy, 2012). However, antibodies can only bind to pathogens that are present in the blood and the extracellular spaces. In contrast, T cells can destroy cells infected with intracellular pathogens derived from either bacteria, parasites or viruses that have an obligate requirement to replicate within host cells that antibodies cannot detect (Murphy, 2012). There are two subsets of T cells, namely $CD4^+$ T helper cells (T_H) and $CD8^+$ cytotoxic T cells, which represent mediators of cell-mediated immune responses.

The adaptive immune system has the ability to mount a specific immune response against a range of pathogens by recognising specific determinants on proteins through their receptors. Once an antigen is recognized by a lymphocyte within the secondary lymphoid tissues, the lymphocyte becomes activated, proliferates and differentiates into an effector cell (Murphy, 2012). The effector lymphocytes have a short lifespan and will persist until the pathogen has been cleared from the circulation, and eventually the effector cells die through the programmed cell death (Murphy, 2012).

At the same time when effector cells differentiate, a subset of these cells is selected to become a stable population of long-lived memory cells (Murali-Krishna et al., 1998, Webb et al., 1994). When memory cells re-encounter with the same pathogen in the future, they can be reactivated and produce a more rapid and stronger immune response to help eliminate the invading pathogen (Murphy, 2012).

Although both B and T cells play indispensable roles in the protection of host against a range of pathogens, the factors that govern their development and function are yet to be entirely delineated. Uncovering these factors and the molecular mechanisms that control these processes will lead to a better understanding of disease states such as B- and T-cell leukaemia, immunodeficiency and autoimmunity syndromes, and may help in the development of new clinical treatments. The work presented in this thesis will focus primarily on B cells in relation to their development while T cells will not be discussed.

1.2 B Lymphocytes

B cells are generated from HSCs primarily in the foetal liver before the birth and in the bone marrow during the postnatal period (Hardy and Hayakawa, 2001), and play a central role in the adaptive immune system. Since their discovery, B cells have been considered as antibody-producing cells. However, recent studies suggest that B cells have broader roles in the immune system, which include the ability to act as antigen presenting cells (Myers, 1991, Rodriguez-Pinto, 2005) and produce cytokines (Pistoia, 1997, Lund, 2008). B cell precursors derived from HSCs follow a well-defined developmental program in the bone marrow characterised by the expression of a variety of specific cell surface molecules driven by the rearrangement status of the immunoglobulin (Ig) gene loci (Hardy and Hayakawa, 2001). Upon the successful production of a functional B cell receptor (BCR) on the surface, B cells exit the bone marrow and enter to the periphery for their further maturation steps (Hardy and Hayakawa, 2001). The mature BCRs on B cells are in the form of Ig molecules, and possess the transmembrane region. Mature B cells search for their cognate antigens during their circulation in the blood and lymph. When a BCR recognizes epitopes on a naïve antigen, the B cell becomes activated and differentiates into either an antibody producing plasma cell that secretes soluble form of antigen specific antibodies with no transmembrane region to clear the pathogen, or they can differentiate into memory B cells to provide a faster and stronger immune response upon a secondary encounter with the same antigen (Murphy, 2012).

In this section of the thesis, I will review early B cell development in the bone marrow and discuss the critical signalling circuits as well as the transcription factors that control B cell development. I will further discuss maturation of B cells into different peripheral subsets and their functional properties.

1.2.1 Early B cell development

Differentiation of B cells from HSCs is one of the best-defined cell differentiation processes in vertebrates and different stages (pre/pro-B, pro-B, pre-B, immature B and mature B cells) can be characterised on the basis of differential expression of surface markers, the status of Ig gene rearrangements, growth factor requirements and expression of genes in the developing B cells in the bone marrow and spleen

(Hardy and Hayakawa, 2001). Its analysis by molecular genetics has illuminated fundamental mechanisms for normal immunity, human immunodeficiency diseases, DNA transcription, rearrangement and repair, cell signalling and cancer. B cell differentiation is currently viewed as proceeding in a graded manner, guided by a complex, self-reinforcing network of B cell-specific transcriptional regulators and receptor signalling systems (Malin et al., 2010a, Ye and Graf, 2007, Mandel and Grosschedl, 2010, Nutt and Kee, 2007). Understanding how the elements of this network are integrated has only begun to be revealed and hinges upon identifying essential missing steps.

The use of cell surface markers as well as the molecular characterisation has defined different B cell populations throughout the development in the bone marrow. Several terminologies have been used to describe these subsets, including the Philadelphia (Hardy and Hayakawa, 2001) and Basel nomenclatures (Osmond et al., 1998). In order to avoid confusion, in this thesis the Philadelphia nomenclature will be used and the corresponding fractions (fractions A, B, C, C`, D and E) defined by Hardy (Hardy et al., 1991) will be supplied in brackets.

The earliest B cell progenitor cells, known as pre/pro-B cells (fraction A) are differentiated from $Ly6D^+$ common lymphoid progenitors (CLPs) (Inlay et al., 2009). Early studies suggested that pre/pro-B cells express B220 on their surface (Figure 1.1), but are not yet committed to the B cell lineage and express low levels of RAG1 and RAG2 proteins (Hardy et al., 1991, Li et al., 1993, Li et al., 1996). Although pre/pro-B cells contain the source of more committed B cell precursors ($CD19^+$ pro-B cells), they were also shown to be competent to differentiate into other lineages including NK cells and plasmacytoid dendritic cells (Rolink et al., 1996, Diao et al., 2004, Pelayo et al., 2005), as well as T cells *in vitro* (Rumfelt et al., 2006).

Pre/pro B cells differentiate into pro-B cells (early and late pro-B cells, fraction B and C, respectively) that express CD19 on their surface, which is believed to be one of the earliest hallmarks of commitment to the B cell lineage (Figure 1.1) (Rolink et al., 1996). Since murine pro-B cells are Interleukin (IL)-7-dependent for their proliferation and survival (discussed below) (Corfe and Paige, 2012), they need to

interact with bone marrow stromal cells that produce IL-7 (Tokoyoda et al., 2004, Kurosaki et al., 2010, Clark et al., 2014).

Pro-B cells express two signalling components known as Igα (CD79a, mb-1) and Igβ (CD79b, B29) (Koyama et al., 1997), which together with the molecular chaperone calnexin are thought to form the pro-BCR on the surface of pro-B cells (Figure 1.1) (Nagata et al., 1997). Although the pro-BCR has been suggested to be a functional receptor in pro-B cells (Meffre et al., 2000), a more direct role for pro-BCR signalling in B cell development remains to be completely delineated.

In order for B cells to generate a diverse repertoire of antigen receptors, Ig heavy chain D to J rearrangements are initiated at the early pro-B cell stage (fraction B) followed by V to DJ rearrangements in late pro-B cell stage (fraction C) to produce a functional Igμ heavy chain protein in the cytoplasm (Figure 1.1). This VDJ recombination is mediated by the RAG1 and RAG2 proteins, which are highly expressed in pro-B cells (Figure 1.1) (Li et al., 1993), and mice deficient for these proteins have a developmental block at the transition from pro-B to pre-B cell stage (Mombaerts et al., 1992, Shinkai et al., 1992). Once produced, the functional Igμ associates with the surrogate light chain (SLC) proteins VpreB and λ5, which are highly expressed on pro-B cells (Sakaguchi and Melchers, 1986, Kudo and Melchers, 1987, Li et al., 1993), as well as the signalling subunits Igα and Igβ, which non-covalently associate with Igμ, to form the precursor (pre)-BCR on their surface (Figure 1.1) (Nishimoto et al., 1991, Karasuyama et al., 1996).

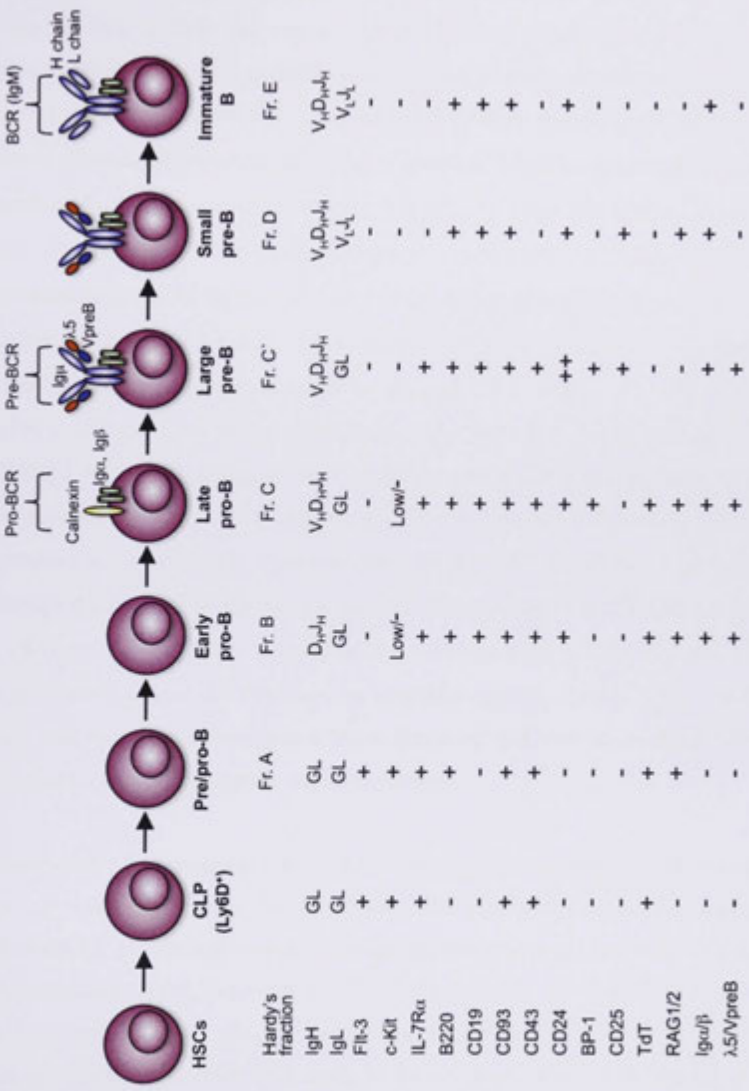

Figure 1.1 The developmental stages of B cells in the bone marrow

A schematic representation of different B cell stages starting from Ly6D$^+$ CLPs to immature B cells. Successive stages, and the phenotypic characteristics used to delineate the different stages are shown.

During the heavy chain gene rearrangements at the pro-B cell stage of B cell development in the bone marrow, the rearrangement of D_H to J_H can occur in three possible reading frames due to an inexact joining mechanism. If D_H to J_H rearrangement occurs in-frame, followed by another in-frame rearrangement of V_H to D_HJ_H, a functional μ chain that can pair with the SLC components is produced. However, a truncated μ protein called Dμ is produced when the rearrangement of D_H elements to J_H elements occurs in reading frame 2 (Reth and Alt, 1984). Dμ appears to have the opposite effect to full-length μ protein and suppresses pre-B cell differentiation as shown by a block in B cell development in the bone marrow of Dμ transgenic mice (Tornberg et al., 1998). Although Dμ can pair with SLCs, Igα and Igβ, and induce some signals through the Dμ-preBCR (Horne et al., 1996, Gong et al., 1996), transgenic expression failed to rescue B cell development in *Rag2*$^{-/-}$ mice as opposed to the correction of RAG-deficient phenotype by expression of full-length μ (Malynn et al., 2002), indicating a defective pre-BCR signalling caused by Dμ production. Interestingly, overexpression of the pro-survival factor BCL-2 did not change the inability of the Dμ transgene to promote *Rag2*$^{-/-}$ pro-B cells into pre-B cells (Wikstrom et al., 2006), suggesting that the block in B cell development of Dμ transgenic mice cannot be explained by impaired survival signals. These findings suggest that counterselection against Dμ at the pro-B cell stage is a critical process for normal B cell development in the bone marrow.

The formation of a functional pre-BCR marks the transition to the pre-B cell stage (large and small pre-B cells, fraction C' and D, respectively), and is an important check-point for the survival, proliferation and differentiation of pre-B cells (Hendriks and Middendorp, 2004, Herzog et al., 2009, Clark et al., 2014, Reth and Nielsen, 2014). Animals deficient for any component of the pre-BCR complex exhibit a partial or complete developmental arrest at the pro-B cell stage of B lymphopoiesis in the bone marrow (Kitamura et al., 1991, Kitamura et al., 1992, Torres et al., 1996, Gong and Nussenzweig, 1996, Mundt et al., 2001, Pelanda et al., 2002). The cells that assemble a functional pre-BCR undergo up to 5 rounds of cell division (clonal expansion) for the selection and expansion of large pre-B cells in order to expand the number of daughter cells with a functional Igμ (Rolink et al., 2000). Large pre-B cells eventually exit the cell cycle and become resting small pre-B cells, which begin

to undergo Ig light chain V to J rearrangement by reactivating the expression of RAG1 and RAG2 proteins (Figure 1.1) (Grawunder et al., 1995). Successful production of complete and in-frame κ or λ light chain marks the second essential check-point and allows pre-B cells to express IgM on the cell-surface (Figure 1.1). These cells are now called immature B cells (fraction E), which leave the bone marrow and emigrate to the periphery to undergo the final steps of B cell maturation.

1.2.2 Signalling events controlling early B cell development

Like other stages, the progress of B cell differentiation from pro-B cells into pre-B cells is tightly regulated process, and in addition to transcriptional control it is dependent on many signalling events in the bone marrow. Especially, signalling through the IL-7R and pre-BCR has been long considered to be fundamental for differentiation of pre-B cells as any defect in these pathways results in a developmental arrest before the pre-B cell stage of B lymphopoiesis (Herzog et al., 2009, Clark et al., 2014, Reth and Nielsen, 2014). Therefore, the role of signalling through the IL-7R and pre-BCR in early B cell development will be discussed in more detail.

1.2.2.1 IL-7R signalling

IL-7 has been suggested to play critical roles in many processes that are required for the survival, proliferation and differentiation of B cells in the adult bone marrow, but is less important for B cell development in the foetal liver (Corfe and Paige, 2012). IL-7, a member of the common gamma (γ_c) chain cytokine family, is a type I cytokine secreted primarily by stromal cells in the foetal liver, bone marrow, spleen and thymus (Tokoyoda et al., 2004). IL-7 binds a heterodimeric receptor that consists of the γ_c chain and IL-7Rα chain. While the γ_c chain is shared with IL-2, IL-4, IL-9, IL-15 and IL-21 and is crucial for the development of lymphocyte populations as mice deficient in γc lack B, T and NK cells (DiSanto et al., 1995, Cao et al., 1995), the IL-7Rα chain is shared with thymic stromal lymphopoietin (TSLP) (Jiang et al., 2005, Alves et al., 2007).

The importance of IL-7 and IL-7R signalling in B lymphopoiesis is revealed by analysis of the phenotype of animals deficient in the genes encoding these proteins,

which exhibited a profound defect of B cell development beyond the pre/pro-B cell stage in the bone marrow (Peschon et al., 1994, von Freeden-Jeffry et al., 1995, Miller et al., 2002). Intriguingly, the defective B cell accumulation in IL-7R$^{-/-}$ mice is more severe compared to that observed in animals deficient for IL-7 (Vosshenrich et al., 2003). Since IL-7Rα is shared with IL-7 and TLSP, these data suggest a possible role for TLSP in early B cell development. In keeping with these findings, TLSP has been suggested to drive the generation of IL-7-independent B cells that exist in IL-7$^{-/-}$ and IL-7R$^{-/-}$ mice (Vosshenrich et al., 2003, Vosshenrich et al., 2004). However, contrary to this notion is the observation that loss of TLSP in IL-7$^{-/-}$ animals did not cause a more severe phenotype compare to those with a single deficiency in IL-7 (Jensen et al., 2008).

Despite an essential role for IL-7 in murine B lymphopoiesis, IL-7 has been shown to be redundant for B cell development in humans as patients carrying mutations in IL-7Rα exhibit a normal peripheral B cell compartment (Puel et al., 1998). These data support the conclusion that B cell development in humans is IL-7-independent, and therefore it remains to be delineated whether human B cells do not require signalling through a cytokine receptor or use an as yet undefined receptor signalling to account for loss of IL-7R signalling during B cell development.

IL-7R signalling controls B cell proliferation, survival and development by activating three major signalling cascades: the janus associated kinase (JAK)- signal transducer and activator of transcription (STAT) pathway, the phosphatidylinositol 3-kinase (PI3K)-AKT pathway, and the mitogen activated protein kinase (MAPK)-ERK pathway (Figure 1.2), which will briefly be discussed below.

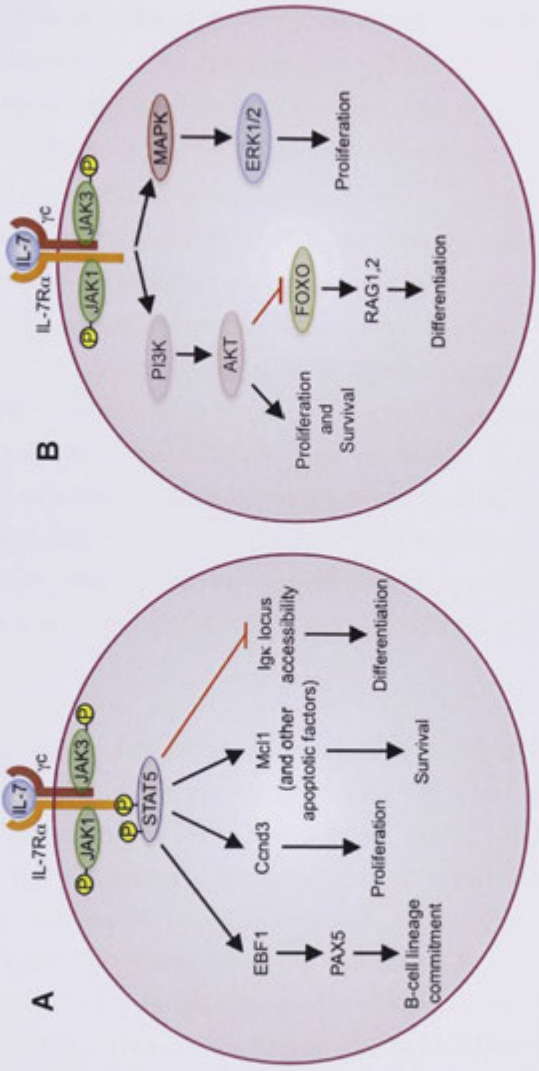

Figure 1.2 Signalling events downstream of the IL-7R

Binding of IL-7 to its receptor leads to activation of JAK-STAT **(A)**, PI3K-AKT and MAPK-ERK **(B)** signalling pathways, which regulate important events that are required for the proliferation, survival and differentiation of pro- and pre-B cells during B cell development in the bone marrow (for details, see the text).

Since the components of the heterodimeric receptor of IL-7 do not possess kinase activity, activation of the constitutively associated JAK1 and JAK3 are required to mediate downstream signalling of the IL-7R. Binding of IL-7 to the IL-7R induces heterodimerization of the α and γ chains, which brings JAK1 and JAK3 together and stimulate their phosphorylation and activation (Figure 1.2A) (Corfe and Paige, 2012). The activated JAK kinases phosphorylate tyrosines on the IL-7Rα chain, which then provide docking sides for STAT family members 5a and 5b (Figure 1.2A) (Corfe and Paige, 2012). The recruitment of STAT5 through phosphorylation of the IL-7Rα chain is an essential event in the initiation of downstream signalling, and leads to its translocation to the nucleus where it functions as a transcription factor (Heltemes-Harris and Farrar, 2012). The importance of the IL-7R-mediated STAT5 activation in the proliferation and survival of B cell precursors has been revealed by studies where animals deficient for either JAK3 or STAT5a/b exhibit a developmental arrest at the pre/pro-B cells stage of B cell development in the bone marrow, a phenotype that mirrors IL-7R-deficient mice (Thomis et al., 1995, Nosaka et al., 1995, Park et al., 1995, Yao et al., 2006). In keeping with these findings, constitutive activation of STAT5 rescues B cell deficiency in mice with IL-7R-deficient signalling (Goetz et al., 2004).

IL-7-mediated activation of STAT5 promotes expression of cyclin D3 (Mandal et al., 2009), whose expression is required for the proliferation of pro- and pre-B cells (Figure 1.2A) (Cooper et al., 2006, Powers et al., 2012), indicating a critical involvement of IL-7R signalling in B cell proliferation. Another important role of STAT5 is the induction of crucial pro-survival factors during early B cell development (Figure 1.2A). Using conditional mutagenesis of STAT5, Malin et al. demonstrated that STAT5 regulates pro-B cell survival by activating the anti-apoptotic protein MCL-1 (Malin et al., 2010b). This is consistent with the finding that MCL-1 deficient mice display a B cell deficiency due to a developmental arrest at the pro-B cell stage of B cell development in the bone marrow (Opferman et al., 2003). In addition to MCL-1, the IL-7-induced JAK-STAT5 pathway also controls pro-B cell survival by regulating the expression of anti-apoptotic proteins BCL-2 and BCL-$_{XL}$ and pro-apoptotic proteins BAX, BAD and BIM (Corfe and Paige, 2012). Importantly, IL-7R-STAT5 signalling is also involved in the repression of light chain

rearrangement in pro-B cells by regulating Igκ locus accessibility (Figure 1.2A) (Johnson et al., 2008).

In addition to the roles in the proliferation and survival of B cells, IL-7R signalling has been suggested to play a critical in B cell specification and commitment. Activation of STAT5 through IL-7R signalling induces expression of EBF1 (Kikuchi et al., 2005), which in turn promotes PAX5 expression (Figure 1.2A) (O'Riordan and Grosschedl, 1999). In agreement with these findings, overexpression of EBF1 or a constitutively active STAT5 rescued B cell development in IL-7-deficient mice (Dias et al., 2005, Kikuchi et al., 2005). Since EBF1, together with PAX5, is an essential transcription factor for the initiation and maintenance of B lineage commitment, these findings suggest that IL-7 further plays a nonredundant role in the regulation of B cell specification and commitment via controlling important B cell-specific transcription factors (Figure 1.2A). Collectively, these data reveal that IL-7R signalling through the JAK-STAT5 pathway plays a vital role in the proliferation, survival and differentiation of murine B cells in the bone marrow.

IL-7R signalling in B cells also activates the PI3K-AKT pathway through binding of the SH2 domain of the PI3K p85 regulatory subunit to Tyr449 of the IL-7Rα chain (Venkitaraman and Cowling, 1994). The activation of PI3K has been shown to be critical for early B cell development as disruption of the p85 subunit or treatment of B cells with PI3K inhibitors resulted in a defective IL-7-induced proliferation and impaired B cell development at the pro-B cell stage (Corcoran et al., 1996, Suzuki et al., 1999, Fleming and Paige, 2001). Accordingly, mice double deficient for p110α and p110δ, the larger catalytic subunits of PI3K, have been recently shown to possess a developmental arrest at the pre-B cell stage of B cell development in the bone marrow (Ramadani et al., 2010). Interestingly, pro-B cells from these mice exhibit impaired proliferation in response to IL-7 (Ramadani et al., 2010). In addition to the role in pro-B cell proliferation, the IL-7R-mediated PI3K-AKT pathway has also been suggested to play a role in pro-B cell survival through inhibition of pro-apoptotic proteins by AKT (Corfe and Paige, 2012, Clark et al., 2014).

The IL-7R/PI3K-AKT signalling pathway is also involved in the regulation of RAG proteins that are required for normal B cell development (Corfe and Paige, 2012, Clark et al., 2014). Given that FOXO1, a transcription factor negatively regulated by the PI3K-AKT pathway, directly controls the expression of *Rag1* and *Rag2* (Amin and Schlissel, 2008, Herzog et al., 2008), it is plausible that the IL-7R/PI3K-AKT pathway mediates *Rag1* and *Rag2* expression by controlling the expression of members of the FOXO family (Figure 1.2B). In agreement with this notion, a recent study revealed that attenuation of IL-7R signalling leads to robust induction of *Rag1* and *Rag2* via upregulation of FOXO1 due to diminished AKT activation (Ochiai et al., 2012). Consistently, in the absence of p110α and p110δ pro-B cells exhibit dysregulated *Rag1* and *Rag2* expression (Ramadani et al., 2010). These findings collectively suggest that IL-7R signalling-mediated PI3K-AKT activation is also important for proliferation and differentiation of B cell precursors in the bone marrow.

The binding of IL-7 to its receptor also leads to the activation of the MAPK/ERK pathway (Figure 1.2B) (Corfe and Paige, 2012), but the mechanism is less clear. ERK has been shown to be a target of both IL-7R and pre-BCR signalling, and treatment of cells with ERK inhibitors prohibits survival and proliferation of pro- and pre-B cells in response to IL-7 (Fleming and Paige, 2001). Consistently, deletion of both ERK1 and ERK2 in mice caused a developmental arrest at the pro-B cell stage of B lymphopoiesis (Yasuda et al., 2008). These findings suggest that IL-7R signalling activates the MAPK/ERK pathway, which in turn controls important events in B lymphopoiesis in the bone marrow.

The studies on the role of IL-7R signalling in B cell development absolutely suggest a critical involvement of IL-7R signalling in the different signalling processes that are required for proliferation, survival and differentiation of B cells in the bone marrow.

1.2.2.2 Pre-BCR signalling

A functional production of Igμ via in-frame VDJ gene recombination in pro-B cells leads to their assembly with the SLC proteins λ5 and VpreB, together with signal-

transducing proteins Igα and Igβ to form the pre-BCR on their surface (Figure 1.3) (Nishimoto et al., 1991, Karasuyama et al., 1996). The expression and signalling through the pre-BCR is an important check-point in early B cell development, which was apparent by the *in vivo* studies where mutations in genes encoding components of the pre-BCR signalling complex or its associated tyrosine kinases cause a partial or complete developmental arrest at the pro-B cell stage of B cell development (Kitamura et al., 1991, Kitamura et al., 1992, Torres et al., 1996, Gong and Nussenzweig, 1996, Mundt et al., 2001, Pelanda et al., 2002). Importantly, mutations in human λ5 cause a severe block in B cell development (Minegishi et al., 1998), suggesting that expression and signalling of the pre-BCR is also required for normal B cell development in humans.

Despite the similarities in the formation of signalling complexes, one of the fundamental differences between the pre-BCR and mature BCR is how the signalling is initiated. Expression of the pre-BCR on the surface is considered to be sufficient for the autonomous initiation of signalling (Herzog et al., 2009, Clark et al., 2014, Reth and Nielsen, 2014), but this idea remains controversial. Recent studies have suggested that pre-BCR activation relies on a soluble extracellular ligand present in the bone marrow environment. These studies identified Heparin and Galectin 1 on stromal cells as possible natural ligands for the pre-BCR (Bradl and Jack, 2001, Gauthier et al., 2002). However, the finding that *in vitro* proliferation and differentiation of pre-B cells mediated by pre-BCR signalling is independent of the bone marrow and foetal liver environment contradicts the requirement for the soluble ligand for pre-BCR activation (Rolink et al., 2000). An alternative model proposes that pre-BCR signalling is initiated upon autoaggregation of pre-BCRs on the cell surface (Ohnishi and Melchers, 2003). This notion is supported by the data that the positively charged non-immunoglobulin portion of λ5 mediates spontaneous pre-BCR aggregation to facilitate the initiation of signalling (Ohnishi and Melchers, 2003).

The pre-B stage is characterised by an initial proliferation stage (large pre-B cells) at which the number of cells expressing functional pre-BCRs is increased, followed by

a maturation stage (small pre-B cells) at which the rearrangements of Ig light gene loci occur (Herzog et al., 2009, Clark et al., 2014, Reth and Nielsen, 2014).

Upon expression of the pre-BCR, the SRC-family protein tyrosine kinases phosphorylate tyrosine residues in immunoreceptor tyrosine-based activation motifs (ITAMs) in the cytoplasmic tails of Igα and Igβ (Figure 1.3) (Sanchez et al., 1993, Flaswinkel and Reth, 1994). The SRC-family of kinases include Blk, Lyn and Fyn, but animals deficient in any one member of these kinases display normal B cell development in the bone marrow (Texido et al., 2000, Hibbs et al., 1995, Nishizumi et al., 1995, Stein et al., 1992). However, Lyn/Fyn/Blk triple knock out mice show a developmental arrest at the pro-B cell stage of B lymphopoiesis (Saijo et al., 2003). Phosphorylated ITAMs serve as docking sites for the recruitment and activation of spleen tyrosine kinase (SYK), which leads to activation of several downstream pathways (Figure 1.3). The activation of SYK is crucial for signalling through the pre-BCR as mice deficient in SYK have been shown to possess a developmental arrest at the pro-B cell stage and exhibit impaired clonal expansion (Turner et al., 1995, Cheng et al., 1995). T cell receptor associated protein ZAP70, which is mainly expressed in T and NK cells (Au-Yeung et al., 2009), has been suggested to compensate loss of SYK in pre-BCR signalling as double deficient animals exhibit a complete block in B cell development (Schweighoffer et al., 2003).

In the large pre-B cell stage, activation of SYK leads to a proliferative burst via predominantly the MAPK/ERK pathway in order to expand number of cells (Figure 1.3). As already mentioned, this notion has been supported by the evidence that B cells in mice deficient for ERK1/2 display a developmental arrest at the pro-B to pre-B cell transition, as well as a diminished pre-BCR-mediated expansion of pro-B cells (Yasuda et al., 2008). ERK is also activated through IL-7R signalling, which enables pre-BCR expressing cells to respond to the limiting concentration of IL-7 (Fleming and Paige, 2001). *In vivo* analysis of mice lacking both receptors confirm the requirement of IL-7R and pre-BCR signalling in the initial expansion of pre-B cells (Erlandsson et al., 2005). These *in vitro* and *in vivo* studies suggest that IL-7R signalling and to a lesser extent pre-BCR signalling act synergistically to control the expansion of large pre-B cells by activating the MAPK/ERK pathway (Figure 1.3).

SYK also activates the PI3K-AKT pathway that is required for the survival and metabolism of pre-B cells (Reth and Nielsen, 2014).

The clonal expansion of large pre-B cells is restricted up to 5 rounds of cell division (Rolink et al., 2000), after which large pre-B cells exit the cell cycle and differentiate into resting small pre-B cells. Although the precise mechanism(s) that controls the decision to undergo cell-cycle arrest and differentiate into small pre-B cells are not clear, the pre-BCR signalling-mediated downregulation of the expression of SLCs, and eventually the expression of the pre-BCR, has been suggested to account for exit of cells from the cycle (Parker et al., 2005). However, it was later shown that downregulation of pre-BCR expression is not required for the development of pre-B cells, nor for the cell-cycle arrest (van Loo et al., 2007). A recent report by Ochiai et al. revealed that a self-regulatory network between IL-7R and pre-BCR signalling plays a critical role in the decision between clonal expansion and cell-cycle arrest and differentiation (Ochiai et al., 2012). The authors demonstrate that attenuation of signalling through the IL-7R at the pre-B cell stage leads to the induction of genes that are necessary for pre-BCR signalling. The onset of pre-BCR signalling then induces a positive feedback loop that further reduces signalling through the IL-7R and strengthens signalling through the pre-BCR. Together, the reduction in IL-7 signalling and the onset of pre-BCR signalling leads to a progression from cell proliferation during the large pre-B cell stage to cell differentiation at the small pre-B cell stage. The caveat of the study was that the authors used pre-B cell lines from IRF4/8$^{-/-}$ mice, which have a developmental block at the pre-B cell stage (Lu et al., 2003), and it would be interesting to test if a similar mechanism acts in normal pre-B cells.

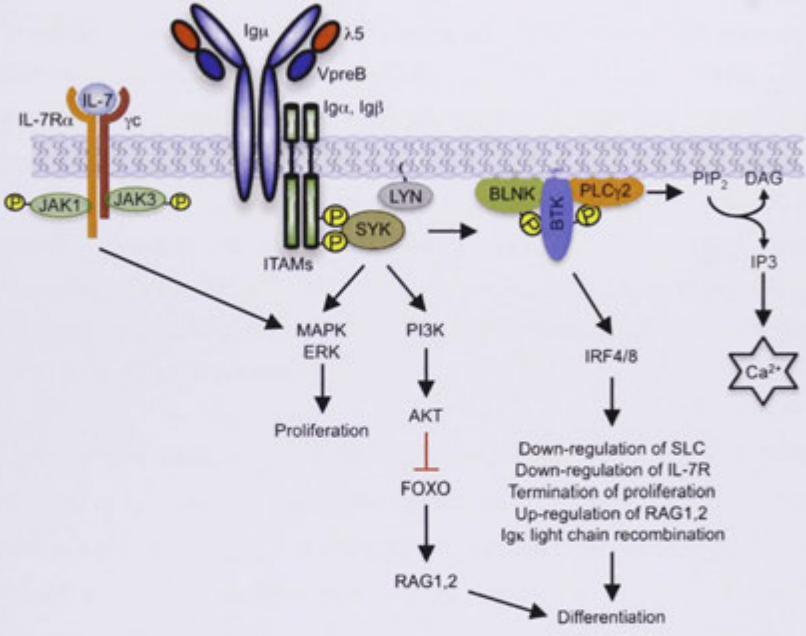

Figure 1.3 Signalling events downstream of the pre-BCR

In concert with IL-7R signalling, pre-BCR signalling in large pre-B cell stage activates the MAPK/ERK pathway that promotes a clonal expansion phase in order to increase number of cells expressing a functional pre-BCR. Pre-BCR signalling in small pre-B cells, on the other hand, terminates the proliferation and promotes the recombination of light chain through a BLNK/BTK/PLCγ2 dependent pathway. In the latter pathway, activation of FOXO by attenuated PI3K-AKT signalling also contributes to the light chain rearrangement by activating expression of RAG1 and RAG2 (Modified from Hendriks and Middendorp, 2004).

The transition of large pre-B cells toward to the small pre-B cells is associated with the SYK-mediated activation of BLNK/BTK/PLCγ2 pathway (Figure 1.3). SYK phosphorylates BLNK on multiple tyrosine residues, and BLNK in turn acts as a scaffold protein to provide docking sides for BTK and PLCγ2, which come together form a complex that induces pre-B cell differentiation (Figure 1.3) (Reth and Nielsen, 2014). Activation of PLCγ2 through BLNK and BTK results in hydrolysis of PIP2 to IP3 and diacylglycerol (DAG), which causes intracellular Ca^{2+} mobilisation and activation of Ca^{2+} dependent enzymes (Figure 1.3) (Reth and Nielsen, 2014). Mice deficient for BLNK or BTK display developmental arrest at the large pre-B cell stage (Flemming et al., 2003, Middendorp et al., 2002). Moreover, pre-B cells from the deficient mice exhibited increased expression of SLC and pre-BCR, and pre-BCR-dependent expansion (Flemming et al., 2003, Middendorp et al., 2002). These findings suggest that BLNK and BTK play a crucial role in the repression of pre-BCR expression, and thus limit signalling and proliferation emanating from the pre-BCR at the large pre-B cell stage (Figure 1.3).

In addition to the activation of BTK/PLCγ2 axis, BLNK also participates in the activation of Igκ germline transcription and recombination by promoting IRF4, whose expression is thought to promote Igκ recombination (Figure 1.3) (Muljo and Schlissel, 2003, Ma et al., 2006, Johnson et al., 2008, Lu et al., 2003). As already mentioned, defective activation of PI3K-AKT due to loss of IL-7R signalling results in increased FOXO1 expression, which also contributes to Ig light gene recombination by inducing RAG1 and RAG2 expression (Figure 1.3) (Amin and Schlissel, 2008, Herzog et al., 2008). Collectively, these findings suggest that SYK-mediated activation of BLNK/BTK/PLCγ2 pathway mainly orchestrates the differentiation of large-pre B cells into small pre-B cells by terminating IL-7R-dependent proliferation and inducing recombination of the Ig light chain loci (Figure 1.3).

1.2.3 Transcriptional control of early B cell development

The development of B cells is a highly ordered process, and in addition to cytokines and their receptors it is mediated by several transcriptional factors, which are DNA binding proteins that orchestrate many important events in cells through the

induction or suppression of target genes. The transcriptional regulatory factors are thought to function in a sequential and interdependent manner (Mandel and Grosschedl, 2010, Nutt and Kee, 2007). Although recent advances in flow cytometric analysis of B cell development using additional surface markers have enabled scientists to dissect different stages of B cell development from HSCs, the transcriptional regulation of these stages remains to be fully resolved (Mandel and Grosschedl, 2010, Nutt and Kee, 2007). The well-determined transcription factors that play essential roles in priming of the lymphoid lineages as well as the B cell lineage will be briefly discussed below.

The transcription factor **PU.1** (encoded by *Sfpi1*), a member of the ETS family of transcription factors, plays an indispensable role in the generation of early progenitors of lymphocytes and myeloid cells. PU.1 is exclusively expressed in early progenitors with a similar expression profile in HSCs, CLPs and common myeloid progenitors (CMPs) (Back et al., 2005, Nutt et al., 2005). Mice deficient for *Sfpi1* lack B and T lymphocytes, monocytes and granulocytes, but have normal megakaryocytes and erythroid progenitors (Scott et al., 1994, McKercher et al., 1996), suggesting a role for PU.1 in the generation of lymphoid and myeloid progenitors. Consistent with this idea, multipotent progenitors (MPPs) expressing a PU.1 transcriptional reporter can develop into monocytes, granulocytes and lymphoid progenitors, but not into megakaryocyte and erythroid cells (Arinobu et al., 2007). Further analysis of *Sfpi1*$^{-/-}$ animals revealed that loss of PU.1 results in a reduction in the number of lymphoid-primed multipotent progenitor (LMPPs), which are unable to give rise to B cell precursors (Scott et al., 1997). Evidence supporting this is the study where PU.1-deficient haematopoietic progenitors was shown to fail to express Flt3 and IL-7R transcripts, whose expression is vital for the generation of LMPPs and survival of early B-cell progenitors, respectively (DeKoter et al., 2002). Consistently, mice with conditional inactivation of PU.1 possess a defect in the accumulation of CLP cells (Dakic et al., 2005).

With respect to the B cell lineage, studies with PU.1 conditional knockout mice at the pro-B cell stage revealed a normal B cell development and function (Polli et al., 2005, Ye et al., 2005). Moreover, sorted CLPs with an inactivated PU.1 also differentiate into the B cell lineage *in vitro* (Iwasaki et al., 2005). Collectively, these

findings suggest that PU.1 is required for normal B cell accumulation at or before the CLP stage during the development from HSCs, but is not essential for further B cell differentiation.

Ikaros (encoded by *Ikzf1*), the founding member of a small family of transcription factors, is also critical for specification in lymphoid and B cell lineages as it is expressed in all haematopoietic lineages including HSCs and MPPs (Georgopoulos et al., 1992, Morgan et al., 1997, Klug et al., 1998, Kelley et al., 1998, Papathanasiou et al., 2009). Ikaros deficient MPPs display impaired differentiation of CLPs, which results in a defect in the accumulation of lymphoid lineages including B, NK and foetal T cells despite the presence of some T cell progenitors in the thymus and mature T cells in the periphery (Georgopoulos et al., 1994, Wang et al., 1996). Like PU.1-deficient mice, loss of Ikaros in haematopoietic progenitors fail to express Flt3 (Nichogiannopoulou et al., 1999), suggesting a role for Ikaros in the accumulation of LMPPs. However, a recent study using an Ikaros promotor-driven reporter gene illustrated a normal generation of the LMPP population in the bone marrow of Ikaros-deficient mice, but these cells were unable to generate B and T cells, and have reduced expression of IL-7R and RAG1 (Yoshida et al., 2006). These studies suggest that Ikaros is most likely dispensable for the development of LMPPs, but required for their progression into lymphoid lineages.

In addition to its role in priming lymphoid lineages, Ikaros also plays a direct role in B cell development. Mice with a hypomorphic allele of Ikaros exhibit a developmental block at the pro-B cell stage of B cell development in the bone marrow (Kirstetter et al., 2002). Additionally, pro-B cells from these mice fail to form IL-7 dependent colonies *in vitro*, and display diminished levels of transcript for the genes encoding RAG1, RAG2, TdT and λ5 as well as Flt3 and IL-7R (Kirstetter et al., 2002, Yoshida et al., 2006). More recently three independent studies confirmed the vital role for Ikaros in early B cell development in the bone marrow (Heizmann et al., 2013, Schwickert et al., 2014, Joshi et al., 2014). These studies identified crucial roles for Ikaros in activating the downstream of pre-BCR signalling, controlling cell migration and adhesion (Schwickert et al., 2014, Joshi et al., 2014). Collectively, these studies reveal that Ikaros is a critical transcription factor in various aspects of early B cell development from HSCs.

Another transcription factor that plays a crucial role in priming of the lymphoid lineage from MPPs is the basic helix-loop-helix transcription factor **E2A** (encoded by *Tcfe2a*), which occurs in two splice variants E12 and E47. Animals deficient for E2A have reduced numbers of LMPPs and CLPs (Borghesi et al., 2005, Dias et al., 2008, Semerad et al., 2009). In cooperation with the other transcription factors PU.1 and Ikaros, E2A has been suggested to activate lymphoid-specific genes in LMPPs (Ramirez et al., 2010).

In regard to B cell differentiation, E2A-deficient mice exhibit a block during early B cell development prior to onset of Ig gene rearrangements (Bain et al., 1994, Zhuang et al., 1994, Bain et al., 1997, Beck et al., 2009), revealing a critical role for E2A in B cell development in the bone marrow. E2A also plays a role in the specification of the B cell lineage by initiating and maintaining the expression of the B cell fate transcription factors EBF1 and PAX5 (discussed below) (Bain et al., 1994, Seet et al., 2004, Kwon et al., 2008). The E2A transcription factor can bind to the EBF promoter to regulate EBF1 expression (Smith et al., 2002). Moreover, the E2A proteins, together with HeLa E-box binding protein (HEB), activate the expression of FOXO1 in CLPs (Welinder et al., 2011), whose expression together with E2A induces EBF1 expression. EBF1 and FOXO1, in turn, activate a positive intergenic feedback circuitry, which is important for the establishment of B cell identity (Mansson et al., 2012). These findings suggest that E2A plays a vital role in B cell development through transcriptionally priming of lymphoid lineages as well as initiation of the B cell gene program.

EBF1, an essential B-lineage specification factor, is expressed exclusively in early B cell stages, but not in late stages of B cell development or T and non-lymphoid cells (Hagman et al., 1991, Feldhaus et al., 1992, Hagman et al., 1993). The expression of EBF1 is controlled by the transcription factor E2A (Smith et al., 2002) and IL-7R signalling (Kikuchi et al., 2005). Analysis of mice lacking EBF1 revealed a requirement for EBF1 in B cell development beyond the pre/pro-B cell stage in the bone marrow (fraction A) (Lin and Grosschedl, 1995). Pre/pro-B cells from EBF1 deficient mice failed to express B cell specific genes including *Cd79a*, *Cd79b*, *Igll1* and *VpreB1* (Lin and Grosschedl, 1995). The crucial role of EBF1 in early B cell development was further revealed by studies where ectopic expression of EBF1

alone was sufficient to compensate for loss of IL-7, IL-7Rα, PU.1, Ikaros or E2A during early B cell development in the bone marrow (Seet et al., 2004, Dias et al., 2005, Kikuchi et al., 2005, Medina et al., 2004, Reynaud et al., 2008). Recently, conditional inactivation of *Ebf1 in vitro* and *in vivo* at various B cell stages also identified a crucial role for EBF1 in pro-B cell survival, proliferation and signalling (Gyory et al., 2012, Vilagos et al., 2012). Moreover, multiple lines of evidence demonstrate that EBF1 also regulates B cell gene networks, maintain B cell identity and prevent development of non-B cell lineages through repression of genes encoding various transcription factors of alternative cell fates (Pongubala et al., 2008, Thal et al., 2009, Treiber et al., 2010, Lukin et al., 2011, Nechanitzky et al., 2013). Collectively, these studies suggest that EBF1 functions as a key transcription factor at multiple stages of B cell development in the bone marrow via regulation of important compartments of transcription factor and signalling networks.

The transcription factor **PAX5** is only expressed in B cells (from the pro-B cell to mature B cell stage) within the haematopoietic lineage (Barberis et al., 1990, Adams et al., 1992, Fuxa and Busslinger, 2007), and is considered to be a master regulator gene for B cell development. Early studies showed that PAX5-deficient mice failed to accumulate B cell progenitors in the foetal liver, but B cell development in the adult bone marrow progressed up to the pro-B cell stage (Urbanek et al., 1994, Nutt et al., 1997b, Nutt et al., 1997a), indicating an essential requirement for PAX5 beyond the pro-B cell stage of adult B lymphopoiesis. The expression of genes encoding the transcription factors PU.1, Ikaros, E2A and EBF1 is unaffected in PAX5-deficient pro-B cells (Nutt et al., 1997b), suggesting that PAX5 functions downstream of these transcription factors. Like EBF1, PAX5 was reported to maintain B cell identity and thus promotes B cell development through activation of genes involved in BCR signalling, adhesion and migration, as well as suppression of genes that are required for differentiation into non-B cell lineages. This was confirmed by analysis of PAX5-deficient pro-B cells that were able to differentiate into different haematopoietic cell types (Kozmik et al., 1992, Nutt et al., 1999, Souabni et al., 2002, Schebesta et al., 2002, Mikkola et al., 2002, Delogu et al., 2006, Schebesta et al., 2007). This notion has been further confirmed by a study where mature B cells from mice with a conditionally inactivated PAX5 were shown to

dedifferentiate into early uncommitted progenitors, which eventually give rise to T cells in the thymus of T-cell deficient mice (Cobaleda et al., 2007).

As already mentioned, EBF1 expression is controlled by the transcription factor E2A as well as by the IL-7R signalling (Smith et al., 2002, Kikuchi et al., 2005). E2A-induced EBF1 binds to the *Pax5* promoter region and activates PAX5 expression in pro-B cells (Decker et al., 2009). PAX5 in turn promotes EBF1 expression by binding to the *Ebf1* promoter (Roessler et al., 2007). This provides a positive feedback loop between EBF1 and PAX5 to enable pro-B cells to reinforce the B cell genetic program and to commit these cells to the B cell lineage. These studies suggest that PAX5, in concert with EBF1, is a vital transcriptional factor for B cell fate specification and commitment. They play critical roles in activation of B cell-specific genes and suppression of non-B cell lineage genes as well as maintenance of B cell identity and control of multiple determinants of B cell development.

The transcription factors interferon regulatory factors 4 and 8 (**IRF4,8**) are mainly expressed in the immune system, and were shown to play a critical role in B cell development via multiple mechanisms (Lu et al., 2003, Ma et al., 2006, Ma et al., 2008). IRF4, whose expression is elevated by pre-BCR signalling, alone is vital for the promotion of light chain rearrangement and transcription in pre-B cells in the bone marrow (Ma et al., 2006, Johnson et al., 2008, Pathak et al., 2008). Similarly, IRF8 alone also plays a role in the specification, commitment and differentiation of B cells from HSCs through regulation of a transcriptional network including PU.1 and EBF1 (Wang et al., 2008). Furthermore, animals deficient for both IRF4 and 8 (IRF4,8$^{-/-}$) exhibited a developmental arrest at the cycling pre-B cell stage in the bone marrow, and failed to down-regulate the pre-BCR (Lu et al., 2003). These results suggest that transcription factors IRF4 and 8, both alone and together, control different aspects of B cell development in the bone marrow.

1.2.4 Generation of a functional B cell population in the periphery

Upon productive rearrangement of the Ig heavy and light chain loci IgM is expressed on the surface of immature B cells, which are ready to leave the bone marrow and enter the periphery to complete their maturation (Figure 1.4) (Samitas et al., 2010). Occasionally, immature B cells that possess an autoreactive receptor are not deleted

during the earlier stages of B lymphopoiesis. Therefore, immature B cells need to be checked first for self-reactivity before they leave the bone marrow, and the clonotypes bearing receptors with high affinity for self-antigens must be either eliminated or silenced in order to maintain self-tolerance (Figure 1.4). Several studies using transgenic mice have shown that mechanisms for censoring the autoreactive BCRs include receptor editing (secondary gene rearrangement) (Gay et al., 1993, Tiegs et al., 1993, Radic et al., 1993, Halverson et al., 2004), clonal deletion (Nemazee and Burki, 1989) and anergy (Goodnow et al., 1988). Relevant to the existence of the self tolerance check-point at the immature stage of B cell development in the bone marrow is the observation that only 10 to 20% of all newly produced B cells have been estimated to enter the mature B cell compartment in mice (Allman et al., 1993, Rolink et al., 1998), and this ratio was shown to be between 25 and 45% of all immature B cells in humans (Wardemann et al., 2003).

Immature B cells that pass the self-reactivity check-point leave the bone marrow as recent immigrants called transitional (T)-1 cells and migrate to the spleen for their final stages of maturation (Figure 1.4) (Loder et al., 1999). Multiple lines of evidence suggest that negative selection of immature B cells by clonal deletion in response to basal (tonic) BCR signalling continues to occur at the T1 stage of the peripheral maturation as BCR crosslinking induces increased apoptosis at this stage (Carsetti et al., 1995, Su and Rawlings, 2002, Petro et al., 2002). T1 cells express high level of IgM but low levels of IgD and CD21, and give rise to T2 cells, which represent a distinct population of $IgM^{hi}IgD^{hi}CD21^{hi}CD23^{+}$ (Figure 1.4) (Loder et al., 1999). T2 cells are exclusively found in the primary follicles of the spleen but not in the lymph node or bone marrow, and they possess the ability to further differentiate into mature B cell subpopulations (Loder et al., 1999, Teague et al., 2007). A subsequent study by Allman et al. suggested the existence of a third transitional population of immature peripheral B cells, and re-defined the three distinct subsets based on the surface phenotype of $CD93^{+}IgM^{hi}CD23^{-}$ (T1), $CD93^{+}IgM^{hi}CD23^{+}$ (T2) and $CD93^{+}IgM^{lo}CD23^{+}$ (T3) (Figure 1.4) (Allman et al., 2001). The authors confirmed the existence of a developmental sequence in which T1 cells differentiate into T2 B cells, which constitute the mature B cell compartments (Allman et al., 2001). Importantly, several lines of evidence suggest that all T3 cells are naturally anergic B cells as these cells were unable to give rise to mature B cells and were

hyporesponsive to BCR stimulation (Figure 1.4) (Merrell et al., 2006, Teague et al., 2007, Liubchenko et al., 2012).

Similar to early B cell development in the bone marrow, the peripheral maturation of immature B cells also possesses distinct requirements for their survival and differentiation. A self-antigen-induced BCR signalling is suggested to be indispensable for B cell survival as well as for the differentiation of transitional B cells into mature B cells. This notion is supported by studies where ablation of BCR signalling via deletion or inactivation of genes encoding BCR signalling components including *Btk*, *Blnk*, *Pik3ap1*, *Plcg2* and *Vav1*/*Vav2*/*Vav3* resulted in a failure in the accumulation of mature B cells in the periphery (Khan et al., 1995, Pappu et al., 1999, Hashimoto et al., 2000, Yamazaki et al., 2002, Fujikawa et al., 2003, Kraus et al., 2004, Vigorito et al., 2005). These findings reveal the importance of tonic signalling in the survival of transitional immature B cells and their differentiation into mature B cell populations.

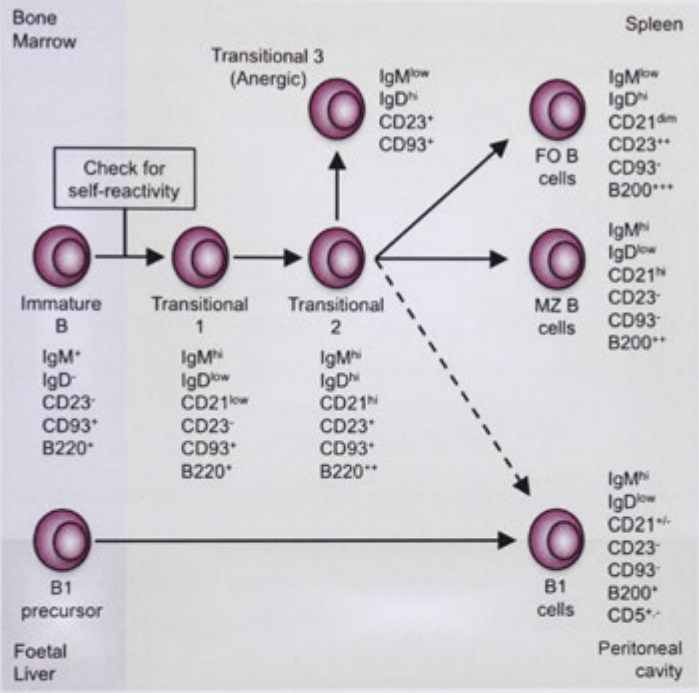

Figure 1.4 A schematic representation of B cell maturation in the periphery
Immature B cells that express IgM on their surface leave bone marrow and migrate to the periphery as transitional (T) 1 cells. Newly formed T1 cells give rise to T2 cells, which eventually differentiate into mature B cell subsets including FO B cells and MZ B cells. While some T2 cells differentiate into T3 cells, which mainly consist of anergic B cells, some of them are thought to differentiate into B1 cells (mainly B1b cells). Recent evidence suggests that the development of B1 cells can also be derived from the precursors in the foetal liver and bone marrow. The phenotypic characteristics of the different subsets are shown. FO B, follicular B cells; MZ B, marginal zone B cells (Modified from Samitas et al., 2010).

In addition to the tonic BCR signalling, immature B cells depend on growth factors for their survival. In particular, the cytokine B cell-activating factor (BAFF), which is predominantly produced by neutrophils, monocytes and macrophages, is essential for survival of T2 cells as well as mature B cells via the alternative NFκB pathway (Mackay et al., 2010, Gardam and Brink, 2014). Mice deficient for BAFF exhibit a B cell developmental arrest at the T1 stage and have almost no mature B cells despite a normal B cell development in the bone marrow (Batten et al., 2000, Schiemann et al., 2001, Gross et al., 2001). Conversely, overexpression of BAFF resulted in an expansion in the number of peripheral B cells, which led to severe autoimmune diseases (Mackay et al., 1999, Groom et al., 2002). Although BAFF is able to bind to three TNF family receptors, BCMA, TACI and BAFFR, the latter appears to be the crucial receptor for governing the effects of BAFF (Ng et al., 2004). This notion was further supported by evidence that BAFFR-null mice exhibit a very similar phenotype to that observed in BAFF-deficient animals (Shulga-Morskaya et al., 2004).

The generation and maintenance of functional mature B cell populations in the periphery is important for the effective protection against a vast range of infectious agents. Mature B cells can be divided into three subsets that differ with respect to their localisation, expression of different surface markers and function, namely follicular (FO) B cells, marginal zone (MZ) B cells and B1 cells (Figure 1.4). The strength of the ligand-independent tonic BCR signalling appears to play a key role in the commitment of immature B cells to a mature FO versus MZ B cell fate, with weak signalling favours the development of MZ B cells while strong signalling favours the development of FO B cells (Pillai and Cariappa, 2009).

FO B cells that differentiate from T2 cells (Figure 1.4) are the main effector B cells that make up the majority of mature B cells in the periphery. They are localised into the primary follicles of B cell zones in the spleen, and are responsible for immune responses against T-dependent antigens (Allman and Pillai, 2008). Once FO B cells become activated and with the help from Th cells they differentiate into short-lived extrafollicular plasma cells that produce IgM, which is the first line of humoral immune responses (Goodnow et al., 2010, Hamel et al., 2012). Alternatively, activated FO B cells can migrate into the specialized microenvironments within the

secondary lymphoid tissues, known as germinal centres (GC), where B cells undergo clonal expansion, somatic hypermutation and affinity maturation for effective humoral immune responses and for the generation of memory B-lymphocytes (Goodnow et al., 2010, Hamel et al., 2012).

MZ B cells, on the other hand, localise in the marginal sinus regions of the spleen and they play a crucial role in host protection against T-independent antigens such as blood-borne antigens. Like FO B cells, MZ B cells also originate from T2 immature B cells (Figure 1.4), which contain substantial numbers of MZ precursors (Srivastava et al., 2005). MZ B cells are considered to be innate-like cells as upon T-independent activation they are able to rapidly proliferate and differentiate into low-affinity antibody-producing plasmablasts with 3-4 days (Oliver et al., 1999, Martin et al., 2001). In addition to their role in T-independent immune responses, MZ B cells also function as antigen-presenting cells by transporting immune complexes that contain antigens from the marginal sinus to follicular dendritic cells in the splenic follicles (Ferguson et al., 2004, Cinamon et al., 2008). Moreover, MZ B cells have been shown to present antigen to T cells and activate them far better than FO B cells (Attanavanich and Kearney, 2004). These data suggest a potential role for MZ B cells in T-dependent immune responses.

B1 cells have self-renewal ability and are mainly found in the pleural and peritoneal cavities. They account for nearly 5% of the total B cell population with fewer numbers in the spleen (Hayakawa et al., 1983). The chemokine CXCL13 has been shown to control B1 cell homing to the peritoneal cavities as CXCL13-deficient B1 cells were largely found in the spleen and exhibited a defective antibody response (Ansel et al., 2002). Although initially CD5 expression on their surface was thought to distinguish B1 cells from the conventional B (B2) cells (Hayakawa et al., 1983), it was later found that not all B1 cells express CD5 on their surface, and B1 cells can be divided into two subpopulations, namely B1a cells ($CD5^+$) and B1b cells ($CD5^-$) (Kantor et al., 1992).

The development of B1 cells takes place earlier than FO B cells in ontogeny (Godin et al., 1993), and occurs both before the birth and in the first weeks of post-natal life (Baumgarth, 2011). B1 cell development is believed to be different from the

development of B2 cells, but it is less understood and different models have been suggested to explain. The first model is known as the "lineage hypothesis", which proposes existence of two distinct B cell precursors that give rise to different B cell subpopulations (Figure 1.4) (Herzenberg, 2000, Dorshkind and Montecino-Rodriguez, 2007). Evidence supporting this notion was shown by studies where a precursor population in the foetal liver and bone marrow was shown to give rise to B1 cells (Montecino-Rodriguez et al., 2006, Tung et al., 2006, Esplin et al., 2009). The second model, known as the "induced differentiation hypothesis", proposes that all B cells derive from a common precursor (Figure 1.4) and the appearance of B1 cells is dependent on the encounter with naturally occurring antigens (Berland and Wortis, 2002). Baumgarth recently proposed a third hypothesis named the "two-pathway model" for B1 cell development in which both the lineage and induced differentiation hypothesis coexist to warrant the generation of a functional B1 cell population (Baumgarth, 2011). With respect to their functional properties, B1 cells participate in the antigen-stimulated T-independent antibody responses with their ability to produce natural antibodies (IgM) and thus provide the earliest antibody response against antigens (Berland and Wortis, 2002, Allman and Pillai, 2008). B1 cells have also been suggested to participate in T-independent immune responses at the mucosal sites by producing IgA (Berland and Wortis, 2002, Allman and Pillai, 2008).

1.2.5 B cell activation and formation of GC B cells

Once a functional mature B cell population is generated in the periphery, mature B cells search their cognate antigen by circulating through the blood and the lymph. The encounter of antigen with naïve B cells occurs in the secondary lymphoid tissues in most cases. Engagement of the BCR by its cognate antigen is not sufficient for B cell activation, as B cells need a second signal from Th cells, and recognition of the antigen with its cognate BCR leads to migration of B cell to the T cell zone near the follicle to receive this help. The membrane protein CD40 ligand, which is highly expressed by activated Th cells, activates the B cell surface receptor CD40 to promote the survival and proliferation of B cells (Elgueta et al., 2009). The gain of a second signal from Th cells is central for the activation and proliferation of B cells as cells that fail to receive this signal undergo apoptotic death or anergy in a T-dependent response (Goodnow et al., 2010). The activated B cells express the CD28

ligands CD80 and CD86 to activate CD4 Th cells (Goodnow et al., 2010), which upon activation proliferate and produce cytokines, which in turn enable B cells to survive and proliferate (Goodnow et al., 2010).

Activation of B cells through the BCR results in either differentiation into GC B cells or becoming short-lived plasma cells producing IgM antibodies with low affinity (Goodnow et al., 2010). GCs are specialized microenvironments within the secondary lymphoid tissues where B cells undergo clonal expansion, somatic hypermutation and affinity maturation for effective humoral immune responses and for the generation of memory B-lymphocytes (Vinuesa and Cyster, 2011, Crotty, 2011). In GCs, B cells undergo an extensive proliferation phase. Class switch recombination also mainly occurs in GCs in order for B cells to switch their Igs to a different constant region for different effector functions (Goodnow et al., 2010). Furthermore, within the GCs, B cells also undergo somatic hypermutation, resulting in an increase in antigen affinity (Goodnow et al., 2010). Some of the activated cells eventually either differentiate into antibody secreting plasma cells or become memory B cells (Goodnow et al., 2010).

T Follicular helper (T_{FH}) cells are a recently identified subset of $CD4^+$ T cells that provide essential help to B cells to trigger formation of GCs (Vinuesa and Cyster, 2011, Crotty, 2011). During a T-dependent immune response, the differentiation of normal numbers of T_{FH} cells is a crucial step as failure of T_{FH}-cell differentiation results in impaired GC formation and a lack of high-affinity antibody production (Johnston et al., 2009, Nurieva et al., 2009, Yu et al., 2009). In contrast, increased numbers of T_{FH} cells results in aberrant production of autoantibodies and the development of autoimmune diseases (Hu et al., 2009, Linterman et al., 2009).

In conclusion, the formation of GC B cells as well as T_{FH} cells is an important step for the effective humoral responses, and dysregulation of the GC responses is associated with several immune system disorders (Vinuesa et al., 2009, Klein and Dalla-Favera, 2008).

1.3 Plasma Membrane Lipid Asymmetry

The plasma membrane in eukaryotes envelops cells and consists of a bilayer structure based on the distribution of aminophospholipids, which was first shown in human erythrocytes (Gorter and Grendel, 1925). One of the unique features of the plasma membrane is the asymmetric distribution of the specific phospholipids between the two leaflets of the bilayer. While most of the plasma membranes contain phosphatidylcholine (PC) and sphingomyelin (SM) on the exoplasmic leaflet, phosphatidylserine (PS) and phosphatidylethanolamine (PE) are mainly confined to the cytoplasmic leaflet (Bretscher, 1972, Gordesky and Marinetti, 1973). PC is the most prevalent lipid, which constitutes 40 – 50% of total lipids in the plasma membrane, whereas PE and PS only account for 25% and 12% of the total membrane lipids, respectively (Daleke, 2008). The presence of other lipids such as phosphatidylinositol (PI) and phosphatidic acid (PA) is less abundant and restricted to the cytoplasmic leaflet (Butikofer et al., 1990, Gascard et al., 1991).

The establishment and dynamic maintenance of the non-random distribution of phospholipids is important for normal membrane functions, and has been implicated in many cellular processes including blood coagulation, apoptosis and vesicle formation (Leventis and Grinstein, 2010). The restriction of PS in the cytoplasmic leaflet is particularly important as it mediates important biological functions. PS in the cytoplasmic leaflet activates Protein Kinase C beta and provides a docking site for a range of other signalling proteins including GTPases (Ras and Rho) and non-receptor tyrosine kinases (e.g. Src) (Leventis and Grinstein, 2010). In contrast to their role in the cytoplasmic leaflet, PS also initiates important biological processes upon exposure on the surface. During the platelet activation PS accumulates on the exoplasmic leaflet via the scramblase activity (discussed below), which initiates the blood coagulation cascade through the activation of several blood proteins like clotting factor V, VIII and X (Leventis and Grinstein, 2010). Exposure of PS on the surface of cells is also critical for the recognition and clearance of apoptotic cells. During the early stages of cell death, PS is no longer restricted to the inner leaflet and is exposed on the exoplasmic leaflet, which provides an "eat-me" signal that can be recognized by specific PS receptors expressed on macrophages for their engulfment (Fadok et al., 1992).

As mentioned above, asymmetry of the plasma membrane is critical but it does not exist autonomously, and has to be actively generated by two groups of ATP-dependent transporters embedded in the membrane (Figure 1.5A). ATP-binding cassette (ABC)-type transporters (floppases) are responsible for active transport of specific lipids such as PC to the exoplasmic leaflet (Pomorski and Menon, 2006). "Flipping" of PS and PE into the inner leaflet against their concentration gradient is greatly accelerated by flippases, which are members of the P4-type ATPase family of 10-transmembrane domain proteins (Figure 1.5B) (Tang et al., 1996, van der Velden et al., 2010, Paulusma and Elferink, 2010). The third group of transporters, known as scramblases, are believed to disrupt the lipid asymmetry generated by energy-dependent transporters via mediating the rapid bidirectional movement of all types of phospholipids (Figure 1.5A) (Bevers and Williamson, 2010). In contrast to energy-dependent flippases and floppases, scramblases become activated by elevation of intracellular Ca^{2+} concentration (Bevers and Williamson, 2010).

1.3.1 Phospholipid flippases

The presence of an asymmetric distribution of phospholipids was first shown in human erythrocytes (Bretscher, 1972, Gordesky and Marinetti, 1973), which provide a great model for the study of membrane lipids as erythrocytes lack nuclei and they are closely associated with their plasma membrane (Daleke, 2008). In 1984, Seigneuret and Devaux were the first to identify the existence of an phospholipid translocase that catalyses the movement of specific spin-labelled lipid analogues from the outer leaflet of the plasma membrane to the inner leaflet in human erythrocytes (Seigneuret and Devaux, 1984). This process requires ATP for function, as vanadate inhibits translocation (Seigneuret and Devaux, 1984), and selectively transports PS and, to lesser extent PE. Since the first evidence for the phospholipid translocase activity, a huge amount of work has been done for the molecular identification and characterisation of these transporters, and it was later shown that proteins belong to the P4-type ATPase family catalyse the flipping of phospholipids (Tang et al., 1996, van der Velden et al., 2010, Paulusma and Elferink, 2010).

The P4-type ATPases are integral membrane proteins and expressed in eukaryotes (van der Mark et al., 2013). The proteins consist of 10 transmembrane segments with a phosphorylation domain, a nucleotide binding domain, an actuator domain and

both N- and C-terminal tails (Figure 1.5B). While there are 14 members in humans (ATP8A1, ATP8A2, ATP8B1, ATP8B2, ATP8B3, ATP8B4, ATP9A, ATP9B, ATP10A, ATP10B, ATP10D, ATP11A, ATP11B and ATP11C) and 15 in mice (all present in humans and ATP8B5), there are only 5 members in yeast (Drs2, Dnf1, Dnf2, Dnf3 and Neo1) (Sebastian et al., 2012).

Like other P-type ATPases, the proper function of the P4-type ATPases requires the formation of a heterodimeric complex with a β-subunit. The members of the cell divisional control 50 (CDC50) protein family, that is evolutionary conserved in yeast, plants and mammals, have been suggested to act as the β-subunit (Saito et al., 2004). CDC50 proteins possess two putative transmembrane domains separated by a large glycosylated extracellular domain (Figure 1.5B). Although the β-subunit is believed to be required for the release of the P4-type ATPase from the ER (van der Mark et al., 2013, Lopez-Marques et al., 2013), their contribution to the subcellular localisation and the determination of substrate specificity is still unclear. Recent studies in *Arabidopsis thaliana* and yeast revealed that the CDC50 is not involved in the recognition of different phospholipid substrates, and the P4-type ATPase itself determines the substrate specificity (Lopez-Marques et al., 2010, Baldridge and Graham, 2012). Despite the existence of 14 the P4-type ATPases in humans (15 in mice), there are only 3 CDC50 proteins expressed in mammals (CDC50A-C) (Katoh and Katoh, 2004), indicating that one CDC50 protein can associate with multiple P4 ATPases. However, the specific role of CDC50 proteins in the localisation and the determination of substrate specificity of the P4-type ATPases in mammals remains elusive.

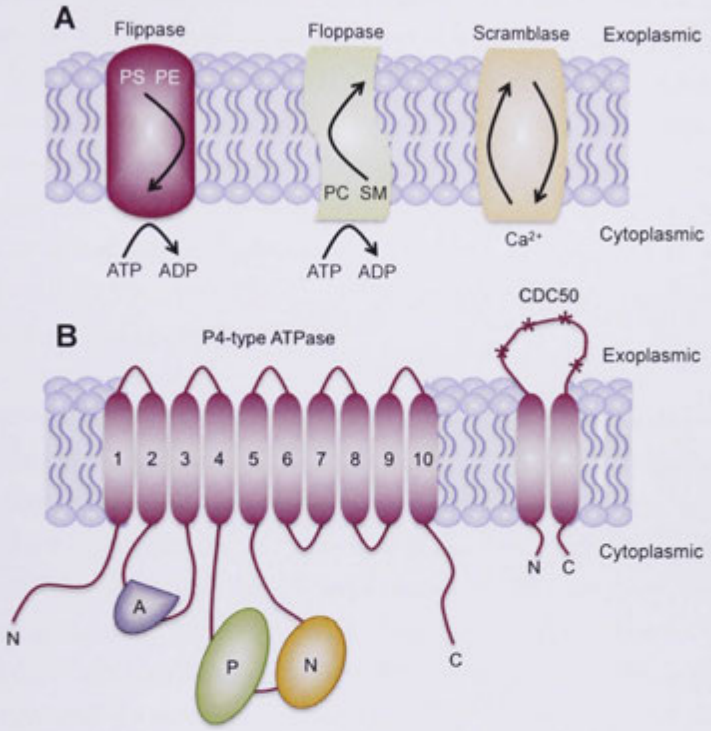

Figure 1.5 The generation and dynamic maintenance of phospholipid asymmetry by lipid transporters

(A) Asymmetric distribution of phospholipids in the biological membranes is a hallmark of cell survival and function. Three different groups of enzymes are involved in the movement of phospholipid molecules between the two leaflets of the plasma membranes. While ATP-dependent flippases catalyse the inward movement of predominantly phosphatidylserine (PS), and to a lesser extent phosphatidylethanolamine (PE), ATP-dependent floppases transport phosphatidylcholine (PC) and sphingomyelin (SM) from the cytosolic leaflet to the exoplasmic leaflet of the bilayer. Scramblases, on the other hand, are activated by Ca^{2+}, and mediate bidirectional movement of lipids without substrate specificity. **(B)** The predicted topology of the P4-type ATPases (α-subunit) and CDC50 (β-subunit) is shown. The P4-type ATPases have ten transmembrane domains, cytosolic actuator (A), phosphorylation (P), the nucleotide binding (N) domains and N- and C-termini. CDC50 subunit possesses two transmembrane domains, short cytosolic N- and C-termini, and multiple putative glycosylation sites as indicated by asterisks.

1.3.1.1 Evidence that the P4-type ATPases are phospholipid flippases

Although the biochemical activity of flippases has been known for a long time, their identification and characterisation is still unclear. The evidence that the P4-type ATPases are involved in the inward movement of lipids originates from studies in yeast. In 1996, Tang et al. showed in yeast that a Drs2 null mutant is defective in ATP-dependent transport of NBD-labelled PS (Tang et al., 1996). Subsequent studies revealed that other members, Dnf1 and Dnf2 reside in the plasma membrane and mediate the transport of NBD-labelled PE, PS and PC from the outer to the inner leaflet of plasma membrane (Pomorski et al., 2003). Recently, reconstitution of flippase activity with purified Drs2 has also been implicated in the translocation of PS (Zhou and Graham, 2009).

Further evidence for the involvement of P4-type ATPases in the translocation of phospholipids came from the studies in higher eukaryotes. For instance, the Arabidopsis protein ALA1, which is homologous with Drs2 in yeast, has been shown to act as a flippase (Gomes et al., 2000). Consistently, the P4-type ATPase TAT-1 in *Caenorhabditis elegans* facilitates the inward transport of PS in germ cells (Darland-Ransom et al., 2008). As discussed further below, mammalian flippases ATP8A1, ATP8A2, ATP8B1 and ATP8B3 have been shown to be involved in the translocation of phospholipid between the two leaflets of the bilayer in different cell types (Levano et al., 2012, Zhu et al., 2012, Cai et al., 2009, Wang et al., 2004). These findings collectively suggest that members of the P4-type ATPase family have the ability to translocate specific phospholipids (predominantly PS) from the cytoplasmic leaflet to the exoplasmic leaflet of biological membranes, thereby acting as a flippase.

1.3.1.2 Evidence that the P4-type ATPases are involved in vesicle-mediated protein transport

In addition to phospholipid translocase activity, the P4-type ATPases have been suggested to play an important role in vesicle-mediated protein trafficking in the Golgi and endosomal systems (Graham, 2004). The first evidence for involvement of the flippases in vesicular transport was demonstrated in yeast. The mutant Drs2, which predominantly localises to the *trans*-Golgi network where clathrin-coated vesicles bud, exhibited impaired formation of clathrin-coated vesicles (Chen et al., 1999). Using different mutant flippases in yeast, subsequent studies confirmed that

the P4-type ATPases were involved in the vesicle-mediated protein transport (Hua et al., 2002, Pomorski et al., 2003). The involvement of the flippase family in the biogenesis of intracellular transport vesicles within the endocytic and secretory pathways has also been demonstrated in higher organisms including *Arabidopsis thaliana* and *Caenorhabditis elegans* (Poulsen et al., 2008, Ruaud et al., 2009, Chen et al., 2010) as well as in mammalian cells (Xu et al., 2009). These findings suggest a nonredundant function for the P4-type ATPases in secretory vesicle formation, but their physiological functions in mammalian systems remain to be fully uncovered.

1.3.1.3 Physiological importance of the P4-type ATPases in mammals

As already mentioned, the cellular functions of the P4-type ATPases have mostly been pinpointed by genetic analysis in yeast and the role of the 15 P4-type ATPases in mice (14 in humans) (Sebastian et al., 2012) and other mammals is mostly unexplored (van der Mark et al., 2013). The flippases that have been linked to the physiological functions in mammals will be briefly highlighted below.

The plasma membrane aminophospholipid translocase activity of ATP8A1 has been recently shown using knock out mice. ATP8A1 knock-out hippocampal cells displayed increased PS exposure on their surface compared to cells from heterozygous and control mice (Levano et al., 2012). ATP8A1-deficient animals also showed a delayed hippocampus-dependent learning, and hyperactivity. Interestingly, despite the expression of ATP8A1 in erythrocyte membranes (Soupene and Kuypers, 2006), erythrocytes from the deficient mice exhibit no increased exposure of PS at the surface, and this was explained by a compensatory increase of ATP8A2 in erythrocytes from *Atp8a1*$^{-/-}$ mice (Levano et al., 2012).

A homologue of ATP8A1, ATP8A2 is highly expressed in photoreceptor outer segments of retina, brain, spinal cord and testis (Coleman et al., 2009, Cacciagli et al., 2010, Zhu et al., 2012). Loss of ATP8A2 in mice led to the development of neurodegeneration in the central and peripheral nervous system, and deficient mice exhibited an impaired flippase activity (Zhu et al., 2012). *In vitro* transfection of cells defective in non-endocytic uptake of PS with ATP8A2 revealed an increase in PS translocation activity, confirming that ATP8A2 is a phospholipid flippase (Zhu et al., 2012). Moreover, a recent study illustrated that *Atp8a2*$^{-/-}$ mice displayed shortened

retinal photoreceptor outer segments and decreased photoreceptor viability (Coleman et al., 2014), indicating a role for ATP8A2 in normal visual and auditory function as well as the survival of photoreceptor and spiral ganglion. In agreement with murine findings, patients with a mutation in *ATP8A2* have been shown to display cerebellar ataxia, mental retardation and disequilibrium syndrome (Cacciagli et al., 2010, Onat et al., 2013). These data collectively suggest a critical role for the P4-type ATPase ATP8A2 in the development of neurological disorders as well as in normal vision.

ATP8B1 is the first member of the P4-type ATPase family that has been related to a human disease. It is expressed in many tissues such as liver, pancreas, small intestine, bladder and prostate (van der Mark et al., 2013). Mutations in human *ATP8B1* have been associated with familial intrahepatic cholestasis characterised by a defective bile salt extraction from liver into bile (Bull et al., 1998, Klomp et al., 2004). Further mouse studies revealed that ATP8B1 is important for normal phospholipid asymmetry of the canalicular membrane, and hepatocytes from ATP8B1-deficient animals were shown to be more sensitive to bile salt-induced membrane damage (Paulusma et al., 2006, Cai et al., 2009).

ATP8B3 is expressed in spermatozoa, and is required for asymmetric distribution of PS between the two leaflets of the sperm plasma membrane (Wang et al., 2004, Gong et al., 2009). Despite normal sperm morphology and motility, sperm from the deficient animals exhibited compromised *in vitro* fertilization capability (Wang et al., 2004), suggesting a possible role for ATP8B3 in the formation of acrosome and sperm function during fertilization.

The heterozygous deletion of ATP10A (also known as ATP10C) in mice is associated with diet-induced obesity, type-2 diabetes, non-alcoholic fatty liver disease and as well as the development of insulin resistance and regulation of glucose uptake in adipose tissue and skeletal muscle (Dhar et al., 2004, Dhar et al., 2006). Similarly, C57BL/6J mice carrying a stop codon in exon 12 of *Atp10d* (Flamant et al., 2003) have been shown to be prone to develop obesity, hyperglycemia and hypertension upon a high-fat diet (Surwit et al., 1988, Surwit et al., 1991, Rebuffe-Scrive et al., 1993), suggesting a potential role for flippases in the development of obesity and type-2 diabetes.

Despite the studies revealing the physiological importance of flippases in mammals, further characterisation and functional properties of different flippases are needed to fully understand pathophysiology of flippase-related diseases such as intrahepatic cholestasis in humans.

1.3.2 Phospholipid floppases

The second group of lipid transporters, known as floppases, which mediate the movement of phospholipids from the inner leaflet to the outer leaflet of biological membranes, has been identified in erythrocytes using spin- or NBD-labelled lipids (Bitbol and Devaux, 1988, Connor et al., 1992). ABC-type transporters catalyse active transport of specific lipids to the exoplasmic leaflet, and the most characterised members are ABCA1, ABCB1 (also known as MDR1), ABCB4 (also known as MDR2 in mice or MDR3 in humans) and ABCC1, but the role of these transporters in mammals is largely unknown. ABCB4 has been implicated in the secretion of PC into the bile (Smit et al., 1993). Subsequent studies further demonstrated a critical involvement for ABCB1 and ABCB4 in the outward translocation of different lipids including platelet activation factor, PC, PE, and SM (van Helvoort et al., 1996, Ernest and Bello-Reuss, 1999, Raggers et al., 2001, Morita et al., 2007). Other members of the ABC-type transporter family, ABCB11 as well as ABCG5 and ABCG8 have also been implicated in intrahepatic cholestasis (Wang et al., 2001), and biliary excretion of cholesterol (Berge et al., 2000). In conclusion, despite that many ABC transporters have been suggested to exist (Nagao et al., 2010), their characterisation and mechanism of action needs further evaluation to be fully delineated.

1.3.3 Phospholipid scramblases

The physiological importance of phospholipid scrambling has been documented in several important events (Bevers and Williamson, 2010). As already mentioned, loss of plasma phospholipid asymmetry and subsequent exposure of PS on the surface is a feature of the activation of blood coagulation cascades as well as recognition of apoptotic cells, and dependent on the activity of lipid scrambling (Williamson et al., 1992). The disruption of plasma membrane lipid asymmetry via scramblase activity was first discovered in blood platelets (Bevers et al., 1983). This activity has been suggested to be important for exposure of PS on the surface that provides a platform

for the assembly of complexes of the blood coagulation cascade (Bevers et al., 1983, Bevers and Williamson, 2010). Exposure of PS on the surface has also been shown to be critical for the recognition and clearance of apoptotic cells by macrophages (Fadok et al., 1992), and subsequent studies have shown that PS externalisation on apoptotic cells is mediated by scramblases (Verhoven et al., 1995, Bratton et al., 1997). These results suggest that a fine-tuned scramblase activity is vital for normal blood coagulation and recognition and clearance of apoptotic cells.

Activation of scramblases is regulated by cytoplasmic Ca^{2+} concentration, and alterations in Ca^{2+} concentration can disrupt lipid asymmetry, followed by an accelerated flippase activity within human erythrocytes (Henseleit et al., 1990). Consistently, Ca^{2+}-induced loss of lipid asymmetry can be regenerated by reactivation of flippases that can pump phospholipids such as PS back to the cytoplasmic leaflet upon removal of Ca^{2+} (Comfurius et al., 1990, Verhoven et al., 1992). Moreover, the duration of Ca^{2+}-triggered scramblases activity in erythrocytes has been shown to depend on Ca^{2+} levels (Williamson et al., 1992), and has also been observed in different cell types including lymphocytes (Williamson et al., 2001). These results suggest that asymmetric distribution of specific phospholipid can be established and maintained by energy-dependent transporters, and this asymmetry is disrupted by the activity of Ca^{2+}-induced scramblases.

The physiological importance of phospholipid scrambling has been first shown in a patient with Scott syndrome in which platelets are unable to form a procoagulant activity due to a reduced surface exposure of PS resulting in moderate to severe bleeding (Weiss et al., 1979, Rosing et al., 1985). In addition to platelets, erythrocytes and lymphocytes from these patients exhibited an impaired Ca^{2+}-induced PS exposure on the surface (Bevers et al., 1992). EBV-transformed B cells from patients with Scott syndrome also displayed a defective Ca^{2+}-induced lipid scrambling (Williamson et al., 2001). Intriguingly, when these cells were driven into apoptosis, they were able to expose PS normally on their surface, suggesting the existence of two different activation pathways determined by their dependency on intracellular Ca^{2+} (Williamson et al., 2001, Bevers and Williamson, 2010).

Despite that biochemical activity of scramblases has been known for a long time, their characterisation is incomplete. Several studies attempted to purify the putative scramblases in erythrocytes and platelets (Basse et al., 1996, Comfurius et al., 1996, Zhou et al., 1997, Wiedmer et al., 2000), but whether the isolated proteins exert scramblese activity is controversial. A potential phospholipid scrambles (TMEM16F) has recently been identified, and shown to play an important role in lipid scrambling in platelets during blood coagulation by forming a Ca^{2+}-activated cation channel (Suzuki et al., 2010, Yang et al., 2012). In keeping with these findings, mutations in *TMEM16F* were found in patients with Scott syndrome (Suzuki et al., 2010, Castoldi et al., 2011), suggesting a critical role for TMEM16F in lipid scrambling.

1.3.4 Role of lipid transporters in the immune system

As mentioned above, the plasma membrane is organised into specialized substructures, such as asymmetrical concentration of specific phospholipids between the exoplasmic and cytoplasmic leaflets in eukaryotic cells that facilitates many immunological signalling events (Lingwood and Simons, 2010, Leventis and Grinstein, 2010). Despite the importance of lipid transporters in the establishment and maintenance of the membrane lipid asymmetry, their direct or indirect involvement in the development and function of cells of the immune system remains to be uncovered. This is basically due to the paucity of *in vivo* genetic tools. Therefore, it is crucial to develop *in vivo* animal models to be able to study the role of the aminophospholipid transporters within the immune system.

1.4 Discovery of Novel Immune Regulatory Genes by *N*-Ethyl-*N*-nitrosourea (ENU) Mutagenesis

1.4.1 Developing model organisms

Despite an extensive research in cellular, molecular and clinical immunology in recent decades, there remain many important questions to be resolved. For instance, what factors control the development, homeostasis and function of immune cells? How are the important signalling pathways in the immune system initiated and terminated? How does organization of the eukaryotic plasma membrane into specialized substructures in lymphocytes facilitate important biological functions? How can immunological diseases such as autoimmunity, allergy and transplant rejection develop in human and is it possible to find potential cures and therapies for these devastating diseases?

Scientists have been striving to answer these questions by examining the biological function of genes in humans. However, human studies have been hampered by the difficulties in accessing the human biological samples and genetic heterogeneity in families. In order to overcome these limitations, scientists have made use of a variety of model genetic organisms (e.g. *Drosophila melanogaster*, *Caenorhabditis elegans*, *Danio rerio* and *Mus musculus*) to study mutations that affect the pathogenesis and biochemical pathways of immunological disorders that have clinical relevance in humans.

In particular the laboratory mouse, *Mus musculus*, has gained the most attention in biomedical research as comparative genomics revealed that nearly 90% of mouse genes are conserved in the human genome (Waterston et al., 2002), suggesting that most findings in mice possibly have a corresponding effect in humans. In addition to the genomic and physiological similarities between mice and humans, their availabilities, ease of handling, high reproductive rates in a relatively short time frame and low cost make the laboratory mice a suitable model organism for biomedical research. Therefore, the generation of mouse models through genetic engineering enables the scientists not only to identify genes involved in different biological processes, but also to develop novel therapies for human diseases based on a detailed pathophysiological understanding.

1.4.2 Genomic approaches for modifying the mouse genome to study immune system disorders

Two distinct approaches have been widely used to generate mouse models for identification and functional characterisation of novel genes in human diseases and immunity studies; gene-driven (reverse genetic) and phenotype-driven (forward genetic). The gene-driven approach mainly involves the use of "knock out" models in which a target gene is completely or partially deleted from the mouse genome followed by analysis of the resulting phenotype (Thomas and Capecchi, 1987). Recently, an alternate gene modification method has been described harnessing the adaptive immune system of bacteria and archaea termed clustered regularly interspaced short palindromic repeats (CRISPR)/CRISPR-associated systems (Cas) (Cong et al., 2013, Mali et al., 2013). This evolved immune system uses short RNA to directly target the foreign nucleic acids (Horvath and Barrangou, 2010), and this feature has been used for gene modifications in mammals (Cong et al., 2013, Mali et al., 2013). Employing the CRISPR/Cas9 system, it was shown that mice carrying mutations in multiple genes can be obtained through only one-step generation within weeks (Wang et al., 2013). Moreover, mice that contain both reporter and conditional mutations can also be created (Yang et al., 2013).

The generation of mouse models using gene-driven approach is particularly valuable when a single gene is known to be the primary cause of a disease so that an animal model can be generated to examine the function of the gene. However, gene-driven approaches sometimes result in homozygous lethality during embryonic development, because target genes might be crucial for the early embryogenesis, thereby preventing postnatal analysis of mice. Another limitation of the "knock out" technology is the examination of only one gene at a time.

On the other hand, phenotype-driven screens for example ENU mutagenesis have gained enormous attention in the last two decades as they provide a unique, unbiased approach to discover new genes of previously unknown functions in major physiological systems including the immune system, the reproductive system and behavioural studies (Nelms and Goodnow, 2001, Hoyne and Goodnow, 2006, Gondo, 2008, Yates et al., 2009, Jamsai and O'Bryan, 2010, Liu et al., 2011, Oliver and Davies, 2012, Moresco et al., 2013). A number of laboratories around the world have

been harnessing ENU mutagenesis to unveil new genes and characterise novel disease pathways. One of the major advantages of ENU mutagenesis over the "knock out" technology is the introduction of point mutations in the germline, which inactivates or alters the function of individual protein domains or splice products rather than making a null allele (Nelms and Goodnow, 2001). Moreover, ENU mutagenesis does not require prior knowledge or assumption about a particular gene; therefore the possibility of identifying a novel gene with important functions in physiological systems is relatively high.

A phenotype-driven ENU mutagenesis screen has also been used at the Immunogenomics Laboratory at the John Curtin School of Medical Research to identify novel genes with important roles in the immune system. For the last decade, using ENU mutagenesis our laboratory has discovered many genes with previously unknown function or they revealed novel functions of well known target genes including *Carma1*, *Ikaros*, *Roquin*, *Zap70*, *Hnrpll*, *Dock8*, *Zbtb7b*, *Sppl2a*, *Prkcb* and *Zfp318* (Jun et al., 2003, Papathanasiou et al., 2003, Vinuesa et al., 2005, Siggs et al., 2007, Wu et al., 2008, Randall et al., 2009, Enders et al., 2012, Bergmann et al., 2013, Teh et al., 2013, Enders et al., 2014). These genes have been shown to control many different immunological processes.

1.4.3 ENU mutagenesis screen

ENU, the alkylating agent, was found as a strong chemical mutagen in mice (Russell et al., 1979) that induces a high rate of random base-pair substitutions, typically A→T or A→G transversions in mouse spermatogonial stem cells (Hitotsumachi et al., 1985, Nelms and Goodnow, 2001, Moresco et al., 2013).

For the ENU screen at the John Curtin School of Medical Research, 90 mg ENU / kg mouse body weight is intraperitoneally administered to the male wild-type C57BL/6 mice. This induces one point mutation per 1.54 Mb in spermatogonial stem cells of Generation (G) 0 mice (Andrews et al., 2012, Bull et al., 2013). The ENU-treated G0 males are then bred with wild-type females to generate G1 offspring bearing various independently induced mutations (Figure 1.6). While a screen of dominant mutations with visible phenotypes or detectable changes can be carried out in the G1 founders, G3 mice derived from the interbreeding of G1 and G2 populations is used to screen

for recessive traits (Nelms and Goodnow, 2001). In the three-generation scheme to conduct genome wide recessive screens, a G1 male mouse is paired with an unrelated G1 female (Figure 1.6). Since each of these G1 parents carries approximately 45 protein variants, a total of ~45 protein variants are brought into each G2 mouse (Figure 1.6). By intercrossing the G2 progeny as brother-sister pairs, a total of ~ 4-5 recessive mutations are brought to homozygosity in each offspring and the remaining genetic mutations (40-41 variants) remain as heterozygous traits in G3 animals (Figure 1.6) (Nelms and Goodnow, 2001, Moresco et al., 2013).

The screening in our laboratory is based on the collection of the peripheral blood from the mutagenised G3 mice, followed by a multi-colour flow cytometry phenotypic screen to detect abnormalities in the development of different immune cell subsets including B cells, T cells and natural killer (NK) cells.

Once a phenotype of interest is uncovered in the G3 offspring it must be confirmed with more technical and biological replicates. Once the trait is established, the underlying mutation has to be identified. In the past, this involved a two generation mapping cross between an affected mouse and a mouse from a different inbred strain, followed by detection of a linked chromosomal region and PCR amplification and Sanger sequencing of all coding regions within the linked interval. However, recent advances in the technology of DNA sequencing have significantly reduced the costs and time required for sequencing and largely abolished the need for extensive mapping crosses (Mardis, 2011, Andrews et al., 2012, Andrews et al., 2013, Bull et al., 2013). Therefore, our laboratory currently uses whole-genome or whole-exome sequencing of individual or multiple affected mice to identify the probable causative variant (Andrews et al., 2012).

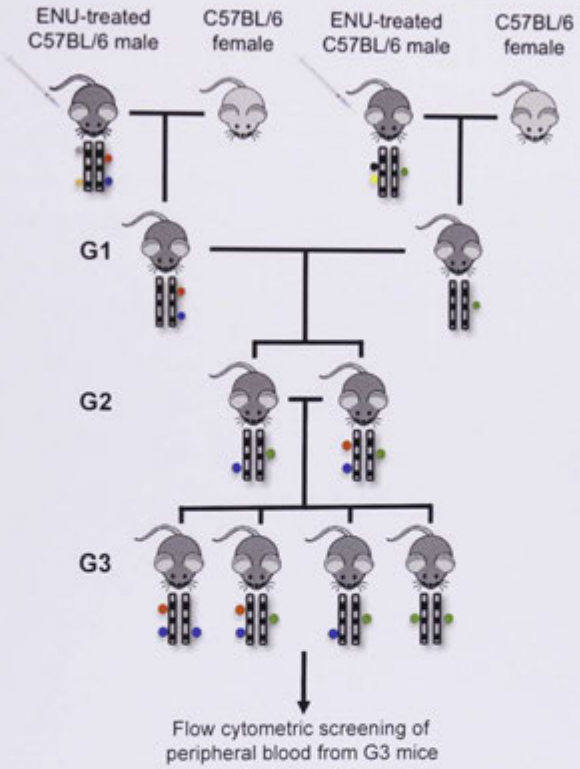

Figure 1.6 The three generation scheme for genome wide screening of recessive phenotypes induced by ENU mutagenesis

The ENU-treated G0 males are bred with females from the same inbred strain to generate G1 offspring bearing various independently induced mutations. In order to conduct genome wide recessive screen, a G1 male mouse is paired with an unrelated G1 female, followed by intercrossing the G2 progeny as brother-sister pairs. Lymphocytes in the peripheral blood of G3 offsprings are then collected and stained with a range of fluorescent antibodies and analysed on flow cytometry for specific phenotype (Modified from Andrews et al., 2012).

1.4.4 Discovery of *Ambrosius* mouse strain with a point mutation in *Atp11c*

1.4.4.1 ENU mutagenesis identifies mice with severe B cell deficiency

During the above mentioned flow cytometry screen, a G3 male mouse from the ENU11B6:221 strain was identified with severely reduced $B220^+$ B cell frequency in blood (Figure 1.7).

The strain was named "*Ambrosius*", and mutant male mice on the B6 background were out-crossed to the CBA mapping strain to facilitate mapping of the ENU-induced mutation. F1 hybrid mice were intercrossed to produce F2 progeny that could be used to map the mutant locus. Hemizygous mutant males or homozygous mutant females and their wild-type littermates were, however, maintained on a C57BL/6 background for further studies reported in this thesis.

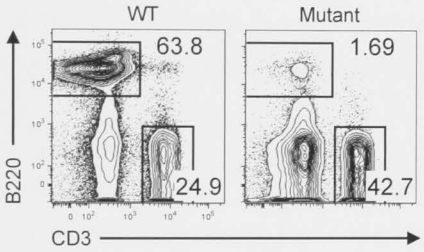

Figure 1.7 Identification of a strain with fewer B cells after ENU-induced mutagenesis
Flow cytometry of $B220^+$ B cells in the blood of wild-type (WT) and mutant mice. Numbers adjacent to outlined areas indicate percentage of $B220^+CD3^-$ B cells (top left) or $B220^-CD3^+$ T cells (bottom right).

1.4.4.2 Next-generation DNA sequencing reveals *Atp11c* mutation in *Ambrosius* mice

Linkage analysis in (B6xCBA)F_2 offspring mapped the mutation to an X-chromosomal region distal to marker rs13483763 at 54,012,901 base pairs (Build NCBI37.1). To capture and sequence Refseq annotated exons in this region of the X-chromosome, a custom Agilent Sureselect targeted DNA capture array was designed and hybridized with fragmented genomic DNA from an *Ambrosius* male mouse (Figure 1.8A). The enriched DNA was sequenced in paired-end mode for 100 cycles on a single lane of an Ilumina GAIIx sequencer. For the bait-targets, the median read depth from a single lane of data was 138 and 96% of the nucleotides were covered with a read depth of 5 or greater. A median read depth of 137 was obtained across all RefSeq exons in the mutation-containing region and a read depth of 5 or greater for approximately 93% of the nucleotides in these exons. Capture and sequencing was performed in replicate at two facilities, yielding highly reproducible results (Yabas et al., 2011).

Within the interval a single mutation was identified in both capture datasets and confirmed by Sanger sequencing, lying in a previously uncharacterised gene, *Atp11c*. This was a G to A substitution in the exon 27 splice donor sequence at the +1 position of intron 27 (Figure 1.8B, C). The normal +1 G nucleotide is invariant in 5′ splice donor sequences and its substitution would be predicted to abolish splicing, either yielding an in-frame UGA stop codon at the 3′ end of exon 27 (Figure 1.8C) or aberrant use of alternative splice donors. Further experiment confirmed skipping of exon 27 and the resulting deletion of 104 bp introduced a frame-shift after amino acid 1010, abolishing the C-terminal residues encoding the last two transmembrane domains and cytoplasmic tail of the ATP11C protein (Yabas et al., 2011).

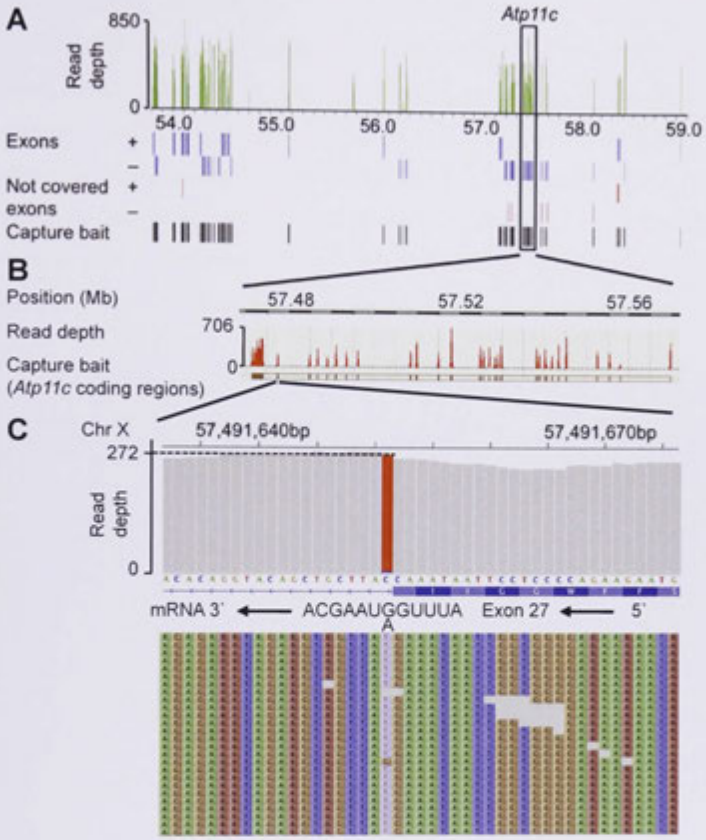

Figure 1.8 Identification of a splice-site mutation in *Atp11c* by next-generation DNA sequencing

(A) Read depth from a single GA2x sequencer lane across the tiled region between 54 and 59 Mb on the X-chromosome. Blue lines below denote all annotated exons on the + and – strand, red lines denote exons with a read depth of less than 5, and black lines denote capture baits used to enrich exons from genomic DNA. *Atp11c* gene is boxed and shown in greater magnification in **(B)** with read depth and chromosomal coordinates (NCBI build 37.1). **(C)** View of *Atp11c* exon 27 splice donor at single nucleotide resolution, read depth across these nucleotides, and sequence of first 30 reads. The C to T change, representing an intronic +1 G to A substitution in the *Atp11c* sense strand and RNA transcript was the only identified discrepancy between ambrosius DNA and the C57BL/6J mouse reference sequence in two independent capture and sequencing runs, and was confirmed by Sanger sequencing.

As mentioned earlier, ATP11C is an integral membrane protein that consists of 10 transmembrane segments, and a member of the P4-type ATPase family, which selectively catalyses the flipping of PS and to lesser extent PE from the exoplasmic to the cytoplasmic leaflet of the plasma membrane (Sebastian et al., 2012, van der Mark et al., 2013). Microarray profiling of *Atp11c* mRNA shows that it is equally expressed in B and T lymphocytes as well as other immune cells (Figure 1.9A, B), and most other tissues with highest expression in liver (Figure 1.10) (Heng and Painter, 2008, Wu et al., 2009), suggesting a possible role for ATP11C in the development and/or function of the immune system as well as other biological systems, which is subject to examination within this thesis.

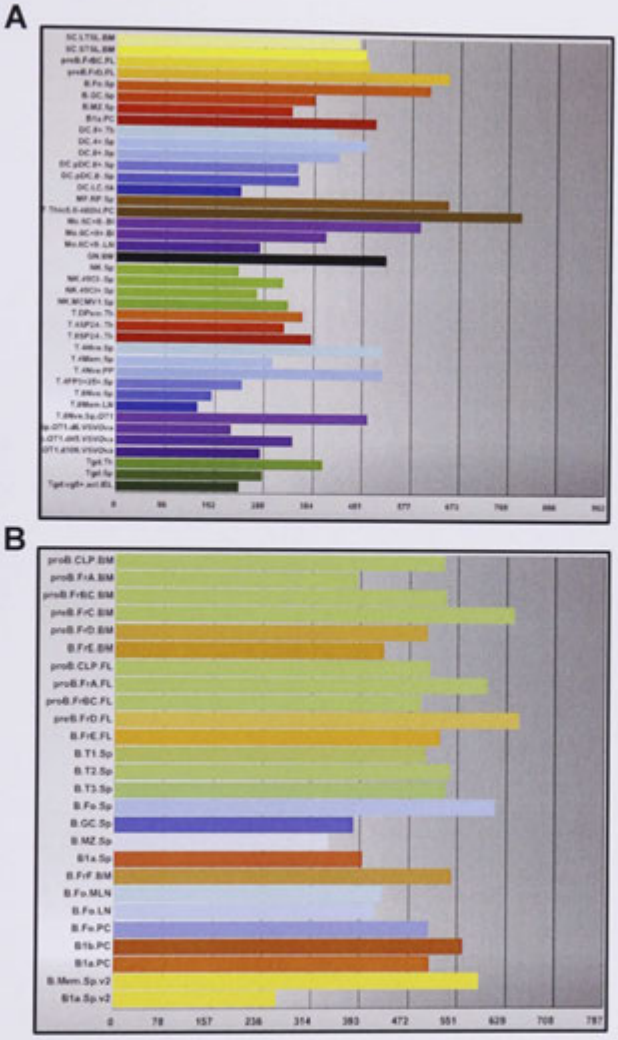

Figure 1.9 The expression profile of *Atp11c* in immune cell subsets

(A) The expression profile of *Atp11c* in the major immune cell groups in the bone marrow, thymus and periphery. **(B)** A detailed graph of *Atp11c* expression in B cell populations in the bone marrow and periphery. Data from the Immunological genome project (Heng and Painter, 2008), and methods of isolation and expression measurement are described on website (www.immgen.org).

Figure 1.10 The expression profile of *Atp11c* in different tissues
BioGPS microarray data comparing *Atp11c* mRNA abundance in the indicated mouse tissues, using the indicated Affymetrix probeset (For details, see Wu et al., 2009).

1.5 Aims of the thesis

In this thesis, I describe two novel ENU variant mouse strains called *Ambrosius* and *18NIH30*. Both strains were identified through a peripheral blood lymphocyte screen using flow cytometry, and carry mutations in the gene encoding the aminophospholipid translocase ATP11C, which is thought to play a role in the establishment and maintenance of lipid asymmetry in biological membranes. The affected mice had significantly reduced numbers of B cells in the bone marrow and periphery due to a developmental block in the early B cell development. In addition, ATP11C-deficient mice were anaemic.

Both mutant strains provide a unique resource and have enabled me to address the fundamentally important question of the role of the putative lipid transporter ATP11C within the immune system as well as erythrocyte biology. The studies presented in this thesis provide new insights into the control of B cell development by the distribution and turnover of phospholipids in membranes through the putative phospholipid transporter ATP11C. Moreover, the findings of this thesis also suggest ATP11C as a candidate for flippase activity in erythrocytes.

By analysing the particular cellular phenotypes and molecular mechanisms impaired in mutant mice, this study aims to:

- Characterise the immunological phenotype of *Ambrosius* and *18NIH30* mice, and attempt to identify the molecular mechanisms underlying the cellular phenotype observed,
- Investigate if the ATP11C^{amb} mutation has any effect on the generation of immune responses,
- Determine if ATP11C functions as a flippase in cells of the immune system,
- Investigate if ATP11C has any impact on the development and survival of erythrocytes.

CHAPTER 2: Materials and Methods

2.1 Mice

Mouse strains used in this study are described below:

C57BL/6J (B6): Inbred mouse strain was originally obtained from Jackson Laboratories, USA.

C57BL/6-SJL.Ptpc (CD45.1): B6 strain congenic for CD45.1 (Ly5a).

***Atp11c*$^{amb/0}$ (*Ambrosius*) and *Atp11c*$^{18NIH30/0}$ (*18NIH30*):** These mouse strains with a point mutation in *Atp11c* were generated through ENU mutagenesis. The strains were largely maintained either by breeding heterozygous females with wild-type littermates or with wild-type C57BL/6J. For mapping purposes heterozygous females were crossed to the CBA/H strain.

***Rag1*$^{-/-}$:** This mouse strain lacks mature B and T cells due to their inability to activate V(D)J recombination (Mombaerts et al., 1992).

***Vav-Bcl2*-Tg:** This mouse strain has a transgenic expression of the gene encoding the prosurvival protein BCL-2 driven by the promoter of the gene encoding the adaptor VAV (Ogilvy et al., 1999).

***H2Ea-Il7*-Tg:** This mouse strain has a transgenic expression of *Il7* by the Eα promoter of the gene encoding mouse MHC Class II (*H2Ea-Il7*) (Mertsching et al., 1996), and was a kind gift of Professor Jonathan Sprent (Garvan Institute, Sydney).

MD4-Tg: This mouse strain carries rearranged heavy and light chain transgenes encoding the hen egg lysozyme (HEL)-specific monoclonal antibody (Goodnow et al., 1988).

SW$_{HEL}$: This mouse strain carries a heavy-chain VDJ knock-in gene combined with a HEL-specific κ-light chain transgene (Phan et al., 2003), and was a kind gift of Professor Robert Brink (Garvan Institute, Sydney).

***Cd79a*$^{-/-}$:** This mouse strain has a point mutation in *Cd79a* that leads to a premature stop codon in exon 2 (Lina Tze and Anselm Enders, unpublished data).

Mice were genotyped by PCR amplification of DNA isolated from mouse-ear punches. In some experiments, the phenotype of mice was confirmed by analysing lymphocytes in the peripheral blood by flow cytometry.

Except when noted specifically all mice used for this study were between 8-12 weeks old. All experimental mice were maintained on a C57BL/6 background and housed in specific pathogen free conditions at the Australian Phenomics Facility and all animal procedures were approved by the Australian National University Animal Ethics and Experimentation Committee.

2.2 Buffers, solutions and media

Buffers, solutions and media were sourced and/or prepared as described in Table 2.1.

2.3 Flow cytometry analysis

2.3.1 Cell preparation

2.3.1.1 Preparation of lymphoid tissues

Bone marrow, spleen, lymph node and thymus were collected from sacrificed mice into 3 ml of ice-cold cell culture medium or flow cytometry buffer. Bone marrow cells were extracted by pressurised flow of sterile flow cytometry buffer through dissected femurs and tibias. Single cell suspensions from spleen, lymph node and thymus were prepared by passing the tissues through 70 µm nylon mesh filters (BD Biosciences). Red blood cells (RBC) in the spleen samples were removed by incubating splenocytes with 3 ml of RBC lysis buffer in 15 ml centrifuge tubes for 1-2 min at room temperature. Samples were then centrifuged for 4 min at 1340 rpm at 8 °C, followed by discarding the supernatant. The pellets were washed once in 10-13 ml of ice-cold flow cytometry buffer followed by centrifugation and resuspension in 3 ml of flow cytometry buffer.

White blood cells were counted using the ViCELL cell counter (Beckham Coulter Inc.). After cell counting of cells from the bone marrow, spleen, lymph node and thymus, equal number of cells was transferred into the 96-well round-bottom plates at a density of 2 - 2.5x10^6 cells/well and stained with antibodies as detailed below for flow cytometric analysis.

2.3.1.2 Preparation of blood samples

For preparation of peripheral blood samples, 100-150 µl of blood was collected by retro-orbital bleeding into cluster tubes containing 20 µl of 1000 U/ml heparin by the animal technicians at the Australian Phenomics Facility. 160 µl RBC lysis buffer was added to 40 µl of the blood sample in the 96-well round-bottom plates, and was gently mixed and incubated for 3-5 min at room temperature. Samples were centrifuged for 4 min at 1340 rpm at 8 °C, followed by the second lysis with 160 µl RBC lysis buffer, incubation 3-5 min at room temperature and centrifugation for 4 min at 1340 rpm at 8 °C. The pellets were then washed twice in 150-200 µl of ice-cold flow cytometry buffer and stained with antibodies as detailed below for flow cytometric analysis.

For erythrocyte analysis shown in Chapter 9, red blood cell lysis in the bone marrow, spleen and blood samples was not performed.

Table 2.1 Buffers, solutions and media

Phosphate Buffer Saline (PBS) and ddH_20	Obtained from the John Curtin School of Medical Research Media Facility, the Australian National University or purchased (Life Technologies).
Culture Medium	RPMI 1640 (Life Technologies) supplemented with 10 mM HEPES (Sigma-Aldrich), 0.1 mM Non-Essential Amino Acid solution (Life Technologies), 1 mM Sodium Pyruvate (Sigma-Aldrich), 55 µM 2-Merchapthoethanol (Life Technologies), 2% L-glutamate and penicillin/streptomycin (Life Technologies) and 10% heat-inactivated Foetal Calf Serum (FCS) (Life Technologies).
Flow Cytometry Buffer	2% Bovine Serum (BS) (Thermo Fisher Scientific Australia Pty. Ltd.) and 0.1% sodium azide (Australian Chemical Reagents) in PBS.
Red Blood Cell (RBC) Lysis Buffer (10X)	8.99 g ammonium chloride (Sigma-Aldrich), 1 g potassium bicarbonate (Sigma-Aldrich), 37 mg sodium EDTA in 100 mL ddH_20. Buffer was diluted with ddH_20 to 1x prior to use and adjusted to pH 7.3 with hydrochloric acid solution (Sigma-Aldrich).
Conjugation Buffer	0.35 M Mannitol (Univar) and 0.01 M sodium chloride (Chem Supply) in ddH_2O.
ELISA Coating Buffer	0.05 M Carbonate from Na_2CO_3 and $NaHCO_3$ diluted in ddH_20 (pH 9.6).
ELISA Blocking Buffer	1% BS in PBS.
ELISA Dilution Buffer	0.05% Tween 20 (Sigma-Aldrich) and 1% BS in PBS.
ELISA Washing Buffer	0.05% Tween 20 in PBS.
ELISA Developing Buffer	100 mM glycine (BioRad), 0.1 mM of zinc chloride and 1 M of Magnesium chloride (Sigma-Aldrich) in ddH_20, adjusted to pH 10.4 with sodium hydroxide solution.
ELISA Substrate Solution	Two pNPP tablets (Sigma-Aldrich) dissolved in 10 ml of alkaline phosphatase buffer.

2.3.2 Surface antibody staining

Cell suspensions were prepared, counted and equal number of cells aliquoted into the 96-well round-bottom plates as described above. Cells were then incubated with a purified antibody against Fcγ II and III receptors (CD16/32 - BD), that are expressed by B cells, monocyte/macrophages, NK cells and neutrophils in order to block nonspecific binding together with biotinylated antibodies, if applicable. After 30 min incubation at 4 °C in the dark, cells were washed with flow cytometry buffer and centrifuged for 4 min at 1340 rpm at 8 °C. Cells were then incubated with a primary antibody cocktail containing an appropriate combination of the antibodies as well as streptavidin that binds to biotinylated antibody (Table 2.2) each diluted to its optimal concentration in flow cytometry buffer and incubated for 30 min at 4 °C in the dark. Samples were washed with flow cytometry buffer and resuspended in flow cytometry buffer and kept at 4 °C until use.

For erythrocyte analysis shown in Chapter 9, cells from the bone marrow, spleen and blood samples were washed once with flow cytometry buffer followed by centrifugation for 4 min at 1340 rpm at 4 °C. Cells were then stained with a primary antibody cocktail as detailed above and kept at 4 °C until use.

2.3.3 Annexin-V staining

For Annexin-V staining, once cell surface staining was performed cells were washed once with flow cytometry buffer and once with Annexin-V binding buffer (Biolegend). Annexin-V and 7-Aminoactinomycin D (7-AAD) staining were performed in Annexin-V binding buffer at room temperature for 15 min and washed and resuspended in Annexin-V binding buffer and kept at 4 °C until use.

2.3.4 Intracellular staining

Intracellular IgM staining was performed using the Foxp3/Transcription Factor Staining Buffer set from eBioscience. Cell surface staining was performed as detailed above, and cells were washed once with flow cytometry buffer followed by resuspension of the pelleted cells in 50 µl of Fix/Perm solution for 30 min. After one wash with 1x Permeabilisation/wash buffer solution, cells were incubated with appropriately conjugated intracellular antibodies for 30 min. After a final wash step

once with the permeabilisation/wash buffer and once with flow cytometry buffer, cells were resuspended in flow cytometry buffer and kept at 4 °C until use.

For DNA content analysis, bone marrow cells were stained with surface markers and fixed using the eBioscience kit as described above. Cells were then intracellularly stained with 7-AAD.

2.3.5 Phospho-STAT5 staining

Bone marrow cells were prepared as detailed above and were cultured in the absence or presence of various concentrations of IL-7 for various time points. At the end of the culture period, the cells were harvested and stained with cocktail containing antibodies as detailed above. The samples were then fixed by adding paraformaldehyde (final concentration 2-4%) and incubated for 10 min at room temperature. Samples were then washed with PBS followed by centrifugation for 5 min at 1500 rpm at 25 °C and the supernatant was discarded. 1 ml cool methanol was added and samples were incubated at - 80 °C over night. On the next day, cells were incubated an antibody specific for phospho-STAT5 and incubated for 30 minutes at room temperature in the dark. Samples were washed with flow cytometry buffer followed by centrifugation and the supernatant was discarded. Cells were then resuspended in flow cytometry buffer and kept at 4 °C until use.

Flow cytometry analysis was performed using a LSR II or LSR Fortessa flow cytometry (BD Biosciences).

2.3.6 Intracellular Ca^{2+} mobilisation assay

Pro-B cells were sorted from the bone marrow and were loaded with the calcium-sensor dye Indo-1 (Invitrogen) at a final concentration of 5 µM in 1 ml of tissue culture medium. After incubation for 30 min at 37 °C, the cells were washed twice and resuspended with tissue culture medium. Samples were kept on ice until further analysis. The acquisition of data was initiated 30 s before the addition of antibody against CD79b (Clone HM79b, BD) at a final concentration of 10 µg/ml. Ionomycin stimulation was used as a positive control to measure a maximum flux. Data were collected on LSR Fortessa flow cytometry and analysed with FlowJo software.

2.3.7 Cell sorting

2.3.7.1 Flow cytometry sorting

Cell suspensions were prepared by staining single cell suspensions from the bone marrow of mice with appropriate conjugated antibodies in sterile flow cytometry buffer. Pro-B cells were sorted on an Aria I or II flow cytometry (BD Biosciences) and collected in sterile tissue culture medium for culturing.

2.3.7.2 Magnetic-activated cell sorting (MACS)

Pro-B cells from the bone marrow of *Rag1*$^{-/-}$ and *Atp11c*$^{amb.0}$ *Rag1*$^{-/-}$ double deficient mice were Macs sorted according to manufacturer's specifications using CD19 microBeads (Miltenyi Biotec,). Briefly, cell suspensions were prepared from the bone marrow of mice followed by red blood cell lysis and determination of cell numbers. Cells were then incubated with CD19 microBeads for 15 min at 4 °C in the dark followed by centrifugation and separation using Macs separator column. Positively selected pro-B cells were then washed and used for further analysis.

Table 2.2 List of antibodies used in flow cytometry analysis

Antibody	Clone	Conjugation	Vendor
Annexin-V		Pacific Blue	Biolegend
BP-1	6C3	PE	Biolegend
CD3	145-2C11	AF 700	eBioscience
CD4	RM4-5	AF 700	Biolegend
CD4	GK1.5	Biotin	BD
CD5	53-7.3	APC	eBioscience
CD5	53-7.3	Biotin	BD
CD8a	53-6.7	Biotin	BD
CD8a	53-6.7	PE Cy7	Biolegend
CD11b	M1/70	APC AF 750	eBioscience
CD11b	M1/70	Biotin	BD
CD11c	HL3	Biotin	BD
CD19	eBio1D3	AF 700	eBioscience
CD19	1D3	APC	BD
CD19	eBio1D3	Biotin	eBioscience
CD19	1D3	PE	BD
CD21/35	7G6	FITC	BD
CD21/35	7G6	PE	BD
CD23	B3B4	Pacific Blue	Biolegend
CD23	B3B4	PE	BD
CD23	B3B4	PE Cy7	eBioscience
CD24	91	Biotin	SouthernBiotech
CD24	M1/69	Pacific Blue	Biolegend
CD25	PC61	APC	BD
CD25	7D4	Biotin	BD
CD25	7D4	FITC	BD
CD43	S7	FITC	BD
CD43	S7	PE	BD
CD44	IM7	APC	BD
CD44	IM7	Pacific Blue	Biolegend
CD45	30-F11	FITC	BD
CD45R/B220	RA3-6B2	APC	BD
CD45R/B220	RA3-6B2	A700	BD
CD45R/B220	RA3-6B2	Biotin	BD
CD45R/B220	RA3-6B2	FITC	BD
CD45R/B220	RA3-6B2	PerCP	BD
CD45.1	A20	AF 700	Biolegend
CD45.1	A20	FITC	BD
CD45.1	A20	PE	BD
CD45.2	104	APC	eBioscience
CD45.2	104	Pacific Blue	Biolegend

CD45.2	104	PerCP Cy5.5	BD
CD71	C2	Biotin	BD
CD71	C2	PE	BD
CD93	AA4.1	APC	BD
CD93	AA4.1	Biotin	eBioscience
CD95	Jo2	PE Cy7	BD
CD117 (c-Kit)	ACK2	APC AF 780	eBioscience
CD127	A7R34	PE	eBioscience
CXCR5	2G8	Biotin	BD
Flt3	A2F10	PE Cy5	eBioscience
GL-7	GL7	FITC	BD
Gr-1	RB6-8C5	APC Cy7	BD
Gr-1	RB6-8C5	Biotin	BD
IgD	11-26c	Biotin	eBioscience
IgD	11-26c.2a	PerCP Cy5.5	Biolegend
IgD	11-26c	FITC	eBioscience
IgM	II/41	APC	BD
IgM	II/41	Biotin	BD
IgM	II/41	PE Cy7	eBioscience
NK1.1	PK136	APC	BD
NK1.1	PK136	Biotin	BD
PD-1	J43	PE	eBioscience
pSTAT5	pY694	PE	BD
Sca-1	D7	Pacific Blue	Biolegend
TCRβ	H57-597	APC Cy7	Biolegend
TCRβ	H57-597	Biotin	BD
TCRγδ	GL3	Biotin	BD
Ter119	TER-119	Biotin	BD
Ter119	TER-119	FITC	BD
Ter119	TER-119	PE Cy7	BD
7-AAD		PerCP	Invitrogen

Table 2.3 List of secondary antibodies used in flow cytometry analysis

Secondary antibody	Vendor
APC Streptavidin	BD
Brilliant Violet 605 Streptavidin	Biolegend
PE Cy7 Streptavidin	eBioscience
Q-dot 605 Streptavidin	Invitrogen

2.4 Generation of bone marrow chimeras

2.4.1 Mixed bone marrow chimera

Bone marrow cells with different allotypes of the cell surface marker CD45 were harvested from mutant CD45.2, wild-type CD45.2 and wild-type CD45.1 animals as detailed above. Extracted cells were counted, and mixed at a 1:1 ratio from either wild-type CD45.2 or mutant CD45.2 with wild-type CD45.1. *Rag1*$^{-/-}$ recipient mice were irradiated with a single dose of 450 rads before being intravenously injected with 200 µl of 2-3 x 10^6 bone marrow donor cells for each recipient mouse. In some experiments, bone marrow cells from CD45.1 mutant animals were mixed with CD45.2 bone marrow cells from *Rag1*$^{-/-}$ animals, and injected into *Rag1*$^{-/-}$ recipients. After reconstitution of the haematopoietic system lymphoid tissues were collected from the recipient mice and single cell suspensions were prepared as detailed above for flow cytometry analysis.

2.4.2 100% bone marrow chimera

Bone marrow cells from CD45.1 mutant and CD45.1 wild-type animals were extracted as detailed above. CD45.2 wild-type and CD45.2 mutant recipient mice were irradiated with double doses of 450 rads before being intravenously injected with 200 µl of 2-3 x 10^6 bone marrow donor cells for each recipient mouse. After reconstitution of the haematopoietic system lymphoid tissues were collected from the recipient mice and single cell suspensions were prepared as detailed below for flow cytometry analysis.

All chimeric recipients received neomycin and polymixin B prophylactic antibiotics in the drinking water for 4 weeks after reconstitution.

2.5 Carboxyfluorescein succinimidyl ester (CFSE) labelling

Macs-sorted pro-B cells were labelled with the intracellular and membrane permeable dye CFSE (Molecular Probes) according to the method described (Quah and Parish, 2012). Briefly, purified cells were resuspended to 1x10^8/ml in 20 °C RPMI 1640 medium supplemented with 10% FCS and a final concentration of 10 µM of CFSE added to 1 ml aliquots of lymphocytes with immediate vortexing. Cells were incubated at 20 °C for 5 min, then washed 3 times with RPMI 1640

supplemented with 10% FCS.

2.6 Cell culture

Flow purified pro-B cells from control and mutant mice were counted by trypan blue exclusion. 5 - 6 x 10^4 pro-B cells were seeded per well onto 96-well flat-bottom plates in sterile tissue culture medium and incubated at 37 °C and 5% CO_2 for up to 7 days in the presence of 25 ng/ml of IL-7 (R&D Systems). At the end of the cultivation period, cells were counted by trypan blue exclusion and stained with appropriate antibodies to cell surface markers for flow cytometry analysis.

In some experiments, Macs purified $CD19^+$ pro-B cells from *Rag1*$^{-/-}$ and *Atp11c*^{ambi0} *Rag1*$^{-/-}$ double deficient mice were labelled with the membrane permeable dye CFSE as described above. 10^5 pro-B cells were then seeded per well onto 96-well flat-bottom plates in sterile tissue culture medium and incubated at 37 °C and 5% CO_2 for 4 days in the absence or presence of various concentrations of IL-7. At the end of the cultivation period, cells were stained with appropriate antibodies to cell surface markers for flow cytometry analysis and the percentage of proliferating cells in response to IL-7 was determined by CFSE dilution.

2.7 Immunofluorescence microscopy

Spleen cryo-sections (10µm) were fixed in acetone and blocked with 5% mouse serum, followed by detection of B cell follicles and T cell zones with anti-mouse B220-PE (RA3-6B2, BD) and anti-mouse CD3-FITC (145-2C11, BD) antibodies. Slides were analysed on an Olympus IX 71 fluorescence microscope.

2.8 Functional assessment of B cells

2.8.1 Assessment of antibody responses to T-dependent and -independent antigens

2.8.1.1 Immunisations

Primary immunisation was done by intraperitoneal injection of 300 µl (150 µl to each side of the abdomen) PBS containing 50 µg alum-precipitated chicken γ

globulin (alum-CGG) (Biosearch) and 1 x 10^8 heat- and formalin-inactivated *Bordetella pertussis* bacteria (Lee Laboratories). Mice were bled at 2 and 4 weeks post primary immunisation. Booster immunisations were 50 µg alum-precipitated CGG coupled to the hapten azo-benzene-arsonate (ABA) and 25 µg nitrophenyl-Ficoll (Biosearch) in 300 µl PBS. Mice were bled 6 days post-secondary immunisation. Blood samples were diluted at a 1:5 ratio in PBS. Followed by centrifugation for 4 min at 1340 rpm at 8 °C. Plasma samples were collected, and stored at -20 °C for further analysis of the quantification of the antibody content by enzyme-linked immunosorbent assay (ELISA).

2.8.1.2 ELISA

High protein-binding 96-well flat-bottom plates were coated with 100 µl/well of antigens of interest (diluted in Coating Buffer) and incubated overnight at 4 °C. Next day, unbound antigen was removed by washing plates three times with washing buffer. Blocking buffer was then added (150 µl/well) to prevent non-specific binding, followed by a 1 hour incubation at 37 °C. Blocking buffer was removed and plates were washed three times with washing buffer. Thawed and appropriately diluted plasma samples (diluted in dilution buffer) were added (100 µl/well) to each well, followed by a 1-hour incubation at 37 °C. After removal of solution and repeat of washing step, plates were further incubated with 100 µl of alkaline phosphatase conjugated secondary antibodies for 1 hour at 37 °C, followed by a washing step. 150 µl of substrate solution was then added to each well and incubated at 37 °C until sufficient yellow colour develops. Plates were read on a Plate Reader (ThermoMax; Molecular Devices) and the absorbance of each well was measured at 405nm and 650nm. The background absorbance was determined by measuring at 650nm, and was subtracted from all data points.

2.8.2 Assessment of HEL-specific GC formation

2.8.2.1 Conjugation of HEL-SRBCs

Sterile Sheep Red Blood Cells (SRBCs) were washed three times with 50 ml sterile PBS or until the supernatant was transparent. SRBCs were then washed with 20 ml of conjugation buffer followed by incubation with conjugation buffer with HEL (HEL-SRBC) or without (Mock-SRBC) for 10 minutes on ice on a rocking platform. In order to cross-link HEL to SRBCs 1-Ethyl-3-(3-dimethylaminopropyl)

carbodiimide (Sigma) was added to the samples and continued rocking for 30 minutes. SRBCs were then washed three times with PBS, and the number of cells was determined.

Successful conjugation was confirmed by staining cells with APC-conjugated HyHel9 antibody (a kind gift of Professor Robert Brink), followed by flow cytometry analysis.

2.8.2.2 Adoptive transfer experiments

To test HEL-specific GC formation, Ambrosius mice were crossed to CD45.1 allotyped SW_{HEL} transgenic mice, and an adoptive transfer system was used. Splenocytes containing 10^5 congenically CD45.1-labelled HEL-binding B cells from donor *Atp11c*$^{+/0}$ SW_{HEL} transgenic and *Atp11c*$^{amb/0}$ SW_{HEL} transgenic mice were intravenously injected into non-irradiated CD45.2 wild-type recipient mice in combination with $2x10^8$ Mock-conjugated (control) or HEL-conjugated SRBCs. The percentage and total number of wild-type and mutant derived HEL-specific GC B cells were determined by flow cytometry analysis.

2.8.3 Assessment of T_{FH} formation

Mice were intravenously injected with $2x10^8$ SRBCs and the frequency and absolute number of T_{FH} cells were determined by flow cytometry analysis.

2.9 Phospholipid translocase (Flippase) activity assay

Flippase activity assays were performed with mutant and wild-type bone marrow, spleen and thymic cells using the fluorescent analogues of PS, 1-palmitoyl-2-{12-[(7-nitro-2-1,3-benzoxadiazol-4yl)amino]dodecanoyl}-*sn*-glycero-3-phosphoserine (ammonium salt) (C_{12}-NBD-PS) and 1-palmitoyl-2-{6-[(7-nitro-2-1,3-benzoxadiazol-4-yl)amino]hexanoyl}-*sn*-glycero-3-phosphoserine (ammonium salt) (C_6-NBD-PS) (Avanti Polar Lipids, Inc.). Equal numbers of CD45.1$^+$ marked wild-type cells and CD45.2$^+$ marked mutant cells were mixed and washed with pH 6.0 Hanks' Balanced Salt Solution (HBBS) (Life Technologies) supplemented with 5.5 mM D-glucose and 20 mM HEPES and pre-warmed to 15 °C (and 37 °C in some experiments). Cells were then incubated with 5 µM NBD-labelled PS in 200 µl of

the same solution for the indicated time points at 15 °C (and 37 °C in some experiments). To stop the flipping of NBD-PS and remove the unbound NBD-PS from the cell surface, cells were immediately placed on ice and incubated with HBBS supplemented with 5.5 mM D-glucose, 20 mM HEPES, 1% fatty acid free bovine serum albumin (BSA) (Sigma-Aldrich) for 5 min. After 5 min cells were centrifuged for 4 min at 1500 rpm at 8 °C and washed twice in HBBS supplemented with 5.5 mM D-glucose and 20 mM HEPES. Cells were then transferred to a 96-well plate and stained with fluorescently labelled antibodies as described before and analysed on a LSR II or LSR Fortessa flow cytometry (BD Biosciences).

The flippase activity assay in erythrocytes was performed using the same method except that samples from mutant and control animals were kept in the different tubes, as red blood cells do not express CD45.

The percentage of C_{12}-NBD-PS or C_6-NBD-PS uptake in ATP11C-deficient cells relative to wild-type cells was calculated by the formula [geometric MFI of wild-type or Amb NBD-PS(T_8) / geometric MFI of wild-type NBD-PS(T_{30})] × 100.

2.10 Microarray analysis

For the microarray analysis, $5x10^4$-$1x10^5$ 7AAD$^-$B220$^+$IgD$^-$IgM$^-$CD24^{int}CD43$^+$BP-1$^-$ pro-B cells were sorted from *Atp11c*$^{+/0}$ and *Atp11c*$^{amb/0}$ animals. Sorted cell pellets were snap-frozen and shipped on dry ice to the Miltenyi Biotec Genomic Service Department, Germany for Agilent Whole Genome Microarray Service.

2.11 Analysis of haematological parameters

100 µl of blood was mixed with 100 µl of flow cytometry buffer and run on an ADVIA 2120 Haematology System (Siemens Healthcare Diagnostics) for the analysis of blood parameters.

2.12 Clinical chemistry

Mutant mice and their control littermates were first culled and then bled by cardiac puncture and blood samples were rested for 0,5 – 1 h at room temperature. Samples

were then centrifuged for 10 min at 4000 rpm, and sera were collected and frozen at -20 °C for further analysis. Determination of serum concentrations of alanine aminotransferase, aspartate aminotransferase, bilirubin and iron parameters were assayed by automated procedures in the Department of Pathology, The Canberra Hospital.

2.13 Tumour harvest and histology

Liver tumours, and surrounding liver tissue were removed and fixed in 10% neutral buffered formalin. Liver sections (4 µm) were cut from paraffin-embedded blocks and stained with haematoxylin and eosin (H&E) for histological examination.

2.14 Determination of erythrocyte lifespan using *in vivo* CFSE-labelling and lifespan modelling

In vivo life span measurements using CFSE, in conjunction with mathematical modelling were performed based on the method described (Coupland et al., 2010). Mutant mice and their control littermates were intravenously injected with 50 µl of 10 mM CFSE in dimethyl sulfoxide mixed with 100µl PBS. Erythrocyte analysis was performed at various time points by taking 5 µl blood from the tail tip and mixing it with 45 µl acid citrate dextrose. Blood loss was controlled via cauterisation and lidocaine gel was used on the tail tip to minimize pain. Within 30 min of sample collection, 10 µl blood/acid citrate dextrose mixture was added to 990 µl PBS, and the samples were then analysed by flow cytometry. Erythrocytes were identified using their characteristic log forward and side scatter parameters. To determine the extent of CFSE labelling of erythrocytes at each time point, fluorescence was measured on the FITC channel, with the percentage of CFSE-positive erythrocytes being followed over time to determine lifespan.

Erythrocyte lifespans were obtained by curve fitting using the lognormal model as previously described (Coupland et al., 2010). Matlab's nonlinear least-squares estimator lsqnonlin was used to perform the data fitting.

2.15 Cation measurement in erythrocytes

Intra- and extracellular Na^+ and K^+ levels were determined using Ultra High Pressure Liquid Chromatography (UHPLC; Dionex) linked to a Charged Aerosol Detector (CAD; Dionex) based on the method described (Winterberg et al., 2012). 10 µl-heparinised blood was separated by centrifugation into erythrocyte and plasma fractions. The erythrocytes were washed (x1) with a 250 mM $MgSO_4$ solution to replace extracellular Na^+ and K^+. The resulting cell pellet and 1 µl of the plasma were added to 200 and 100 µl, respectively, of 40/60 v/v 20 mM ammonium sulphate pH 5/acetonitrile, to precipitate proteins. The samples were centrifuged and 10 µl aliquots of the resulting supernatant solutions were subjected to the HPLC analysis.

2.16 Scanning electron microscopy (SEM) analysis of erythrocytes

Cells attached to coverslips were fixed with 2% v/v glutaraldehyde in 0.1 M sodium cacodylate overnight at 4 °C and post-fixed with 1% w/v osmium tetroxide for 1.5 hours at room temperature. The samples were dehydrated using a graded ethanol series, then critical point dried, mounted on aluminium stubs, and sputter-coated with gold prior to imaging. Images were taken using a Zeiss Ultraplus FESEM.

2.17 Osmotic fragility test

Peripheral blood from wild-type and ATP11C-deficient mice was diluted to an approximate haematocrit of 10% with PBS followed by a further 1 in 10 dilution in NaCl solutions of varying osmolarity (0.1%-0.8% w/v NaCl in H_2O). After incubation for 30 min at room temperature, samples were centrifuged and the absorbance of the supernatant solutions measured at 540 nm (A_{540}) using a microplate reader (ThermoMax; Molecular Devices). Percentage haemolysis of the cells in each solution was calculated based on the A_{540} value relative to that obtained for cells suspended (and thereby lysed) in H_2O.

2.18 Statistical analysis

For comparison of only two groups, the two-tailed student *t* test was used. When multiple experimental groups were being compared, One-Way Analysis of Variance

(ANOVA), followed by pair-wise comparison with a Bonferroni port-test were used. For all statistical analysis, differences were taken to be significant when $P < 0.05$. All statistical analysis was performed using GraphPad Prism 5 (GraphPad Software).

CHAPTER 3: Initial characterisation of strains with fewer B-lymphocytes after ENU-induced mutagenesis: developmental arrest at the pro-B cell stage of B cell development

Contents of Figure 3.1A, 3.2, 3.3, 3.4B-D, 3.6, 3.7, and 3.8A appeared in:

Mehmet Yabas, Charis E. Teh, Sandra Frankenreiter, Dennis Lal, Carla M. Roots, Belinda Whittle, Daniel T. Andrews, Yafei Zhang, Narci C. Teoh, Jonathan Sprent, Lina E. Tze, Edyta M. Kucharska, Jennifer Kofler, Geoffrey C. Farell, Stefan Bröer, Christopher C. Goodnow and Anselm Enders (2011). "ATP11C is critical for the internalization of phosphatidylserine and differentiation B lymphocytes". *Nature Immunology*, 12(5):441-449.

Contributions from others:

- Dr. Charis E. Teh, Mrs. Edyta M. Kucharska and Dr. Anselm Enders provided technical help in cell preparation in some experiments.
- Mrs. Debbie Howard provided technical help in the irradiation of mice and intravenous injection of cells in the bone marrow chimera experiments.

3.1 Preamble

The strain named "*Ambrosius*" was discovered through ENU mutagenesis by the selective reduction of B cells in the peripheral blood of male mice. The causative point mutation was mapped to the X-chromosomal *Atp11c* gene of mutant mice, which encodes the putative aminophospholipid transporter ATP11C that contributes to the generation and maintenance of plasma membrane lipid asymmetry. In this chapter of the thesis, I characterise the immunological phenotype of *Ambrosius* mice as well as *18NIH30* mice, which were identified during the course of my studies, structured around the initially observed B cell phenotype.

3.2 ATP11C-deficient mice exhibit severe B cell deficiency

I first confirmed the B cell deficiency in the peripheral blood of $Atp11c^{amb/0}$ mice using a large cohort (Figure 3.1A). Analysis of the peripheral blood of female mice demonstrated that homozygous females have also severely reduced B cell frequency similar to hemizygous mutant male mice (Figure 3.1B). In contrast, heterozygous females had normal percentage of B cells in the peripheral blood (Figure 3.1B). These data indicate that loss of ATP11C in mice results in B cell deficiency syndrome.

3.3 Developmental block at the transition from pro-B to pre-B cell stage of B cell development in the bone marrow of ATP11C-deficient animals

B cells develop from the pluripotent HSCs in the bone marrow. Since ATP11C deficiency resulted in loss of B cell population in the peripheral blood, a systematic analysis of B cell subsets was performed in the bone marrow of $Atp11c^{amb/0}$ and control mice to determine if there is a developmental block during early B cell development. While the absolute number of leukocytes was normal (Figure 3.2A), the percentage and number of total B cells were decreased in $Atp11c^{amb/0}$ mice to 15-18% of the numbers in wild-type controls (Figure 3.2B, C). The number of $CD43^{+}CD24^{med}$ pro-B cells was 60% of normal, whereas the number of $CD43^{lo}$ $CD24^{hi}$ pre-B cells and $IgM^{+}IgD^{-}$ immature B cells were only 6% and 1.8% of normal, respectively (Figure 3.2C). $IgM^{+}IgD^{+}$ mature recirculating B cells in the bone marrow were 11% of normal numbers, and these expressed much higher

densities of IgM compared to wild-type littermates (Figure 3.2B, C). Further analysis of sIgM-negative and lineage marker-negative bone marrow B cell progenitors by CD43, CD24 and BP-1 expression showed normal numbers of pre/pro-B cells (Fraction A) in the mutant animals, but progressively reduced numbers of pro-B and pre-B cells in Fractions B, C and C′ (Figure 3.3A, B). These data establish that ATP11C is required for B cells to differentiate normally past the pro-B cell stage.

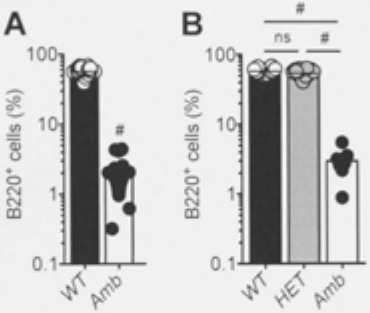

Figure 3.1 Confirmation of B cell deficiency in ATP11C-deficient mice using more biological replicates

(A) Graph shows B220$^+$ cells as a percentage of total lymphocytes in the blood of *Atp11c*$^{+/0}$ (WT) or *Atp11c*$^{amb/0}$ (Amb) male mice. **(B)** Graph shows B220$^+$ cells as a percentage of total lymphocytes in the blood of *Atp11c*$^{+/+}$ (WT), *Atp11c*$^{amb/+}$ (HET) or *Atp11c*$^{amb/amb}$ (Amb) female mice. Each circle represents a single mouse, and data are pooled from at least three (or two in panel B) independent experiments with three to ten mice per genotype in each. Statistical significance was calculated using the two-tailed Student's *t*-test (A) or One-Way ANOVA analysis, followed by the Bonferroni post-test, with the *P* values comparing each pair of experimental groups shown on the plots (B). ns, not significant; #, $P < 0.0001$.

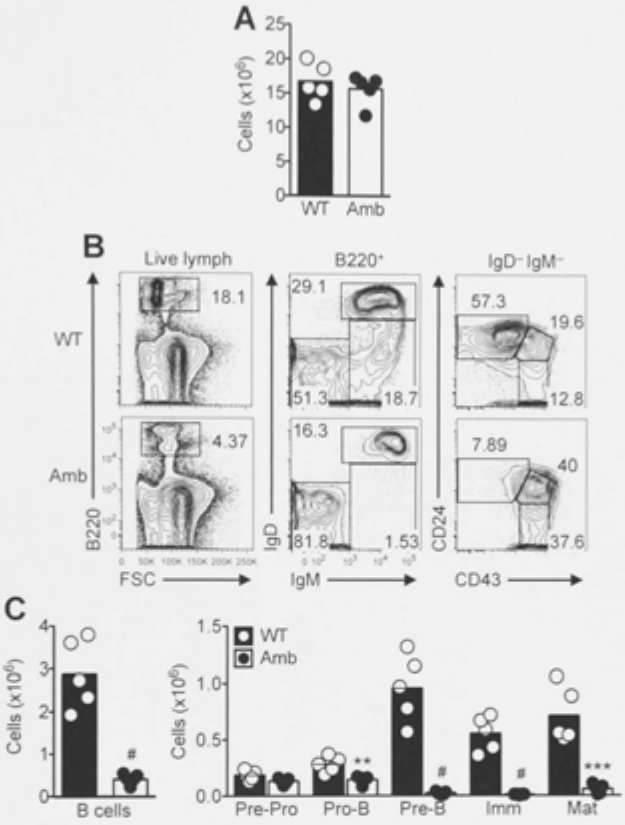

Figure 3.2 The ATP11C^{amb} mutation causes a developmental block at the pro- to pre-B cell transition stage of B cell development in the bone marrow

(A) Graph shows the absolute number of leukocytes in the bone marrow from *Atp11c*$^{+/0}$ (WT) or *Atp11c*$^{amb/0}$ (Amb) mice. **(B)** Representative flow cytometric analysis of bone marrow cells from *Atp11c*$^{+/0}$ (WT) or *Atp11c*$^{amb/0}$ (Amb) mice. Numbers adjacent to outlined areas indicate percentage of B220$^+$ B cells (left); percentage of IgM$^+$IgD$^+$ mature B cells, IgM$^+$IgD$^-$ immature (Imm.) B cells, and IgM$^-$IgD$^-$ pro- and pre-B cells within the B220$^+$ subset (middle); cells gated on B220$^+$ IgM$^-$IgD$^-$ cells, showing the percentage that are CD43$^-$CD24^{hi} pre-B cells, CD43$^+$CD24^{med} pro-B cells and CD43$^+$CD24$^-$ pre-pro-B cells (right). **(C)** Graphs show the absolute number of B cells and indicated B cell subsets in the bone marrow from *Atp11c*$^{+/0}$ (WT) or *Atp11c*$^{amb/0}$ (Amb) mice. Each circle represents a single mouse, and data are representative of at least five independent experiments with two to five mice per genotype in each. Statistical significance was calculated using the two-tailed Student's *t*-test. $^{\#}$, $P < 0.0001$; *** $P < .001$; ** $P < .01$.

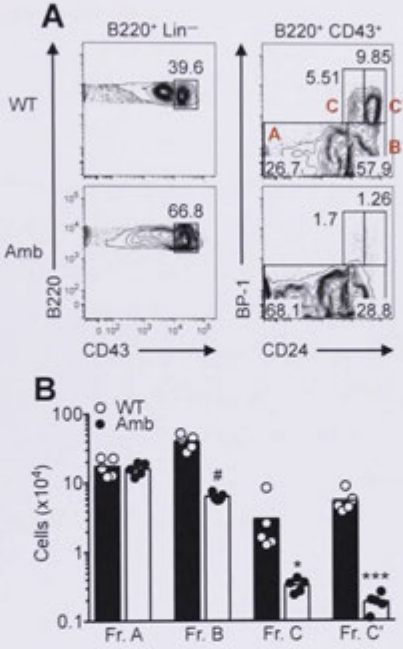

Figure 3.3 Analysis of B cell subpopulations in the bone marrow

(A) Representative flow cytometric analysis of B220, CD43, BP-1 and CD24 surface expression on lineage-negative bone marrow cells of mice from the indicated genotypes. Lineage panel for the analysis contains antibodies against CD4, CD5, CD8, TCRβ, TCRγδ, IgM, Mac-1, CD11c, Ter119, Ly6c, Gr-1 and NK1.1 **(B)** Graph shows the absolute number of Fraction (Fr.) A-C` cell populations as shown in (A). Each circle represents a single mouse, and data are representative of two independent experiments with two to five mice per genotype in each. Statistical significance was calculated using the two-tailed Student's *t*-test. #, $P < 0.0001$; *** $P < .001$; * $P < .05$.

3.4 The ATP11C^{amb} mutation reduces all B cell subsets except MZ B cells in the spleen

The previous set of results revealed that B cell development in the bone marrow of ATP11C-deficient animals is arrested at the pro-B cell stage. As a next step, the effects of ATP11C mutation on peripheral B cell and B cell subsets were examined. Spleens of mutant animals were smaller than those of control mice (Figure 3.4A). In line with a smaller spleen, the number of total leukocytes was reduced in mutant mice compared to their littermate controls (Figure 3.4B). The number of B cells in *Atp11c*$^{amb/0}$ animals was also decreased to 9% of that in wild-type mice (Figure 3.4C, D). Consistent with a reduced production of B cells in the bone marrow, immature B cells in the spleen were decreased to 1% of the numbers in wild-type mice and FO B cells decreased to 5% of the normal number (Figure 3.4C, D). Despite an abnormal surface phenotype of higher CD21 and lower CD23 (Figure 3.4C), immunofluorescent staining of spleen sections illustrated that the FO B cells were located normally (Figure 3.5). By contrast, MZ B cells were present largely in normal numbers in *Atp11c*$^{amb/0}$ mice (Figure 3.4D), so that they made up approximately 40% of all splenic B cells. These data indicate that MZ B cells are unique among B cell subsets by either not requiring or being able to compensate for ATP11C deficiency.

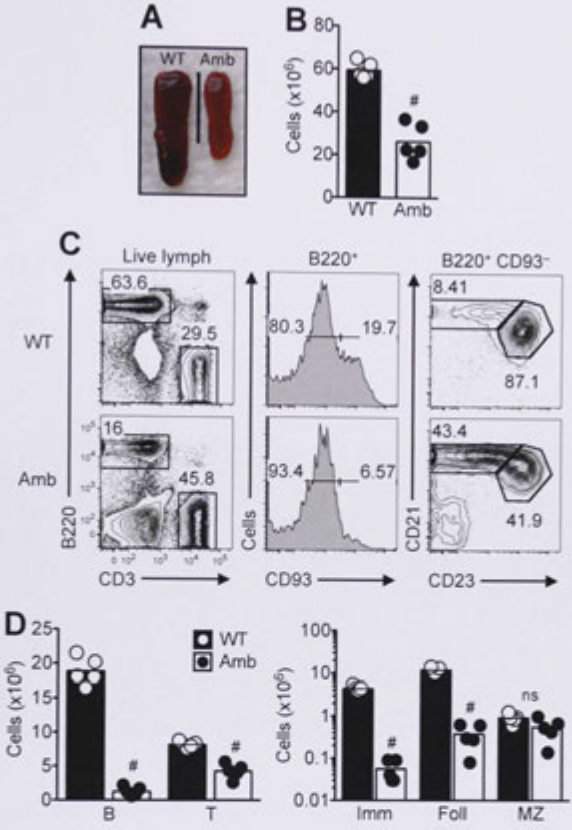

Figure 3.4 The ATP11C^{amb} mutation reduces all B cell subsets except MZ B cells in the spleen

(A) Spleen size in *Atp11c*$^{+/0}$ (WT) or *Atp11c*$^{amb/0}$ (Amb) mice. Bar, 1 cm. **(B)** Graph shows the absolute number of leukocytes in the spleen from *Atp11c*$^{+/0}$ (WT) or *Atp11c*$^{amb/0}$ (Amb) mice. **(C)** Representative flow cytometric analysis of B cell subpopulations in the spleen from *Atp11c*$^{+/0}$ (WT) or *Atp11c*$^{amb/0}$ (Amb) mice. Numbers adjacent to outlined areas indicate percentage of B220^{+} B cells and CD3^{+} T cells (left); percentage of B220^{+}-gated cells that are CD93^{-} mature B cells and CD93^{+} immature (Imm) B cells (middle); percentage of the CD21^{hi}CD23^{-} marginal zone (MZ) and the CD21^{med}CD23^{+} follicular (Foll) B cell subset within the B220^{+}CD93^{-} mature B cells (right). **(D)** Graphs show the absolute number of B cells, T cells and indicated B cell subsets in the spleen from *Atp11c*$^{+/0}$ (WT) or *Atp11c*$^{amb/0}$ (Amb) mice. Each circle represents a single mouse, and data are representative of at least five independent experiments with two to five mice per genotype in each. Statistical significance was calculated using the two-tailed Student's *t*-test. ns, not significant; #, $P < 0.0001$.

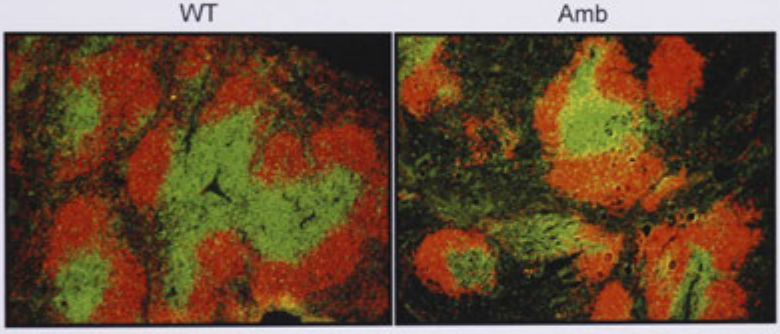

Figure 3.5 Normal localisation of the residual B cells in the spleen of ATP11C-deficient mice.

Spleen cryosections from *Atp11c*$^{+/0}$ (WT) and *Atp11c*$^{amb/0}$ (Amb) mice were stained with fluorescently labelled antibodies to detect B cells (B220) and T cells (CD3).

3.5 Loss of B1 cells in the peritoneal cavity of ATP11C-deficient mice

B1 cells are known as innate-like cells and involved in the early defence against pathogens (Berland and Wortis, 2002). Unlike mature recirculating B cells (also referred to as "conventional" or "B2" cells), B1 cells are most abundant in the peritoneal cavity, and can be identified using specific surface markers (Berland and Wortis, 2002). To investigate whether the ATP11C^{amb} mutation has any effect on the development of B1 cells, B1 cells in the peritoneal cavity of *Atp11c*$^{+/0}$ and *Atp11c*$^{amb/0}$ animals were analysed. There was a slight reduction in the total number of leukocytes in the peritoneal cavity of *Atp11c*$^{amb/0}$ mice (Figure 3.6A). Both the B1 (CD23$^-$) and B2 (CD23$^+$) B cell subsets were decreased to less than 10% of normal (Figure 3.6B, C). Further analysis of B1 cell subsets based on CD5 expression revealed that both CD5$^+$ B1a and CD5$^-$ B1b cells are equally affected by the mutation as the absolute number of both populations was significantly reduced (Figure 3.6B, C). These results indicate that in addition to its role in the development of conventional B2 cells in the bone marrow and spleen, ATP11C has a critical role in the accumulation of B1 cells in the peritoneal cavity.

3.6 A cell-autonomous requirement for ATP11C in B cell revealed by mixed bone marrow chimera

The results presented above showed that ATP11C plays an important role in the development of B cells in the bone marrow. In order to test if the effect of the ATP11C^{amb} mutation on B cell numbers is due to a cell intrinsic or extrinsic effect, mixed bone marrow chimeras were generated. Recipient *Rag1*$^{-/-}$ mice, lacking both B and T lymphocytes, were irradiated with one dose of 450 rad irradiation, and were then reconstituted with an equal mixture of CD45.1-marked *Atp11c*$^{+/0}$ and CD45.2 *Atp11c*$^{amb/0}$ bone marrow cells (Figure 3.7A). As a control, a group of mice were reconstituted with a mixture of CD45.1-marked *Atp11c*$^{+/0}$ and CD45.2 *Atp11c*$^{+/0}$ bone marrow cells (Figure 3.7A). The recipient mice were sacrificed 12-14 weeks after the transplantation, and the relative reconstitution of each chimeric mouse by *Atp11c*$^{+/0}$ or *Atp11c*$^{amb/0}$ CD45.2$^+$ haematopoietic stem cells was gauged by the percentage of donor derived B, T and NK cells that were CD45.2$^+$ in the spleen of recipient mice.

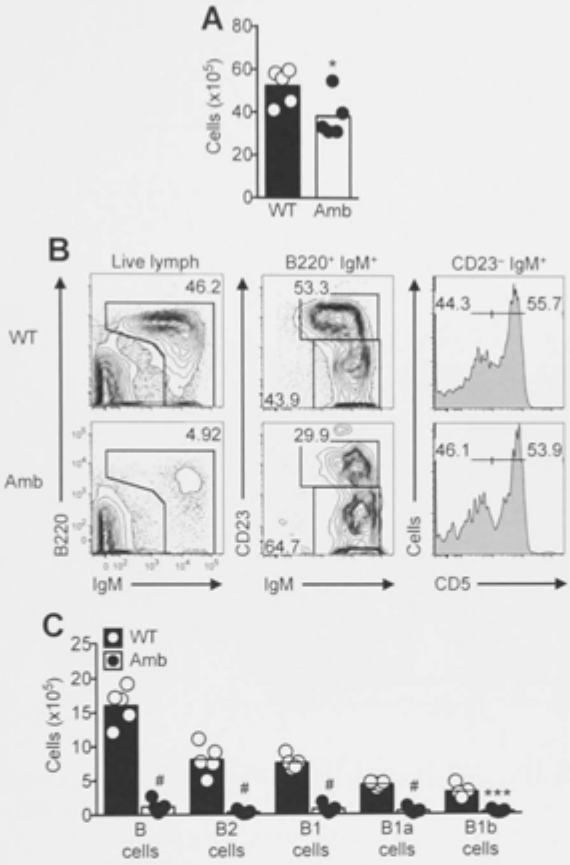

Figure 3.6 Effect of the ATP11C^{amb} mutation on peritoneal B cells.

(A) Graph shows the absolute number of leukocytes in the peritoneal cavity wash from *Atp11c*$^{+/0}$ (WT) or *Atp11c*$^{amb/0}$ (Amb) mice. **(B)** Representative flow cytometric analysis of the frequency of B cells and B cell subpopulations in the peritoneal cavity of *Atp11c*$^{+/0}$ (WT) and *Atp11c*$^{amb/0}$ (Amb) mice. Numbers adjacent to outlined areas indicate percentage of B220^{+}IgM^{+} B cells (left); percentage of B220^{+}IgM^{+}-gated cells that are CD23^{+} B2 cells and CD23^{-} B1 cells (middle); percentage of the CD5^{+} B1a and the CD5^{-} B1b B cell subset within the CD23^{-}IgM^{+} B1 cells (right). **(C)** Graphs show the absolute number of B cells and indicated B cell subsets in the peritoneal cavity wash from *Atp11c*$^{+/0}$ (WT) or *Atp11c*$^{amb/0}$ (Amb) mice. Each circle represents a single mouse, and data are representative of two independent experiments with three to five mice per genotype in each. Statistical significance was calculated using the two-tailed Student's *t*-test. $^{\#}$, $P < 0.0001$; *** $P < .001$; * $P < .05$.

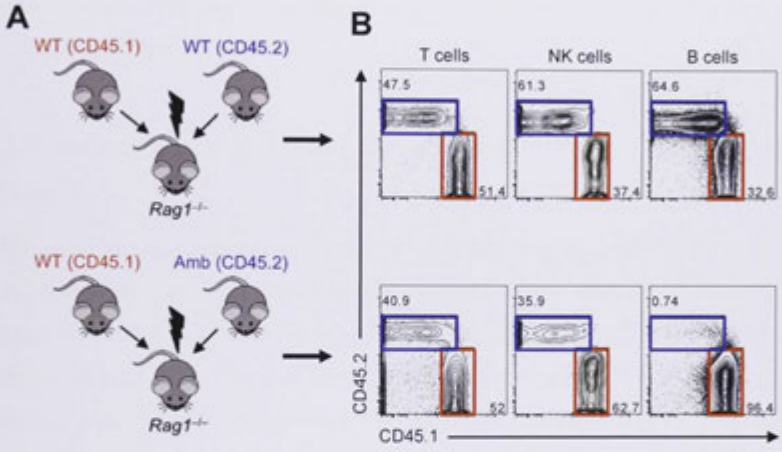

Figure 3.7 B cell deficiency in *Atp11c*$^{amb/0}$ mice is due to a cell-autonomous requirement for ATP11C within B cells.

(A) Bone marrow cells from CD45.1$^+$ *Atp11c*$^{+/0}$ (WT) mice was mixed with equal numbers of bone marrow cells from CD45.2$^+$ *Atp11c*$^{+/0}$ or *Atp11c*$^{amb/0}$ (Amb) mice and injected intravenously into irradiated *Rag1*$^{-/-}$ animals. **(B)** 12 weeks after reconstitution the recipient mice were analysed by flow cytometry for the percentage of CD45.1$^+$ versus CD45.2$^+$ CD3$^+$ T cells, NK1.1$^+$ NK cells and B220$^+$ B cells in the spleen. Data are representative of two independent experiments with four to six mice per genotype in each.

The results showed that there is no significant difference in the ratio of *Atp11c*$^{+/0}$ derived B cells, T cells and NK cells in the spleen of recipient mice (Figure 3.7B). In contrast, the requirement for normal ATP11C in B cells was found to be cell autonomous as *Atp11c*$^{amb/0}$ B cells represented only 1% of B cells in the periphery of chimeric recipients (Figure 3.7B). In the same mixed chimeras, *Atp11c*$^{amb/0}$ T cells and NK cells nevertheless accumulated in approximately equal proportions to their wild-type counterparts, establishing that there is little or no competitive disadvantage of mutant cells in T cells, NK cells or their haematopoietic progenitors (Figure 3.7B). Taken together, these results illustrate that ATP11C controls B cell development in a cell-intrinsic manner.

3.7 Identification and phenotypic characterisation of second allele, *18NIH30*

While analysing the *Ambrosius* mice, flow cytometric screening of blood from ENU-mutagenised mouse pedigrees identified another strain with a reduced B cell frequency in the peripheral blood of male animals (Figure 3.8A). An *Atp11c* mutation identified by Sanger sequencing in this strain (*18NIH30*) also disrupts an invariant, essential splice donor nucleotide but in the preceding exon 26 splice donor sequence (intronic +2T to G: TCTGAAGg*t*aga to AACTCTGAAGg*g*taga). To directly compare the phenotype of both strains, a comparative B cell analysis in the bone marrow and spleen of both *Atp11c* mutants and wild-type control was performed in the same experiment. Phenotypic comparison of *Atp11c*$^{amb/0}$ and *Atp11c*$^{18NIH30/0}$ animals showed that both strains have similarly reduced B cell numbers in the bone marrow due to a developmental arrest at the pro-B cells (Figure 3.8B). Likewise, while the number of total B, immature B and FO B cells was severely reduced, MZ B cells remained mostly unaffected in the spleen of *Atp11c*$^{amb/0}$ and *Atp11c*$^{18NIH30/0}$ mice (Figure 3.8C). Thus, the discovery of a second allele confirms the requirement of ATP11C at the pro-B cell stage of B cell development in the bone marrow.

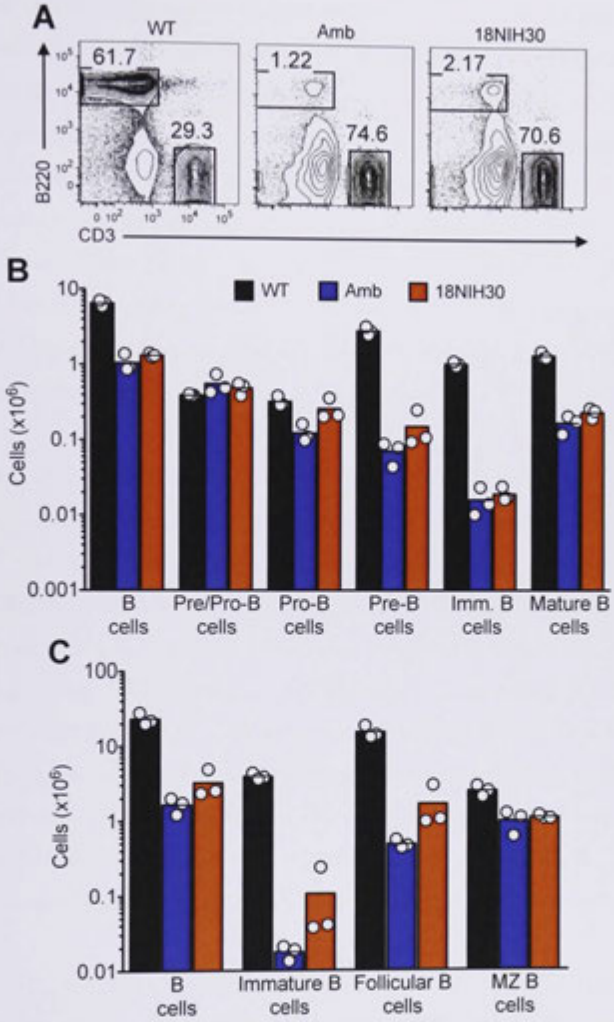

Figure 3.8 Discovery and initial characterisation of second allele, *18NIH30*.
(A) Flow cytometry of B220$^+$ B cells in the blood of *Atp11c*$^{+/0}$ (WT), *Atp11c*$^{amb/0}$ (Amb) and *Atp11c*$^{18NIH30/0}$ (18NIH30) mice. Numbers adjacent to outlined areas indicate percentage of B220$^+$CD3$^-$ B cells (top left) or B220$^-$CD3$^+$ T cells (bottom right). **(B, C)** Graphs show the absolute number of B cells and B cell subsets in the (B) bone marrow and (C) spleen of *Atp11c*$^{+/0}$ (WT), *Atp11c*$^{amb/0}$ (Amb) and *Atp11c*$^{18NIH30/0}$ (18NIH30) mice. Each circle represents a single mouse.

3.8 Chapter summary and discussion

This chapter examined the immunological characteristics of two independent mouse strains identified through ENU mutagenesis that exhibited severely reduced B cell frequency in the peripheral blood caused by splice-site mutations in *Atp11c*. The detailed flow cytometric analysis of mutant animals revealed a developmental block of B cell differentiation at the pro-B cell stage, leading to reduced B cell numbers in the bone marrow and periphery. In addition to conventional B cells, B1 cells in the peritoneal cavity of mutant mice were severely reduced compared to their control littermates, but MZ B cells in the spleen of mutant mice remained unaffected by the mutation. A cell-autonomous requirement for ATP11C within B cells was revealed through mixed bone marrow chimeras.

The developmental arrest at the transition from pro- to pre-B cells in ATP11C mutant mice is similar to that observed in some other mouse models including *Rag1*$^{-/-}$ or *Rag2*$^{-/-}$ mice and other mice deficient in the expression and signalling through the pre-BCR (Mombaerts et al., 1992, Shinkai et al., 1992) (Kitamura et al., 1991, Kitamura et al., 1992, Torres et al., 1996, Gong and Nussenzweig, 1996, Mundt et al., 2001, Pelanda et al., 2002). Formation and signalling through the pre-BCR is a key step in pre-B cell development, because upon successful rearrangement of Ig heavy chain it signals the proliferation and differentiation of pre-B cells and initiates light chain recombination (Clark et al., 2014). Therefore, it is possible that the ATP11C^{amb} mutation may cripple formation and/or signalling through the pre-BCR, which could result in a developmental block in B cell development of ATP11C mutant animals.

Mice lacking IL-7, a critical growth factor for the survival and proliferation of pro-B cells, or its receptor IL-7R also have a defect in early B cell development (von Freeden-Jeffry et al., 1995, Peschon et al., 1994). Although the developmental arrest in these mice is already at the pre/pro-B cell stage, it is still possible that ATP11C may have a quantitative or qualitative influence on the expression and/or signalling through the IL-7R. Moreover, one of the critical roles for IL-7 is to control pro-B cell survival by regulating important pro- and anti-apoptotic proteins (Corfe and Paige, 2012). It is also possible that ATP11C-deficient pro- or/and pre-B cells undergo excessive apoptosis due to possibly an impaired signalling through the IL-7R. As

will be discussed in the next chapter, I tried to answer these questions by crossing ATP11C-deficient mice to mouse strains with transgenic overexpression of IL-7 or the anti-apoptotic protein BCL-2.

In conclusion, ATP11C deficiency in mice causes a B cell deficiency syndrome due to a developmental arrest in B lymphopoiesis in the bone marrow. Although the mechanism(s) by which ATP11C affects B cell development is unclear and will be a focus of later chapters in this thesis, the availability of the novel ENU variant mouse strains provide excellent model organisms to investigate the role of ATP11C in B cell biology as well as other important biological systems.

CHAPTER 4: Examination of the compromised pathway in ATP11C-deficient B cells by crossing *Atp11c*$^{amb/0}$ with animals carrying transgenes encoding the BCR, BCL-2 and IL-7

Contents of this chapter appeared in:

Mehmet Yabas, Charis E. Teh, Sandra Frankenreiter, Dennis Lal, Carla M. Roots, Belinda Whittle, Daniel T. Andrews, Yafei Zhang, Narci C. Teoh, Jonathan Sprent, Lina E. Tze, Edyta M. Kucharska, Jennifer Kofler, Geoffrey C. Farell, Stefan Bröer, Christopher C. Goodnow and Anselm Enders (2011). "ATP11C is critical for the internalization of phosphatidylserine and differentiation B lymphocytes". *Nature Immunology*, 12(5):441-449.

4.1 Preamble

In the previous chapter, loss of ATP11C has been shown to cause a B cell deficiency due to a developmental arrest at the transition of pro-B to pre-B cells, but the precise mechanism(s) underlying the observed phenotype in *Atp11c*$^{amb/0}$ mice remains unknown. Since the transition from pro- to pre-B cells is dependent on signalling through the IL-7R and successful rearrangement of Ig heavy chain genes (Clark et al., 2014), in this chapter I tested if defects in these processes and subsequent apoptosis caused the developmental block in *Atp11c*$^{amb/0}$ mice. I explored the possible compromised pathway(s) in ATP11C-deficient B cells by crossing mutant mice with: (1) MD4 or SW_{HEL} transgenic mice with Ig heavy and light chain genes already rearranged; (2) *Vav-Bcl2* transgenic mice to inhibit apoptosis or (3) *H2Ea-Il7* transgenic mice with greatly increased IL-7. In this chapter, B cell development in the bone marrow and accumulation of B cell subsets in the spleen of ATP11C-deficient mice carrying one of these transgenes will be examined.

4.2 Partial restoration of B cell deficiency in *Atp11c*$^{amb/0}$ mice by a BCR transgene

Once a functionally Ig heavy chain is produced at pro-B cell stage, it leads to the assembly of a membrane complex together with the transmembrane proteins Igα, Igβ, and the SLC molecules λ5 and VpreB. This complex is known as pre-BCR and it initiates a signalling cascade, which is a crucial check-point in B cell development in the bone marrow (Herzog et al., 2009, Clark et al., 2014). I first wanted to test if a failure of pre-BCR signalling is responsible for the defect in *Atp11c*$^{amb/0}$ B cells and if the presence of recombined heavy- and light-chain transgenes corrects B cell deficiency in *Atp11c*$^{amb/0}$ mice. To do so, I analysed B cell subpopulations in the bone marrow and spleen of *Atp11c*$^{+/0}$ and *Atp11c*$^{amb/0}$ mice with or without a BCR transgene (MD4) that is specific for HEL protein (Goodnow et al., 1988). In MD4 transgenic mice, the rearranged Ig heavy and light chain transgenes are normally activated during the pro-B cell stage, bypassing and suppressing RAG-mediated recombination of the endogenous Ig-genes (Goodnow et al., 1988). This lowers the number of pro-B cells and pre-B cells to 12% and 2% of normal numbers, respectively, replacing them with IgM^+ IgD^- immature B cells that are present in

normal numbers in the bone marrow (Table 4.1 and Figure 4.1). Whereas the ATP11C^{amb} mutation decreased the number of pro-B cells in non-transgenic mice, it increased the number of pro-B cells in *Atp11c*$^{amb/0}$ MD4 transgenic mice to 150% of the numbers in control MD4 animals with normal ATP11C (Table 4.1 and Figure 4.1). The number of immature B cells in the bone marrow of *Atp11c*$^{amb/0}$ MD4 animals was nevertheless only partly restored to 11% of the numbers in *Atp11c*$^{+/0}$ MD4 mice, whereas circulating B cells in the bone marrow and total B cells in the spleen were partly restored to 37% of those in MD4 transgenic mice with normal ATP11C (Table 4.1 and Figure 4.1).

Atp11c$^{amb/0}$ mice were also crossed with HEL transgenic (SW_{HEL}) mice, which carry a heavy-chain VDJ knock-in gene combined with a HEL-specific κ-light chain transgene (Phan et al., 2003). A similar magnitude of rescue occurred in SW_{HEL} mice with a rearranged *Igh* gene targeted in its normal location, but only when combined with a rearranged transgenic light chain (Figure 4.2). Collectively, these results suggest that bypassing the pre-BCR signalling step partially overcomes the B cell deficiency, but does not completely eliminate the need for ATP11C.

ATP11C	Transgene	Pre/Pro-B cells	Pro-B cells	Pre-B cells	Immature B cells	Mature B cells	Mice (*n*. BM)	Splenic B cells	Mice (*n*. Spleen)
WT	None	3.99 ± 0.25	4.10 ± 0.42	28.66 ± 2.04	12.50 ± 1.20	14.29 ± 0.89	14	20.06 ± 1.87	11
Amb	None	5.55 ± 0.36	2.22 ± 0.42	1.74 ± 0.34	0.24 ± 0.04	1.75 ± 0.25	13	1.73 ± 0.20	10
WT	*Vav-Bcl2*	5.53 ± 0.48	6.48 ± 0.65	21.48 ± 5.72	17.60 ± 1.65	69.63 ± 13.55	4	101.10 ± 11.84	4
Amb	*Vav-Bcl2*	6.22 ± 0.49	4.78 ± 0.96	6.22 ± 1.37	3.12 ± 0.26	9.98 ± 1.06	6	6.18 ± 1.37	6
WT	*H2Eα-Il7*	2.36 ± 0.56	19.26 ± 2.28	262.00 ± 36.5	36.36 ± 3.86	1.66 ± 0.31	5	153.30 ± 18.25	3
Amb	*H2Eα-Il7*	5.33 ± 0.21	2.33 ± 0.40	1.68 ± 0.43	0.25 ± 0.03	6.30 ± 1.45	4	7.78 ± 1.94	2
WT	MD4	2.53 ± 0.29	0.50 ± 0.06	0.73 ± 0.13	15.97 ± 0.89	10.07 ± 0.84	3	10.82 ± 1.64	3
Amb	MD4	3.28 ± 0.32	0.70 ± 0.03	0.66 ± 0.03	1.98 ± 0.39	4.90 ± 1.04	5	3.00 ± 0.23	5

Table 4.1 B cells in the spleen and B cell subpopulations in bone marrow

The numbers are expressed as mean values $x10^5$ ± S.E.M in the bone marrow and $x10^6$ ± S.E.M in the spleen. B cells ($B220^+$ in live lymphocytes gate) in the spleen. Mature B cell (IgD^+IgM^+ in $B220^+$ gate), Immature B cells (IgD^-IgM^+ in $B220^+$ gate), Pre-B cell ($CD24^{hi}CD43^-$ in IgD^-IgM^- gate), Pro-B cell ($CD24^{int}CD43^+$ in IgD^-IgM^- gate), Pre/Pro-B cell ($CD24^-CD43^+$ in IgD^-IgM^- gate) in the bone marrow. *n* represents number of mice analysed for each genotype.

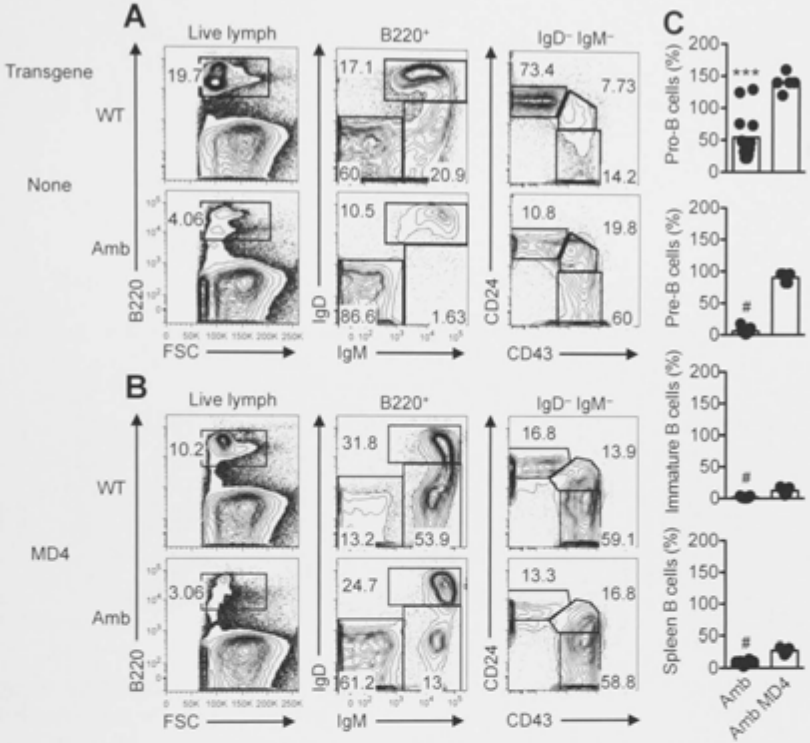

Figure 4.1 Partial correction of B cell phenotype in ATP11C-deficient mice by a BCR transgene

Representative flow cytometric analysis of B cell subpopulations in the bone marrow of **(A)** non-transgenic mice with WT or mutant (Amb) ATP11C, **(B)** ATP11C WT or Amb mice expressing rearranged *Igh* and *Igk* transgenes from the MD4 strain. Numbers adjacent to outlined areas indicate percentage of $B220^+$ B cells (left); percentage of IgM^-IgD^+ mature B cells, IgM^+IgD^- immature (Imm.) B cells, and IgM^-IgD^- pro- and pre-B cells within the $B220^+$ subset (middle); cells gated on $B220^+$ IgM^-IgD^- cells, showing the percentage that are $CD43^-CD24^{hi}$ pre-B cells, $CD43^+CD24^{med}$ pro-B cells and $CD43^+CD24^-$ pre-pro-B cells (right). **(C)** Graphs show the relative number of pro-B, pre-B, immature B cells in the bone marrow and B cells in the spleen of $Atp11c^{amb/0}$ mutant mice with the MD4 BCR transgene, as a percentage of the mean number in $Atp11c^{+/0}$ WT control animals carrying the same transgene. Each circle represents one mouse, and data are pooled from multiple experiments with one to five mice per genotype in each. Statistical significance was calculated using the two-tailed Student's *t*-test. $^{\#}$, $P < 0.0001$; *** $P < .001$.

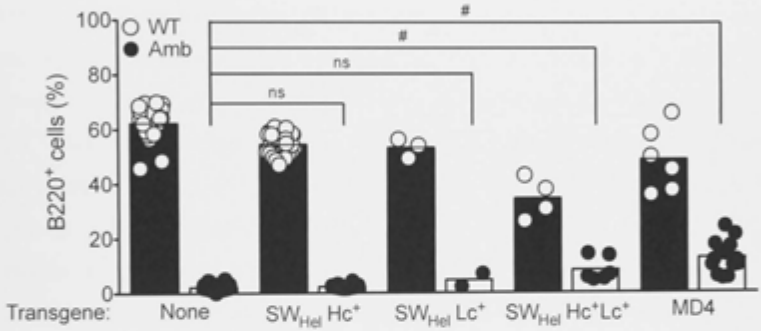

Figure 4.2 Limited rescue of B cells in the blood of ATP11C-deficient animals by overexpression of transgenic BCRs

$B220^+$ B cells (% of lymphocytes) in the blood of mice from the indicated genotypes. SW_{HEL} mice have a rearranged HEL-specific VDJ exon knocked into the heavy chain locus and a rearranged HEL-specific κ light-chain transgene. The MD4 mice carry several copies of rearranged HEL-specific heavy and light chain transgenes, co-integrated at one site on Chromosome 17 several cM distal to *H2*. Each circle represents one mouse, and data are pooled from multiple experiments with one to five mice per genotype in each. ns, not significant; Statistical significance was calculated using the two-tailed Student's *t*-test. #, $P < 0.0001$.

4.3 Enforced expression of BCL-2 fails to drive B cell development in *Atp11c*$^{amb/0}$ mice

BCL-2 is an anti-apoptotic protein that promotes cell survival through the inhibition of programmed cell death, apoptosis caused through the cell intrinsic or mitochondrial pathway (Vaux et al., 1988, Hockenbery et al., 1990). In order to test if diminished mitochondrial apoptosis restores the B cell deficiency in mutant animals, *Atp11c*$^{amb/0}$ mice with transgenic expression of the gene encoding the pro-survival protein BCL-2 driven by the promoter of the gene encoding the adaptor VAV (*Vav-Bcl2* mice) were generated (Ogilvy et al., 1999). Consistent with the published report (Ogilvy et al., 1999) *Vav-Bcl2* greatly increased the number of mature B cells in control siblings with normal ATP11C (Table 4.1 and Figure 4.3). The number of pre-B cells in *Atp11c*$^{amb/0}$ *Vav-Bcl2* mice was 29% of the number in *Atp11c*$^{+/0}$ *Vav-Bcl2* controls, representing a partial restoration compared to 6% of normal numbers in *Atp11c*$^{amb/0}$ mutants without *Vav-Bcl2* (Table 4.1 and Figure 4.3). The pre-B cells in *Atp11c*$^{amb/0}$ *Vav-Bcl2* mice nevertheless failed to increase expression of CD24 (Figure 4.3) and CD25 (Figure 4.4), whose expressions are increased in pre-B cells. Immature B cells were also partly rescued in *Atp11c*$^{amb/0}$ *Vav-Bcl2* animals, although they still represented only 17% of the numbers in *Atp11c*$^{+/0}$ *Vav-Bcl2* controls (Table 4.1 and Figure 4.3). Likewise splenic B cells remained at 6% of the numbers in *Atp11c*$^{+/0}$ *Vav-Bcl2* controls and 31% of wild-type mice (Table 4.1 and Figure 4.3). Collectively, these results indicate that suppression of apoptosis by enforced BCL-2 expression is unable to correct the B cell developmental abnormalities caused by ATP11C deficiency.

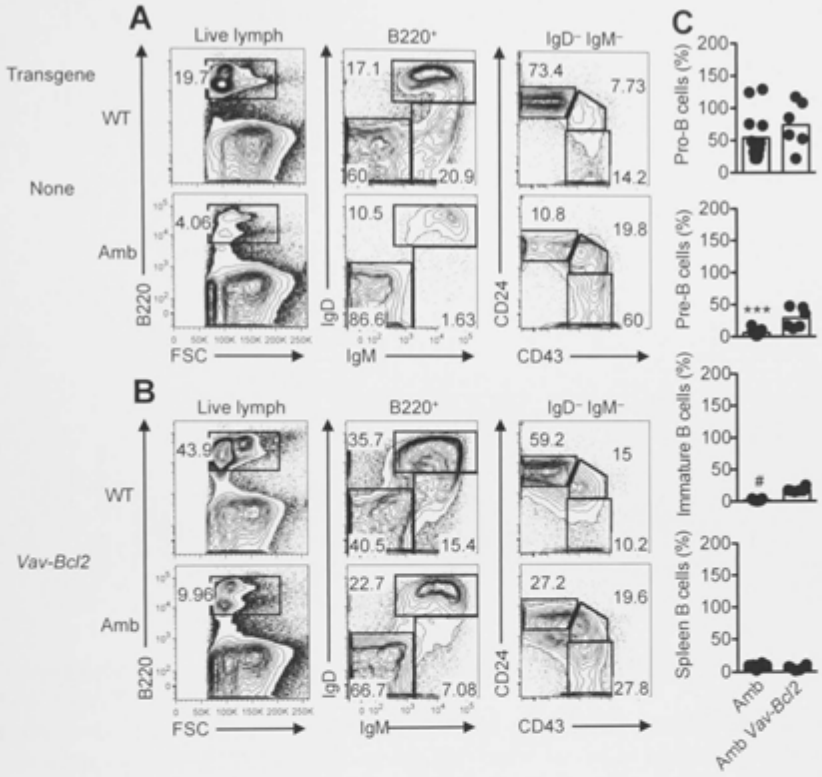

Figure 4.3 Enforced expression of BCL-2 fails to drive B cell development in *Atp11c*$^{amb\,0}$ mice

Representative flow cytometric analysis of B cell subpopulations in the bone marrow of **(A)** non-transgenic mice with wild-type (WT) or mutant (Amb) ATP11C, **(B)** ATP11C WT or Amb mice with enforced expression of BCL-2 under the control of the VAV-promoter (*Vav-Bcl2*). Numbers adjacent to outlined areas indicate percentage of B220$^+$ B cells (left); percentage of IgM$^+$IgD$^+$ mature B cells, IgM$^+$IgD$^-$ immature (Imm.) B cells, and IgM$^-$IgD$^-$ pro- and pre-B cells within the B220$^+$ subset (middle); cells gated on B220$^+$ IgM$^-$IgD$^-$ cells, showing the percentage that are CD43$^-$CD24^{hi} pre-B cells, CD43$^+$CD24^{med} pro-B cells and CD43$^+$CD24$^-$ pre-pro-B cells (right). **(C)** Graphs show the relative number of pro-B, pre-B, immature B cells in the bone marrow and B cells in the spleen of *Atp11c*$^{amb\,0}$ mutant mice with the BCL-2 transgene, as a percentage of the mean number in *Atp11c*$^{+\,0}$ WT control animals carrying the same transgene. Each circle represents one mouse, and data are pooled from multiple experiments with one to five mice per genotype in each. Statistical significance was calculated using the two-tailed Student's *t*-test. $^{\#}$, $P < 0.0001$; *** $P < .001$.

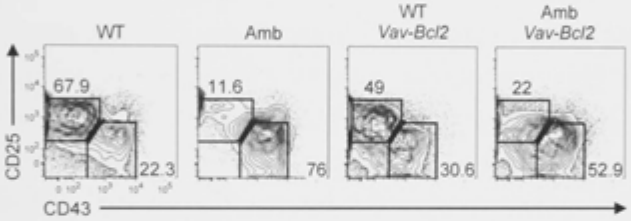

Figure 4.4 Over-expression of BCL-2 fails to upregulate CD25 expression in pre-B cells from *Atp11c*$^{amb/0}$ mice

Representative flow cytometric profiles of $CD25^{-}CD43^{+}$ pro-B cells and $CD25^{+}CD43^{-}$ pre-B cells within the $IgM^{-}IgD^{-}B220^{lo}$ bone marrow cells from mice of the indicated genotypes. Note that the *Vav-Bcl2* transgene increases the percentage of $CD43^{-}$ cells in *Atp11c*$^{amb/0}$ animals, but these cells show little increase in CD25. The data are representative of two independent experiments with two to three mice per genotype in each.

4.4 ATP11C deficiency abolishes effects of an *Il7* transgene

IL-7 is an essential cytokine for early B development in mice and signals through the IL-7R (Corfe and Paige, 2012). Analysis of the bone marrow of mice deficient for IL-7 or IL-7Rα showed that B cell development is arrested at the uncommitted pre-pro-B cell stage (von Freeden-Jeffry et al., 1995, Peschon et al., 1994). To investigate whether elevated IL-7 rescues the B cell phenotype in *Atp11c*$^{amb/0}$ animals, ATP11C mutant animals were crossed to *H2Ea-Il7* mice with transgenic expression of *Il7* driven by the Eα promoter of the gene encoding mouse major histocompatibility complex class II (*H2Ea-Il7* mice) (Mertsching et al., 1996). Due to the elevated IL-7, *H2Ea-Il7* transgenic mice with a normal *Atp11c* gene exhibited a 5-fold increase in bone marrow pro-B cells and 10-fold increase in pre-B cell numbers relative to wild-type mice (Table 4.1 and Figure 4.5), consistent with published analysis (Mertsching et al., 1996). By contrast, there was no effect of the increased IL-7 on the number of pro-B, pre-B, or immature B cells in *Atp11c*$^{amb/0}$ *H2Ea-Il7* mice compared to *Atp11c*$^{amb/0}$ mice without the IL-7 transgene (Table 4.1 and Figure 4.5). Increased IL-7 was therefore unable to rescue development of ATP11C-deficient B cells, and instead the mutation abolished the effects of transgenic IL-7 on pro-B and pre-B cells in the bone marrow.

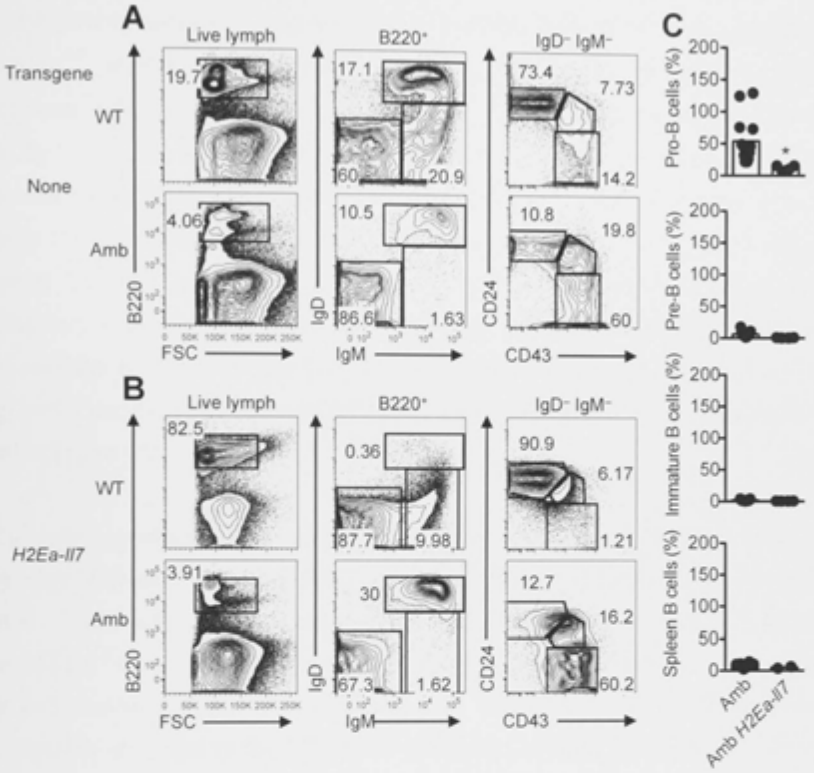

Figure 4.5 ATP11C deficiency abolishes effects of an *Il7* transgene

Representative flow cytometric analysis of B cell subpopulations in the bone marrow of **(A)** non-transgenic mice with wild-type (WT) or Mutant (Amb) ATP11C, **(B)** ATP11C WT or Amb mice over-expressing IL-7 under the control of the MHC II Eα gene promoter (*H2Ea-Il7*). Numbers adjacent to outlined areas indicate percentage of $B220^+$ B cells (left); percentage of IgM^+IgD^+ mature B cells, IgM^+IgD^- immature (Imm.) B cells, and IgM^-IgD^- pro- and pre-B cells within the $B220^+$ subset (middle); cells gated on $B220^+$ IgM^-IgD^- cells, showing the percentage that are $CD43^-CD24^{hi}$ pre-B cells, $CD43^+CD24^{med}$ pro-B cells and $CD43^+CD24^-$ pre-pro-B cells (right). **(C)** Graphs show the relative number of pro-B, pre-B, immature B cells in the bone marrow and B cells in the spleen of $Atp11c^{amb/0}$ mutant mice with the *Il7* transgene, as a percentage of the mean number in $Atp11c^{+/0}$ WT control animals carrying the same transgene. Each circle represents one mouse, and data are pooled from multiple experiments with one to five mice per genotype in each. Statistical significance was calculated using the two-tailed Student's *t*-test. * $P < .05$.

4.5 Less transition of *Atp11c*$^{amb/0}$ pro-B cells from Ig$^-$ to Ig$^+$ cells

To further characterise the developmental block in bone marrow B cells I performed staining for cytoplasmic μ (cμ) heavy chains in surface IgM$^-$ B220^{lo} cells, comparing *Atp11c*$^{+/0}$ or *Atp11c*$^{amb/0}$ animals with mice homozygous for null mutations eliminating the RAG1 recombinase or the CD79α subunit of the pre-BCR and BCR. In *Atp11c*$^{+/0}$ mice, 65% of sIgM$^-$ B220^{lo} cells were cμ$^+$ and these were CD24^{hi} due to normal pre-BCR signalling (Figure 4.6). No sIgM$^-$ B220^{lo} cells were cμ$^+$ in *Rag1*$^{-/-}$ mice (Figure 4.6A), consistent with their inability to recombine the heavy chain genes. 15% of sIgM$^-$B220^{lo} cells were cμ$^+$ in *Cd79a*$^{-/-}$ marrow, and their low frequency and lower CD24 expression is consistent with the inability of the pre-BCR to assemble and signal (Figure 4.6A, B). Compared to this baseline, the frequency of cμ$^+$ cells was even lower in *Atp11c*$^{amb/0}$ mice, representing only 5% of sIgM$^-$B220^{lo} cells (Figure 4.6).

Cμ$^+$ cells normally exhibit a heightened proliferative response to IL-7 as a result of synergy between IL-7R and pre-BCR signalling (Fleming and Paige, 2001, Marshall et al., 1998), so that cμ$^+$ cells among sIgM$^-$ B220^{lo} cells are preferentially expanded in *H2Ea-Il7* transgenic mice (Figure 4.6A, B). Like the earlier data on pro-B and pre-B cell numbers (Table 4.1 and Figure 4.5), this effect of *H2Ea-Il7* was also completely abolished by the ATP11C^{amb} mutation, so that the low frequency of cμ$^+$ cells in *Atp11c*$^{amb/0}$ marrow remained unchanged by the *Il7* transgene (Figure 4.6A, B).

Next I wanted to examine if the proliferative capacity of B cells was diminished by ATP11C deficiency *in vivo*. Flow cytometric staining for DNA content in bone marrow pre/pro-B (CD24$^-$Cμ$^-$), pro-B (CD24$^+$Cμ$^-$) and pre-B cells (CD24$^+$Cμ$^+$) revealed increased frequencies of mutant pro-B cells and pre-B cells with greater than 2n DNA, indicating that a greater proportion of mutant pro-B and pre-B cells were in S or G2+M phases of cell cycle (Figure 4.7).

CD24 was increased on cμ$^+$ cells in *Atp11c*$^{amb/0}$ bone marrow cells compared to *Cd79a*$^{-/-}$ and *Rag1*$^{-/-}$ bone marrow cells, but only to half of the levels on normal cμ$^+$ cells (Figure 4.6A, B). When the need for Ig-gene rearrangement and pre-BCR

signalling was bypassed in MD4 transgenic mice, ATP11C deficiency still greatly reduced the frequency of $B220^{lo}$ B cells that expressed the Ig genes and instead there was an expanded population of pro-B cells that had not yet activated Ig transgene expression (Table 4.1 and Figure 4.8). Collectively, these results indicate that the onset of H-chain expression and formation and/or signalling through the pre-BCR is both diminished in the absence of normal ATP11C.

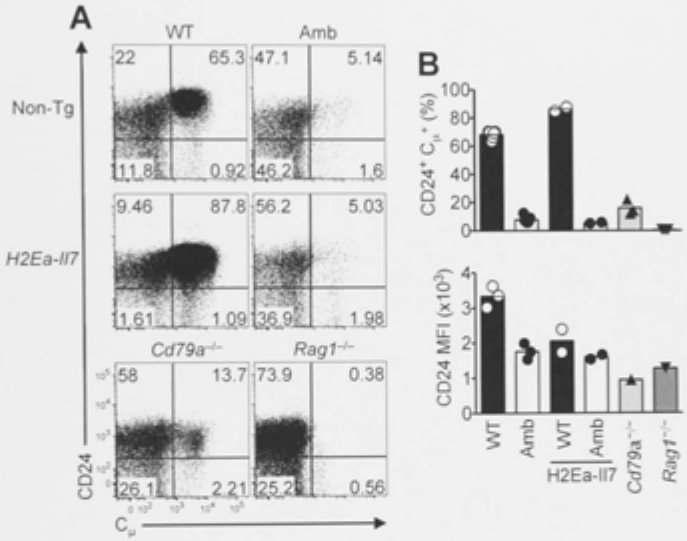

Figure 4.6 Decreased pro-B cell transition from Ig^- to Ig^+ cells in the bone marrow of *Atp11c*$^{amb.9}$ mice

(A) Representative flow cytometric analysis of the surface expression of CD24 and intracellular expression of IgM (Cμ) gated on surface $IgM^-B220^{lo}7AAD^-$ B cells in bone marrow from non-transgenic or IL-7 transgenic mice with wild-type (WT) or mutant (Amb) ATP11C, or from *Cd79a*$^{-/-}$ and *Rag1*$^{-/-}$ mice. Numbers indicate percent of gated cells in each quadrant. **(B)** Percent of intracellular IgM^+ $CD24^+$ cells gated as in (A), and mean fluorescence intensity (MFI) of CD24 staining on these cells. The data are representative of three different experiments with one to three mice per genotype in each.

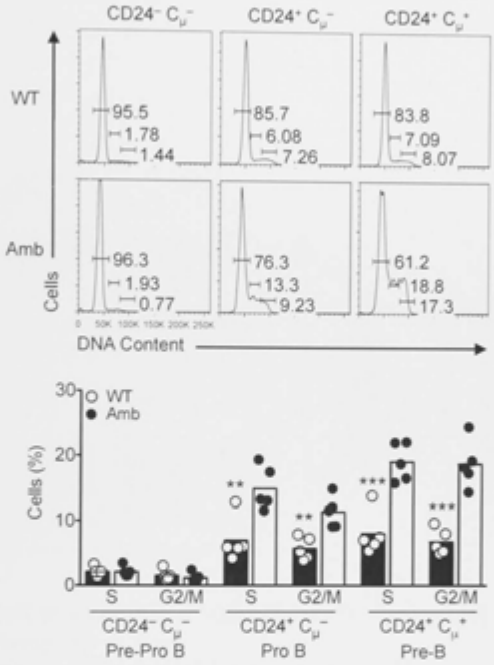

Figure 4.7 Cell cycle analysis of B cell precursors in the bone marrow of *Atp11c*$^{amb.9}$ animals

Representative flow cytometric analysis of the cell cycle of CD24$^-$Cμ$^-$ pre/pro-B, CD24$^+$Cμ$^-$ pro-B and CD24$^+$Cμ$^+$ pre-B cells from *Atp11c*$^{+.0}$ (WT) and *Atp11c*$^{amb.0}$ (Amb) mice. The percentages of cycling cells (G0/1, S and G2/M phase) are indicated. Graph shows % of CD24$^-$Cμ$^-$ pre/pro-B, CD24$^+$Cμ$^-$ pro-B and CD24$^+$Cμ$^+$ pre-B cells that are in S and G2/M phase. Data are representative of two different experiments with two to five mice per genotype in each. Statistical significance was calculated using the two-tailed Student's *t*-test. *** $P < .001$; ** $P < .01$.

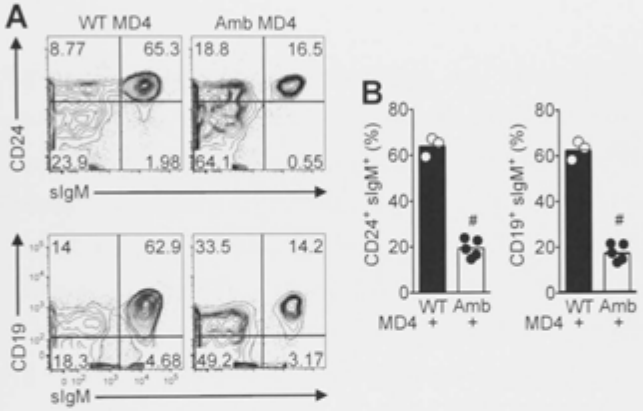

Figure 4.8 Impaired accumulation of sIgM$^+$ B cells in the bone marrow of *Atp11c*$^{amb/0}$ mice with a BCR transgene

Analysis of bone marrow from *Atp11c*$^{+/0}$ (WT) and *Atp11c*$^{amb/0}$ (Amb) mice expressing the rearranged MD4 *Igh* and *Igk* transgenes, showing the percentage of B220^{low}IgD$^-$ cells expressing surface IgM and CD24 (top) or CD19 (bottom). Graphs are combined from three different experiments with one to three mice per genotype in each. Statistical significance was calculated using the two-tailed Student's *t*-test. #, $P < 0.0001$.

4.6 Chapter summary and discussion

This chapter examined whether the developmental block in B cell differentiation caused by the ATP11C^{amb} mutation could be rescued by bypassing antigen receptor gene rearrangement or by providing pro-survival signals to progenitor B cells in the form of growth factor signals through IL-7 or overexpression of the anti-apoptotic protein BCL-2. While introduction of a BCR transgene with functionally rearranged Ig heavy and light loci in ATP11C-deficient mice partially corrected B cell deficiency, overexpression of BCL-2 or IL-7 was incapable of rescuing B cell development in *Atp11c*$^{amb/0}$ animals.

In the BCR transgenic mice, the rearranged Ig heavy and light chain transgenes are normally activated during the pro-B cell stage, leading to a redundant pre-BCR signalling during B lymphopoiesis (Goodnow et al., 1988). Interestingly, crossing ATP11C-deficient animals to MD4 or SW_{HEL} transgenic mice resulted in a partial rescue in B cell numbers in the bone marrow and spleen, and both heavy and light chain transgenes were required for the correction. In contrast to the results presented here, B cell deficiency in pre-BCR deficient λ5 and RAG-1 has been corrected by expression of rearranged light or heavy chain transgenes (Spanopoulou et al., 1994, Pelanda et al., 1996). These results suggest that B cells developing in the bone marrow of ATP11C-deficient mice may have impaired signalling through the pre-BCR. Consistent with this notion, further analysis revealed that ATP11C-deficient mice have reduced Cμ$^+$ pre-B cells in the bone marrow, and these cells express lower levels of CD24, whose expression is upregulated by the pre-BCR signalling. The frequency of Cμ$^+$ cells in mutant mice was lower than that of *Cd79a*$^{-/-}$ mice, which are deficient in pre-BCR signalling, as CD79α constitutes an important component of the pre-BCR (Torres et al., 1996). These data collectively suggest a role for ATP11C in the expression and/or signalling through the pre-BCR.

IL-7 plays critical roles in the survival, proliferation and differentiation of pro- and pre-B cells (Corfe and Paige, 2012). Given the importance of IL-7 in early B cell development, it is likely that impaired signalling through the IL-7R could explain the phenotype in mutant mice. In keeping with this notion, there was no phenotypic difference between mutant mice and mutant mice with an *Il7* transgene, suggesting

that in the absence of ATP11C developing B cells may have a defect in IL-7R signalling. This lack of signalling through the IL-7R could cause increased apoptosis of developing B cells in ATP11C mutant mice. Recently, Malin et al. suggested that BCL-2, an important anti-apoptotic survival protein that prevents cells from undergoing mitochondrial apoptosis (Youle and Strasser, 2008), could replace the survival, but not proliferative function of IL-7R signalling in pro-B cells (Malin et al., 2010b). The authors showed that transgenic expression of BCL-2 in mice deficient for IL-7R resulted in a partial increase in the number of pro-, pre- and total B cell numbers in the bone marrow (Malin et al., 2010b). However, no rescue in B cell development and numbers of mature B cells was observed in ATP11C-deficient mice with transgenic expression of BCL-2. These results collectively suggest that the developmental arrest at the pro-B cell stage of B lymphopoiesis in ATP11C-deficient mice is more fundamental than simply a diminished survival signal or through increased apoptosis.

A synergistic interaction between the IL-7R and pre-BCR signalling has been suggested to mediate the transition from pro- to pre-B cells in the bone marrow (Fleming and Paige, 2002), suggesting that a defect in one pathway could possibly affect another pathway. Therefore, one hypothesis for the developmental arrest in B lymphopoiesis of ATP11C-deficient mice would be that the ATP11C^{amb} mutation might influence either IL-7R or pre-BCR signalling, which leads to disruption of another pathway. The possible effect(s) of the ATP11C^{amb} mutation on these signalling pathways are, therefore, noteworthy and will be examined in more detail in the next chapter.

CHAPTER 5: Analysing the components of the IL-7R and pre-BCR signalling as a candidate pathway responsible for the defect in B cells from *Atp11c*$^{amb/0}$ mice

Contents of Figure 5.1, and 5.2 appeared in:

Mehmet Yabas, Charis E. I, Sandra Frankenreiter, Dennis Lal, Carla M. Roots, Belinda Whittle, Daniel T. Andrews, Yafei Zhang, Narci C. Teoh, Jonathan Sprent, Lina E. Tze, Edyta M. Kucharska, Jennifer Kofler, Geoffrey C. Farell, Stefan Bröer, Christopher C. Goodnow and Anselm Enders (2011). "ATP11C is critical for the internalization of phosphatidylserine and differentiation B lymphocytes". *Nature Immunology*, 12(5):441-449.

Contributions from others:

- Mr. Hannes Bergmann provided technical help in the sample preparation and organisation of the microarray experiment.
- Mrs. Debbie Howard provided technical help in the irradiation of mice and intravenous injection of cells in the bone marrow chimera experiments.

5.1 Preamble

The IL-7R signalling and expression and signalling through the pre-BCR are two crucial processes for pre-B cell development in the bone marrow (Herzog et al., 2009, Clark et al., 2014, Reth and Nielsen, 2014). The findings in the previous chapter suggest that ATP11C might play a role in these two signalling pathways. Therefore, in this chapter the effect of the ATP11C^{amb} mutation on signalling through the IL-7R and pre-BCR will be examined.

5.2 The effect of the ATP11C^{amb} mutation on IL-7R signalling

5.2.1 Normal IL-7Rα (CD127) expression in ATP11C-deficient pro-B cells

Pro- and pre-B cells express the IL-7Rα at the cell surface and internalise the receptor after binding to IL-7, which mediates crucial signalling events required for normal B cell development in the bone marrow (Corfe and Paige, 2012). I first wanted to determine whether the *in vivo* IL-7 unresponsiveness in *Atp11c*$^{amb.0}$ pro-B cells could be explained by the lack of IL-7R expression. Bone marrow cells were stained for surface expression of IL-7Rα by flow cytometry, and pro-B cells from *Atp11c*$^{amb.0}$ mice displayed an increased expression of IL-7Rα. A similar increase in IL-7Rα expression was also observed on pro-B cells in *Atp11c*$^{amb.0}$ mice with an *H2Ea-Il7* transgene compared to wild-type controls (Figure 5.1A, B). This increased expression was similar to IL-7Rα expression on bone marrow cells of pre-BCR deficient animals (*Cd79a*$^{-/-}$ and *Rag1*$^{-/-}$) (Figure 5.1B). The increased IL-7Rα expression *Cd79a*$^{-/-}$ and *Rag1*$^{-/-}$ animals could possibly be due to a compensatory increase as these mice are defective in the later development stage, that is pre-BCR signalling. These data indicate that the absence of an *in vivo* response to the *Il7* transgene in *Atp11c*$^{amb.0}$ mice is not explained by failure to express the receptor, but could be due to a defect in responding to IL-7.

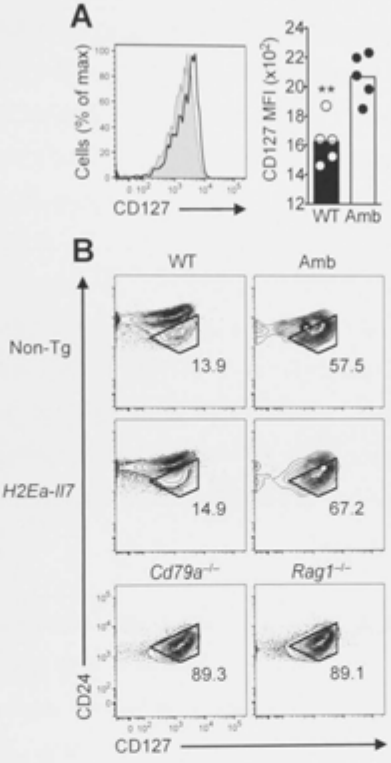

Figure 5.1 Increased IL-7Rα expression on pro-B cells from *Atp11c*$^{amb/0}$ mice

(A) Expression of CD127 (IL-7Rα) on CD24^{med}CD19^{+}IgM^{-}B220^{lo} pro-B cells from *Atp11c*$^{+/0}$ (WT, shaded area) and *Atp11c*$^{amb/0}$ (Amb, black line) mice. Graph shows the MFI of CD127 expression on pro-B cells from multiple animals of each genotype. **(B)** Panels below show representative flow cytometric analysis of CD24 versus CD127 on CD19^{+}IgM^{-} B220^{lo}7AAD^{-} cells in bone marrow from non-transgenic or IL-7 transgenic mice with wild-type (WT) or mutant (Amb) ATP11C, or from *Cd79a*$^{-/-}$ and *Rag1*$^{-/-}$ mice. The subset of CD24^{med} pro-B cells is shown in the gate. Data are representative of three different experiments with one to three mice per genotype in each. Statistical significance was calculated using the two-tailed Student's *t*-test. ** $P < .01$.

5.2.2 Pro-B cells from *Atp11c*$^{amb/0}$ mice are able to proliferate normally in response to high concentration of IL-7 *in vitro*

In vitro culture of pro-B cells in the presence of high doses of IL-7 induces a strong proliferation, and this can be used to measure signalling through the IL-7R. Therefore, I next examined the competence of the mutant pro-B cells to undergo *in vitro* proliferation and to become IgM$^+$ cells in response to IL-7 signalling. Pro-B cells from mutant and wild-type animals were flow sorted and cultured in the presence of high concentration of IL-7 (25 ng/ml), and analysed 7 days after culture. The mutant and wild-type pro-B cells increased in numbers identically over 7 days (Figure 5.2A), indicating that pro-B cells isolated from *Atp11c*$^{amb/0}$ mice exhibited a normal proliferative response to IL-7 relative to pro-B cells from *Atp11c*$^{+/0}$ animals. However, when the differentiation of these cells was analysed by measuring the fraction that had become small pre-B and sIgM$^+$ immature B cells, a much lower fraction of the mutant pro-B cells had differentiated compared to control cells (Figure 5.2B). These results indicate that the ATP11C^{amb} mutation does not interfere with IL-7R-induced proliferation of pro-B cells, but disrupts their differentiation into IgM$^+$ B cells.

5.2.3 ATP11C-deficient pro-B cells display a defective proliferation response to the limiting concentration of IL-7 *in vitro*

I next wanted to determine the ability of mutant pro-B cells to proliferate in the presence of a wide range of IL-7 concentrations *in vitro*. Because expression of pre-BCR on pro-B cells has been suggested to control the ability of cells to respond to the limiting concentration of IL-7 (Marshall et al., 1998, Fleming and Paige, 2001), I used mice on a RAG-deficient background. This allows me to examine the effect of the ATP11C^{amb} mutation on IL-7R signalling in isolation without any interference from possibly also affected pre-BCR signalling. CD19$^+$ pro-B cells from the bone marrow of *Rag1*$^{-/-}$ and *Atp11c*$^{amb/0}$ *Rag1*$^{-/-}$ double deficient mice were magnetically enriched, labelled with the cell proliferation dye CFSE and cultured in the absence and presence of different concentrations of IL-7 for 4 days. At the of culture period, cells were analysed by flow cytometry and proliferation was determined by the percentage of CFSE diluting cells.

Consistent with the published data (Marshall et al., 1998, Fleming and Paige, 2001), pro-B cells from *Rag1*$^{-/-}$ animals showed no response to lower concentration of IL-7, and some proliferation when the IL-7 concentration reached 20 picogram/ml (Figure 5.3). However, nearly all cells proliferated once the IL-7 concentration reached 1 ng/ml (Figure 5.3). Likewise, the data revealed that pro-B cells isolated from *Atp11c*$^{amb/0}$ *Rag1*$^{-/-}$ double deficient animals also exhibit no proliferation in response to low concentrations of IL-7 (Figure 5.3). The proliferative capacity of the *Atp11c*$^{amb/0}$ *Rag1*$^{-/-}$ pro-B cells was similar to that observed with the *Rag1*$^{-/-}$ pro-B cells, but there was a small concentration range where IL-7 was permissive for proliferation of the *Rag1*$^{-/-}$ cells but not the double deficient pro-B cells (Figure 5.3). Since *Rag1*$^{-/-}$ mice have essentially normal IL-7R signalling, the similar proliferation profile of pro-B cells in *Rag1*$^{-/-}$ and *Atp11c*$^{amb/0}$ *Rag1*$^{-/-}$ double deficient animals in response to the high concentrations of IL-7 suggests a normal IL-7R signalling in ATP11C-deficient pro-B cells. However, it should be noted that this experiment was performed only once, and needs to be repeated to test whether the small differences in proliferation of ATP11C-deficient pro-B cells in response to low concentrations of IL-7 is reproducible.

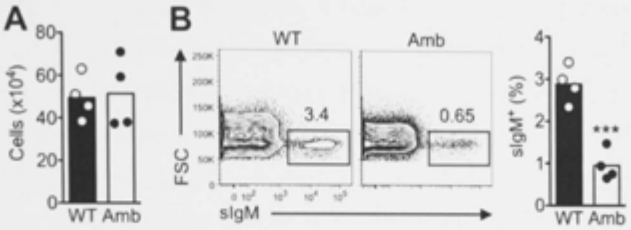

Figure 5.2 Normal *in vitro* proliferation of flow-sorted ATP11C-deficient pro-B cells in response to high concentration of IL-7, but defective differentiation into sIgM$^+$ cells
Flow sorted pro-B cells from *Atp11c*$^{+/0}$ (WT) and *Atp11c*$^{amb/0}$ (Amb) mice were cultured in the presence of 25 ng/ml IL-7 for 7 days. **(A)** Graph shows absolute number of cells after 7 days culture of sorted pro-B cells in the presence of 25 ng/ml IL-7. **(B)** Representative flow cytometric plots showing the percentage of surface IgM$^+$ cells out of all live B220$^+$ cells after 7 day culture of sorted pro-B cells in the presence of 25 ng/ml IL-7. Statistical significance was calculated using the two-tailed Student's *t*-test. *** $P < .001$.

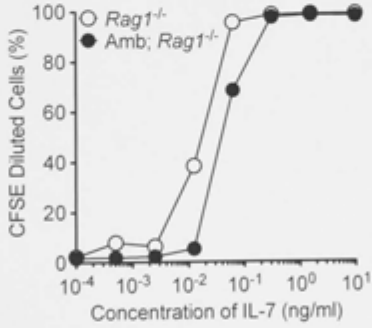

Figure 5.3 Defective *in vitro* proliferation of Macs-sorted pro-B cells from *Atp11c*$^{amb/0}$ *Rag1*$^{-/-}$ double deficient mice in response to low concentrations of IL-7
Macs sorted CD19$^+$ pro-B cells from *Rag1*$^{-/-}$ and *Atp11c*$^{amb/0}$ *Rag1*$^{-/-}$ (Amb; *Rag1*$^{-/-}$) mice were labelled with the cell proliferation dye CFSE and cultured in the absence or presence of various concentrations of IL-7 for 4 days. Graph shows the percentage of CFSE diluted cells after 4 days culture of sorted pro-B cells in the absence or presence of various concentrations of IL-7.

5.2.4 Loss of ATP11C does not compromise STAT5 phosphorylation in pro-B cells upon IL-7 stimulation *in vitro*

The signalling of IL-7/IL-7R is mediated through the JAK-STAT pathway that leads to STAT5 activation (Hofmeister et al., 1999). The results shown above indicate that pro-B cells from ATP11C-deficient animals proliferated normally in response to high concentrations of IL-7, suggesting a most likely intact signalling through the IL-7R. To further support this, *Rag1*$^{-/-}$ and *Atp11c*$^{amb.0}$ *Rag1*$^{-/-}$ double deficient pro-B cells were cultured for 20 minutes *in vitro* with 0.02 and 10 ng/ml IL-7 and stained intracellularly with anti-pSTAT5.

The data shown in Figure 5.4 indicates that *Rag1*$^{-/-}$ and *Atp11c*$^{amb.0}$ *Rag1*$^{-/-}$ double deficient pro-B cells cultured alone or with different concentrations of IL-7 displayed equivalent levels of p-STAT5 expression that increased in a dose dependent manner in response to IL-7 (Figure 5.4). Therefore, these results indicate that the membrane proximal signalling events downstream of IL-7R is not compromised in ATP11C-deficient pro-B cells.

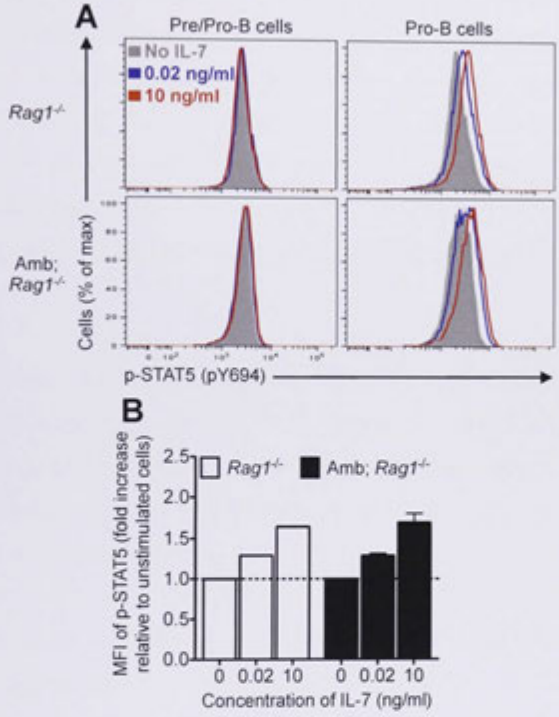

Figure 5.4 Normal IL-7-induced STAT5 phosphorylation in pro-B cells from *Atp11c*$^{amb/0}$ *Rag1*$^{-/-}$ double deficient mice

(A) Representative overlay histograms comparing p-STAT5 (pY694) expression on *Rag1*$^{-/-}$ and *Atp11c*$^{amb/0}$ *Rag1*$^{-/-}$ (Amb; *Rag1*$^{-/-}$) double deficient pre/pro-B and pro-B cells cultured in the absence or presence of 0.02 and 10 ng/ml of IL-7 for 20 min. Cells were then fixed, permeabilised and stained with p-STAT5 intracellularly. **(B)** Graph shows the fold change in MFI of p-STAT5 expression on pro-B cells in the presence of IL-7 over media alone. Data are representative of two independent experiments.

5.3 The effect of the ATP11C^{amb} mutation on pre-BCR signalling

5.3.1 *In vivo* cross-linking of Igβ on pro-B cells from ATP11C-deficient animals fails to induce pre-B cell differentiation

Given that ATP11C-deficient animals have a developmental block at the pro- to pre-B transition and show a defective proliferative capacity in response to low concentrations of IL-7 similar to the pre-BCR deficient mice, I hypothesised that a specific failure in the expression and/or signalling through the pre-BCR could explain the B cell deficiency in mutant animals. To test this hypothesis, I took advantage of the experimental system in which treatment of *Rag2*$^{-/-}$ mice with an antibody against Igβ (CD79b) can mimic pre-BCR signalling and induce differentiation of RAG2-deficient pro-B cells into pre-B cells *in vivo* (Nagata et al., 1997).

Mixed bone marrow chimeras were set up as shown in Figure 5.5 to test the ability of pro-B cells from *Rag1*$^{-/-}$ and *Atp11c*$^{amb/0}$ mice to respond anti-Igβ antibody treatment under the same experimental conditions (Figure 5.5). *Rag1*$^{-/-}$ recipient mice were given one dose of irradiation prior to intravenous injection of bone marrow cells mixed at a 1:1 ratio from CD45.2 *Rag1*$^{-/-}$ and CD45.1 *Atp11c*$^{amb/0}$ mice (Figure 5.5). Five to eight weeks post reconstitution recipient mice were given a single intraperitoneal injection of PBS or 200μg antibody against Igβ, and B cells in the bone marrow were examined by flow cytometry (Figure 5.5).

Seven days after treatment there was an increase in the number of *Rag1*$^{-/-}$-derived total B cells in the bone marrow of recipient mice treated with anti-Igβ compared to those injected with PBS (Figure 5.6A, B). The antibody treatment also induced differentiation of *Rag1*$^{-/-}$-derived pro-B cells into pre-B cells as determined by a 17-fold increase in the number cells that express the pre-B cell marker CD25 on their surface (Figure 5.6A, B). The increase in total B and pre-B cell numbers in anti-Igβ injected recipient mice cannot be attributed to the different number of leukocytes in different recipients, because the number of non-B cells in anti-Igβ treated recipients was comparable to that in PBS injected recipients (Figure 5.6B). In contrast, anti-Igβ injection had no impact on mutant-derived pro-B cells in recipient mice as the number of mutant derived total B cells and CD25^{+} pre-B cells were not increased

upon anti-Igβ treatment compared to mutant cells from PBS-treated recipient mice (Figure 5.6A, B).

Pre-B cell differentiation from RAG-deficient pro-B cells after anti-Igβ treatment could also be confirmed by the expression of different pro- and pre-B cell surface markers (Nagata et al., 1997). While antibody treatment induces down-regulation of pro-B cell markers such as CD43 and C-Kit, the expression of pre-B cell markers such as CD25 and BP-1 are up-regulated, and these phenotypic changes are linked to the transition from pro-B cells to pre-B cells (Nagata et al., 1997). Consistent with the published data (Nagata et al., 1997), expression of CD25 was up-regulated, and expression of CD43 and C-Kit was down-regulated in *Rag1*$^{-/-}$-derived B cells after anti-Igβ antibody treatment (Figure 5.6A and 5.7). Moreover, antibody treatment caused changes in the side and forward scatter profiles of B cells derived from *Rag1*$^{-/-}$ bone marrow cells (Figure 5.7). However, none of these changes was observed in B cells derived from *Atp11c*$^{amb.0}$ bone marrow cells after anti-Igβ antibody treatment (Figure 5.7). These data indicate that pro-B cells from the bone marrow of ATP11C-deficient animals fail to respond to Igβ cross-linking *in vivo*.

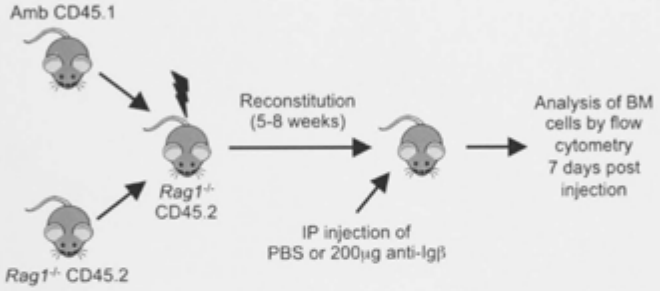

Figure 5.5 Experimental design of mixed bone marrow chimera approach to test whether cross-linking of Igβ induces differentiation of ATP11C-deficient-derived pro-B cells into pre-B cells

Bone marrow chimeric mice were generated by the injection of congenic (CD45.1) bone marrow cells from *Atp11c*$^{amb\,0}$ (Amb) animals mixed at a 1:1 ratio with *Rag1*$^{-/-}$ bone marrow cells (CD45.2) into irradiated *Rag1*$^{-/-}$ recipients (CD45.2). 5-8 weeks after reconstitution, the recipient mice were intraperitoneally injected with PBS or 200μg anti-Igβ antibody, and B cells in the bone marrow of the recipient mice were analysed 7 days post treatment by flow cytometry.

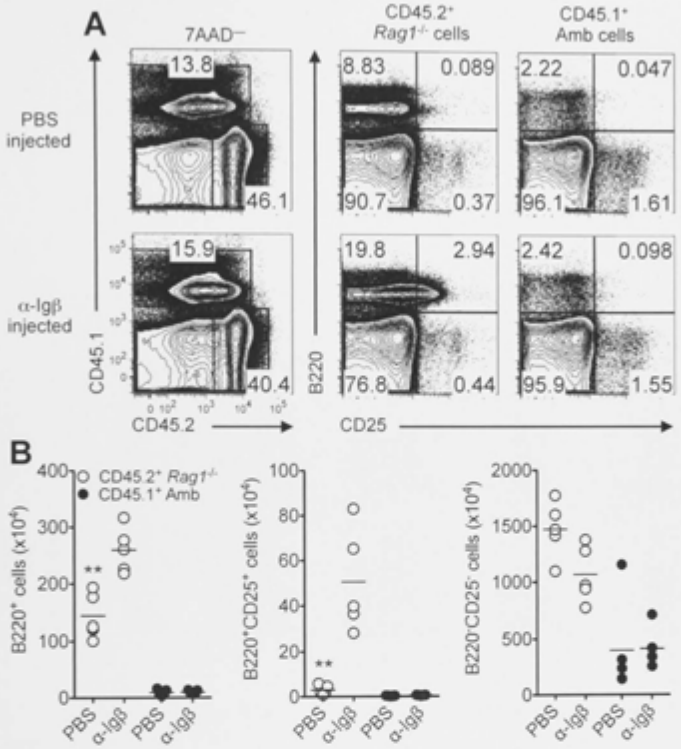

Figure 5.6 Defective Igβ-mediated pro- to pre-B cell transition in *Atp11c*$^{amb\,0}$-derived bone marrow cells

(A) Representative flow cytometric analysis of bone marrow cells from PBS or anti-Igβ treated-chimeric recipients that were irradiated and reconstituted with a mixture of CD45.2$^+$ *Rag1*$^{-/-}$ and CD45.1$^+$ *Atp11c*$^{amb\,0}$ (Amb) bone marrow cells. Numbers adjacent to outlined areas indicate percentage of CD45.2$^+$ *Rag1*$^{-/-}$- and CD45.1$^+$ *Atp11c*$^{amb\,0}$ (Amb)-derived cells (left); percentage of B220$^+$CD25$^-$ pro-B cells, B220$^+$CD25$^+$ pre-B cells, and B220$^-$CD25$^-$ non-B cells within the CD45.2$^+$ and CD45.1$^+$ donor derived cells (middle and right). **(B)** Graphs show absolute number of CD45.2$^+$ *Rag1*$^{-/-}$- and CD45.1$^+$ *Atp11c*$^{amb\,0}$ (Amb)-derived B220$^+$ total B cells (left), B220$^+$CD25$^+$ pre-B cells (middle) and B220$^-$CD25$^-$ non-B cells (right) in the bone marrow of chimeric recipients that were treated with PBS or anti-Igβ antibody. Each circle represents a single mouse, and data are pooled from two different experiments. Statistical significance was calculated using the two-tailed Student's *t*-test. ** $P < .01$.

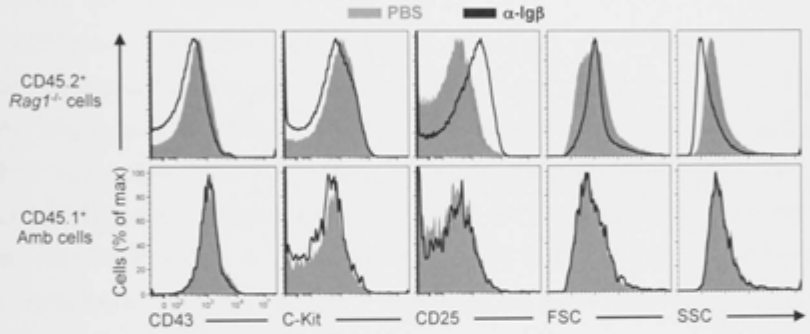

Figure 5.7 Anti-Igβ treatment fails to upregulate pre-B cell markers in *Atp11c*$^{amb/0}$-derived bone marrow cells

Representative flow cytometric analysis of surface expression of CD43, C-Kit, CD25, Forward Scatter (FSC) and Side Scatter (SSC) on CD45.2$^+$ *Rag1*$^{-/-}$- and CD45.1$^+$ *Atp11c*$^{amb/0}$ (Amb)-derived 7AAD$^-$B220$^+$ B cells within the chimeric recipients that were treated with PBS or anti-Igβ antibody. Data are representative of two independent experiments with two to three mice in each.

5.3.2 *In vivo* cross-linking of Igβ on *Atp11c*$^{amb/0}$ *Rag1*$^{-/-}$ double deficient pro-B cells fails to induce pre-B cell differentiation

The *in vivo* Igβ-stimulation-induced pre-B cell differentiation system was also tested in *Atp11c*$^{amb/0}$ mice on a RAG-deficient background in order to exclude any possible effect of pre-B cells that are present in ATP11C-deficient mice. *Rag1*$^{-/-}$ and *Atp11c*$^{amb/0}$ *Rag1*$^{-/-}$ double deficient animals were injected with anti-Igβ antibody, and the number of total B and pre-B cells in the bone marrow was determined seven days post treatment as detailed above.

Consistent with the published results (Nagata et al., 1997) and results shown above, anti-Igβ antibody treatment led to an increase in the number of total B cells and CD25^{+} pre-B cells in *Rag1*$^{-/-}$ mice compared to those injected with PBS (Figure 5.8A, B). In contrast, there was no such increase in the number of total B and pre-B cells in the bone marrow of anti-Igβ antibody treated *Atp11c*$^{amb/0}$ *Rag1*$^{-/-}$ mice compared to PBS treated *Atp11c*$^{amb/0}$ *Rag1*$^{-/-}$ mice (Figure 5.8A, B). While antibody treatment caused changes in the expression of pro- and pre-B cell markers as well as forward and side scatter profiles in B cells from *Rag1*$^{-/-}$ mice, no such changes were observed in bone marrow cells from *Atp11c*$^{amb/0}$ *Rag1*$^{-/-}$ animals injected with Igβ (Figure 5.9).

5.3.3 *In vivo* cross-linking of Igβ on *Atp11c*$^{amb/0}$ *Rag1*$^{-/-}$ double deficient pro-B cells fails to induce Ca^{2+} mobilisation

Upon activation, signalling through the BCR results in intracellular Ca^{2+} flux (Kurosaki et al., 2010). To further test the signalling capacity of the pre-BCR in *Atp11c*$^{amb/0}$ *Rag1*$^{-/-}$ mice, I examined the ability of flow sorted pro-B cells from *Atp11c*$^{amb/0}$ *Rag1*$^{-/-}$ animals to induce Ca^{2+} flux after anti-Igβ cross-linking. Consistent with the published data (Schwickert et al., 2014), treatment with anti-Igβ antibody led to an increase in Ca^{2+} mobilisation in pro-B cells from RAG1-deficient mice (Figure 5.10), indicating that anti-Igβ crosslinking in pro-B cells induces pre-BCR signalling-dependent Ca^{2+} release. However, pro-B cells from *Atp11c*$^{amb/0}$ *Rag1*$^{-/-}$ animals displayed no Ca^{2+} mobilisation upon anti-Igβ treatment, despite a comparable baseline intracellular concentration of Ca^{2+} to RAG-deficient pro-B cells and equivalent increase in Ca^{2+} mobilisation in response to treatment with the Ca^{2+}

ionophore ionomycin (Figure 5.10). These data suggest a defective Igβ-induced pre-BCR signalling-driven Ca^{2+} flux in ATP11C-deficient pro-B cells.

These data illustrate that the differentiation of pre-B cells mediated by an antibody treatment against Igβ is impaired in ATP11C-deficient B cells, suggesting an essential role for ATP11C in the formation and/or signalling through the pre-BCR.

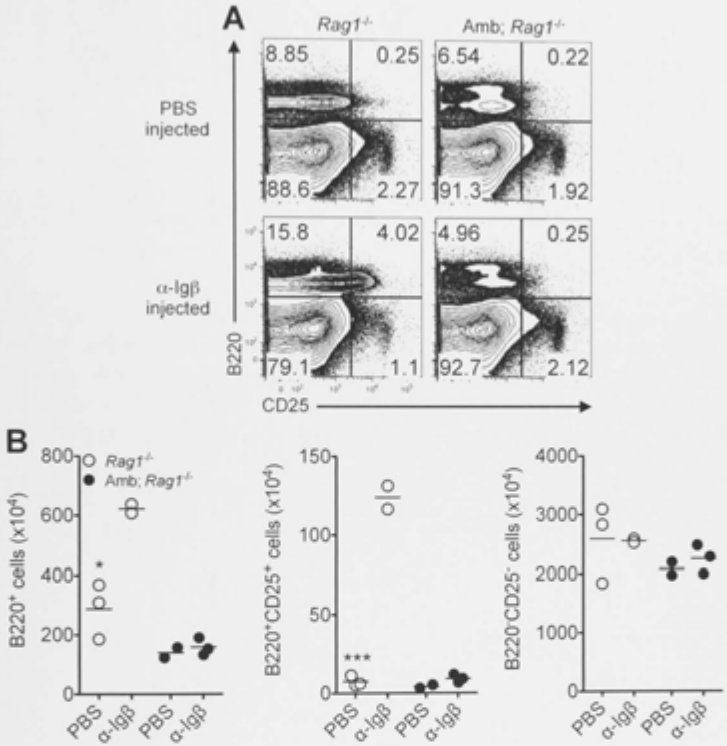

Figure 5.8 Defective Igβ-mediated pro- to pre-B cell transition in *Atp11c*$^{amb\,0}$ *Rag1*$^{-/-}$ double deficient animals

(A) Representative flow cytometric analysis of bone marrow cells from PBS or anti-Igβ antibody treated *Rag1*$^{-/-}$ and *Atp11c*$^{amb\,0}$ *Rag1*$^{-/-}$ (Amb; *Rag1*$^{-/-}$) mice. Numbers adjacent to outlined areas indicate percentage of B220^{+}CD25^{-} pro-B cells, B220^{+}CD25^{+} pre-B cells, and B220^{-}CD25^{-} non-B cells within the 7AAD^{-} lymphocytes. **(B)** Graphs show absolute number of B220^{+} total B cells (left), B220^{+}CD25^{+} pre-B cells (middle) and B220^{-}CD25^{-} non-B cells (right) PBS or anti-Igβ antibody treated *Rag1*$^{-/-}$ and *Atp11c*$^{amb\,0}$ *Rag1*$^{-/-}$ (Amb; *Rag1*$^{-/-}$) mice. Each circle represents a single mouse. Statistical significance was calculated using the two-tailed Student's *t*-test. *** $P < .001$; * $P < .05$.

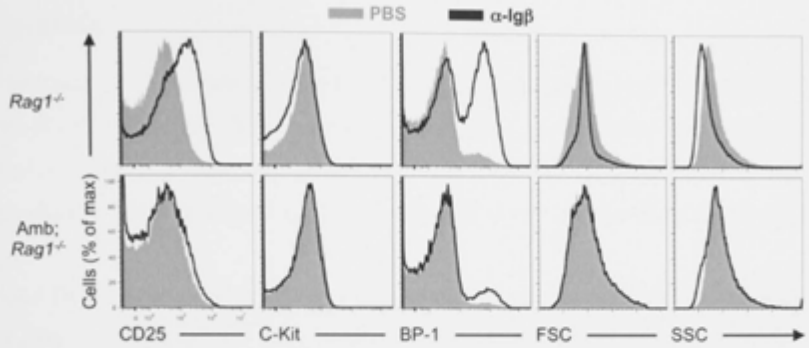

Figure 5.9 Anti-Igβ treatment fails to upregulate pre-B cell markers in *Atp11c*$^{amb\,0}$ *Rag1*$^{-/-}$ double deficient pro-B cells

Representative flow cytometric analysis of surface expression of CD25, C-Kit, BP-1, Forward Scatter (FSC) and Side Scatter (SSC) on 7AAD^{-}B220^{+} B cells from the bone marrow of PBS or anti-Igβ antibody treated *Rag1*$^{-/-}$ and *Atp11c*$^{amb\,0}$ *Rag1*$^{-/-}$ (Amb; *Rag1*$^{-/-}$) mice.

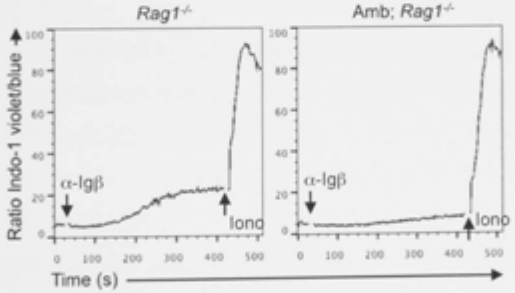

Figure 5.10 Pro-B cells from *Atp11c*$^{amb\,0}$ *Rag1*$^{-/-}$ double deficient animals fail to induce anti-Igβ-induced Ca^{2+} flux

Flow cytometry analysis of Ca^{2+} measurements after stimulation with anti-Igβ in sorted pro-B cells from *Rag1*$^{-/-}$ and *Atp11c*$^{amb\,0}$ *Rag1*$^{-/-}$ (Amb; *Rag1*$^{-/-}$) mice. Flow sorted pro-B cells were incubated with Indo-1 and analysed on flow cytometry for Ca^{2+} mobilisation after stimulation. Ionomycin (Iono) is used as a positive control. Arrows indicate addition of the stimuli. Data are representative of three independent experiments with one to two mice in each.

5.4 Microarray analysis in pro-B cells for the characterisation of dysregulayed genes that are associated with IL-7R and pre-BCR signalling

I next wanted to compare the pattern of gene expression in *Atp11c*$^{+/0}$ and *Atp11c*$^{amb/0}$ pro-B cells to identify differentially regulated genes. A microarray gene expression analysis was undertaken on flow-sorted 7AAD$^-$B220$^+$IgD$^-$IgM$^-$CD24^{int}CD43$^+$BP-1$^-$ pro-B cells from control and mutant animals (~95% pure populations after sorting).

5.4.1 Dysregulation of IL-7R signalling-related genes in ATP11C-deficient pro-B cells

The first set of genes examined were those whose expression is controlled by IL-7R signalling. The binding of IL-7 to its receptor leads to activation JAK-STAT5 pathway, which promotes pro-B cell survival by regulating anti-apoptotic proteins BCL-2, BCL-$_{XL}$ and MCL-1 and pro-apoptotic proteins BAX, BAD and BIM (Corfe and Paige, 2012). As shown in Table 5.1, the expression of a range of pro- and anti-apoptotic genes including *Mcl1*, *Bax* and *Bad* was reduced in mutant pro-B cells, but the expression of *Bcl2* and *Bcl2l1* remained unaltered compared to pro-B cells from control mice (Table 5.1).

Activation of STAT5 mediated by IL-7R signalling also promotes *Ccnd3* (Mandal et al., 2009), whose expression is required for pro- and pre-B cell proliferation (Cooper et al., 2006, Powers et al., 2012). Consistent with the data that mutant pro-B cells are able to proliferate normally in response to elevated level of IL-7 *in vitro*, mutant pro-B cells had normal *Ccnd3* expression compared to those from control animals (Table 5.1). STAT5 activation also plays an important role in B cell specification and commitment by inducing EBF1 expression (Kikuchi et al., 2005), which in turn promotes PAX5 expression (Figure 1.2A) (O'Riordan and Grosschedl, 1999). The mRNA level of *Ebf1*, but not *Pax5*, was decreased in ATP11C-deficient pro-B cells compared to those from control animals (Table 5.1).

Activation of the PI3K-AKT pathway by IL-7 signalling negatively regulates the transcription factor FOXO1 that directly controls the expression of *Rag1* and *Rag2* (Amin and Schlissel, 2008, Herzog et al., 2008). Therefore, I also looked at the

expression of the genes encoding FOXO1, RAG1 and RAG2, and found a significant reduction in the *Foxo1* transcript in pro-B cells from ATP11C mutant mice (Table 5.1). However, the level of *Rag1* and *Rag2* transcripts in mutant pro-B cells was not significantly reduced compared to control mice (Table 5.1).

Expression of a range of genes that are required for signalling through the IL-7R was also examined. mRNA levels of genes encoding STAT5A and STAT5B were significantly reduced in mutant pro-B cells compared to cells from control animals while the expression of *Jak1* and *Jak3* was mostly comparable (Table 5.2). However, these data are at odds with results of normal phosphorylation of STAT5 upon *in vitro* IL-7 stimulation.

Gene	Systematic Name	WT Pro-B cells (n=3)	Amb Pro-B cells (n=3)	Fold Change	*P*
Mcl1	NM_008562	894 ± 33	510 ± 50	- 1.75	0.0030
Bcl2	NM_177410	31 ± 1	34 ± 7	+ 1.10	0.6466
Bcl2l1	NM_009743	425 ±22	372 ± 42	- 1.14	0.3304
Bax	NM_007527	366 ± 16	267 ± 19	- 1.37	0.0161
Bad	NM_007522	348 ± 15	241 ± 27	- 1.44	0.0263
Ccnd3	NM_007632	3182 ± 119	3474 ± 516	- 1.09	0.6106
Ebf1	NM_007897	779 ± 17	492 ± 83	- 1.58	0.0277
Pax5	NM_008782	41 ± 4	31 ± 8	- 1.32	0.3313
Foxo1	NM_019739	711 ± 21	460 ± 50	- 1.55	0.0096
Rag1	NM_009019	535 ± 73	323 ± 39	- 1.66	0.0619
Rag2	NM_009020	405 ± 41	261 ± 48	- 1.55	0.0848

Table 5.1 Microarray analysis of genes encoding downstream of IL-7R signalling

Table shows the mean ± S.E.M. of relative expression values as estimated by microarray analysis for a set of genes encoding downstream of IL-7R signalling in sorted pro-B cells from *Atp11c*$^{+/0}$ (WT) and *Atp11c*$^{amb/0}$ (Amb) mice. The data were generated by hybridisation of RNA to Agilent microarrays. Statistical significance was calculated using the two-tailed Student's *t*-test.

Gene	Systematic Name	WT Pro-B cells (n=3)	Amb Pro-B cells (n=3)	Fold Change	*P*
Stat5a	NM_011488	62 ± 2	47 ± 4	- 1.32	0.0249
Stat5b	NM_011489	147 ± 6	106 ± 12	- 1.39	0.0373
Jak1	NM_146145	431 ± 46	323 ± 48	- 1.33	0.1790
Jak3	NM_001190830	103 ± 7	70 ± 11	- 1.47	0.0650

Table 5.2 Microarray analysis of genes encoding components of IL-7R signalling

Table shows the mean ± S.E.M. of relative expression values as estimated by microarray analysis for a set of genes encoding the components of IL-7R signalling in sorted pro-B cells from *Atp11c*$^{+/0}$ (WT) and *Atp11c*$^{amb/0}$ (Amb) mice. The data were generated by hybridisation of RNA to Agilent microarrays. Statistical significance was calculated using the two-tailed Student's *t*-test.

5.4.2 Microarray analysis of pro-B cells reveals dysregulated expression of genes related to the pre-BCR signalling

I also compared the expression of genes involved in the assembly and signalling through the pre-BCR. The levels of *Syk* and *Btk*, which are downstream of the pre-BCR signalling, were significantly reduced in pro-B cells from ATP11C-deficient mice despite normal expression of *Blnk* and *Plcg2*, which are also downstream of the pre-BCR (Table 5.3). Src-family protein tyrosine kinases Blk, Fyn and Lyn were shown to play an essential role in B cell development through pre-BCR-mediated NFκB activation as triple knock out exhibited a developmental block in early B cell development (Saijo et al., 2003). Intriguingly, there was a downward trend of gene expression of *Blk* and *Fyn* but these were not significant whereas *Lyn* expression was significantly reduced in pro-B cells of ATP11C-deficient mice compared to those in control animals (Table 5.3). The analysis of genes encoding the key components of the pre-BCR complex illustrated that pro-B cells from mutant animals also exhibit significantly reduced expression of these genes including *Vpreb1*, *Vpreb2*, *Vpreb3*, *Igll1*, *Cd79a* and *Cd79b* (Table 5.4).

There are a number of genes encoding important transcription factors involved in the specification and commitment of B cell lineage including Ikaros-1, E2A, and IRF4. The transcript levels of genes encoding these transcription factors as well as the transmembrane receptor CD93 were significantly reduced in pro-B cells from *Atp11c*$^{amb/0}$ mice compared to those from *Atp11*$^{+/0}$ animals (Table 5.5). Moreover, expression of other B-cell specific genes such as *Irf8* and *Cd19* showed also a trend towards reduced expression in mutant pro-B cells without the differences reaching statistically significance (Table 5.5). These data collectively suggest that the ATP11C^{amb} mutation causes a reduced gene expression pattern for most known genes that are involved in the pre-BCR signalling and B-cell lineage specification and commitment.

In conclusion, the data from the microarray analysis together with results shown above suggest that the ATP11C^{amb} mutation has apparently no direct effect on the signalling through the IL-7R. Similar to pre-BCR-deficient *Rag1*$^{-/-}$ mice, the inability of mutant pro-B cells to proliferate in response to lower levels of IL-7 and the presence of few differential changes in the expression of IL-7R signalling-related

genes in ATP11C-deficient pro-B cells could possibly be due to a diminished later developmental stage (i.e. pre-BCR signalling). Indeed, the defective Igβ-mediated pre-B cell expansion together with the microarray results suggest that ATP11C is crucial for the expression and/or signalling through the pre-BCR. However, further studies are needed to validate the microarray results and also dissect which stage of the pre-BCR signalling is specifically affected by the ATP11C^{amb} mutation.

Gene	Systematic Name	WT Pro-B cells (n=3)	Amb Pro-B cells (n=3)	Fold Change	P
Syk	NM_011518	1001 ± 56	613 ± 72	- 1.63	0.0131
Btk	NM_013482	682 ± 30	473 ± 66	- 1.44	0.0422
Blnk	NM_008528	7546 ± 141	5624 ± 772	- 1.34	0.0706
Plcg2	NM_172285	1963 ± 34	1508 ± 217	- 1.30	0.1065
Blk	NM_007549	34 ± 4	21 ± 2	- 1.62	0.0576
Lyn	NM_001111096	14 ± 0.6	8 ± 0.3	- 1.75	0.0007
Fyn	NM_001122893	32 ± 2	24 ± 4	- 1.33	0.1296

Table 5.3 Microarray analysis of genes encoding downstream of pre-BCR signalling

Table shows the mean ± S.E.M. of relative expression values as estimated by microarray analysis for a set of genes encoding downstream of pre-BCR signalling in sorted pro-B cells from *Atp11c*$^{+/0}$ (WT) and *Atp11c*$^{amb/0}$ (Amb) mice. The data were generated by hybridisation of RNA to Agilent microarrays. Statistical significance was calculated using the two-tailed Student's *t*-test.

Gene	Systematic Name	WT Pro-B cells (n=3)	Amb Pro-B cells (n=3)	Fold Change	P
Igll1	NM_001190325	3117 ± 108	1856 ± 232	- 1.70	0.0078
Vpreb1	NM_016982	13389 ± 512	8703 ± 1093	- 1.54	0.0178
Vpreb2	NM_016983	2056 ± 28	1209 ± 96	- 1.70	0.0011
Vpreb3	NM_009514	10448 ± 299	6814 ± 980	- 1.53	0.0238
Cd79a	BC027633	2050 ± 81	1260 ± 152	- 1.63	0.0102
Cd79b	NM_008339	4853 ± 279	3186 ± 367	- 1.52	0.0223

Table 5.4 Microarray analysis of genes encoding components of pre-BCR signalling

Table shows the mean ± S.E.M. of relative expression values as estimated by microarray analysis for a set of genes encoding the components of pre-BCR signalling in sorted pro-B cells from *Atp11c*$^{+/0}$ (WT) and *Atp11c*$^{amb/0}$ (Amb) mice. The data were generated by hybridisation of RNA to Agilent microarrays. Statistical significance was calculated using the two-tailed Student's *t*-test.

Gene	Systematic Name	WT Pro-B cells (n=3)	Amb Pro-B cells (n=3)	Fold Change	P
Ikzf1	NM_001025597	194 ± 7	120 ± 15	- 1.62	0.0103
Tcf3	NM_011548	833 ± 11	542 ± 65	- 1.54	0.0114
Irf4	NM_013674	285 ± 29	155 ± 22	- 1.84	0.0224
Irf8	NM_008320	971 ± 85	782 ± 40	- 1.24	0.1153
Cd19	NM_009844	1939 ± 175	1263 ± 246	- 1.54	0.0885
Cd93	NM_010740	3640 ± 155	2302 ± 337	- 1.58	0.0226

Table 5.5 Microarray analysis of genes encoding B-cell lineage genes

Table shows the mean ± S.E.M. of relative expression values as estimated by microarray analysis for a set of genes encoding B cell lineage transcription factors as well as B cell specific proteins in sorted pro-B cells from *Atp11c*$^{+/0}$ (WT) and *Atp11c*$^{amb/0}$ (Amb) mice. The data were generated by hybridisation of RNA to Agilent microarrays. Statistical significance was calculated using the two-tailed Student's *t*-test.

5.4 Chapter summary and discussion

This chapter examined the role of ATP11C in the outcome of signalling through the IL-7R and pre-BCR that are each essential for the development of pre-B cells (Herzog et al., 2009, Clark et al., 2014, Reth and Nielsen, 2014). Pro-B cells from ATP11C-deficient animals expressed elevated levels of IL-7Rα on their surface, compared to control cells, and displayed a normal proliferative response to high concentrations of IL-7 *in vitro*. In contrast, the proliferative response of mutant pro-B cells in response to limiting concentrations of IL-7 was reduced. This observation mirrored the phenotype seen in pre-BCR deficient *Rag2*$^{-/-}$ animals (Marshall et al., 1998, Fleming and Paige, 2001). Further analysis revealed that ATP11C-deficient pro-B cells failed to differentiate into pre-B cells in response to anti-Igβ crosslinking. These results suggest that IL-7R signalling is possibly not affected by the ATP11C^{amb} mutation, but the problem could be in the formation and/or signalling through the pre-BCR.

Although the results of this chapter suggest that signalling through the IL-7R appears to be intact in ATP11C-deficient pro-B cells, there are some inconsistencies that cannot be resolved based on the current data. The microarray analysis demonstrated that the expression of some genes encoding downstream of IL-7 signalling was reduced in mutant pro-B cells. While this could be a direct effect of ATP11C deficiency on signalling through the IL-7R, it can also occur as a result of the developmental defect observed in ATP11C-deficient mice. Many of the target genes identified through the microarray assay remain to be validated by real time PCR as well as flow cytometry. Moreover, since IL-7 signals through three different pathways, namely JAK-STAT, PI3K-AKT and MAPK-ERK (Corfe and Paige, 2012), the results presented above cannot rule out the possibility that IL-7R-mediated activation of the PI3K-AKT and MAPK-ERK pathways might also be defective in mutant mice. Therefore, in addition to the downstream of JAK-STAT, IL-7R-driven activation of these pathways and their downstream molecules also need to be tested in mutant pro-B cells.

Expression and signalling through the pre-BCR is essential for the development of pre-B cells as animals deficient for any components of the pre-BCR show a

developmental arrest at the pro-B cell stage (Herzog et al., 2009, Clark et al., 2014, Reth and Nielsen, 2014). Studies using pre-BCR deficient animals reported that expression of the pre-BCR could improve the ability of pro-B cells to respond to low concentrations of IL-7 *in vitro* (Marshall et al., 1998, Fleming and Paige, 2001). These studies showed that pre-BCR-deficient *Rag2*$^{-/-}$ pro-B cells fail to proliferate in response to limiting concentration of IL-7 (picogram) (Marshall et al., 1998, Fleming and Paige, 2001). However, pro-B cells from *Rag2*$^{-/-}$ animals proliferated normally when IL-7 is abundant (nanogram) (Marshall et al., 1998, Fleming and Paige, 2001). A similar proliferation profile of mutant pro-B cells in response to the different concentrations of IL-7 suggests that the ATP11C^{amb} mutation may have an influence on the expression and/or signalling through the pre-BCR. The examination of the pre-BCR signalling in mutant mice revealed that *in vivo* Igβ-mediated pre-B cell differentiation is impaired in the absence of ATP11C. Consistently, microarray analysis revealed that ATP11C-deficient pro-B cells express some of the pre-BCR- and B cell lineage-related genes at a lower level compared to cells from control animals, supporting a critical involvement of ATP11C in formation and/or signalling through the pre-BCR in the bone marrow.

Because initial studies failed to find a significant Ca^{2+} flux upon crosslinking of Igβ in pro-B cells, it was thought that the main difference of pre-BCR and mature BCR signalling was the intracellular Ca^{2+} signalling (Nagata et al., 1997). However, a recent study revealed that anti-Igβ treatment is able to induce Ca^{2+} mobilisation in sorted pro-B cells from RAG-deficient mice (Schwickert et al., 2014). Consistent with the recent report, *Rag1*$^{-/-}$ pro-B cells treated with anti-Igβ antibody led to an intracellular Ca^{2+} flux. In contrast, antibody-treated mutant pro-B cells were deficient in Ca^{2+} mobilisation, suggesting a functional defect in pre-BCR signalling in ATP11C-deficient cells. These results suggest that ATP11C-deficient pro-B cells may have reduced signalling through the pre-BCR, most likely caused by a reduced expression of key signalling components but possibly also through a more direct effect. Therefore, pro-B cells cannot receive important signals through the pre-BCR, which then increase the ability to respond to limiting concentrations of IL-7. Further studies are needed to explore these possibilities.

Collectively, these results indicate that the ATP11C^{amb} mutation may lead to a defect in the assembly and/or signalling through the pre-BCR. This notion may also explain the results that the small changes in the expression of IL-7R signalling-related genes observed in pro-B cells of ATP11C-deficient mice could be due to the defective pre-BCR signalling, as both IL-7R and pre-BCR pathways are thought to act synergistically to control B cell development (Fleming and Paige, 2002). However, further studies are required to determine whether mutant pro-B cells express CD79b in order for them to respond to antibody treatment, and if so which stages of pre-BCR formation and/or signalling were disrupted in pro-B cells from *Atp11c*$^{amb/0}$ animals.

CHAPTER 6: Humoral immune response in the absence of ATP11C

Contents of Figure 6.1 appeared in:

Mehmet Yabas, Charis E. Teh, Sandra Frankenreiter, Dennis Lal, Carla M. Roots, Belinda Whittle, Daniel T. Andrews, Yafei Zhang, Narci C. Teoh, Jonathan Sprent, Lina E. Tze, Edyta M. Kucharska, Jennifer Kofler, Geoffrey C. Farell, Stefan Bröer, Christopher C. Goodnow and Anselm Enders (2011). "ATP11C is critical for the internalization of phosphatidylserine and differentiation B lymphocytes". *Nature Immunology*, 12(5):441-449.

Contributions from others:

- Mrs. Edyta M. Kucharska and Dr. Anselm Enders performed the experiment and generated the data in Figure 6.1.
- Mrs. Debbie Howard provided technical help in the irradiation of mice and intravenous injection of cells in the bone marrow chimera experiments.

6.1 Preamble

As discussed in the previous chapters, one of the key defence mechanisms of the immune system is the secretion of antibodies by B-lymphocytes. For the effective production of antibodies specific to an invading pathogen or in response to vaccinations, migration of B-lymphocytes to the GC is essential. GCs are the specialized microenvironments within the secondary lymphoid tissues where activated B cells undergo clonal expansion, somatic hypermutation and affinity maturation for effective humoral immune responses and for the generation of memory B-lymphocytes (Jacob et al., 1991, Berek et al., 1991, Liu et al., 1996). T_{FH} cells, a recently identified subset of $CD4^+$ T cells, have been shown to provide essential help to trigger GC B cell formation (Vinuesa and Cyster, 2011, Crotty, 2011). During a T-dependent immune response, the differentiation of normal numbers of T_{FH} cells is a crucial step as failure of T_{FH}-cell differentiation results in impaired GC formation and a lack of high-affinity antibody production (Johnston et al., 2009, Nurieva et al., 2009, Yu et al., 2009). In contrast, increased numbers of T_{FH} cells results in aberrant production of autoantibodies and the development of autoimmune diseases such as systemic lupus erythematosus (Hu et al., 2009, Linterman et al., 2009).

In the previous chapters, it has been shown that ATP11C-deficiency in mice results in loss of FO B cells in the spleen due to a developmental block at the pro- to pre-B transition in the bone marrow. However, *Atp11c*$^{amb/0}$ mice have some mature B cells that are mainly composed of MZ B cells in the spleen. The aim of this chapter is to evaluate the functional capacity of the residual mature B cells in the spleen of *Atp11c*$^{amb/0}$ mice.

6.2 Variably reduced primary and secondary antibody response by *Atp11c*$^{amb/0}$ B cells

To test whether *Atp11c*$^{amb/0}$ B cells are able to produce antibodies against different antigens, mutant animals and their control littermates were immunised with formalin fixed and heat inactivated *Bordetella pertussis* (*BP*) and alum-precipitated chicken γ globulin (CGG) coupled to the hapten azo-benzene-arsonate (ABA). 2 weeks post

primary immunisation plasma from the blood of mice was collected, and tested for the presence of antibodies against the immunogens by ELISA. The analysis showed a variably reduced primary antibody response to both antigens in the mutant animals (Figure 6.1A). Booster immunisation with ABA-CGG 6 weeks later again showed variably decreased antibody response to the CGG protein carrier while antibodies to the ABA hapten – which depends upon antibody hypermutation and selection in GC (Hande et al., 1998) - was almost absent in all mutant animals (Figure 6.1B).

T cell-independent (TI) antibody responses were also examined by immunisation with the T-cell independent antigen, NP-Ficoll and the production of antigen-specific IgM antibodies were monitored. It was found that *Atp11c*$^{amb/0}$ mice made a normal IgM antibody response to NP-Ficoll (Figure 6.1B). A normal antibody response to NP-Ficoll by B cells from *Atp11c*$^{amb/0}$ mice can possibly be explained by normal numbers of MZ B cells in the spleen of mutant mice as MZ B cells are the major B cell subpopulation that are able to respond to TI antigens (Martin et al., 2001). Taken together, the results from immunisation experiments indicate that the profound decrease in circulating mature B cells in *Atp11c*$^{amb/0}$ mice causes a variable humoral immune deficiency in response to T-dependent antigens.

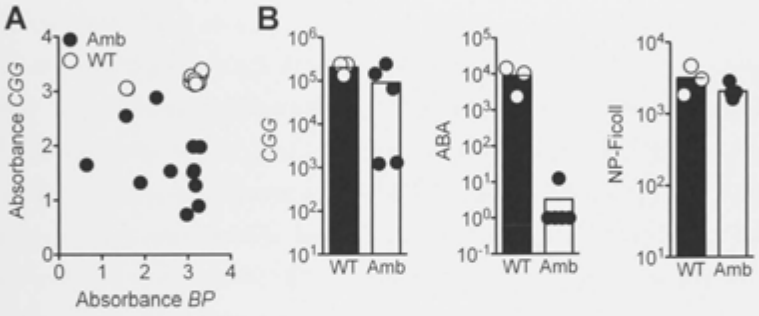

Figure 6.1 Variable humoral immune deficiency in ATP11C-deficient mice
(A) Primary antibody response in the plasma of *Atp11c*$^{+/0}$ (WT, open circle) and *Atp11c*$^{amb/0}$ (Amb, black filled circle) animals 14 days after immunisation with inactivated *Bordetella pertussis* (*BP*) and alum-precipitated chicken γ globulin (CGG) coupled to the hapten azo-benzene-arsonate (ABA). **(B)** Graphs show antibody response to CGG, the hapten ABA, and NP-Ficoll in the plasma of *Atp11c*$^{+/0}$ (WT) and *Atp11c*$^{amb/0}$ (Amb) animals 6 days after booster immunisation. Each circle represents a single mouse.

6.3 ATP11C is dispensable for the generation of GC B cells

The immunisation results presented above demonstrated that while mutant mice still have some antibody responses to *BP* and CGG, the response to ABA is completely absent (Figure 6.1B). Since antibody response to the ABA hapten depends on antibody hypermutation and selection in GCs (Hande et al., 1998), these results raise a possibility of the requirement for ATP11C in the formation of GC within the secondary lymphoid tissues. To test this, a system established by Professor Robert Brink, Garvan Institute of Medical Research, Australia, was used (Brink et al., 2008). Wild-type and ATP11C-deficient mice were crossed with CD45.1 SW_{HEL} mice, which carry a heavy-chain VDJ knock-in gene combined with a HEL-specific κ-light chain transgene (Phan et al., 2003). In this system, mice transgenic for both the heavy and light chain have about 10-25% of B cells specific for HEL. After adoptive transfer into wild-type recipient mice and immunisation with SRBCs conjugated to HEL, the expansion and formation of GC by the HEL-specific donor B cells can be monitored. An important feature of this model is that the HEL specific B cells are able to undergo class switch recombination and somatic hypermutation when challenged with immunogenic HEL in wild-type host that provides functional T cell help (Phan et al., 2003, Phan et al., 2005, Phan et al., 2006, Paus et al., 2006).

To test if ATP11C plays any role in GC formation, 10^5 congenically labelled $CD45.1^+$ HEL-binding B cells isolated from the spleen of donor *Atp11c*$^{+/0}$ SW_{HEL} transgenic and *Atp11c*$^{amb/0}$ SW_{HEL} transgenic mice were intravenously injected into CD45.2 wild-type recipient mice in combination with $2x10^8$ Mock-conjugated (control) or HEL-conjugated SRBCs (Figure 6.2). SRBC immunisation induces GC formation and selection, and the percentage and total number of wild-type and mutant derived HEL-specific GC B cells were determined by flow cytometry.

At various time points after injection, spleens from the recipient mice were collected and analysed for the formation of HEL-specific GC. Flow cytometric analysis revealed a comparable frequency and absolute number of all GC B cells in the spleen of wild-type recipients as indicated by staining for $B220^+GL\text{-}7^+CD95^+$ cells, confirming the ability of SRBCs to induce similar number of GC B cell formation in all recipient animals (Figure 6.3A, B). Therefore, any difference in the formation of

HEL-specific GC B cells cannot be attributed to differences in the total number of GC B cells formed in the different wild-type recipients. Surprisingly, accumulation of HEL-specific GC B cells was not compromised by the ATP11C^{amb} mutation as the percentage and number of CD45.1^{+}HEL^{+} GC B cells formed by *Atp11c*$^{amb/0}$ cells at different time points is comparable to that of wild-type control cells (Figure 6.3A, C). These results indicate that ATP11C is not required for the formation and long-term survival of HEL-specific GC B cells.

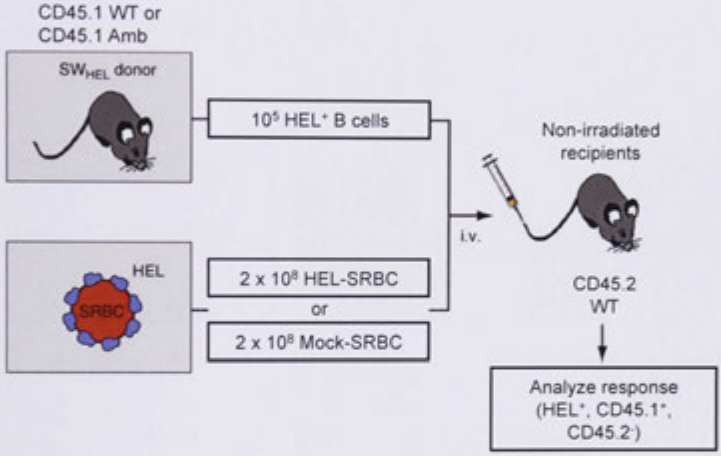

Figure 6.2 Experimental approach to test the formation of HEL-specific GC B cells
CD45.2 wild-type recipient mice were intravenously injected with HEL-specific *Atp11c*$^{+/0}$ (WT) or *Atp11c*$^{amb/0}$ (Amb) B cells from SW$_{HEL}$-transgenic mice (congenically labelled with CD45.1), and immunised with Mock-conjugated or HEL-conjugated SRBCs. At different time points after injection, splenocytes from the recipient mice were analysed for HEL-specific donor derived GC B cells by flow cytometry (Modified from Brink et al., 2008).

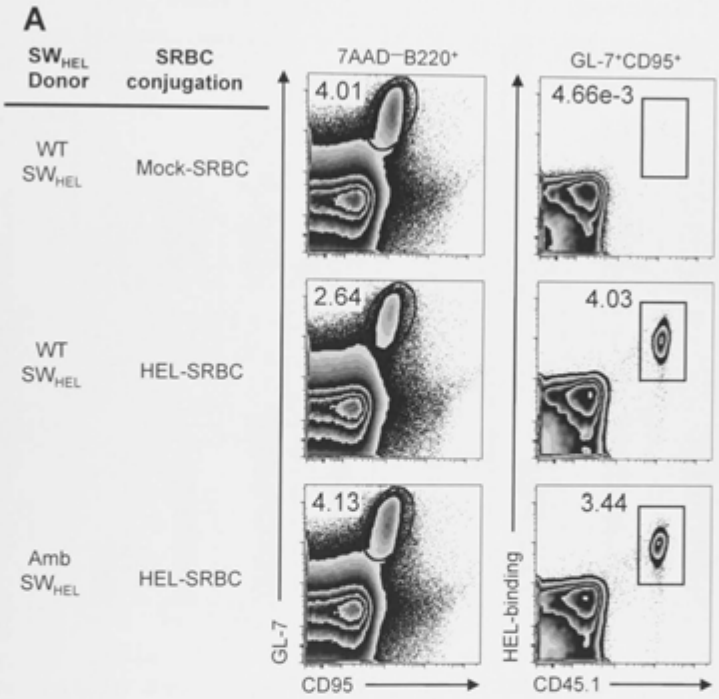

Figure 6.3 ATP11C is not required for the generation of HEL-specific GC B cells
(A) Representative flow cytometric analysis of spleen cells from wild-type recipient mice given adoptive transfer of HEL-specific *Atp11c*$^{+/0}$ (WT) or *Atp11c*$^{amb/0}$ (Amb) B cells from SW$_{HEL}$-transgenic mice (congenically labelled with CD45.1), and immunised with Mock-conjugated or HEL-conjugated SRBCs. The flow cytometric plots show GL-7$^+$CD95$^+$ GC B cells (left panel), and HEL$^+$CD45.1$^+$ donor-derived HEL-specific GC B cells (right panel).

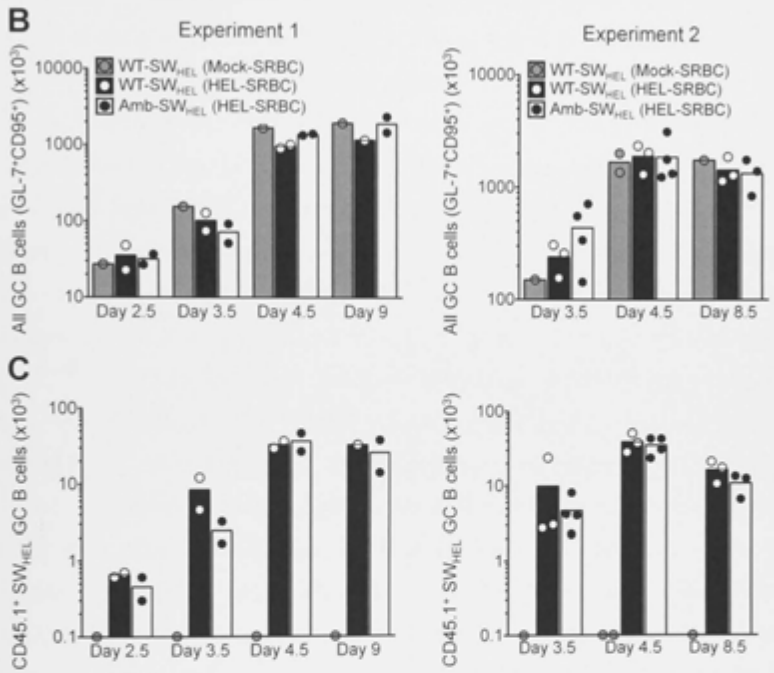

Figure 6.3 ATP11C is not required for the generation of HEL-specific GC B cells

(B) Bar graphs show the total number of GC B cells 2.5, 3.5, 4.5, 8.5 and 9 days after immunisation with Mock- or HEL-conjugated SRBCs in wild-type recipient mice that received HEL-specific B cells from *Atp11c*$^{+/0}$ SW$_{HEL}$-transgenic (WT-SW$_{HEL}$) or *Atp11c*$^{amb/0}$ SW$_{HEL}$-transgenic (Amb-SW$_{HEL}$) mice. **(C)** Bar graphs show the total number of HEL-specific donor-derived GC B cells 2.5, 3.5, 4.5, 8.5 and 9 days after immunisation with Mock- or HEL-conjugated SRBCs in wild-type recipient mice that received HEL-specific B cells from *Atp11c*$^{+/0}$ SW$_{HEL}$-transgenic (WT-SW$_{HEL}$) or *Atp11c*$^{amb/0}$ SW$_{HEL}$-transgenic (Amb-SW$_{HEL}$) mice. Each circle represents an individual mouse, and data shown are from two different experiments.

6.4 ATP11C is not required for the formation of T_{FH} cells

T cell help is required for the generation of GC B cells, and a subset CD4 T cells, termed T_{FH} cells has been shown to provide this essential help to trigger GC B cell formation (Vinuesa and Cyster, 2011, Crotty, 2011). As shown above, I found that while *Atp11c*$^{amb/0}$ mice show defective antibody response to the ABA hapten, the formation of antigen specific GC B cells in SW_{HEL} system is intriguingly normal. It should be noted that in this system the T cell help is provided by the recipient wild-type cells. Therefore, one hypothesis could be that *Atp11c*$^{amb/0}$ mice have a defect in the development of T_{FH} cells, thus B cells in the mutant mice cannot receive the essential help from T cells to form GCs. Given that the development of normal T_{FH} numbers is dependent on the availability of normal B cell numbers, and that mutant mice have reduced B cell numbers, mixed bone marrow chimera experiment was performed in order to test this possibility. Congenic bone marrow cells from *Atp11c*$^{amb/0}$ (CD45.2) and their *Atp11c*$^{+/0}$ littermates (CD45.2) were collected, equally mixed with *Atp11c*$^{+/0}$ bone marrow cells (CD45.1) and injected into irradiated *Rag1*$^{-/-}$ mice (Figure 6.4). The recipient mice were immunised with SRBCs 10-12 weeks after reconstitution, and spleens of the recipient mice were analysed 6 and 12 days after immunisation by flow cytometry (Figure 6.4). Since the reconstitution of $CD4^+$ T cells in the periphery of chimeric recipients is not affected by the ATP11C^{amb} mutation (Figure 3.7B in Chapter 3), the percentage of donor derived T_{FH} cells was compared to donor derived $CD4^+$ T cells to test whether the mutation has any effect on the T_{FH} differentiation.

As shown in Figure 6.5A, T_{FH} cells can be identified as $CXCR5^{hi}PD\text{-}1^{hi}$ in $CD4^+$ T cells 6 and 12 days after immunisation. In control chimeras, the percentage of CD45.2 T_{FH} cells derived from wild-type bone marrow was comparable to the proportion of CD45.2 cells among non-T_{FH} $CD4^+$ cells on day 6 and day 12 after immunisation (Figure 6.5B). Similarly, the percentage of CD45.2 *Atp11c*$^{amb/0}$ derived T_{FH} cells was comparable to the frequency of $CD45.2^+$ non-T_{FH} CD4 T cells in the spleen of recipients mice both 6 and 12 days post immunisation (Figure 6.5B). These data therefore suggest that ATP11C is redundant for the generation and survival of T_{FH} cells.

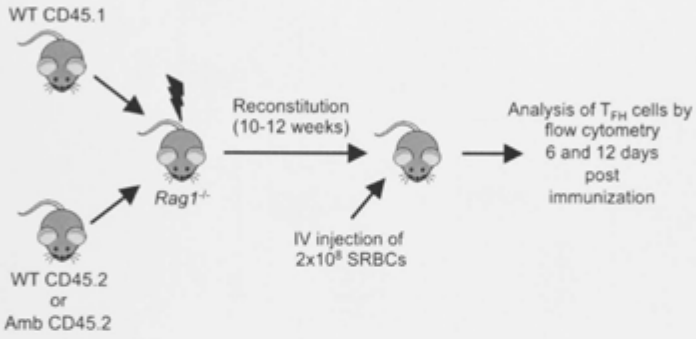

Figure 6.4 Experimental approach to test the formation of *Atp11c*$^{+/0}$ (WT) and *Atp11c*$^{amb/0}$ (Amb) derived T_{FH} cells in the spleen of mixed bone marrow chimeric recipients after SRBCs immunisation

Bone marrow chimeric mice were generated by the injection of congenic (CD45.2) bone marrow cells from *Atp11c*$^{+/0}$ (WT) and *Atp11c*$^{amb/0}$ (Amb) animals mixed at 1:1 ratio with *Atp11c*$^{+/0}$ (WT) bone marrow cells (CD45.1) into irradiated *Rag1*$^{-/-}$ recipients. 10-12 weeks after reconstitution, the recipient mice were immunised with SRBCs, and spleens of the recipient mice were analysed 6 and 12 days post immunisation by flow cytometry.

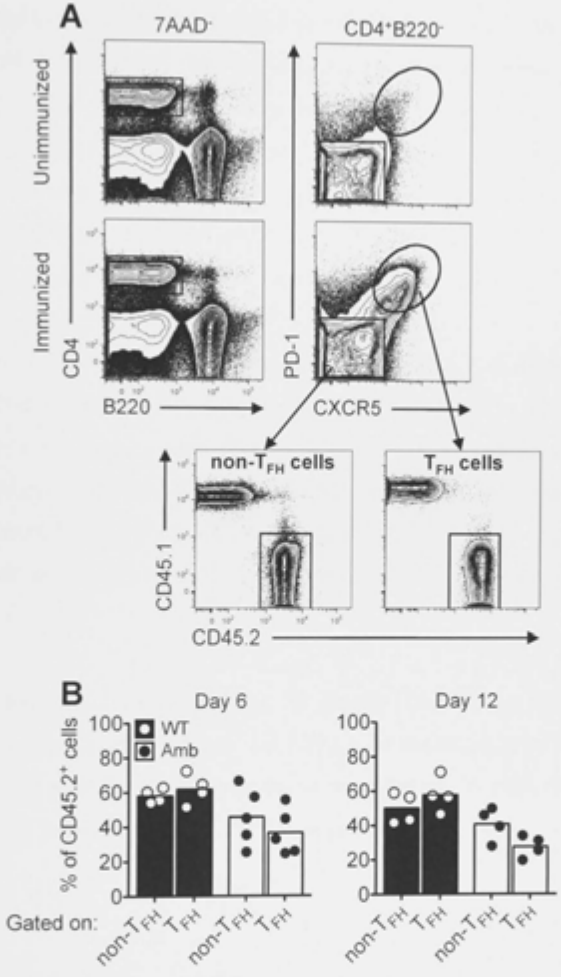

Figure 6.5 ATP11C is not required for the differentiation of T_{FH} cells

(A) Representative flow cytometric analysis of spleen cells from bone marrow chimeric recipient mice shows the gating strategy to determine donor derived non-T_{FH} and T_{FH} cells that are accumulated in the recipient mice 6 and 12 days after immunisation with SRBCs. **(B)** Graphs show the percentage of CD45.2$^+$ *Atp11c*$^{+/+}$ (WT) or *Atp11c*$^{amb/+}$ (Amb) derived non-T_{FH} and T_{FH} cells as shown in (A). Each circle represents an individual mouse, and data are representative of two independent experiments with three to five mice per genotype in each.

6.5 Normal formation of GC B and T_{FH} cells in intact *Atp11c*$^{amb/0}$ mice

Next, intact *Atp11c*$^{amb/0}$ mice and their control littermates were immunised with SRBCs, and the formation of GC B and T_{FH} cells 7 and 14 days post immunisation was determined. Interestingly, the frequency of GC B cells formed in *Atp11c*$^{amb/0}$ mice was higher than their control littermates at both 7 and 14 days after SRBCs-immunisation (Figure 6.6A, upper left panel). However, the absolute number of GC B cells formed in *Atp11c*$^{amb/0}$ mice was significantly reduced (Figure 6.6A, upper right panel), but this is most likely a reflection of the reduced number of total B cells in the spleen of *Atp11c*$^{amb/0}$ mice (Figure 3.4C, D in Chapter 3).

T_{FH} formation in intact *Atp11c*$^{amb/0}$ animals after SRBCs immunisation was also tested. The differentiation of T_{FH} cells in immunised *Atp11c*$^{amb/0}$ mice appeared to be slightly lower both 7 and 14 days after SRBCs-immunisation (Figure 6.6B, bottom left panel). Similar to the number of GC B cells, *Atp11c*$^{amb/0}$ mice had significantly reduced T_{FH} numbers (Figure 6.6B, bottom right panel), but again this most likely reflects the reduced number of total lymphocytes in *Atp11c*$^{amb/0}$ mice (Figure 3.4B in Chapter 3).

Collectively, these results together with the results from SW_{HEL} and mixed bone marrow chimera experiments indicate that ATP11C is not required for the generation of GC B or T_{FH} cells *in vivo* despite its requirement for B cells to differentiate normally past the pro-B cell stage in the bone marrow.

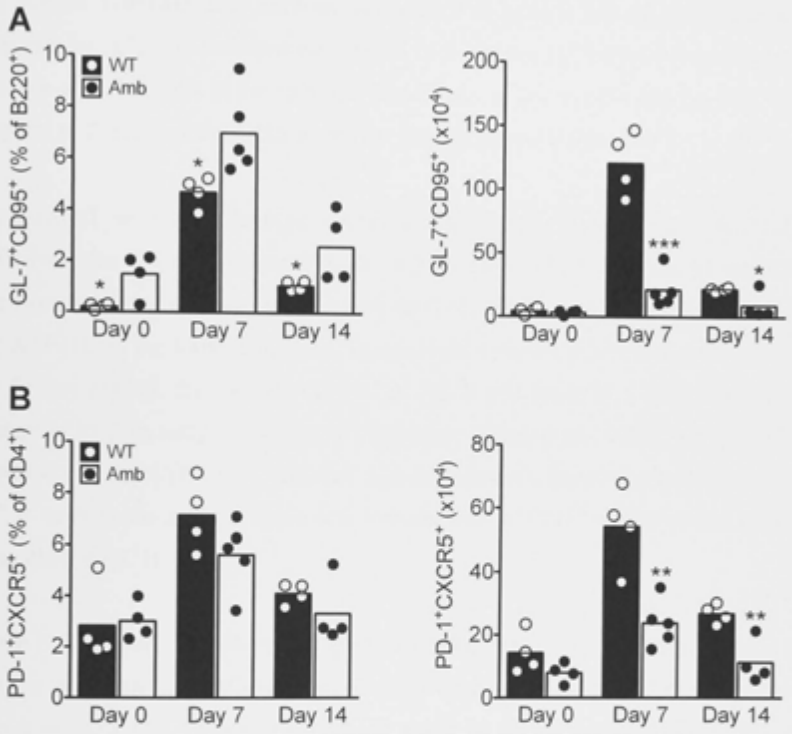

Figure 6.6 Normal GC B and T_{FH} formation in intact ATP11C-deficient mice

(A) Graphs show the percentage and absolute number of GC B cells formed in *Atp11c*$^{+/Y}$ (WT) and *Atp11c*$^{amb/Y}$ (Amb) mice 7 and 14 days after SRBC immunisation. **(B)** Graphs show the percentage and absolute number of T_{FH} cells occurred in *Atp11c*$^{+/Y}$ (WT) and *Atp11c*$^{amb/Y}$ (Amb) mice 7 and 14 days after SRBC immunisation. Day 0 values represent unimmunised mice. Each circle represents an individual mouse. Statistical significance was calculated using the two-tailed Student's *t*-test. *** $P < .001$; ** $P < .01$; * $P < .05$.

6.6 Chapter summary and discussion

In this chapter, the functional capacity of B cells that are present in *Atp11c*$^{amb/0}$ mice was examined. Immunisation experiments revealed that *Atp11c*$^{amb/0}$ mice showed a variable reduced primary and secondary antibody response to T-dependent antigens, but normal T-independent antibody response. The normal T-independent immune response by ATP11C-deficient mice could be explained by the presence of normal number of MZ B cells in the spleen of these mice, as MZ B cells and B1 cells both respond to T-independent antigens *in vivo* (Fagarasan and Honjo, 2000).

Analysis of secondary immune response interestingly revealed that ATP11C-deficient mice show no response to the ABA hapten, which depends on antibody hypermutation and selection in GCs (Hande et al., 1998), suggesting a possible role for ATP11C in the formation of GC B cells within the secondary lymphoid tissues. To further explore the role of ATP11C in GC B cell function, I used the SW_{HEL} system to analyse antigen-specific GC formation (Brink et al., 2008). These studies revealed that the ATP11C^{amb} mutation does not affect the generation and survival of GC B cells in the spleen. These data indicate that ATP11C is dispensable for the formation of GC B cells.

In the SW_{HEL} system, wild-type recipient mice that provide T cell help were used to test the ability of ATP11C-deficient SW_{HEL} transgenic B cells to form GC B cells (Brink et al., 2008). Thus, one hypothesis would be the involvement of ATP11C in T_{FH} formation in intact mutant mice. However, this was not the case as following immunisation T cells from ATP11C mutant mice were able to differentiate into T_{FH} cells, which identified that ATP11C is not required for T_{FH} cell differentiation.

Despite normal GC B and T_{FH} cell formation in the presence of ATP11C deficiency, *Atp11c*$^{amb/0}$ mice showed a defective immune response to the ABA hapten. Since B cells found in mutant mice are primarily MZ B cells, one possibility is that *Atp11c*$^{amb/0}$ mice have a limited receptor repertoire that could limit the ability of mutant B cells to recognise a diverse range of protein antigens. Thus, it would be interesting to determine the diversity of BCRs within mature B cells from ATP11C-deficient mice.

Activated B cells within the GCs undergo affinity maturation and somatic hypermutation in order to produce antibodies with increased affinity for antigen (Goodnow et al., 2010). Thus, another possibility to explain the defective response to ABA despite normal GC formation is the involvement of ATP11C in these latter processes. Consistent with this notion, it has been suggested that affinity maturation and B cell memory can be generated independent of GC formation in the case of lymphotoxin-alpha-deficiency (Matsumoto et al., 1996). Therefore, it is possible that although ATP11C-deficient mice have a normal GC B cell formation, they may not be able to undergo somatic hypermutation or isotype switching in response to GC centre triggers. The future experiments will also be needed to explore this possibility.

It should also be noted that the immunisation screen used in this study was designed to test Th1 and Th2 function in the ENU-mutagenised mice. In addition to T_{FH} cells, polarisation of Th cell differentiation into the Th1 and Th2 cells also contributes to the quality of the immune responses. Having seen a variably reduced antibody production to T-dependent antigens would suggest a potential impact of ATP11C on the differentiation and functional properties of naïve T cells into effector Th1 or Th2 cells, which will be noteworthy for future studies.

Collectively, the results presented in this chapter suggest that ATP11C is dispensable for the activation of mature B cells through the BCR, despite a critical involvement in the formation and/or efficient signalling of the pre-BCR during early B cell development.

CHAPTER 7: ATP11C deficiency causes a biochemical defect in phosphatidylserine internalisation

Some contents of Figure 7.2, 7.3, 7.4, 7.5, 7.6 and 7.19 appeared in:

Mehmet Yabas, Charis E. Teh, Sandra Frankenreiter, Dennis Lal, Carla M. Roots, Belinda Whittle, Daniel T. Andrews, Yafei Zhang, Narci C. Teoh, Jonathan Sprent, Lina E. Tze, Edyta M. Kucharska, Jennifer Kofler, Geoffrey C. Farell, Stefan Bröer, Christopher C. Goodnow and Anselm Enders (2011). "ATP11C is critical for the internalization of phosphatidylserine and differentiation B lymphocytes". *Nature Immunology*, 12(5):441-449.

Contributions from others:

- Prof. Stefan Bröer contributed to the establishment of the flippase assay.

7.1 Preamble

The previous chapters immunologically characterised two ENU-induced mouse strains with point mutations in *Atp11c*, which encodes the putative aminophospholipid translocase ATP11C. Since ATP11C is thought to serve as a flippase that contributes to the generation and maintenance of the plasma membrane lipid asymmetry through translocation of phospholipids between the two leaflets of the bilayer, some important mechanistic questions remain unanswered: does ATP11C function as a flippase in the biological membranes? And if so, how does a possible defective flippase activity in B cells from ATP11C-deficient animals cause B cell deficiency? These are important questions because the results will not only illustrate for the first time whether ATP11C is a flippase, but also provide mechanistic insight into the B cell phenotype observed in mutant animals. Therefore, this part of the thesis will examine the functional consequences of the ATP11C^{amb} and ATP11C^{18NIH30} mutations on PS internalisation across the plasma membrane of cells of the immune system.

7.2 Aminophospholipid translocation (Flippase) activity assay

As discussed in Chapter 1, phospholipids in the plasma membrane of most eukaryotic cells are asymmetrically distributed between the two leaflets of the plasma membrane with PS and PE being predominantly confined to the cytosolic leaflet (Sebastian et al., 2012, van der Mark et al., 2013). In 1984, Seigneuret and Devaux were the first to show the energy-driven translocation of spin-labelled PS and PE from the external leaflet of erythrocyte membranes to the cytosolic leaflet, indicating that the lipid asymmetry is generated by aminophospholipid translocase or flippase activity (Seigneuret and Devaux, 1984). Since then fluorescent and spin-labelled phospholipid analogues have been extensively used to quantitatively measure the movement of phospholipids between the two leaflets of the plasma membranes. Short-chain fluorescent phospholipid analogues such as NBD-PS have been most commonly used to test the translocation activity in different cell types as they are selectively transported to the cytosolic leaflet of plasma membranes by aminophospholipid translocases. In order to test flippase activity in different haematopoietic lineages from ATP11C-deficient animals I also used fluorescently labelled PS analogues.

7.3 A developmental stage-specific defect in C_{12}-NBD-PS internalisation in pro-B stage of B cell development in the bone marrow of *Atp11c*$^{amb/0}$ mice

ATP11C is believed to function as a flippase that transports phospholipid from the outer leaflet of the plasma membrane to the inner leaflet (Sebastian et al., 2012, van der Mark et al., 2013). As revealed in Chapter 3, mutations in the *Atp11c* gene led to a developmental arrest at the pro-B cell stage of differentiation. Therefore, I focused on this population of B lineage precursors as well as other haematopoietic lineages for aminophospholipid flippase activity. To test whether pro-B cells from mutant animals exhibit an impaired PS translocation, congenically marked bone marrow cells from *Atp11c*$^{amb/0}$ CD45.2 and *Atp11c*$^{+/0}$ CD45.1 control animals were mixed at a 1:1 ratio and incubated for various amounts of time with the fluorescent PS analogue, C_{12}-NBD-PS (Figure 7.1). Any dye remaining in the exoplasmic leaflet was then extracted by incubation with excess fatty acid free BSA. The mutant and control cell subsets were distinguished by antibody staining, and analysed by flow cytometry (Figure 7.1).

I found that C_{12}-NBD-PS fluorescence in *Atp11c*$^{amb/0}$ and *Atp11c*$^{+/0}$ B cell subsets increased rapidly as a result of transmembrane movement of the analogue, and approached saturation by 12 minutes at 37°C (Figure 7.2). The rate of C_{12}-NBD-PS translocation was homogeneously less in mutant pro-B cells compared to those from control mice (Figure 7.2). Interestingly, the flippase defect appeared specific for the pro-B cell stage, as other B cell subsets in the bone marrow of *Atp11c*$^{amb/0}$ animals including pre/pro-B, immature B and mature B cells exhibited a normal flippase activity (Figure 7.2). It would also be interesting to compare the flippase activity in mutant pre-B cells. However, because pre-B cells are present in very low number in ATP11C-deficient mice, it was not possible to analyse sufficient pre-B cells in the flippase assay to make a reliable comparison between wild-type and ATP11C-deficent pre-B cells.

I also analysed other haematopoietic lineages including NK1.1$^+$ NK cells, TCRβ$^+$ T cells, Mac-1$^+$Gr-1$^+$ myeloid cells and Ter119$^+$ red cells in the bone marrow, and found that all cell types from *Atp11c*$^{amb/0}$ animals show a normal flippase activity

compared to those in control animals (Figure 7.3). Similarly, analysis of different B cell subsets including immature, FO and MZ B cells and other leukocyte lineages in the spleen revealed that all cell types from *Atp11c*$^{amb/0}$ animals also show a normal C_{12}-NBD-PS internalisation compared to those from control animals (Figure 7.4A, B).

Because ATP11C-deficient animals may have increased number of apoptotic cells and these cells may have reduced flippase activity, I next examined whether the defective flippase activity in mutant pro-B cells can be overcome by the introduction of a transgene that encodes the pro-survival protein BCL-2 that prevents cells from apoptosis. I found that the decreased C_{12}-NBD-PS flippase activity in *Atp11c*$^{amb/0}$ pro-B cells could not be corrected by enforced expression of BCL-2 (Figure 7.5).

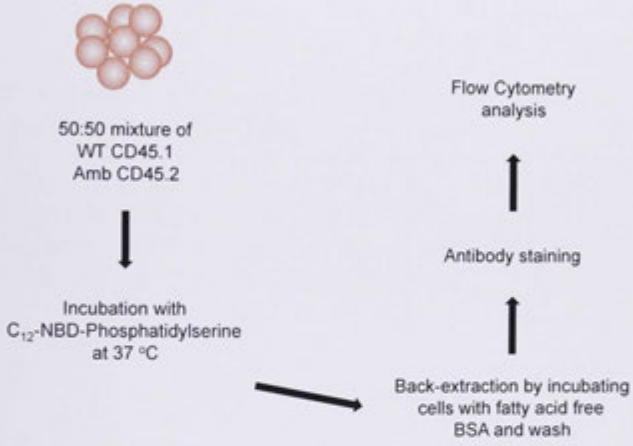

Figure 7.1 Aminophospholipid translocase (Flippase) activity assay
Cells from the bone marrow, spleen and thymus of CD45.2 *Atp11c*$^{ameA\,0}$ and CD45.1 *Atp11c*$^{+\,0}$ control animals were mixed at a 1:1 ratio and incubated for various amounts of time with the fluorescent PS analogue (C_{12}-NBD-PS). Any dye remaining in the exoplasmic leaflet was then extracted with fatty acid free bovine serum albumin (BSA) and washed away. Different cell subsets were distinguished by antibody staining, and analysed on a flow cytometer.

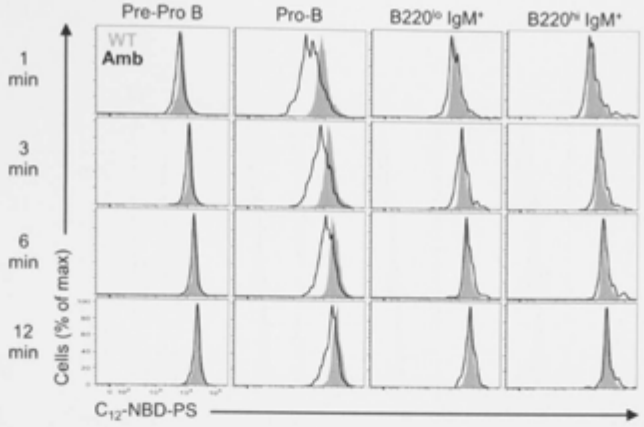

Figure 7.2 A lineage- and developmental stage-specific defect in C_{12}-NBD-PS internalisation in pro-B cells from ATP11C-deficient mice

Representative C_{12}-NBD-PS fluorescence profiles after 1, 3, 6 and 12 min incubation in pre/pro-B, pro-B, $B220^{lo}IgM^{+}$ B, and $B220^{hi}IgM^{+}$ B cells in the bone marrow from *Atp11c*$^{amb\,0}$ (Amb, black lines), compared to the corresponding CD45.1-marked of *Atp11c*$^{+\,0}$ (WT, shaded grey) cells in the same tube. Data are representative of at least three independent experiments with one mouse per genotype in each.

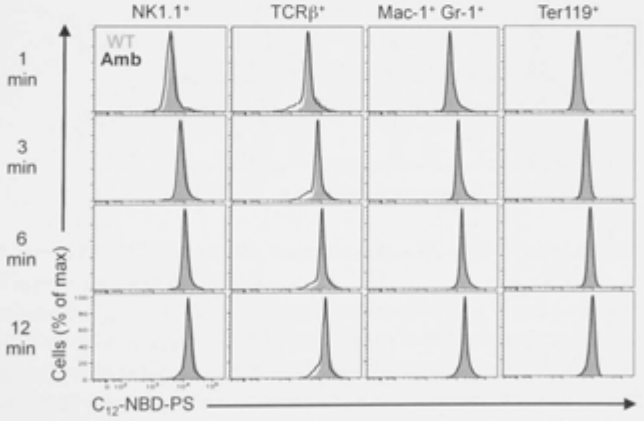

Figure 7.3 The ATP11C^{amb} mutation does not affect C_{12}-NBD-PS translocation into NK, T, myeloid cells and erythrocytes in the bone marrow

Representative C_{12}-NBD-PS fluorescence profiles after 1, 3, 6 and 12 min incubation in $NK1.1^{+}$ NK cells, $TCR\beta^{+}$ T cells $Mac\text{-}1^{+}Gr\text{-}1^{+}$ Myeloid cells and $Ter119^{+}$ red cells in the bone marrow from *Atp11c*$^{amb\,0}$ (Amb, black lines), compared to the corresponding CD45.1-marked of *Atp11c*$^{+\,0}$ (WT, shaded grey) cells in the same tube. Data are representative of at least two independent experiments with one mouse per genotype in each.

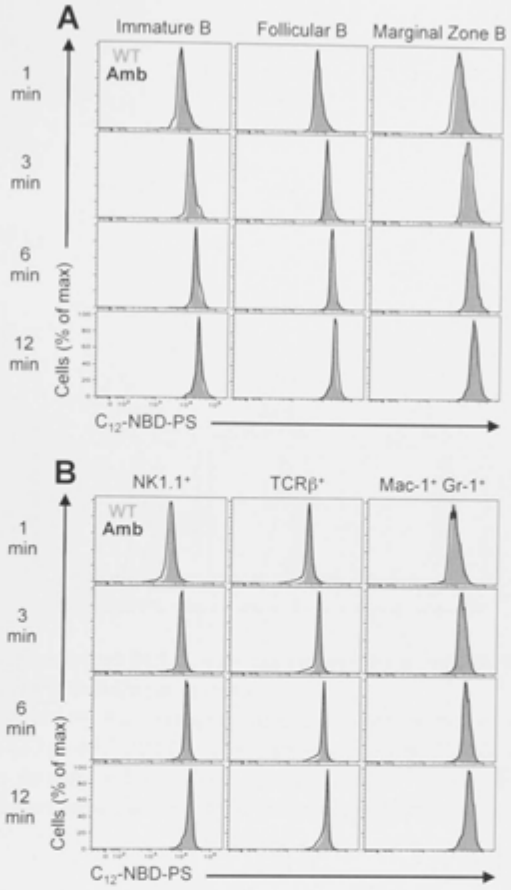

Figure 7.4 The ATP11C^{amb} mutation does not affect C_{12}-NBD-PS translocation into B, NK, T and myeloid cells in the spleen

(A) Representative C_{12}-NBD-PS fluorescence profiles after 1, 3, 6 and 12 min incubation in Immature B, Follicular B and Marginal Zone B cells in the spleen from *Atp11c*$^{amb/0}$ (Amb, black lines), compared to the corresponding CD45.1-marked of *Atp11c*$^{+/0}$ (WT, shaded grey) cells in the same tube. Data are representative of three independent experiments. **(B)** Representative C_{12}-NBD-PS fluorescence profiles after 1, 3, 6 and 12 min incubation in NK1.1$^+$ NK cells, TCRβ$^+$ T cells and Mac-1$^+$Gr-1$^+$ Myeloid cells in the spleen from *Atp11c*$^{amb/0}$ (Amb, black lines), compared to the corresponding CD45.1-marked of *Atp11c*$^{+/0}$ (WT, shaded grey) cells in the same tube. Data are representative of at least two independent experiments with one mouse per genotype in each.

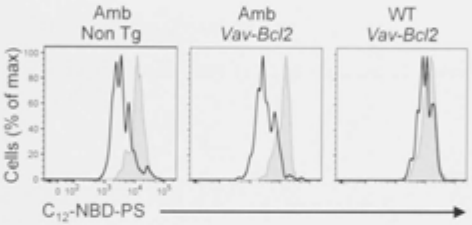

Figure 7.5 Overexpression of BCL-2 does not correct the impaired flippase activity in pro-B cells from ATP11C-deficient animals

Representative C_{12}-NBD-PS fluorescence profiles after 1 min incubation in pro-B cells from *Atp11c*$^{amb/0}$ (Amb) or *Atp11c*$^{+/0}$ (WT) mice lacking or carrying the *Vav-Bcl2* transgene (black lines), compared to the corresponding CD45.1-marked *Atp11c*$^{+/0}$ pro-B cells (shaded grey) in the same tube. Data are representative of two independent experiments with one mouse per genotype in each.

7.4 A developmental stage-specific defect in C_{12}-NBD-PS translocation in DN and DP stages of T cell development in the thymus of *Atp11c*$^{amb/0}$ mice

While peripheral T cell numbers are normal in ATP11C-deficient animals, I wanted to test whether developing thymocytes have a normal flippase activity. Thymocytes from *Atp11c*$^{amb/0}$ CD45.2 and *Atp11c*$^{+/0}$ CD45.1 control animals was mixed, incubated with C_{12}-NBD-PS for various amounts of time at 37°C, and analysed on the flow cytometry. Interestingly, $CD4^-CD8^-$ double negative (DN) and $CD4^+CD8^+$ double positive (DP) thymocytes from *Atp11c*$^{amb/0}$ animals were found to have a reduced flippase activity (Figure 7.6). Similar to pro-B cells, the flippase deficit was stage-specific for DN and DP stages as flippase activity was normal in $CD4^+$ or $CD8^+$ single positive (SP) thymocytes and in mature T cells in bone marrow or spleen (Figure 7.3, Figure 7.4B and Figure 7.6). However, the reduction in flippase activity does not cause an obvious defect in DP cell differentiation into SP cells (data shown in Chapter 8).

Taken together, these data show that ATP11C is critical for phospholipid flipping in a developmental stage-dependent way and that pro-B cells are peculiarly sensitive to reduced flippase activity.

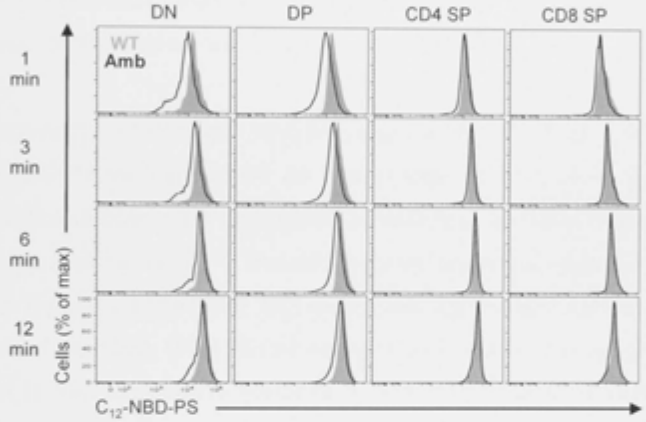

Figure 7.6 A lineage- and developmental stage-specific defect in C_{12}-NBD-PS internalisation in DN and DP stages of T cell development in the thymus of ATP11C-deficient mice

Representative C_{12}-NBD-PS fluorescence profiles after 1, 3, 6 and 12 min in CD4 and CD8 double negative (DN) or double positive (DP), and CD4 or CD8 Single Positive (SP) cells in the thymus from *Atp11c*$^{amb/0}$ (Amb, black lines), compared to the corresponding CD45.1-marked of *Atp11c*$^{+/0}$ (WT, shaded grey) cells in the same tube. Data are representative of three independent experiments with one mouse per genotype in each.

7.5 Optimization of the flippase activity assay: Utilization of a more suitable PS analogue

The measurements of PS internalisation by different type of haematopoietic lineages shown so far were performed using C_{12}-NBD-PS (16:0-12:0 NBD-PS) at 37 °C. The results revealed relatively modest differences of flippase activity between control and ATP11C-deficient pro-B cells as well as DN and DP thymocytes. Because it was shown that C_6-NBD-PS (16:0-6:0 NBD-PS), which is different from the C_{12}-NBD-PS by the length of the *sn-2* chain to which the NBD fluorescence marker is attached (Figure 7.7A), is a more sensitive PS analogue to measure flippase activity (Hanada and Pagano, 1995), I wanted to compare the two different analogues.

As a comparison, I isolated and incubated bone marrow cells from wild-type mice with C_{12}-NBD-PS and C_6-NBD-PS for various time points at 15 °C, followed by back-extraction of fluorescent lipid remaining with fatty acid free BSA. Incubating cells with the analogues at 15 °C insured that the PS internalisation detected was due only to the flippase activity rather than non-specific endocytosis of PS micelles (van Genderen and van Meer, 1995). Translocation of the C_6-NBD-PS analogue increased more than 10-fold compared to that of the C_{12}-NBD-PS analogue at indicated time points (Figure 7.7B). Because these data confirm that C_6-NBD-PS is far a more suitable PS analogue to measure flippase activity, I repeated the PS internalisation assay for all haematopoietic cells from wild-type and ATP11C mutant mice using C_6-NBD-PS.

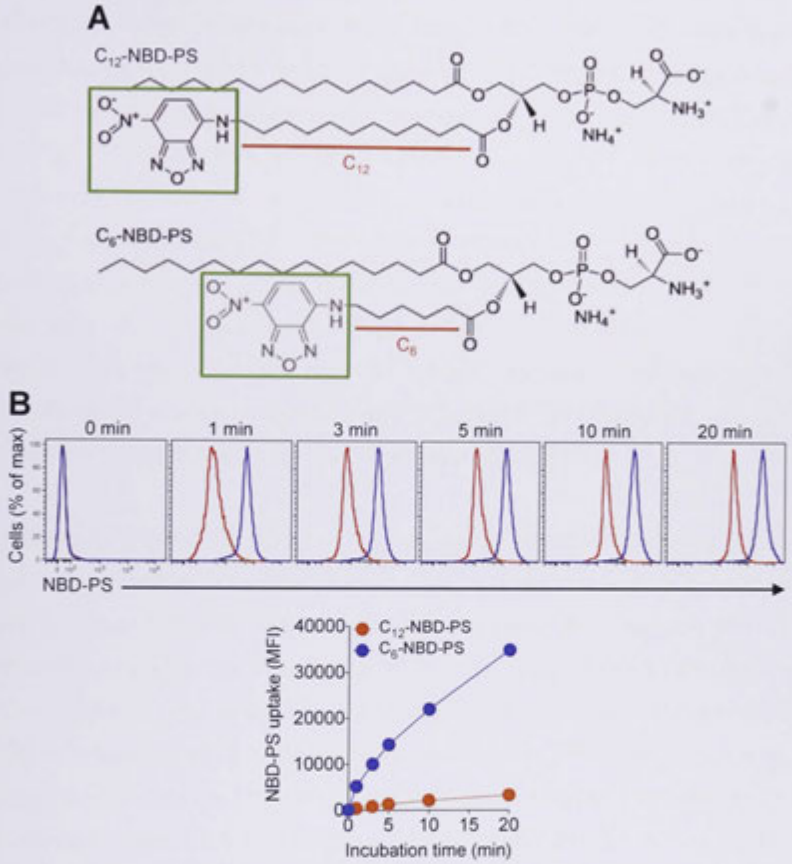

Figure 7.7 C_6-NBD-PS is a more sensitive analogue for the PS translocation assay
(A) The structures of PS analogues C_{12}-NBD-PS and C_6-NBD-PS which are tagged with NBD (green) on its *sn-2* acyl chain of 12 and 6 carbons, respectively (Modified from http://avantilipids.com). **(B)** Representative C_{12}-NBD-PS (red) and C_6-NBD-PS (blue) fluorescence profiles after 0, 1, 3, 5, 10 and 20 min incubation in IgM^+ B cells from the bone marrow of wild-type mice. Graph shows C_{12}-NBD-PS (red) and C_6-NBD-PS (blue) geometric mean fluorescence intensity (MFI) of IgM^+ B cells from the bone marrow of wild-type mice at different incubation times. Data are from one experiment with one mouse.

7.6 Haematopoietic lineages from *Atp11c*$^{amb/0}$ animals exhibit a defective C_6-NBD-PS flippase activity

Having established the most suitable analogue, the flippase activity assays in different haematopoietic lineages in the bone marrow, spleen and thymus were repeated using C_6-NBD-PS at 15 °C. Analysis of different B cell subpopulations revealed that all B cell subsets including pre/pro-B, pro-B, pre-B, B200^{lo}IgM^{+} and B220^{hi}IgM^{+} B cells from the bone marrow of *Atp11c*$^{amb/0}$ animals showed a significantly reduced rate of C_6-NBD-PS internalisation compared to those from *Atp11c*$^{+/0}$ animals (Figure 7.8). The lower internalisation of C_6-NBD-PS could not be corrected over time as ATP11C-deficient cells had decreased C_6-NBD-PS uptake even after 30 min incubation (Figure 7.8). Measurement of C_6-NBD-PS internalisation into B cell subsets in the spleen demonstrated that the rate of C_6-NBD-PS uptake was also notably reduced in splenic B cell subsets from *Atp11c*$^{amb/0}$ animals compared to those from control animals (Figure 7.9).

To determine whether the defective flippase activity is specific for B cell subsets, I measured the uptake of C_6-NBD-PS into different leukocyte subsets including NK cells, T cells and myeloid cells in the bone marrow and spleen, and into different T cell subsets in the thymus. I found that NK1.1^{+} NK cells, TCRβ^{+} T cells, and Mac-1^{+}Gr-1^{+} myeloid cells in the bone marrow and spleen of *Atp11c*$^{amb/0}$ animals also exhibit a lower rate of C_6-NBD-PS uptake compared to those from control animals (Figure 7.10 and Figure 7.11). Moreover, analysis of different T cell subsets in the thymus demonstrated that DN, DP, CD4 SP and CD8 SP thymocytes from ATP11C-deficient animals showed a significantly reduced C_6-NBD-PS uptake compared to the corresponding thymocytes in wild-type mice (Figure 7.12).

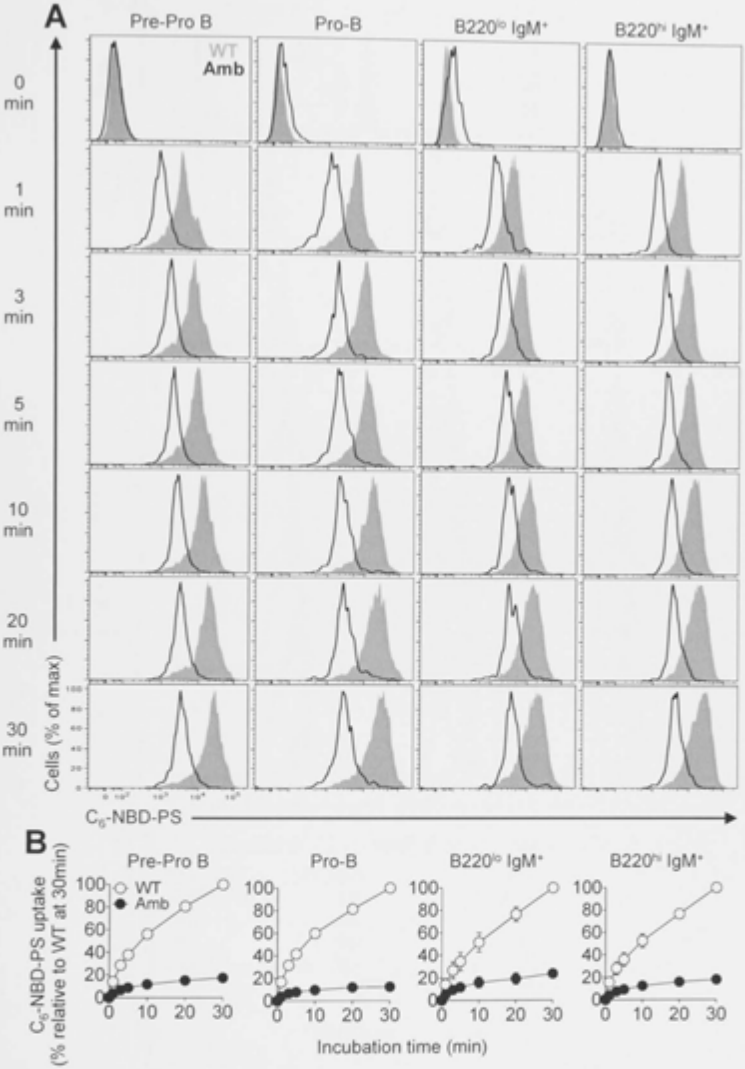

Figure 7.8 The ATP11C^{amb} mutation decreases C_6-NBD-PS translocation into all B cell subsets in the bone marrow

(A) Representative C_6-NBD-PS fluorescence profiles after 0, 1, 3, 5, 10, 20 and 30 min incubation in B cell subsets from the bone marrow of *Atp11c*$^{amb/0}$ (Amb, black lines), compared to the corresponding CD45.1-marked of *Atp11c*$^{-/0}$ (WT, shaded grey) cells in the same tube. **(B)** Graphs represent mean ± S.E.M of the percentage of C_6-NBD-PS uptake relative to WT at 30 min. Data are pooled from two independent experiments with one mouse per genotype in each.

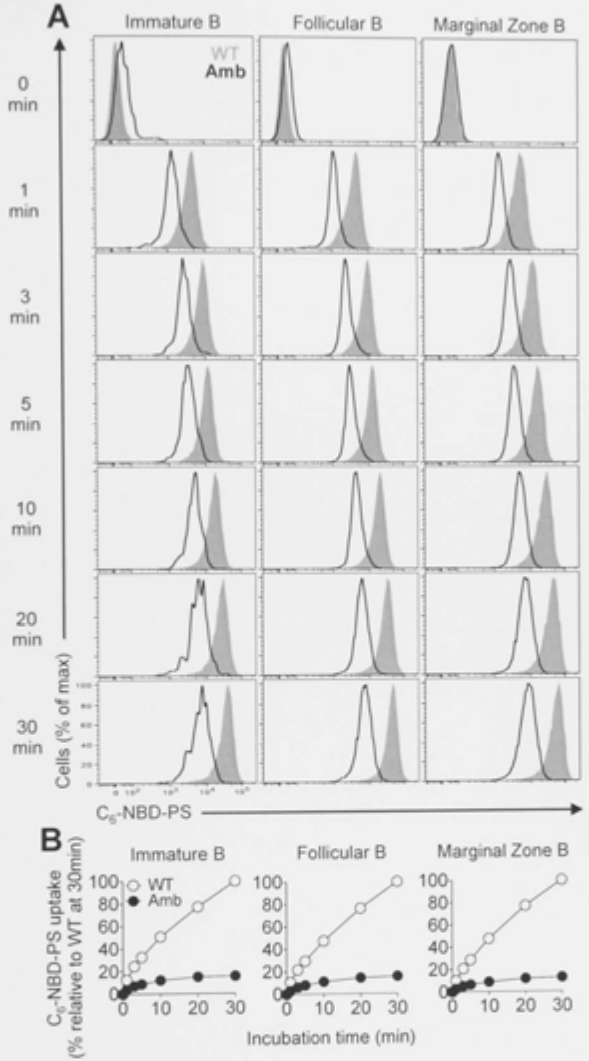

Figure 7.9 The ATP11C^{amb} mutation decreases C_6-NBD-PS translocation into all B cell subsets in the spleen

(A) Representative C_6-NBD-PS fluorescence profiles after 0, 1, 3, 5, 10, 20 and 30 min incubation B cell subsets from the spleen of *Atp11c*$^{amb/0}$ (Amb, black lines), compared to the corresponding CD45.1-marked of *Atp11c*$^{+/0}$ (WT, shaded grey) cells in the same tube. **(B)** Graphs represent mean ± S.E.M of the percentage of C_6-NBD-PS uptake relative to WT at 30 min. Data are pooled from three independent experiments with one mouse per genotype in each.

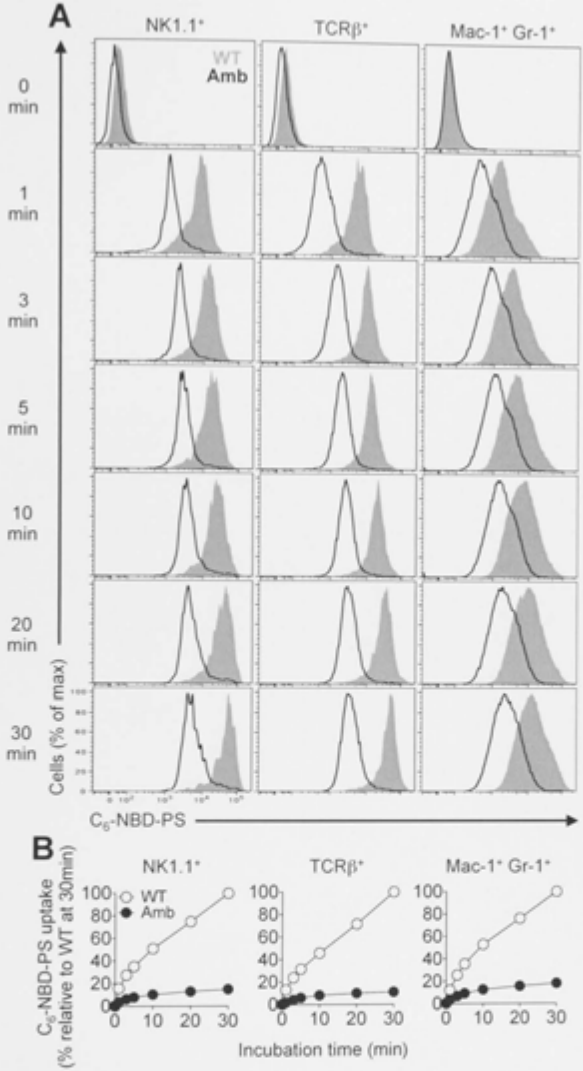

Figure 7.10 The ATP11C^{amb} mutation decreases C_6-NBD-PS translocation into different lineages in the bone marrow

(A) Representative C_6-NBD-PS fluorescence profiles after 0, 1, 3, 5, 10, 20 and 30 min incubation in NK1.1$^+$ NK cells, TCRβ$^+$ T cells and Mac-1$^+$Gr-1$^+$ Myeloid cells from the bone marrow of *Atp11c*$^{amb.0}$ (Amb, black lines), compared to the corresponding CD45.1-marked of *Atp11c*$^{+.0}$ (WT, shaded grey) cells in the same tube. **(B)** Graphs represent mean ± S.E.M of the percentage of C_6-NBD-PS uptake relative to WT at 30 min. Data are pooled from two independent experiments with one mouse per genotype in each.

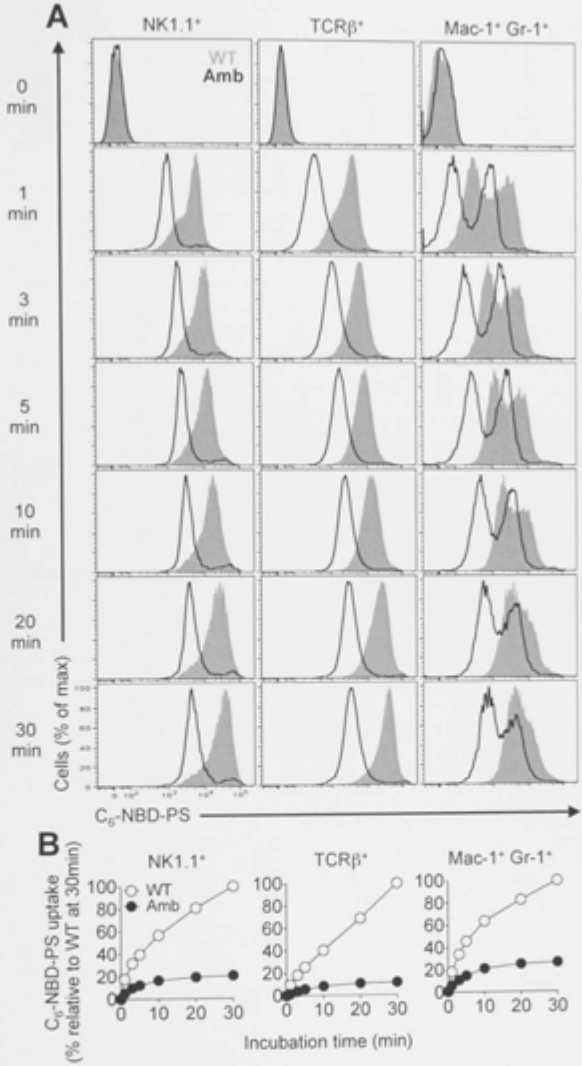

Figure 7.11 The ATP11C^{amb} mutation decreases C_6-NBD-PS translocation into different lineages in the spleen

(A) Representative C_6-NBD-PS fluorescence profiles after 0, 1, 3, 5, 10, 20 and 30 min incubation in NK1.1$^+$ NK cells, TCRβ$^+$ T cells and Mac-1$^+$Gr-1$^+$ Myeloid cells from the spleen of *Atp11c*$^{amb/0}$ (Amb, black lines), compared to the corresponding CD45.1-marked of *Atp11c*$^{+/0}$ (WT, shaded grey) cells in the same tube. **(B)** Graphs represent mean ± S.E.M of the percentage of C_6-NBD-PS uptake relative to WT. Data are pooled from three independent experiments with one mouse per genotype in each.

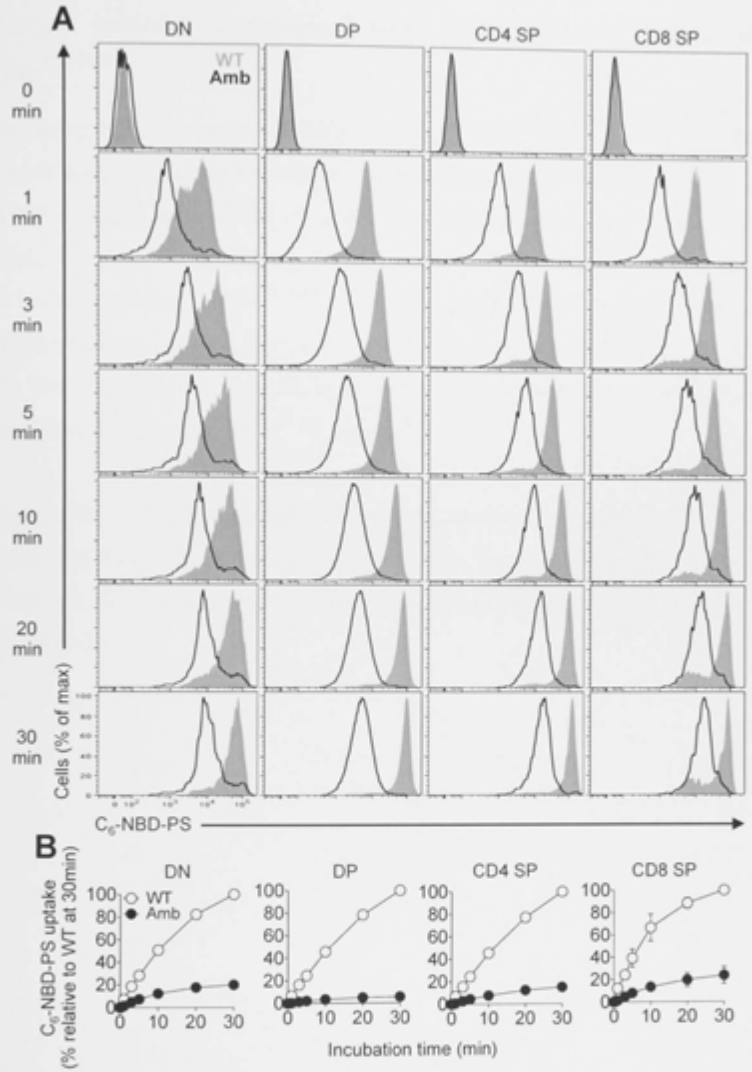

Figure 7.12 The ATP11C^{amb} mutation decreases C_6-NBD-PS translocation into all T cell subsets in the thymus

(A) Representative C_6-NBD-PS fluorescence profiles after 0, 1, 3, 5, 10, 20 and 30 min incubation in CD4 and CD8 double negative (DN) or double positive (DP), and CD4 or CD8 Single Positive (SP) cells from the thymus of *Atp11c*$^{amb/0}$ (Amb, black lines), compared to the corresponding CD45.1-marked of *Atp11c*$^{+/0}$ (WT, shaded grey) cells in the same tube. **(B)** Graphs represent mean ± S.E.M of the percentage of C_6-NBD-PS uptake relative to WT at 30 min. Data are pooled from three independent experiments with one mouse per genotype in each.

7.7 The defective C_6-NBD-PS flippase activity in ATP11C-deficient leukocyte subsets is confirmed using cells from the second allele, *Atp11c*$^{18NIH30/0}$

I also tested different leukocyte subsets from *Atp11c*$^{18NIH30/0}$ mice for C_6-NBD-PS transport activity as described above. I found that the rate of translocation of C_6-NBD-PS from the outer leaflet of the plasma membrane to the inner leaflet in B cell subsets, NK cells, T cells and myeloid cells in the bone marrow and spleen, and in T cells in the thymus of *Atp11c*$^{18NIH30/0}$ is significantly reduced compared to cells from wild-type controls (Figure 7.13, Figure 7.14, Figure 7.15, Figure 7.16 and Figure 7.17). These results show that the defective C_6-NBD-PS translocation activity is also present in cells from *Atp11c*$^{18NIH30/0}$ animals.

Taken together, the data obtained with the more sensitive PS analogue C_6-NBD-PS indicate that ATP11C is a flippase that selectively mediates the inward transport of PS, and that all immune cells from mutant animals are defective in the internalisation of C_6-NBD-PS.

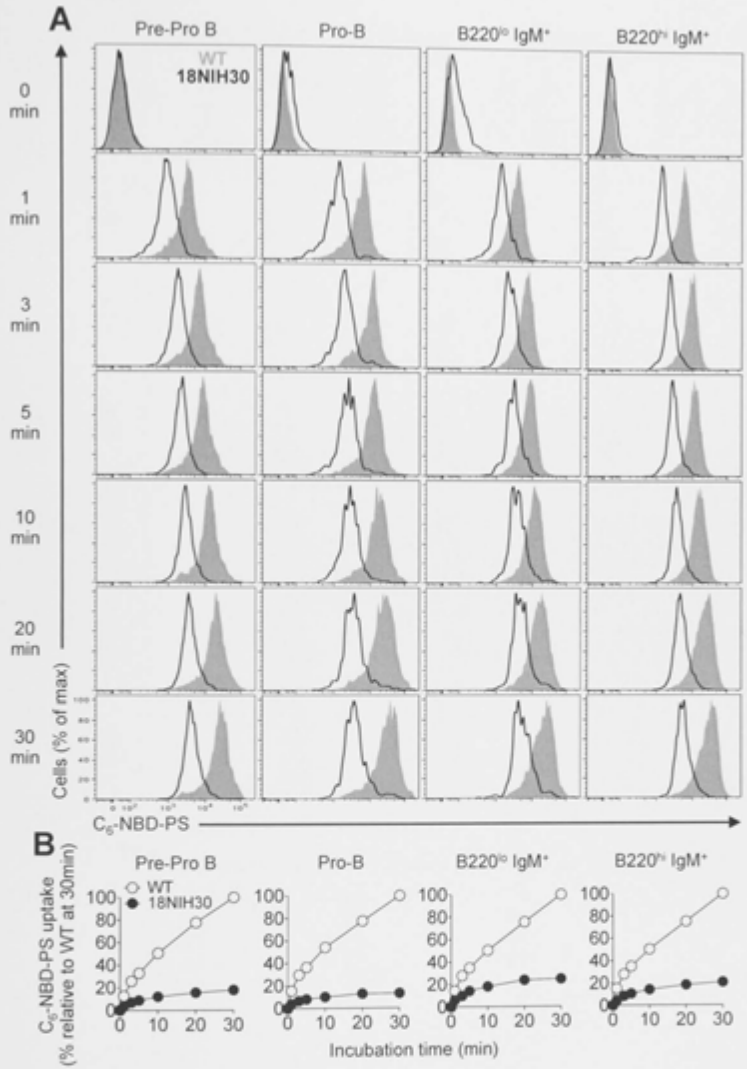

Figure 7.13 The ATP11C^{18NIH30} mutation decreases C_6-NBD-PS translocation into all B cell subsets in the bone marrow

(A) Representative C_6-NBD-PS fluorescence profiles after 0, 1, 3, 5, 10, 20 and 30 min incubation in B cell subsets from the bone marrow of *Atp11c*$^{18NIH30/0}$ (18NIH30, black lines), compared to the corresponding CD45.1-marked of *Atp11c*$^{-/0}$ (WT, shaded grey) cells in the same tube. **(B)** Graphs represent mean ± S.E.M of the percentage of C_6-NBD-PS uptake relative to WT at 30 min. Data are pooled from two independent experiments with one mouse per genotype in each.

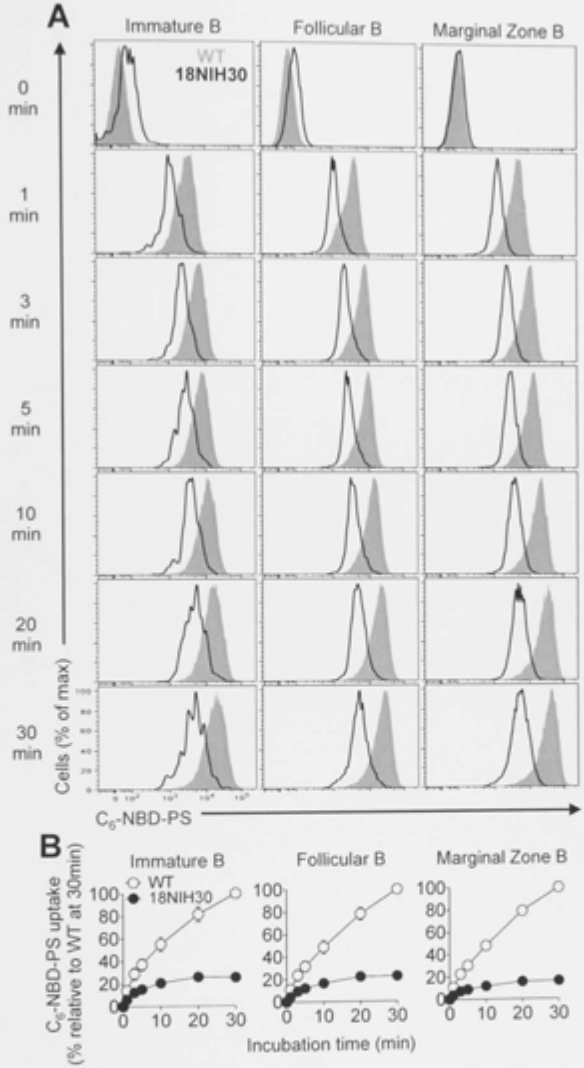

Figure 7.14 The ATP11C^{18NIH30} mutation decreases C_6-NBD-PS translocation into all B cell subsets in the spleen

(A) Representative C_6-NBD-PS fluorescence profiles after 0, 1, 3, 5, 10, 20 and 30 min incubation B cell subsets from the spleen of *Atp11c*$^{18NIH30/0}$ (18NIH30, black lines), compared to the corresponding CD45.1-marked of *Atp11c*$^{-/0}$ (WT, shaded grey) cells in the same tube. **(B)** Graphs represent mean ± S.E.M of the percentage of C_6-NBD-PS uptake relative to WT at 30 min. Data are pooled from two independent experiments with one mouse per genotype in each.

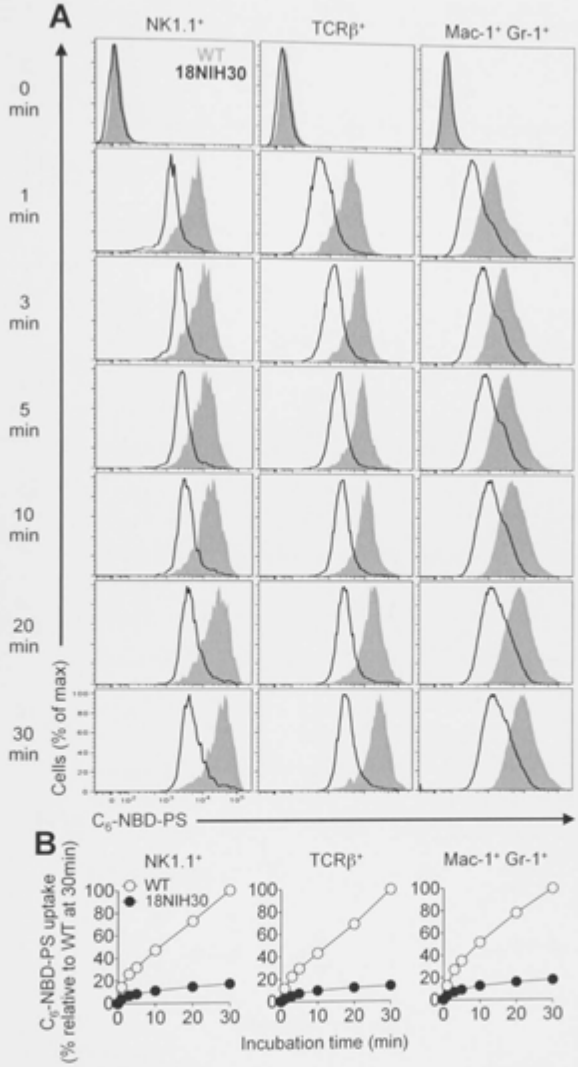

Figure 7.15 The ATP11C^{18NIH30} mutation decreases C_6-NBD-PS translocation into different lineages in the bone marrow

(A) Representative C_6-NBD-PS fluorescence profiles after 0, 1, 3, 5, 10, 20 and 30 min incubation in NK1.1$^+$ NK cells, TCRβ$^+$ T cells and Mac-1$^+$Gr-1$^+$ Myeloid cells from the bone marrow of *Atp11c*$^{18NIH30/0}$ (18NIH30, black lines), compared to the corresponding CD45.1-marked of *Atp11c*$^{+/0}$ (WT, shaded grey) cells in the same tube. **(B)** Graphs represent mean ± S.E.M of the percentage of C_6-NBD-PS uptake relative to WT at 30 min. Data are pooled from two independent experiments with one mouse per genotype in each.

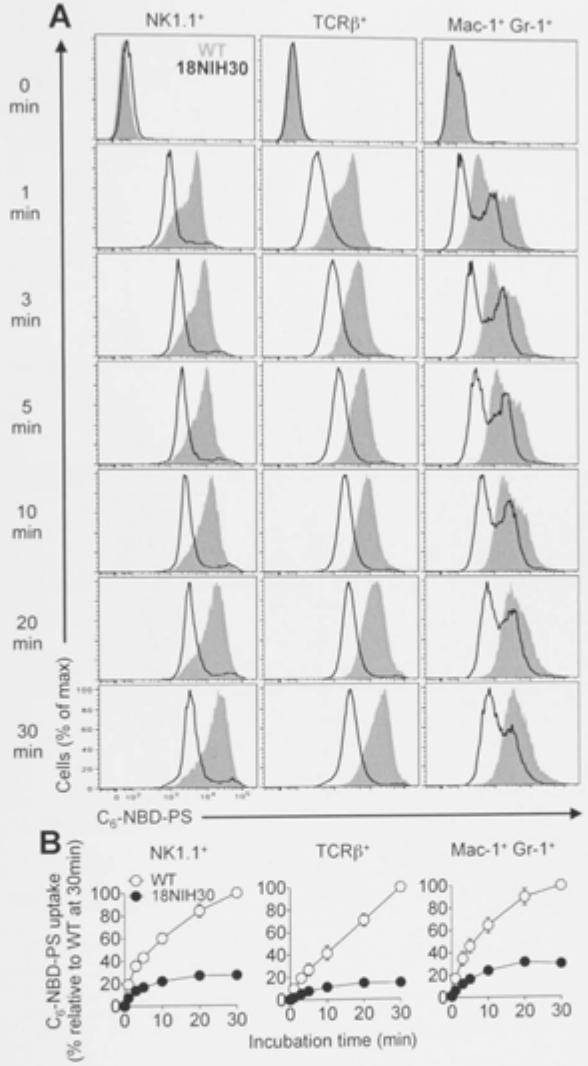

Figure 7.16 The ATP11C^{18NIH30} mutation decreases C_6-NBD-PS translocation into different lineages in the spleen

(A) Representative C_6-NBD-PS fluorescence profiles after 0, 1, 3, 5, 10, 20 and 30 min incubation in NK1.1$^+$ NK cells, TCRβ$^+$ T cells and Mac-1$^+$Gr-1$^+$ Myeloid cells from the spleen of *Atp11c*$^{18NIH30/0}$ (18NIH30, black lines), compared to the corresponding CD45.1-marked of *Atp11c*$^{+/0}$ (WT, shaded grey) cells in the same tube. **(B)** Graphs represent mean ± S.E.M of the percentage of C_6-NBD-PS uptake relative to WT at 30 min. Data are pooled from two independent experiments with one mouse per genotype in each.

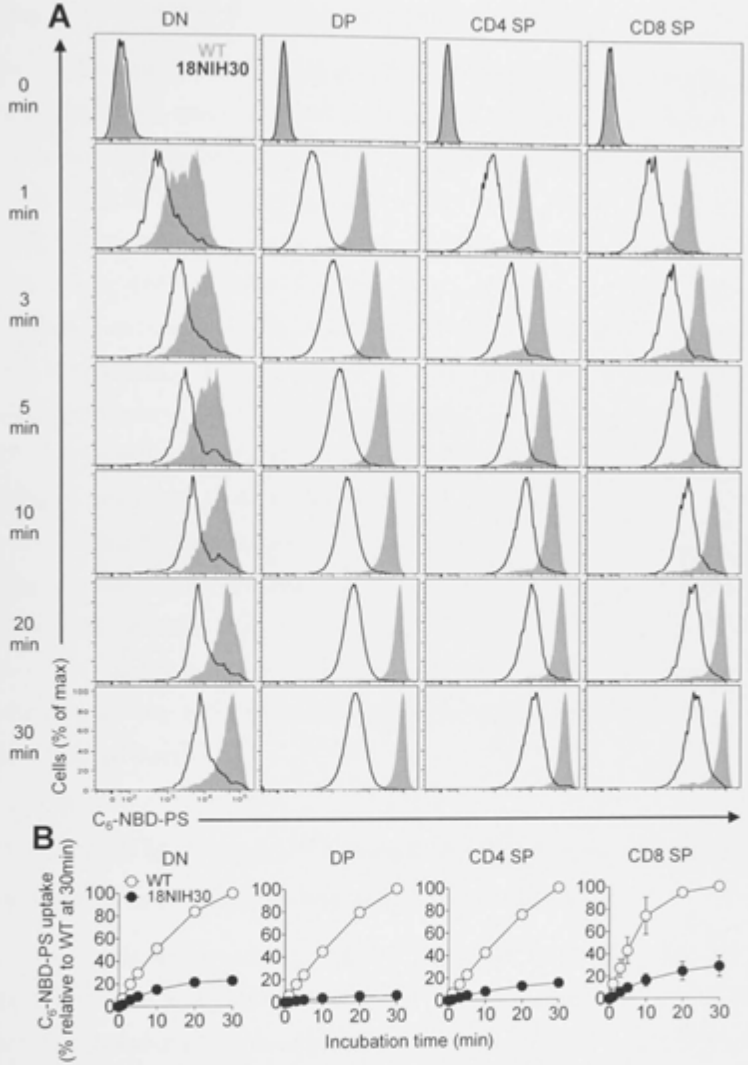

Figure 7.17 The ATP11C^{18NIH30} mutation decreases C_6-NBD-PS translocation into all T cell subsets in the thymus

(A) Representative C_6-NBD-PS fluorescence profiles after 0, 1, 3, 5, 10, 20 and 30 min incubation in CD4 and CD8 double negative (DN) or double positive (DP), and CD4 or CD8 Single Positive (SP) cells from the thymus of *Atp11c*$^{18NIH30/0}$ (18NIH30, black lines), compared to the corresponding CD45.1-marked of *Atp11c*$^{-/0}$ (WT, shaded grey) cells in the same tube. **(B)** Graphs represent mean ± S.E.M of the percentage of C_6-NBD-PS uptake relative to WT at 30 min. Data are pooled from two independent experiments with one mouse per genotype in each.

7.8 Pro-B cells show the highest rate of C_6-NBD-PS internalisation compared to the other B cell subsets in the bone marrow

While flippase assay performed using C_{12}-NBD-PS revealed a stage specific defect in PS internalisation into the mutant pro-B cells, the experiments performed with a more sensitive PS analogue C_6-NBD-PS demonstrated a broader PS translocation defect into the different haematopoietic lineages from ATP11C-deficient animals. These results raise the question why pro-B cells are particularly sensitive to reduced flippase activity as I only observed a cellular defect at the pro-B stage. One possible explanation is an increased need for PS internalisation at this stage. To examine this, I tested the rate of C_6-NBD-PS internalisation in different B cell subpopulations in the bone marrow of wild-type animals. I found that pro-B cells show the highest rate of PS internalisation compared to the other subsets including pre/pro-B, pre-B, $B200^{lo}IgM^+$ and $B220^{hi}IgM^+$ B cells in the bone marrow (Figure 7.18). While the rate of C_6-NBD-PS internalisation in mature B cells and pre/pro-B cells at 30 minutes was 92% and 84% of that in pro-B cells, respectively, it was reduced to 67% in $B200^{lo}IgM^+$ B cells, and to 53% in pre-B cells (Figure 7.18). These results illustrate that different B cell subsets in the bone marrow have different PS translocation activity with pro-B cells showing the highest and pre-B cells showing the lowest flippase activity.

7.9 Pro-B cells from *Atp11c*$^{amb/0}$ animals display normal steady-state PS concentration in the outer plasma membrane leaflet

The reduced flippase activity in *Atp11c*$^{amb/0}$ animals raises the possibility that ATP11C mutations lead to a steady-state increase in the concentration of PS in the exoplasmic plasma membrane leaflet of pro-B cells. To test this hypothesis, bone marrow cells were stained with the PS-binding protein Annexin-V and the membrane-impermeable DNA dye, 7AAD and analysed on a flow cytometry. There was no increased Annexin-V fluorescence on viable $7AAD^-$ pro-B or pre-B cells from *Atp11c*$^{amb/0}$ animals, but the percentage of apoptotic cells staining with both Annexin-V and 7AAD was increased among pre-B cells from *Atp11c*$^{amb/0}$ mice (Figure 7.19). This increase in apoptotic pre-B cells was suppressed by enforced expression of BCL-2 (Figure 7.19).

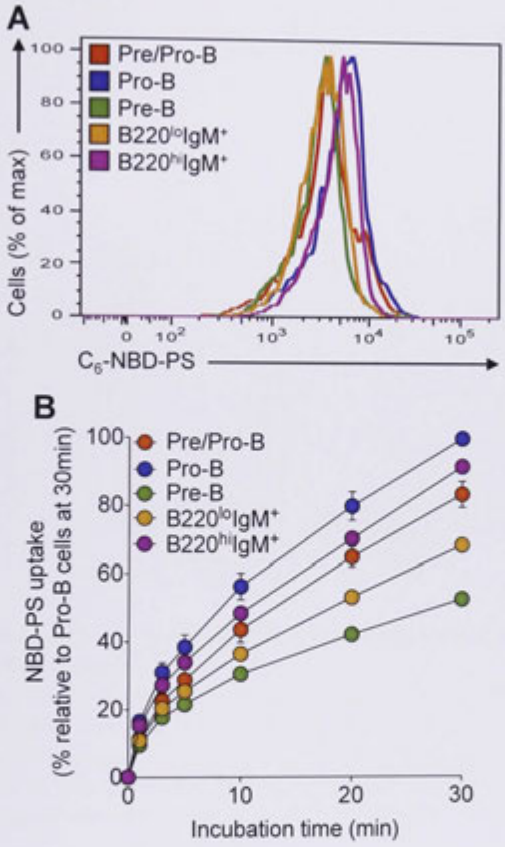

Figure 7.18 The highest rate of PS internalisation into pro-B cells compared to other B cell subsets in the bone marrow

(A) Representative C_6-NBD-PS fluorescence profiles after 1 min incubation in pre/pro-B, pro-B, pre-B, $B220^{lo}IgM^+$ and $B220^{hi}IgM^+$ B cells from the bone marrow of wild-type animals. **(B)** Graph represents mean ± S.D of the percentage of C_6-NBD-PS uptake in different B cell subsets relative to pro-B cells at 30 min. Data are pooled from three independent experiments with one mouse in each.

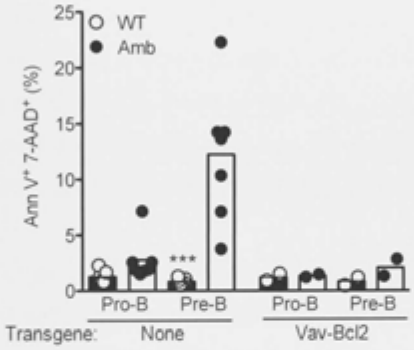

Figure 7.19 Normal surface expression of PS on the exoplasmic leaflet of pro-B cells from ATP11C-deficient animals

Percentage of pro-B or pre-B cells that are apoptotic as measured by positive staining for Annexin-V and 7AAD, from *Atp11c*$^{+/0}$ (WT) and *Atp11c*$^{amb/0}$ (Amb) mice lacking or carrying the *Vav-Bcl2* transgene. Data are from two experiments (non-transgenic) or one experiment (*Vav-Bcl2*) with two to five mice per genotype in each. Statistical significance was calculated using the two-tailed Student's *t*-test. *** $P < .001$.

7.10 Blocking the "eat me" signal fails to rescue the B cell phenotype in *Atp11c*$^{amb/0}$ mice

Despite normal steady-state PS concentration on B cells from *Atp11c*$^{amb/0}$ mice, one hypothesis could still be that PS transiently accumulates on the extracellular leaflet of the plasma membrane due to the impaired flippase function of ATP11C, triggering phagocytosis and destruction by bone marrow macrophages or stromal cells. One way of testing this hypothesis is to block the "eat me" signal on the mutant bone marrow B cells with Diannexin, a homodimer of Annexin-V, which has been suggested to have a higher affinity for PS on the outer leaflet of the plasma membrane as well as an increased *in vivo* half-life compared to Annexin-V (Teoh et al., 2007). If the PS accumulation on pre-B cells is responsible for their destruction in ATP11C-deficient mice and PS accumulation could be adequately saturated by Diannexin, it is expected that treatment would lead to a clear accumulation of pre-B cells within 1-2 days as pre-B cells are rapidly dividing cells.

To examine this hypothesis *Atp11c*$^{amb/0}$ animals and their control littermates were intravenously injected with Diannexin at a concentration that has been shown to be effective in preventing recognition of PS exposing cells by macrophages in hepatic ischemia-reperfusion injury studies (Teoh et al., 2007), and sacrificed 20h after treatment. Another group of mice was treated again with Diannexin 20h after the first injection. The mice of this group were sacrificed 24h after the second Diannexin injection and B cells from the bone marrow and spleen of both groups were analysed on a flow cytometry. Control mice received PBS instead of Diannexin.

Enumeration of B cell subsets in the bone marrow showed no difference in the number of pro-B, pre-B and total B cell numbers in *Atp11c*$^{amb/0}$ animals treated with Diannexin compared to PBS-injected *Atp11c*$^{amb/0}$ animals (Figure 7.20A; left panels). Similarly, there was no difference in the number of total B cell numbers in the spleen of Diannexin-administered *Atp11c*$^{amb/0}$ animals compared to PBS-injected mutant mice (Figure 7.20B; left panel). Likewise, two consecutive daily Diannexin treatments did not cause a significant increase in the number of different B cell subsets in the bone marrow, and number of total B cells in the spleen of *Atp11c*$^{amb/0}$ mice (Figure 7.20A, B; right panels). Collectively, these results suggest that loss of B

cell numbers in the bone marrow and spleen of *Atp11c*^{enu10} animals is likely independent of possible PS accumulation on the surface of pre-B cells due to the defective flippase activity.

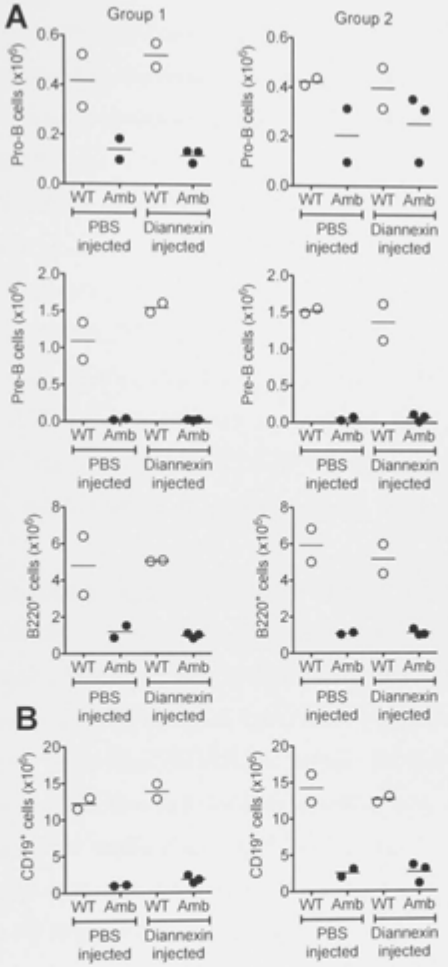

Figure 7.20 Blocking the "eat me" signal by administering Diannexin does not correct B cell phenotype in the bone marrow and spleen of ATP11C-deficient mice

Atp11c$^{+/0}$ (WT) and *Atp11c*$^{amb/0}$ (Amb) animals were intravenously injected with Diannexin and sacrificed 20h after treatment (Group 1). The second group of mice was given another Diannexin treatment 20h after the first treatment. The mice were sacrificed 24h after the second treatment (Group 2). B cells from the bone marrow and spleen of both groups were analyzed on a flow cytometry. Control mice received PBS instead of Diannexin **(A)** Graphs show number of pro-B, pre-B and total B cells in the bone marrow of *Atp11c*$^{+/0}$ (WT) and *Atp11c*$^{amb/0}$ (Amb) mice that were injected with either PBS or Diannexin. **(B)** Graphs show number of total B cells in the spleen of *Atp11c*$^{+/0}$ (WT) and *Atp11c*$^{amb/0}$ (Amb) mice that were injected with either PBS or Diannexin. Each circle represents one mouse, and data are representative of two independent experiments with two to three mice per genotype in each.

7.11 Chapter summary and discussion

The results presented in the previous chapters revealed that ENU-induced point mutations in the gene encoding the putative aminophospholipid translocase ATP11C resulted in a B cell deficiency syndrome in mice. ATP11C is believed to mediate the inward movement of PS, and to lesser extent PE, between the two leaflets of the plasma membrane (Sebastian et al., 2012, van der Mark et al., 2013), but there is no direct evidence for the aminophospholipid translocase activity of ATP11C that has been reported. In this chapter, therefore, the effect of two allelic mutations of the *Atp11c* gene, namely ATP11C^{amb} and ATP11C^{18NIH30} was studied in relation to the aminophospholipid translocation activity. Using the fluorescently labelled PS analogue (C_{12}-NBD-PS), initial experiments revealed that pro-B cells from the bone marrow of *Atp11c*$^{amb/0}$ show a reduced rate of PS internalisation compared to those from control animals, and this defect was specific for only pro-B cells.

A multiple lines of evidence suggest that a more sensitive analogue (C_6-NBD-PS) was available (Hanada and Pagano, 1995), that differed from the original C_{12}-NBD-PS ligand by the length of the *sn-2* chain to which the NBD fluorescence marker is attached. The shorter *sn-2* chain increases the critical micelle concentration of the phospholipid analogue. While C_{12}-NBD-PS can form micelles in aqueous solutions, the C_6-NBD-PS analogue can also exist in its monomeric form. This allows the C_6-NBD-PS to penetrate more easily into a lipid bilayer, and also allows it to back extract with the fatty acid free BSA because of the equilibrium between the monomeric C_6-NBD-PS in solution and in the outer leaflet of the cell membrane.

The utilisation of the more sensitive C_6-NBD-PS analogue revealed that all lymphocyte subsets including B cell subsets, T cells, NK cells as well as myeloid cells in the bone marrow, spleen and thymus of *Atp11c*$^{amb/0}$ animals have a significantly reduced rate of PS internalisation compared to corresponding cells from control animals. Notably, the defective flippase activity was confirmed using cells from mice carrying an independent ATP11C mutant allele (*Atp11c*$^{18NIH30/0}$).

Why are pro-B cells particularly sensitive to the impaired flippase activity despite that all cells of the immune system in mutant mice exhibit slower rate of PS

internalisation? Comparison of PS flippase activity in different B cell subsets in the bone marrow of wild-type mice revealed that pro-B cells display the highest rate of PS internalisation. This finding is interesting because it could indicate that pro-B cells have an increased dependence on PS internalisation, and this could explain the stage specific defect observed in B cell development in the bone marrow of ATP11C-deficient animals. However, the variable internalisation rate did not correlate with gene expression of *Atp11c* in different B cell subpopulations in the bone marrow as it is comparably expressed in pre/pro-, pro-, pre- and immature B cells in the bone marrow (Figure 1.9B in Chapter 1) (Heng and Painter, 2008). Therefore, it is plausible that the cellular defect at the pro-B cell stage of B cell development in the bone marrow of ATP11C-deficient animals could be explained by the defective flippase activity in pro-B cells as they exhibit the highest rate of PS translocation activity compared to the other B cell subsets.

Exposure of PS on the surface of cells is critical for the recognition and clearance of apoptotic cells by macrophages (Fadok et al., 1992). An alternative explanation for the stage specific defect in B lymphopoiesis could be that the impaired flippase activity causes a temporary increased PS concentration on the cell surface this could result in rapid PS-mediated phagocytosis of B cells in ATP11C-deficient mice. However, there was no increase in surface expression of PS on pro-B and pre-B cells from *Atp11c*$^{amb/0}$ animals. Moreover, blocking the "eat me" signal by administering an Annexin-V homodimer, Diannexin, did not rescue the reduced B cell numbers in the bone marrow and spleen of ATP11C-deficient mice. It should be noted that because of the lack of a positive control to show that the Diannexin treatment did block the "eat me" signal in developing B cells, I cannot rule out this possibility and further experiments are needed to test this crucial hypothesis. A definitive experiment will be to cross ATP11C mutant mice with animals that are defective in the engulfment of PS-exposing apoptotic cells by macrophages (i.e. mice lacking the membrane tyrosine kinase c-mer or the PS receptor Tim4 (Cohen et al., 2002, Miyanishi et al., 2007)), and determine whether this genetic ablation rescues the B cell deficiency in ATP11C-deficient mice.

Collectively, these results demonstrate for the first time that the mutations in the gene encoding ATP11C resulted in the diminished flippase activity, and suggest that

ATP11C is a flippase that selectively transports PS from the outer leaflet of the plasma membrane to the inner leaflet. This was confirmed recently by a study where ATP11C was shown to act as a flippase in human cells (Segawa et al., 2014). Segawa et al. also determined the substrate specificity of ATP11C as cells lacking ATP11C failed to flip PS and PE, but not PC, from the exoplasmic to the cytoplasmic leaflet of the bilayer cells (Segawa et al., 2014). Furthermore, the β-subunit of the heterodimeric complex, CDC50, was also required for proper flippase activity (Segawa et al., 2014). Therefore, the results of this chapter together with the findings of Segawa et al. suggest that ATP11C functions as a flippase in the biological membranes.

CHAPTER 8: Analysis of other haematopoietic and non-haematopoietic phenotypes in *Atp11c*$^{amb/0}$ animals

Contents of Figure 8.1, 8.2, 8.12B, C and 8.13 appeared in:

Mehmet Yabas, Charis E. Teh, Sandra Frankenreiter, Dennis Lal, Carla M. Roots, Belinda Whittle, Daniel T. Andrews, Yafei Zhang, Narci C. Teoh, Jonathan Sprent, Lina E. Tze, Edyta M. Kucharska, Jennifer Kofler, Geoffrey C. Farell, Stefan Bröer, Christopher C. Goodnow and Anselm Enders (2011). "ATP11C is critical for the internalization of phosphatidylserine and differentiation B lymphocytes". *Nature Immunology*, 12(5):441-449.

Contributions from others:

- Prof. Narci C. Teoh and Prof. Geoffrey C. Farell provided help in the analysis of samples for Figure 8.12B, C.
- Ms. Anne Prins performed H&E staining of the liver sections for Figure 8.13, and Prof. Narci C. Teoh and Prof. Geoffrey C. Farell assessed the sections at the Canberra Hospital.
- Mrs. Debbie Howard and Ms. Nadine Barthel provided technical help in the irradiation of mice and intravenous injection of cells in the bone marrow chimera experiments.

8.1 Preamble

As shown in Chapter 3, the ATP11C^{amb} and ATP11C^{18NIH30} mutations in mice led to a defect in the accumulation of B cells in the bone marrow and periphery. Consistent with the predicted biochemical function of ATP11C, the previous chapter revealed that B cells from the bone marrow and spleen of *Atp11c*$^{amb/0}$ and *Atp11c*$^{18NIH30/0}$ mice display an impaired flippase activity as measured by decreased uptake of the fluorescent PS analogue C_6-NBD-PS into the plasma membrane compared to B cells from *Atp11c*$^{+/0}$ animals. Interestingly, the defective flippase activity was not specific for B cells and was also detected in other blood lineages including T cells, NK cells and myeloid cells from *Atp11c*$^{amb/0}$ and *Atp11c*$^{18NIH30/0}$ mice. These results raise a possible involvement of ATP11C in the development and homeostasis of multiple cell lineages. Therefore, in this chapter I investigated the effect of the ATP11C^{amb} mutation on the accumulation of haematopoietic progenitor cells in the bone marrow and other non-B cell lineages in the thymus and periphery.

8.2 ATP11C is dispensable for the generation of blood cell progenitors and lineages in the bone marrow

Given that all the cells of the immune system originate from the pluripotent HSCs of the bone marrow, I first tested the effect of the ATP11C^{amb} mutation on the number of progenitors in the bone marrow. Analysis of haematopoietic progenitors including CD127$^-$Lin$^-$C-Kit$^+$Sca-1$^+$Flt3$^-$ haematopoietic stem and progenitor cells, CD127$^-$Lin$^-$ C-Kit$^+$Sca-1$^+$Flt3$^+$ MPPs, and CD127$^+$Lin$^-$CD93$^+$Sca-1^{int}Flt3^{int}C-Kit^{med} CLPs which are the earliest lymphoid progenitors revealed normal or slightly elevated numbers of these populations in the bone marrow of *Atp11c*$^{amb/0}$ mice compared to their wild-type littermates (Figure 8.1).

I next performed a more detailed enumeration of different lineages in the bone marrow, and showed that *Atp11c*$^{amb/0}$ mice have normal number of Mac-1$^+$Gr-1$^+$ myeloid and NK1.1$^+$ NK, slightly lower Ter119$^+$ erythroid and slightly higher number of CD3$^+$ T cells (Figure 8.2). These data indicate that ATP11C is not required for blood cell progenitors and their development into different mature lymphoid and myeloid lineages except B cells.

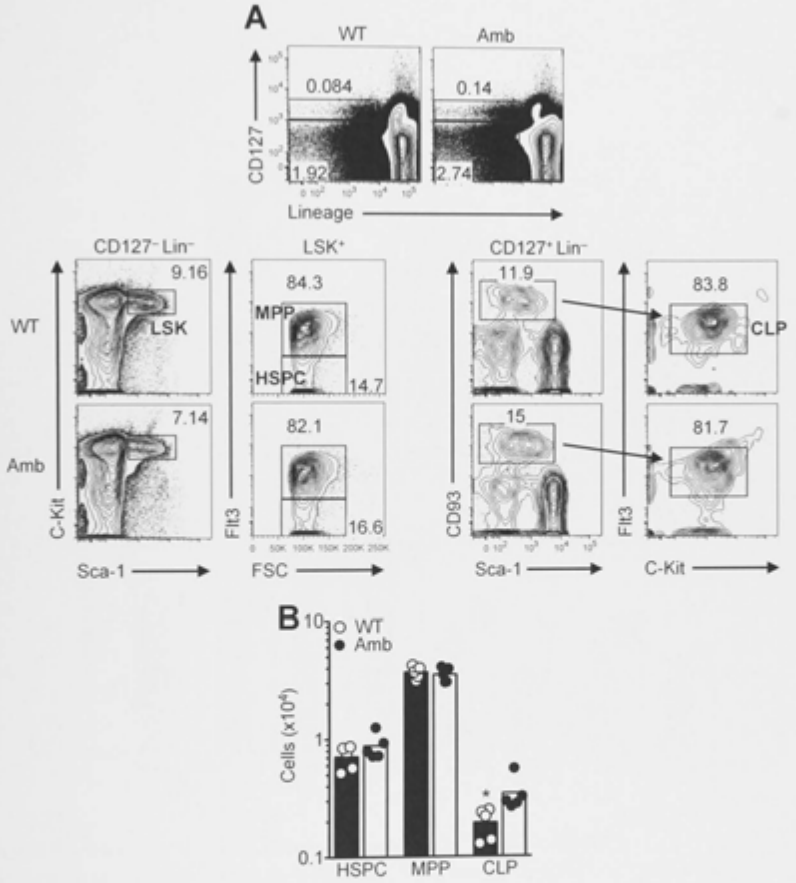

Figure 8.1 Analysis of major blood cell progenitors in the bone marrow

(A) Representative flow cytometric analysis of haematopoietic stem and progenitor cells (HSPC), multipotent progenitors (MPP), and common lymphoid progenitors (CLP) in the bone marrow of *Atp11c*$^{-/0}$ (WT) and *Atp11c*$^{amb/0}$ (Amb) mice. **(B)** Graph shows absolute number of the cell populations gated as in (A), from *Atp11c*$^{-/0}$ (WT) and *Atp11c*$^{amb/0}$ (Amb) mice analysed in two different experiments. Each circle represents a single mouse. Lineage panel for the analysis includes antibodies against CD4, CD5, CD8, TCRβ, TCRγδ, IgM, IgD, B220, CD19, Mac-1, CD11c, Ter119, Ly6c, Gr-1 and NK1.1. Statistical significance was calculated using the two-tailed Student's *t*-test. * $P < .05$.

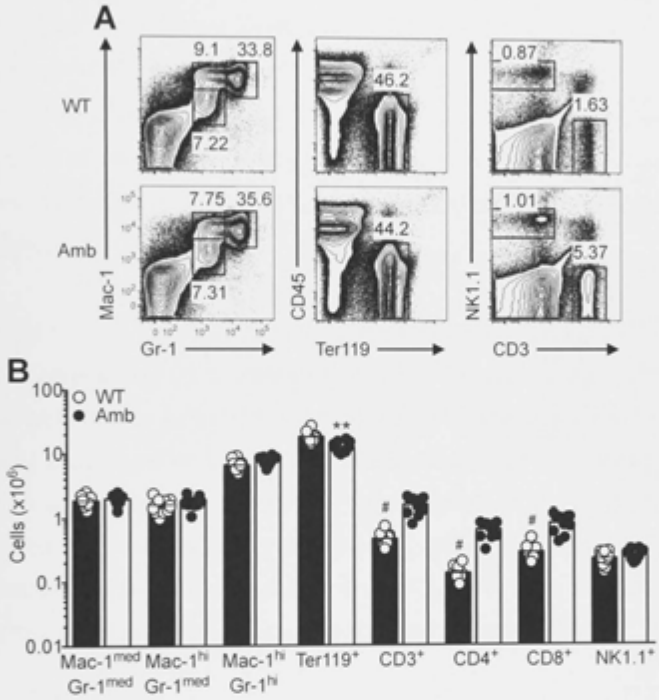

Figure 8.2 Analysis of major blood cell lineages in the bone marrow

(A) Representative flow cytometric analysis of the frequency of Myeloid cells (Mac-1^{med}Gr-1^{med}, Mac-1^{hi}Gr-1^{med} and Mac-1^{hi}Gr-1^{hi} respectively), Erythrocytes (Ter119^{+}), NK cells (NK1.1^{+}) and T cells (CD3^{+}) in the bone marrow of *Atp11c*$^{+/0}$ (WT) and *Atp11c*$^{amb/0}$ (Amb) mice. **(B)** Graph shows absolute number of the indicated cell populations from *Atp11c*$^{+/0}$ (WT) and *Atp11c*$^{amb/0}$ (Amb) mice analysed in two different experiments. Each circle represents a single mouse. Statistical significance was calculated using the two-tailed Student's *t*-test. $^{\#}$ $P < .0001$; *** $P < .001$.

8.3 Normal development of αβ and γδ T cells in the thymus of *Atp11c*$^{amb/0}$ mice

T cell development takes place in the thymus, and follows a well defined cell differentiation process characterised on the basis of expression of cell surface markers (Shortman and Wu, 1996, Zúñiga-Pflücker, 2004). T cells can be differentiated into two different T-cell lineages including alpha-beta (αβ) T cells and gamma-delta (γδ) T cells. Tαβ cells can further be differentiated into different subsets including CD4 SP and CD8 SP cells. While CD4 and CD8 T cells orchestrate different types of cell-mediated immune responses, γδ T cells play critical roles in the immune regulation, primary immune responses and tumour surveillance (Hayday and Pennington, 2007).

As shown in Chapter 7, T cells from the thymus and spleen of *Atp11c*$^{amb/0}$ animals exhibited a lower rate of PS internalisation compared to those in *Atp11c*$^{+/0}$ animals. In order to test whether ATP11C has any role in T cell development and survival, I first isolated thymocytes from *Atp11c*$^{amb/0}$ animals and their control littermates, and stained with surface markers to dissect the different stages of T cell development by flow cytometry. I found that the development of T cells in the thymus of *Atp11c*$^{amb/0}$ mice was normal as the frequency and number of CD4$^+$ SP, CD8$^+$ SP, DN and DP T cells was equivalent to that observed in *Atp11c*$^{+/0}$ mice (Figure 8.3A-C).

A small percentage of thymocytes that successfully rearrange genes encoding a TCRγ and TCRδ chain expresses a mature TCRγδ receptor and becomes Tγδ cells. I found that the number of γδ T cells in the thymus of *Atp11c*$^{amb/0}$ mice was comparable to *Atp11c*$^{+/0}$ controls (Figure 8.3D, E). Collectively, these results suggest that ATP11C is not required for the development of αβ and γδ T cell lineages in the thymus.

8.4 Normal distribution of αβ and γδ T cells in the periphery of *Atp11c*$^{amb/0}$ mice

Having shown that the ATP11C^{amb} mutation has no effect on the development of T cells in the thymus, I next sought to determine whether ATP11C influences the

survival of T cells in the periphery. *Atp11c*$^{+/0}$ and *Atp11c*$^{amb/0}$ animals were sacrificed, and the numbers of αβ and γδ T cells in the spleen and lymph node were enumerated using flow cytometry. As shown in Figure 8.4A ATP11C has no effect on the number of T cells with comparable numbers of αβ and γδ T cells being present in the spleen and lymph node of *Atp11c*$^{amb/0}$ mice.

I also analysed the ratio of CD4 and CD8 T cells in the periphery of *Atp11c*$^{amb/0}$ mice, and found an elevated percentage of CD4^{+} T cells in the spleen of *Atp11c*$^{amb/0}$ mice compared to their wild-type littermates (Figure 8.4B and C). Collectively, these results indicate that ATP11C deficiency in mice has apparently no impact on the development and survival of T cells in the peripheral circulation despite an impaired flippase activity, but seems to have an effect on the CD4/8 ratio in the spleen, which requires further examination.

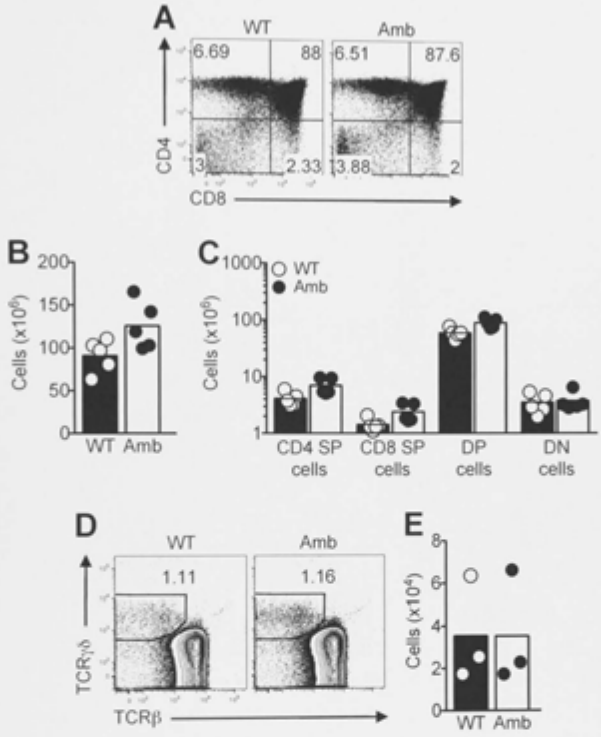

Figure 8.3 Normal T cell development in the thymus of *Atp11c*$^{amb\text{-}0}$ mice

(A) Representative flow cytometric analysis of thymic cells from *Atp11c*$^{+/0}$ (WT) and *Atp11c*$^{amb\text{-}0}$ (Amb) mice. Numbers adjacent to outlined areas indicate percentage of CD4$^+$CD8$^-$ CD4 Single Positive (SP) cells; CD4$^-$CD8$^+$ CD8 Single Positive (SP) cells; CD4$^+$CD8$^+$ Double Positive (DP) cells; CD4$^-$CD8$^-$ Double Negative (DN) cells. **(B, C)** Graphs show absolute number of (B) total thymocytes and (C) T cell subpopulations in the thymus. Each circle represents a single mouse, and data are representative of two independent experiments of three to five mice per genotype in each. **(D)** Representative flow cytometric analysis of γδ T cells from the thymus of *Atp11c*$^{+/0}$ (WT) and *Atp11c*$^{amb\text{-}0}$ (Amb) mice. Cells were pre-gated on CD3$^+$ T cells. Numbers adjacent to outlined area indicates percentage of TCRγδ$^+$TCRβ$^-$ γδ T cells. **(E)** Graph shows absolute number of γδ T cells in the thymus. Each circle represents a single mouse.

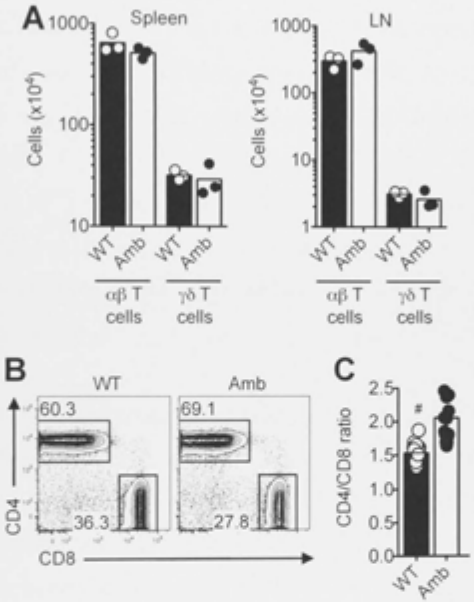

Figure 8.4 Normal distribution of αβ and γδ T cells in the periphery of *Atp11c*$^{amb/0}$ mice
(A) Graphs show absolute number of αβ and γδ T cells in the spleen and lymph node. Each circle represents a single mouse. **(B)** Representative flow cytometric analysis of CD4 and CD8 T cells from the spleen of *Atp11c*$^{-/0}$ (WT) and *Atp11c*$^{amb/0}$ (Amb) mice. Cells were pre-gated on CD3$^+$ T cells. Numbers adjacent to outlined areas indicate percentage of CD4$^+$CD8$^-$ CD4 T cells and CD4$^-$CD8$^+$ CD8 T cells. **(C)** Graph shows the ratio of CD4 and CD8 T cells gated as in (B), from the spleen of *Atp11c*$^{-/0}$ (WT) and *Atp11c*$^{amb/0}$ (Amb) mice analysed in at least four different experiments. Each circle represents a single mouse. Statistical significance was calculated using the two-tailed Student's *t*-test. $^{\#}P < .0001$.

8.5 Normal NK and NKT cell populations in the spleen of *Atp11c*$^{amb/0}$ mice

NK cells play an important role in the innate immune response with the capacity to kill virus infected cells, and contribute to anti-viral and anti-tumour immunity (Yokoyama et al., 2004). Natural Killer T (NKT) cells, on the other hand, arise from DP cells in the thymus and display a restricted TCR repertoire and play a crucial role in immune surveillance in the liver and spleen (Bendelac et al., 2007). Most of NKT cells express NK cell marker NK1.1 and an invariant T-cell receptor α chain that is paired with a limited repertoire of Vβ chains (Bendelac et al., 2007). Similar to other blood lineages, NK cells in the bone marrow and spleen of *Atp11c*$^{amb/0}$ mice also demonstrated reduced C_6-NBD-PS internalisation (Chapter 7). To determine whether the ATP11C^{amb} mutation has any effect on the differentiation and accumulation of NK cells as well as NKT cells, NK1.1^{+}CD3^{-} NK cells and NK1.1^{med}CD3^{med} NKT cells in the spleen of *Atp11c*$^{+/0}$ and *Atp11c*$^{amb/0}$ mice were ascertained by flow cytometry.

As shown in Figure 8.5, accumulation of NK1.1^{+}CD3^{-} and NK1.1^{med}CD3^{med} cells mostly occurred at normal or slightly increased percentages in the spleen of *Atp11c*$^{amb/0}$ animals compared to wild-type controls. The absolute number of both NK and NKT cells were severely reduced compared to their wild-type littermates (Figure 8.5B and C), however this is most likely due to a reduction in total leukocyte numbers in the spleen of mutant mice (Figure 3.4A in Chapter 3). These data thus indicate that ATP11C has likely no effect on NK and NKT cell development or peripheral homeostasis. However, it should be noted that NK1.1 and CD3 are not ideal markers to detect NKT cells, and CD1d alpha-galactosylceramide tetramer together with CD3 must be used to identify the precise NKT cell population.

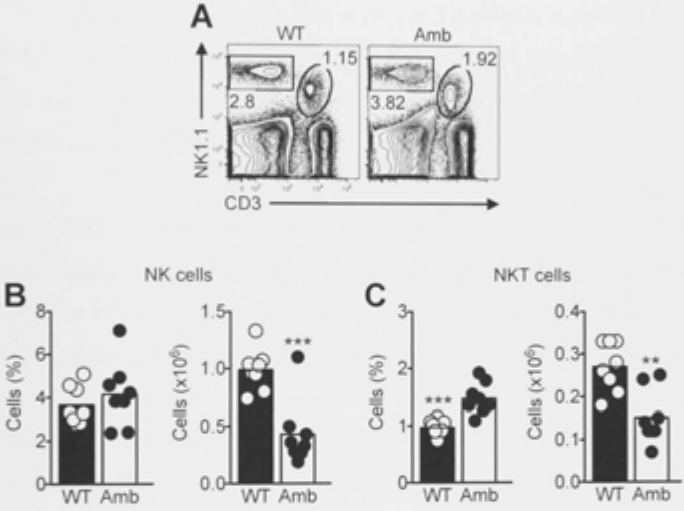

Figure 8.5 Normal frequency of NK and NKT cells in the spleen of *Atp11c*$^{amb/0}$ mice
(A) Representative flow cytometric analysis of spleen cells from *Atp11c*$^{+/0}$ (WT) and *Atp11c*$^{amb/0}$ (Amb) mice. Numbers adjacent to outlined areas indicate percentage of NK1.1^{+}CD3^{-} NK cells and NK1.1^{+}CD3^{+} NKT cells. **(B, C)** Graphs show percentage and absolute number of (B) NK and (C) NKT cells in the spleen of *Atp11c*$^{+/0}$ (WT) and *Atp11c*$^{amb/0}$ (Amb) mice analysed in two different experiments. Each circle represents a single mouse. Statistical significance was calculated using the two-tailed Student's *t*-test. *** $P < .001$; ** $P < .01$.

8.6 ATP11C-deficient environment influences the ability of wild-type HSCs to differentiate into B cell lineage

Having seen that ATP11C does not have a discernable impact on the accumulation of other haematopoietic lineages, I next wanted to test if wild-type HSCs can normally give rise to cells of the immune system in ATP11C-deficient recipient. To do so, I generated non-competitive bone marrow chimeras, in which 100% *Atp11c*$^{+/0}$ and 100% *Atp11c*$^{amb/0}$ bone marrow cells were adoptively transferred alone to both *Atp11c*$^{+/0}$ and *Atp11c*$^{amb/0}$ recipients that were irradiated with two doses of 450 rad (Figure 8.6A). The recipient mice were bled 9 weeks after transfer and leukocytes were analysed by flow cytometry for the donor-derived (CD45.1^{+}) cells in the peripheral blood (Figure 8.6B).

The degree of chimerism was close to 100% regardless of the genotype of the donor or recipient animals as evident from the percentage of CD45.1^{+} donor-derived myeloid cells in the blood of each chimeric recipient (Figure 8.7A). Similarly, the percentage of donor-derived lymphocytes was close to 100% in all groups except that *Atp11c*$^{amb/0}$ bone marrow cells showed an approximately 85% reconstitution in *Atp11c*$^{+/0}$ recipients (Figure 8.7A). Consistent with the findings that ATP11C controls B cell development in a cell intrinsic-fashion (Figure 3.7 in Chapter 3), bone marrow cells from *Atp11c*$^{amb/0}$ animals could not give rise to B cells either in wild-type or in ATP11C mutant recipients (Figure 8.7B).

In the control recipients, on the other hand, the wild-type donor CD45.1^{+} bone marrow cells were able to efficiently differentiate into B cells in wild-type recipients as the percentage of B cells was found to be approximately 70% of total lymphocytes (Figure 8.7B). Remarkably, CD45.1^{+} wild-type derived B cells represented only 9% of total lymphocytes in the blood of *Atp11c*$^{amb/0}$ recipients (Figure 8.7B). In the same chimeras, *Atp11c*$^{+/0}$ T cells nevertheless accumulated in approximately comparable proportion to other groups of recipients (Figure 8.7B). These results surprisingly suggest that the ATP11C^{amb} mutation may also affect some cell extrinsic factors that support B cell development in the bone marrow and/or B cell survival in the periphery.

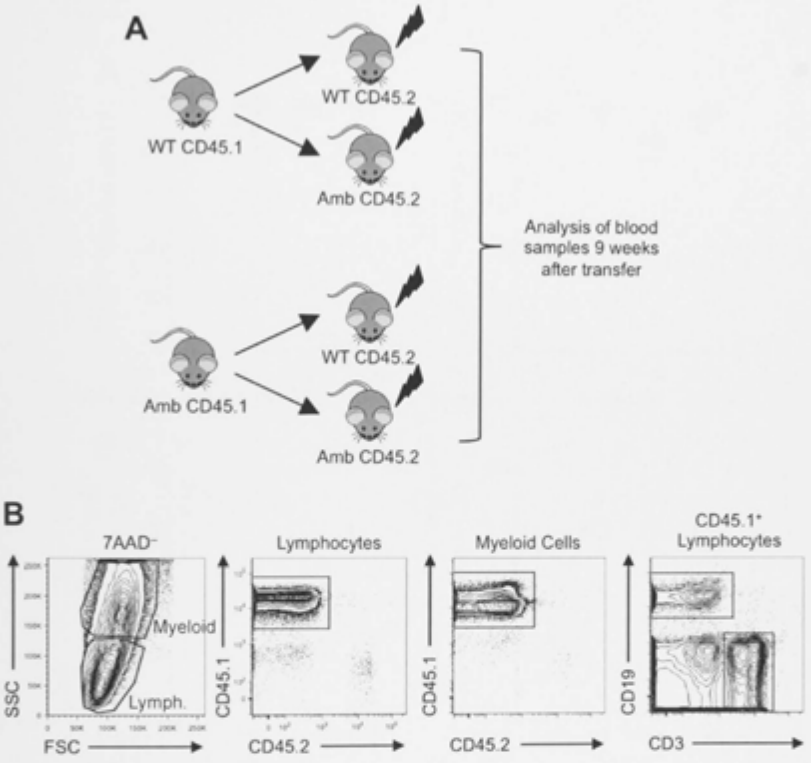

Figure 8.6 Experimental design of noncompetitive bone marrow chimeras, and gating strategy for the analysis of donor-derived cells in the peripheral blood of chimeric recipients

(A) Congenically CD45.1-labelled bone marrow cells from *Atp11c*$^{+/0}$ (WT) and *Atp11c*$^{amb/0}$ (Amb) animals intravenously injected into irradiated CD45.2 *Atp11c*$^{+/0}$ (WT) or *Atp11c*$^{amb/0}$ (Amb) recipients. The recipient mice were bled 9 weeks after transfer and analysed by flow cytometry. **(B)** Gating strategy for flow cytometric analysis of blood samples from the 100% bone marrow chimeric recipients. Donor derived cells in the irradiated hosts can be identified by CD45.1 congenic label.

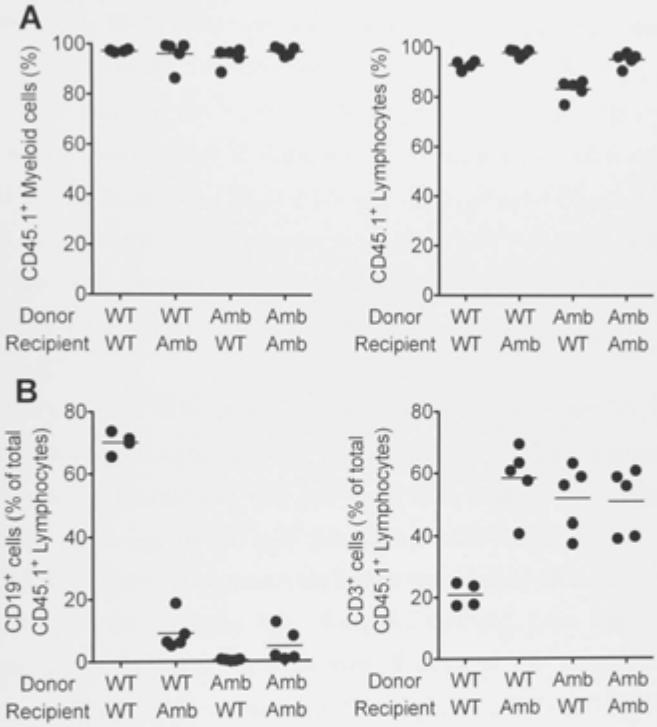

Figure 8.7 Impaired B cell accumulation in the blood of ATP11C-deficient animals that were irradiated and reconstituted with wild-type bone marrow cells

(A) Graphs show the percentage of CD45.1$^+$ donor-derived myeloid cells and lymphocytes (gated as in Figure 8.6B) in the blood of chimeric recipients 9 weeks after transfer. **(B)** Graphs show the percentage of CD19$^+$ B cells and CD3$^+$ T cells within the donor-derived CD45.1$^+$ lymphocytes in the blood of chimeric recipients 9 weeks after transfer. Each circle represents a single mouse.

8.7 Analysis of an ATP11C-deficient mouse that was irradiated and reconstituted with wild-type bone marrow cells

It was unexpected that *Atp11c*$^{amb/0}$ mice reconstituted with *Atp11c*$^{+/0}$ bone marrow cells show defective B cell accumulation in the peripheral blood (9% compared to 70% in the control chimeras). Unfortunately, there was only one *Atp11c*$^{amb/0}$ mouse reconstituted with 100% wild-type bone marrow cells available for the detailed analysis of B cell subsets. Therefore, this mouse was compared to intact *Atp11c*$^{+/0}$ and *Atp11c*$^{amb/0}$ animals. Firstly, B cell development in the bone marrow of the chimeric mouse was analysed to determine if the apparent loss of B cells in the peripheral blood is caused by a block in the early stages of development. Analysis of the B cell development in the bone marrow of the *Atp11c*$^{amb/0}$ mouse reconstituted with wild-type cells showed that the frequency of total B cells in the bone marrow is largely normal compared to that in control mouse (Figure 8.8).

Detailed analysis of B cells subsets revealed that IgD^{+}IgM^{+} mature circulating B cells represent approximately 80% of total B cells in the bone marrow of the *Atp11c*$^{amb/0}$ mouse transplanted with wild-type bone marrow cells (Figure 8.8). However, the percentage of IgD^{-}IgM^{+} immature B cells in the *Atp11c*$^{amb/0}$ mouse transplanted with control bone marrow cells was considerably reduced compared to intact *Atp11c*$^{+/0}$ animal (Figure 8.8). Similarly, IgD^{-}IgM^{-} bone marrow B cell progenitors represented only 12% of total B cells in the *Atp11c*$^{amb/0}$ mouse transplanted with control bone marrow cells compared to 57% and 82% in intact *Atp11c*$^{+/0}$ and *Atp11c*$^{amb/0}$ animals, respectively (Figure 8.8). When these cells were sorted by CD24 and CD43 expression, there was a partial defect at the pro-B cell stage as the percentage of pre-B cells represented 35% of total progenitors compared to 70% in control animal (Figure 8.8). Collectively, these results suggest that there is a defect in early B cell development in the bone marrow of the ATP11C-deficient host that received transplants of wild-type haematopoietic cells, but that mature B cells can develop and survive.

Next, B cell and B cell subsets in the spleen of *Atp11c*$^{+/0}$, *Atp11c*$^{amb/0}$ and chimeric *Atp11c*$^{amb/0}$ mice were analysed. In the *Atp11c*$^{amb/0}$ mouse that was irradiated and reconstituted with wild-type bone marrow cells, the percentage of total B and

immature B cells was increased compared to the intact *Atp11c*$^{amb/0}$ mouse, but it was still lower than in the control animal (Figure 8.9). Interestingly, B cells within the B220^{+}CD93^{-} mature B cells were phenotypically indistinguishable from those in the intact *Atp11c*$^{amb/0}$ mouse with approximately 50% MZ B cells (Figure 8.9). The loss of repopulating activity of wild-type bone marrow cells in the *Atp11c*$^{amb/0}$ mouse was specific for B cells, because bone marrow cells from wild-type mice gave rise to normal percentages in all major haematopoietic lineages including NK cells and T cells in the spleen (Figure 8.10) and T cells in the thymus (Figure 8.11) on transplantation into an irradiated *Atp11c*$^{amb/0}$ mouse.

Taken together, the results from the non-competitive bone marrow chimera experiments suggest that ATP11C may also affect some other cell extrinsic factors that are required for the development of pre-B cells in the bone marrow and accumulation of FO B cells in the spleen. However, these results are preliminary and needed to be confirmed and extended by future experiments.

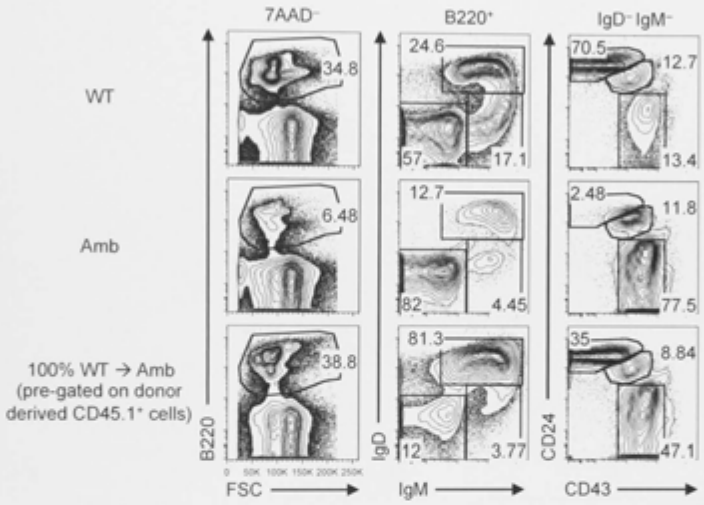

Figure 8.8 A partial developmental arrest at the pro-B cell stage of B-cell development in ATP11C-deficient mouse that was irradiated and transplanted with wild-type bone marrow cells

Representative flow cytometric analysis of bone marrow cells from *Atp11c*$^{+/0}$ (WT) and *Atp11c*$^{amb/0}$ (Amb) animals or an *Atp11c*$^{amb/0}$ (Amb) mouse that was irradiated and reconstituted with *Atp11c*$^{+/0}$ (WT) bone marrow cells. Numbers adjacent to outlined areas indicate percentage of B220^{+} B cells (left); percentage of IgM^{+}IgD^{+} mature B cells, IgM^{+}IgD^{-} immature B cells, and IgM^{-}IgD^{-} precursor B cells within the B220^{+} subset (middle); cells gated on B220^{+} IgM^{-}IgD^{-} cells, showing the percentage that are CD43^{-} CD24^{hi} pre-B cells, CD43^{+}CD24^{med} pro-B cells and CD43^{+}CD24^{-} pre-pro-B cells (right).

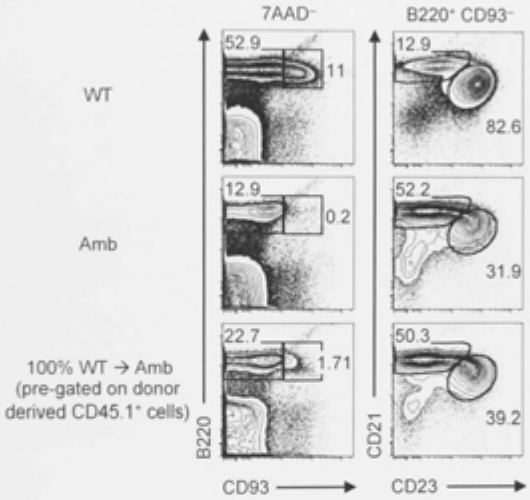

Figure 8.9 Impaired differentiation of wild-type bone marrow cells into mature B cells in the spleen of irradiated ATP11C-deficient host

Representative flow cytometric analysis of splenocytes from *Atp11c*$^{-/0}$ (WT) and *Atp11c*$^{amb/0}$ (Amb) animals or an *Atp11c*$^{amb/0}$ (Amb) mouse that was irradiated and reconstituted with *Atp11c*$^{-/0}$ (WT) bone marrow cells. Numbers adjacent to outlined areas indicate percentage of B220^{+}-gated cells that are CD93^{-} mature B cells and CD93^{+} immature B cells (left); percentage of the CD21^{hi}CD23^{-} marginal zone and the CD21^{med}CD23^{+} follicular B cell subset within the B220^{+}CD93^{-} mature B cells (right).

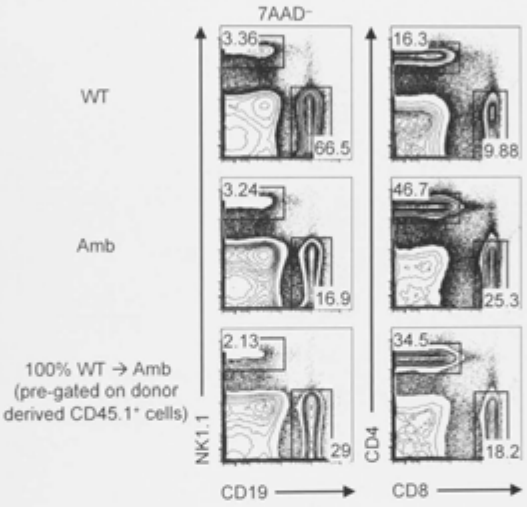

Figure 8.10 Normal differentiation of wild-type bone marrow cells into NK and T cell lineages in the spleen of irradiated ATP11C-deficient host

Representative flow cytometric analysis of splenocytes from *Atp11c*$^{+/0}$ (WT) and *Atp11c*$^{amb/0}$ (Amb) animals or an *Atp11c*$^{amb/0}$ (Amb) mouse that was irradiated and reconstituted with *Atp11c*$^{+/0}$ (WT) bone marrow cells. Numbers adjacent to outlined areas indicate percentage of NK1.1^{+} NK cells and CD19^{+} B cells (left); percentage of CD4^{+} and CD8^{+} T cells (right).

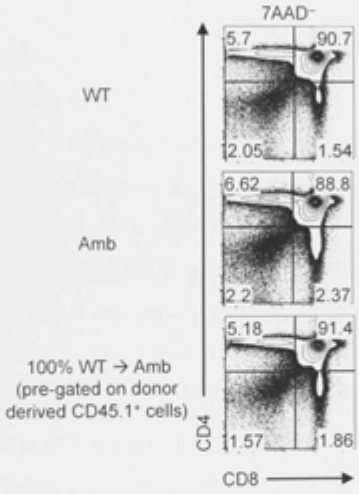

Figure 8.11 Normal differentiation of wild-type bone marrow cells into T cells in the thymus of irradiated ATP11C-deficient host

Representative flow cytometric analysis of thymocytes from *Atp11c*$^{+/0}$ (WT) and *Atp11c*$^{amb/0}$ (Amb) animals or an *Atp11c*$^{amb/0}$ (Amb) mouse that was irradiated and reconstituted with *Atp11c*$^{+/0}$ (WT) bone marrow cells. Numbers adjacent to outlined areas indicate percentage of CD4$^+$ single positive, CD8$^+$ single positive, CD4$^+$CD8$^+$ double positive and CD4$^-$CD8$^-$ double negative T cells.

8.8 Development of liver tumours in *Atp11c*$^{amb/0}$ mice

During the analysis of the blood samples, pronounced yellow coloured plasma from *Atp11c*$^{amb/0}$ animals were noticed (Figure 8.12A). It was found that the yellow coloured plasma is due to a 30-fold increase in unconjugated and conjugated bilirubin (Figure 8.12B). Measurements of liver injury, as measured by the plasma markers alanine aminotransferase and aspartate aminotransferase these were comparable between *Atp11c*$^{amb/0}$ and control animals that are 8-14 weeks of age, but slightly increased with the age (25–30 weeks) in mutant mice (Figure 8.12C).

Necropsy, however, revealed gross or microscopic liver pathology consistent with hepatocellular carcinoma (HCC) in 10 out of 10 *Atp11c*$^{amb/0}$ animals analysed at 6 months of age and not in normal controls. Liver tumours were well to poorly differentiated HCCs containing areas of haemorrhage, necrosis and hypervascularity. Tumour development in these mice was likely to have been preceded by the formation of foci of altered hepatocytes (Figure 8.13). Several such foci were present in liver tissue surrounding the tumours, exhibiting a striking number of mitotic figures, many of which were multipolar with condensed and asymmetric chromatin aggregation (Figure 8.13). Other dysplastic features in *Atp11c*$^{amb/0}$ animals include nuclear anisocytosis, hyperchromasia, pleomorphism and increased nuclear to cytoplasmic ratio (Figure 8.13). By contrast, no such abnormalities were seen in the liver of control littermates. Interestingly, preliminary results seem to indicate that the development of liver tumours in mutant mice is accelerated by an immune stimulation, but further experiments are needed to confirm this, and also test if this is a liver intrinsic defect or related to the abnormalities in the haematopoietic system. These experiments are of considerable interest, but go beyond the scope of my thesis.

8.9 Chapter summary and discussion

As shown in Chapter 7, all cells of the haematopoietic system in ATP11C mutant animals showed an *in vitro* defective flippase activity. These data prompted me to investigate a possible involvement of ATP11C in the differentiation and/or survival of haematopoietic progenitors as well as different blood lineages. I found the number of haematopoietic progenitors in the bone marrow of mutant animals was comparable to those of control mice, indicating that ATP11C had no impact on the

development of haematopoietic progenitors. ATP11C deficiency had also no discernible effect on the accumulation of T cells, NK cells and myeloid cells in the primary and secondary lymphoid tissues despite the fact that the aminophospholipid translocase activity was impaired in all these cells as a result of the ATP11C deficiency. The results suggest that ATP11C is redundant for the development and homeostasis of all other subsets, except B cells, of the immune system.

Despite the expression of ATP11C in a wide range of leukocytes it only appears to be required for B lymphopoiesis. This can possibly be explained by the expression of other P4-type ATPases (14 in mice, 13 in humans) (Sebastian et al., 2012). This notion is supported by the prominent expression of other flippases in specific cell types for example high expression of ATP8A2 in CD4 memory T cells as well as NKT cells, ATP8B1 expression in Langerhans DCs, ATP10A expression in DP T cells (Heng and Painter, 2008). Thus, it would be interesting to test the specific roles of other flippases in the development, homeostasis and function of cells within the immune system by generating knock out mouse models for all P4-type ATPases.

Despite normal T cell development in the thymus of ATP11C-deficient mice, the accumulation of mature T cells in the bone marrow was intriguingly increased. Moreover, the ratio of CD4 vs. CD8 T cells was also increased in the spleen of mutant mice compared to their control littermates. These results suggest that ATP11C is not required for thymic development of T cells, but might play a role in the accumulation, localisation and/or function of mature T cells in the periphery.

It was surprisingly discovered that wild-type bone marrow cells failed to give rise to B cells in lethally irradiated ATP11C-deficient host. This phenotype was also observed with two independent ATP11C mutant alleles (Siggs et al., 2011b). Preliminary data revealed that the wild-type HSCs transplanted into an ATP11C mutant host displayed a partial arrest at the pro- to pre-B cell stage of B cell development. Moreover, the phenotype of splenic B cells in the mutant host that was transplanted with wild-type HSCs was also similar to that seen in intact mutant animals. These results interestingly indicate that ATP11C deficiency may also affect some cell-extrinsic factors that need further examination to be fully delineated.

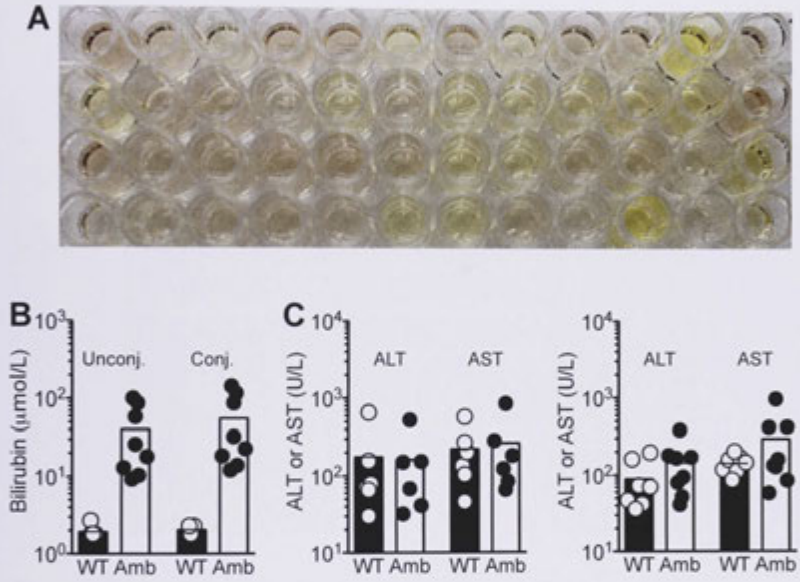

Figure 8.12 Elevated bilirubin level in the plasma of *Atp11c*$^{amb/0}$ mice

(A) Yellow coloured plasma from *Atp11c*$^{amb/0}$ mice. **(B)** Graph shows unconjugated and conjugated bilirubin in the plasma of *Atp11c*$^{+/0}$ (WT) and *Atp11c*$^{amb/0}$ (Amb) mice. The data are representative of at least three independent experiments with four to eight mice per group in each. Each circle represents a single mouse. **(C)** Graphs show alanine aminotransferase (ALT) and aspartate aminotransferase (AST) in the plasma of *Atp11c*$^{+/0}$ (WT) and *Atp11c*$^{amb/0}$ (Amb) mice that were 8-14 weeks (left) or 25-30 weeks old (right). Each circle represents a single mouse and results are shown from two independent experiments.

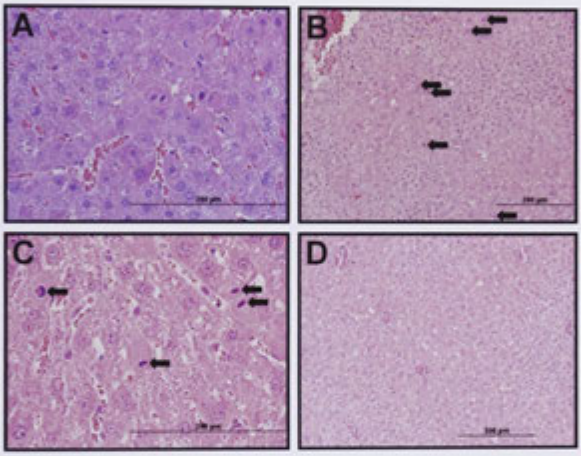

Figure 8.13 Development of hepatocellular carcinoma in *Atp11c*$^{amb\,0}$ mice

(A) Typical dysplastic focus on hematoxylin and eosin (H&E) stained liver section from *Atp11c*$^{amb\,0}$ mice at 6 months (X400 magnification). **(B)** Multiple mitotic figures seen in a representative H&E stained liver tumour section from a *Atp11c*$^{amb\,0}$ mutant mouse (X200 magnification). **(C)** Abnormal mitotic figures with condensed, asymmetric chromatin at higher magnification (X400 magnification). **(D)** Representative H&E stained section of *Atp11c*$^{amb\,0}$ mutant hepatocellular carcinoma (HCCs) at 6 months(X200 magnification).

This chapter also identified that *Atp11c*$^{amb.0}$ mice develop HCC at 6 month of age. The increased expression of *Atp11c* in the liver (Figure 1.10 in Chapter 1) (Wu et al., 2009) supports the conclusion that ATP11C might play a critical role in normal hepatocyte physiology. Consistently, ATP11C has been shown to be critical for the prevention of intrahepatic cholestasis and parturition (Siggs et al., 2011b). Therefore, the development of HCC in mutant mice is of great interest as only a few experimental models are available to study spontaneous development of HCC in mice, but a detailed investigation of this phenotype is beyond the scope of this thesis.

CHAPTER 9: ATP11C-deficient mice exhibit altered erythrocyte shape, anaemia and reduced erythrocyte lifespan

Contents of Figure 9.3, 9.4, 9.6, 9.7, 9.8A, 9.9, 9.10, 9.13A, B, and 9.14 appeared in:

Mehmet Yabas, Lucy A. Coupland, Deborah Cromer, Markus Winterberg, Narci C. Teoh, James D'Rozario, Kiaran Kirk, Stefan Bröer, Christopher R. Parish and Anselm Enders (2014). "Mice deficient in the putative phospholipid flippase ATP11C exhibit altered erythrocyte shape, anemia and reduced erythrocyte lifespan". *The Journal of Biological Chemistry*, 289(28):19531-19537.

Contributions from others:

- Ms. Jennifer Kofler and Ms. Ayla Lorenzo provided technical help for the data in Figure 9.1, Figure 9.2, Figure 9.3, Table 9.1 and Table 9.2.
- Dr. Lucy A. Coupland designed and performed the experiment for the data in Figure 9.6A, and Dr. Deborah Cromer generated Figure 9.6B using the data in Figure 9.6A.
- Ms. Cathy Gillespie and Dr. Lucy A. Coupland generated the images in Figure 9.7A.
- Ms. Anne Prins performed H&E staining of the blood smears in Figure 9.7B.
- Dr. Markus Winterberg and Prof. Kiaran Kirk designed, and Dr. Markus Winterberg performed the experiment for the data in Figure 9.10.
- Prof. Narci C. Teoh provided help in the analysis of samples for the data in Figure 9.11.
- Dr. Lucy A. Coupland injected mice with CFSE and collected blood samples for the data in Figure 9.14B, but staining and flow cytometry analysis performed by myself.
- Prof. Stefan Bröer contributed to the establishment of flippase assay.

9.1 Preamble

Erythrocytes or red blood cells (RBCs) are the most common type of blood cells. Their function is to transport oxygen from the lung to other tissues. Mammalian erythrocytes are unique amongst eukaryotic cells in that they lack nuclei, cytoplasmic structures and organelles. Thus, the structural and functional properties of erythrocytes are closely associated with their plasma membranes (Mohandas and Gallagher, 2008). Like other eukaryotic cells, the erythrocyte membrane consists of a lipid bilayer with an asymmetrical distribution of specific phospholipids between the two leaflets of the bilayer (Daleke, 2008). While PC and SM are predominantly concentrated in the outer monolayer, PS and PE are mainly confined to the cytoplasmic leaflet of the erythrocyte membrane (Daleke, 2008). The generation and maintenance of this asymmetric structure is essential for erythrocyte survival and function (Daleke, 2008, Mohandas and Gallagher, 2008). In particular, localisation of PS to the cytoplasmic leaflet of erythrocytes is crucial, as PS exposure on the surface of erythrocytes plays an essential role in the modulation of the mechanic stability of the membrane through an interaction with the skeletal protein spectrin (An et al., 2004, Manno et al., 2002). PS exposure on the surface of erythrocytes acts as an "eat-me" signal to phagocytes and also can lead to adherence of erythrocytes to the vascular endothelium and activation of surface-dependent plasma blood clotting factors (Daleke, 2008), as well as contributing to the anaemia observed in a wide variety of blood disorders, including sickle cell anaemia and thalassemia (Wood et al., 1996, Kuypers et al., 1998, de Jong et al., 2001, Kean et al., 2002, Yasin et al., 2003).

As already mentioned in the previous chapters, members of the P4-type ATPase family are specialized to serve as 'flippases' that selectively translocate PS, and to a lesser extent PE, into the cytoplasmic leaflet of cell membranes (Daleke, 2007, Sebastian et al., 2012), and this activity was shown for the first time in human erythrocytes (Seigneuret and Devaux, 1984, Daleke and Huestis, 1985). Although there have been a large number of studies related to the asymmetric distribution of phospholipids in the erythrocyte membrane (Daleke, 2003), the role of specific lipid transporters in erythrocyte biology is not well understood. Therefore, in this chapter I aimed at determining the possible role of ATP11C in erythrocyte biology.

9.2 ATP11C-deficient mice exhibit anaemia

In order to test whether ATP11C-deficiency has any effect on the development and survival of erythrocytes, an erythrocyte count in the blood of mutant mice and their control littermates was performed. I found that there were approximately 25% fewer total erythrocytes in the blood of *Atp11c*$^{amb/0}$ (Figure 9.1). However, mutant animals had normal reticulocyte numbers (Figure 9.1).

Separate analysis of peripheral blood of female and male mice demonstrated that ATP11C-deficient female mice have also reduced number of erythrocytes similar to hemizygous mutant male mice (Figure 9.2). In contrast, *Atp11c*$^{amb/+}$ heterozygous female mice had a normal erythrocyte count in the peripheral blood (Figure 9.2). These results reveal that ATP11C deficiency in mice causes anaemia, and suggest that ATP11C plays a significant role in the development and/or survival of erythrocytes.

In order to extend these findings different haematologic parameters were analysed in the blood of mutant mice and their control littermates. I confirmed the reduction in the number of erythrocytes in the blood of mutant mice compared to wild-type among all age groups (Figure 9.3). In line with the lower number of erythrocytes, ATP11C-deficient mice also exhibited a significant decrease in their haemoglobin and haematocrit (Figure 9.3). While the relative proportion of reticulocytes was significantly increased in the blood of ATP11C mutant animals (Table 9.1) the absolute number of reticulocytes was not significantly increased (Figure 9.3). I also analysed mean corpuscular haemoglobin (MCH) and mean corpuscular volume (MCV) which are the average mass of haemoglobin per erythrocyte and the average erythrocyte cell size, respectively. Interestingly, mutant mice had higher MCH in older age groups, and higher MCV among all age groups (Figure 9.3). Together these changes resulted in a reduced corpuscular haemoglobin concentration mean (CHCM) of erythrocytes from ATP11C-deficient mice (Table 9.2).

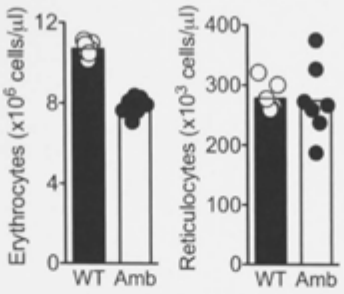

Figure 9.1 Reduced number of erythrocytes in the blood of *Atp11c*$^{amb/0}$ mice
Graphs show number of erythrocytes (left) and reticulocytes (right) in the blood of *Atp11c*$^{+/0}$ (WT) and *Atp11c*$^{amb/0}$ (Amb) mice. Each circle represents a single mouse, and data are representative of two independent experiments.

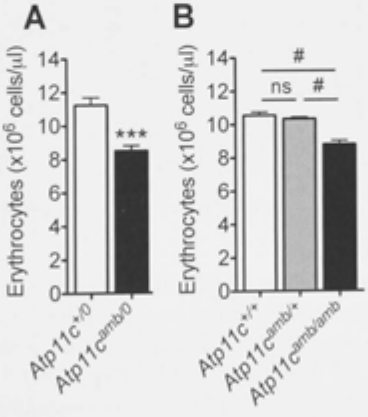

Figure 9.2 Anaemia in mice with a point mutation in *Atp11c*
(A, B) Graphs show the number of erythrocytes in the blood of (A) *Atp11c*$^{+/0}$ and *Atp11c*$^{amb/0}$ male, and (B) *Atp11c*$^{+/+}$, *Atp11c*$^{amb/+}$ and *Atp11c*$^{amb/amb}$ female mice. Bar graphs represent mean ± S.E.M. with four to seven mice per genotype. Statistical significance was calculated using the two-tailed Student's *t*-test (A) or One-Way ANOVA analysis, followed by the Bonferroni post-test, with the *P* values comparing each pair of experimental groups shown on the plots (B). ns, not significant; ***, $P < 0.001$; $^{\#}$, $P < 0.0001$.

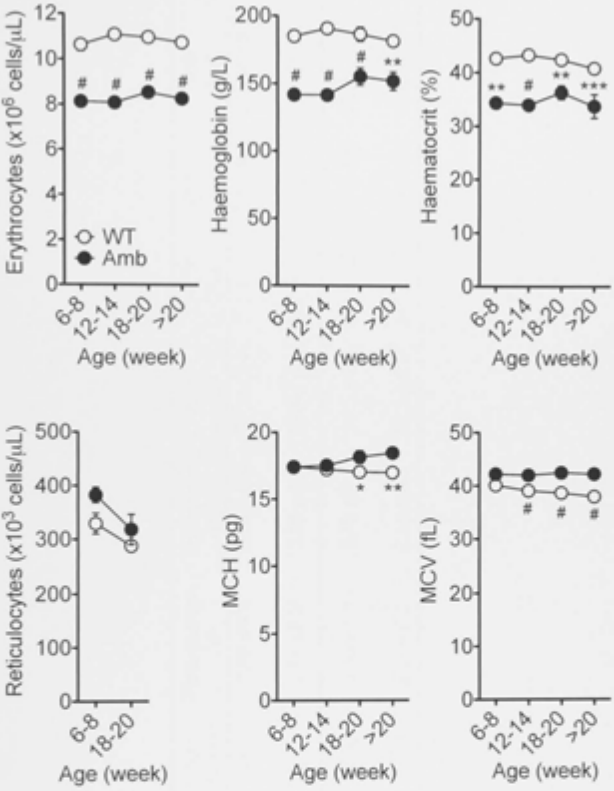

Figure 9.3 The development of anaemia in ATP11C-deficient mice

Graphs show the number of erythrocytes, haemoglobin, haematocrit, the number of reticulocytes, mean corpuscular haemoglobin (MCH) and mean corpuscular volume (MCV) in the blood of *Atp11c*$^{-/0}$ (WT, open circle) and *Atp11c*$^{amb/0}$ (Amb, black filled circle) animals of the indicated age groups. The symbols represent mean ± S.E.M. Data are representative of two independent experiments with four to eight mice per genotype in each. Statistical significance was calculated using One-Way ANOVA analysis, followed by the Bonferroni post-test, with the *P* values comparing each age pair of groups shown on the plots. # $P < 0.0001$; *** $P < 0.001$; ** $P < 0.01$; * $P < 0.05$.

	Age (Week)	Reticulocytes (%)	Reticulocyte Index	MCV (fL)	CHCM (g/L)	RDW (%)	HDW (g/L)	Number of animals
WT	6-8	2.85 ± 0.2	2.84 ± 0.2	57.1 ± 0.3	275 ± 1.1	17.4 ± 0.6	31.7 ± 0.8	4
Amb	6-8	4.24 ± 0.2[c]	3.45 ± 0.3	59.4 ± 0.4[c]	272 ± 0.7	13.3 ± 0.4[d]	29.1 ± 0.2[b]	5
WT	18-20	2.40 ± 0.1	2.40 ± 0.1	56.0 ± 0.1	277 ± 1.3	16.7 ± 0.4	30.1 ± 0.4	4
Amb	18-20	3.37 ± 0.2[b]	2.95 ± 0.3	60.3 ± 0.5[d]	272 ± 1.9	12.9 ± 0.2[d]	28.9 ± 0.5	5

Table 9.1 Reticulocyte analysis in the blood

Analysis of different hematologic parameters on reticulocytes from the blood of *Atp11c*$^{+/+}$ (WT) and *Atp11c*$^{amb/amb}$ (Amb) animals for each age group using an ADVIA 2120 Haematology System. The numbers are expressed as mean ± S.E.M. MCV, mean corpuscular volume; CHCM, corpuscular haemoglobin concentration mean; RDW, red cell distribution width; HDW, haemoglobin distribution width. The reticulocyte index was calculated by multiplying the percentage of reticulocytes with the haematocrit of each mouse divided by the average haematocrit of control mice of the same age. Statistical significance was calculated using One-Way ANOVA analysis, followed by the Bonferroni post-test, with the *P* values comparing each age pair of groups shown on the plots. [b], $P < 0.01$; [c], $P < 0.001$; [d], $P < 0.0001$.

	Age (Week)	MCHC (g/L)	CH (pg)	CHCM (g/L)	RDW (%)	HDW (g/L)	Number of animals
WT	6-8	435 ± 2.9	14.0 ± 0.1	347 ± 1.7	16.2 ± 0.6	23.8 ± 0.4	5
Amb	6-8	413 ± 6.0	14.0 ± 0.1	330 ± 1.6[d]	16.5 ± 0.2	28.4 ± 0.7[d]	4
WT	12-14	441 ± 2.3	13.8 ± 0.2	352 ± 1.3	14.7 ± 0.2	25.8 ± 0.3	8
Amb	12-14	417 ± 0.9[b]	14.2 ± 0.1	336 ± 1.7[d]	15.5 ± 0.1	27.9 ± 0.3[b]	8
WT	18-20	441 ± 1.6	13.7 ± 0.2	353 ± 2.1	15.0 ± 0.2	26.4 ± 0.3	8
Amb	18-20	428 ± 3.4	14.6 ± 0.4[b]	343 ± 3.1[b]	15.5 ± 0.2	26.2 ± 0.7	7
WT	>20	448 ± 8.1	13.3 ± 0.1	351 ± 1.2	16.0 ± 0.4	27.0 ± 0.5	7
Amb	>20	438 ± 9.5	14.5 ± 0.3[c]	343 ± 2.7[a]	15.8 ± 0.5	26.1 ± 0.8	7

Table 9.2 Erythrocyte analysis in the blood

Analysis of different hematologic parameters in the blood of *Atp11c*$^{-/0}$ (WT) and *Atp11c*$^{amb/0}$ (Amb) animals for each age group using an ADVIA 2120 Haematology System. The numbers are expressed as mean ± S.E.M. MCHC, mean corpuscular haemoglobin concentration; CH, cellular haemoglobin; CHCM, corpuscular haemoglobin concentration mean; RDW, red cell distribution width; HDW, haemoglobin distribution width. Statistical significance was calculated using One-Way ANOVA analysis, followed by the Bonferroni post-test, with the *P* values comparing each age pair of groups shown on the plots. [a], $P < 0.05$; [b], $P < 0.01$; [c], $P < 0.001$; [d], $P < 0.0001$.

9.3 Normal erythropoiesis in ATP11C-deficient mice

The data presented above suggest a critical involvement of ATP11C in the development and/or survival of erythrocytes. In order to assess if ATP11C is required for erythropoiesis, I examined the early stages of erythroid development in the bone marrow and spleen. Stepwise analysis of different stages of erythroblast differentiation based on surface marker CD44 and forward scatter profile (Chen et al., 2009) demonstrated that ATP11C-deficient mice have essentially normal erythropoiesis in the bone marrow and spleen (Figure 9.4). The normal erythropoiesis in the bone marrow and spleen of ATP11C-deficient mice was also confirmed using CD71 and Ter119 co-staining (Socolovsky et al., 2001) (Figure 9.5). Collectively, these results indicate that animals deficient for ATP11C have no defect in the early stages of erythropoiesis.

9.4 Erythrocytes from ATP11C-deficient mice have reduced lifespan

As the production of erythrocytes appeared normal in ATP11C-deficient animals, the life span of erythrocytes was investigated using a method developed by Dr. Lucy Coupland from the John Curtin School of Medical Research (Coupland et al., 2010). She injected ATP11C mutant and control mice with the fluorescent dye CFSE, which efficiently labels the erythrocytes, followed by collection of blood from the tail of CFSE-injected mice at different time points and flow cytometric analysis. Interestingly, it was found that erythrocytes from ATP11C-deficient animals exhibit a reduced survival compared to cells from their control littermates as determined by percentage of CFSE-labelled erythrocytes in the blood (Figure 9.6A). Using a mathematical modelling developed by Dr. Deborah Cromer from the University of New South Wales (Coupland et al., 2010), the average survival of erythrocytes was determined. The analysis revealed that erythrocytes from ATP11C mutant animals showed an average lifespan of 25.2 ± 3.5 days, compared to 38.7 ± 3.6 days in the control littermates (presented as means ± S.E.M) (Figure 9.6B). These data clearly indicate that ATP11C plays an important role in the survival of erythrocytes.

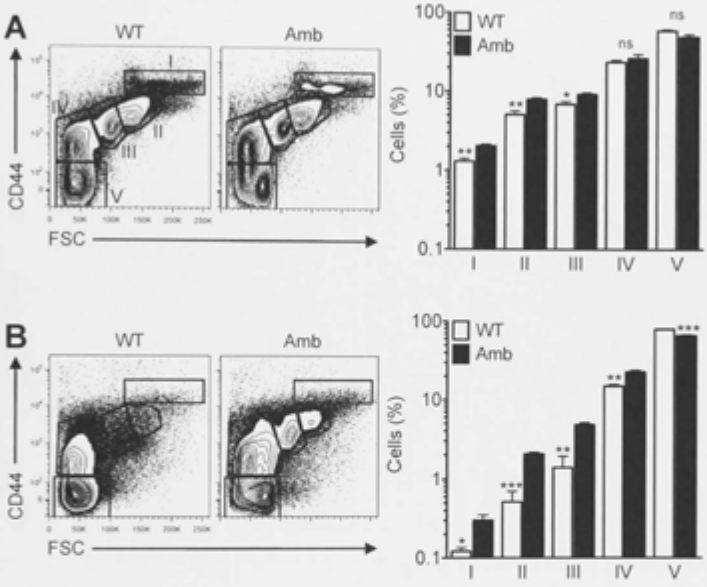

Figure 9.4 Normal erythropoiesis in the bone marrow and spleen of ATP11C-deficient animals

(A, B) Representative flow cytometric dot plots of CD44 and Forward Scatter (FSC) profiles in the (A) bone marrow and (B) spleen of *Atp11c*$^{+/0}$ (WT) and *Atp11c*$^{amb/0}$ (Amb) animals. The plots are pre-gated on CD71^{+} and Ter119^{+} erythrocytes. Bar graphs represent mean ± S.E.M of the percentage of cells in the outlined areas in the flow cytometric plots. Data are representative of two independent experiments with one to four mice per genotype in each. Statistical significance was calculated using the two-tailed Student's *t*-test. ns, not significant; *** $P < .001$; ** $P < .01$; * $P < .05$.

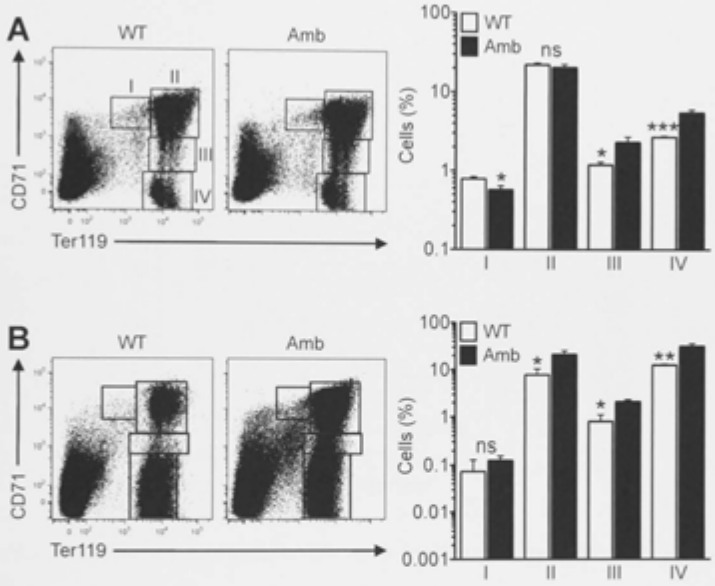

Figure 9.5 Normal erythropoiesis in the bone marrow and spleen of ATP11C-deficient animals

(A, B) Representative flow cytometric dot plots of CD71 and Ter119 profile in the (A) bone marrow and (B) spleen of *Atp11c*$^{+/0}$ (WT) and *Atp11c*$^{amb/0}$ (Amb) animals. Bar graphs represent mean ± S.E.M of the percentage of cells in the outlined areas in the flow cytometric plots. Data are representative of three independent experiments with four to six mice per genotype in each. Statistical significance was calculated using the two-tailed Student's *t*-test. ns, not significant; *** $P < .001$; ** $P < .01$; * $P < .05$.

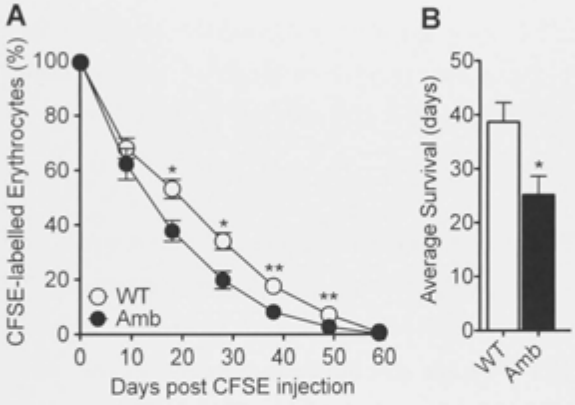

Figure 9.6 A shortened erythrocyte life span in the periphery of ATP11C-deficient animals

(A) Graph shows the percentage of CFSE-labelled erythrocytes in the blood of *Atp11c*$^{+/0}$ (WT, open circle) and *Atp11c*$^{amb/0}$ (Amb, black filled circle) mice after *in vivo* labelling. **(B)** Graph shows the average erythrocyte life span calculated by lognormal modelling from the data presented in (A). The symbols and bar graph represent mean ± S.E.M. Statistical significance was calculated using the two-tailed Student's *t*-test. ** $P < .01$; * $P < .05$.

9.5 ATP11C-deficient erythrocytes form stomatocytes

The composition and asymmetric distribution of phospholipids in the cell membrane is essential for maintaining the normal biconcave shape of erythrocytes (Manno et al., 2002). To examine the morphology of erythrocytes, Ms. Cathy Gillespie and Dr. Lucy Coupland from the John Curtin School of Medical Research performed scanning electron microscopy analysis of erythrocytes from the blood of ATP11C mutant and littermate control mice. As expected red cells from the blood of control animals showed the typical biconcave disc shape (Figure 9.7A, top pictures). Interestingly, distinct changes were observed in erythrocytes from ATP11C-deficient mice with the majority of mutant erythrocytes showing stomatocyte-like morphology (Figure 9.7A, bottom pictures). Peripheral blood smears confirmed the formation of a stomatocyte-like morphology in erythrocytes from ATP11C-deficient mice (Figure 9.7B).

Furthermore, flow cytometry analysis revealed that erythrocytes in the blood and spleen from ATP11C-deficient animals were significantly larger than erythrocytes from control animals as determined by an increase in their forward scatter profile (Figure 9.8A). This increased size was consistent with higher MCV in mutant mice (Figure 9.3), and it was first apparent in mature erythrocytes in the bone marrow, and orthrochromic erythroblasts and reticulocytes in the spleen (Figure 9.8B).

The effect of the mutation on osmotic fragility was also assessed by incubating erythrocytes from ATP11C-deficient mice and control littermates in solutions of varying osmolarity, and measuring the extent of haemolysis. Erythrocytes from ATP11C-deficient mice displayed a normal haemolysis profile, suggesting that their surface-to-volume ratio and cell hydration is comparable to that in erythrocytes from wild-type mice (Figure 9.9).

9.6 No effect of the ATP11C^{amb} mutation on Na^+ and K^+ homeostasis

Stomatocytosis observed in ATP11C-deficient mice may be associated with altered cation transport across the erythrocyte membrane, and a consequent perturbation of erythrocyte Na^+ and K^+ homeostasis (Bruce, 2009). In some cases the cation transport abnormality is enhanced upon reduction of the temperature to which the

cells are exposed (Stewart, 2004). Comparisons of Na^+ and K^+ levels in erythrocytes from *Atp11c*$^{amb/0}$ mice with those in erythrocytes from control mice, using ion chromatography, revealed there to be no difference between the two groups (Figure 9.10A). Measurement of the plasma K^+ concentration in blood samples that had been incubated for 30 min, 1.5 and 3.5 hours at room temperature (in order to enhance any temperature-dependent K^+ leak that might be present) revealed the plasma K^+ concentration of ATP11C-deficient mice to be comparable to that in wild-type mice (Figure 9.10B). Thus, ATP11C deficiency apparently has no significant effect on erythrocyte Na^+ and K^+ homeostasis.

Hereditary stomatocytosis in humans can cause iron overload (Bruce, 2009). Serum iron and transferrin in 8-10 and 18-20 week old ATP11C-deficient mice and their wild-type littermates were measured. Serum iron and transferrin levels were comparable between ATP11C mutant and wild-type animals and between both age groups (Figure 9.11) thus excluding iron overload as a feature of the stomatocytosis seen in these mice.

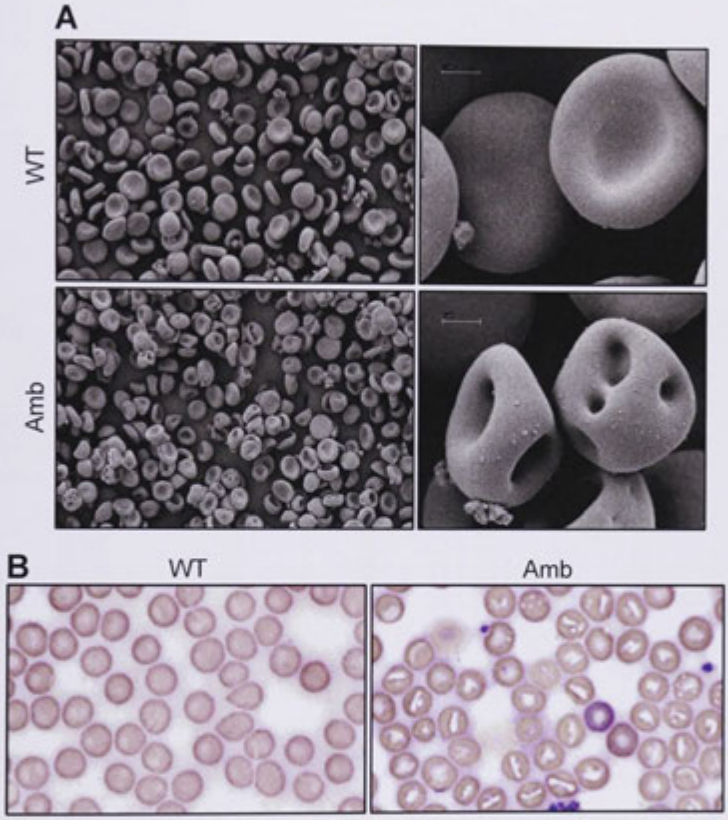

Figure 9.7 ATP11C-deficient erythrocytes have an abnormal shape
(A) Scanning electron microscopic analysis of erythrocytes from the blood of *Atp11c*$^{+/0}$ (WT) and *Atp11c*$^{amb/0}$ (Amb) animals. **(B)** Peripheral blood smears from *Atp11c*$^{+/0}$ (WT) and *Atp11c*$^{amb/0}$ (Amb) animals.

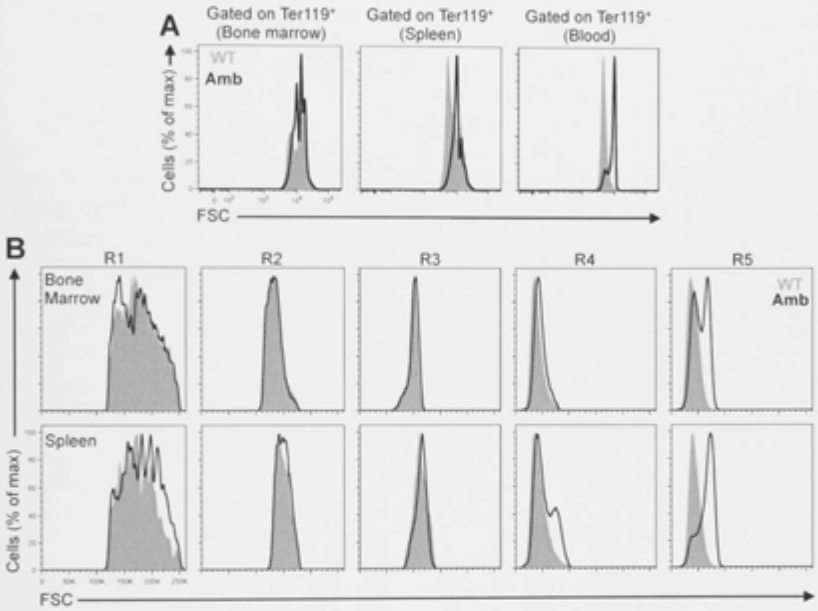

Figure 9.8 Larger mature erythrocytes from *Atp11c*$^{amb/0}$ animals

(A) Representative overlay histograms of forward scatter (FSC) profile in Ter119^{+} erythrocytes from the bone marrow, spleen and blood of *Atp11c*$^{+/0}$ (WT, shaded grey) and *Atp11c*$^{amb/0}$ (Amb, black line) animals. Data are representative of three independent experiments with four to six mice per genotype in each. **(B)** Representative overlay histograms of forward scatter (FSC) profile in different stages of erythroid development (gated as in Figure 9.4) in the bone marrow (top panel) and spleen (bottom panel) of *Atp11c*$^{+/0}$ (WT, shaded grey) and *Atp11c*$^{amb/0}$ (Amb, black line) animals. Data are representative of at least five independent experiments with one to four mice per genotype in each.

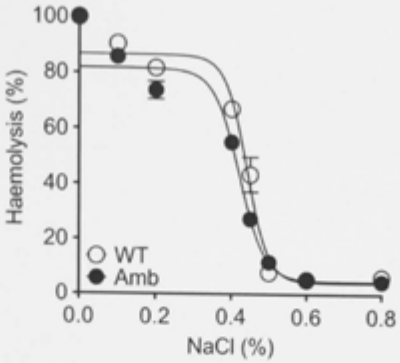

Figure 9.9 Erythrocytes from ATP11C-deficient mice show normal osmotic fragility
Osmotic fragility of erythrocytes from *Atp11c*$^{+/0}$ (WT, open circle) and *Atp11c*$^{amb/0}$ (Amb, black filled circle) mice. The symbols represent mean ± S.E.M of the percentage of haemolysis. Data are representative of three independent experiments with four to five mice per genotype in each.

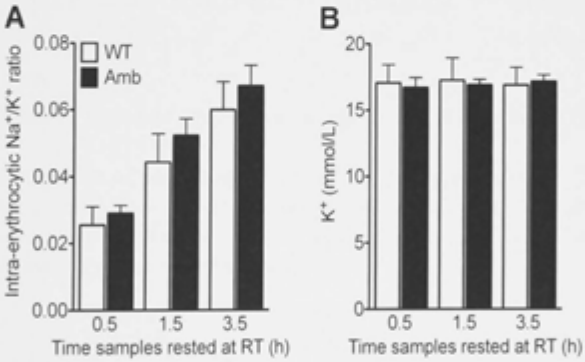

Figure 9.10 Normal intra-erythrocytic and plasma content of cations in ATP11C-deficient mice
(A) Ratio of intra-erythrocytic Na^+ and K^+ of *Atp11c*$^{+/0}$ (WT) and *Atp11c*$^{amb/0}$ (Amb) animals analysed by HPLC within 30 min of blood collection (0.5 h) and after resting at room temperature for 1.5 and 3.5 hours. Bar graph represents mean ± S.E.M of the ratio of intra-erythrocytic Na^+ and K^+ content. **(B)** HPLC measurement of K^+ in the plasma of *Atp11c*$^{+/0}$ (WT) and *Atp11c*$^{amb/0}$ (Amb) animals within 30 min of blood collection (0.5 h) and after resting at room temperature for 1.5 and 3.5 h. Bar graph represents mean ± S.E.M of the plasma K^+ content. Data are representative of two independent experiments with four to five mice per genotype in each.

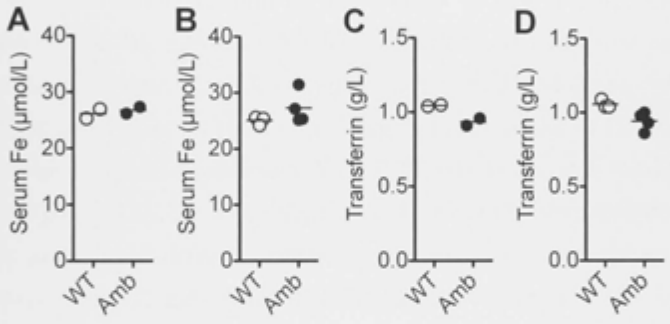

Figure 9.11 Normal iron and transferrin levels in the serum of ATP11C-deficient animals

Graphs show the analysis of iron **(A, B)** and transferrin **(C, D)** in the serum from young (8-10 weeks) **(A, C)** and older (18-20 weeks) **(B, D)** *Atp11c*$^{+/0}$ (WT, open circle) and *Atp11c*$^{amb/0}$ (Amb, black filled circle) animals. Each symbol represents a single sample in which sera from three different mice were pooled.

9.7 Lower flippase activity in erythroblasts from ATP11C-deficient mice

To test if developing erythroblasts or mature erythrocytes have reduced flippase activity, I performed an *in vitro* flippase activity assay using the C_6-NBD-PS. I first tested flippase activity in the different erythroid stages (Proerythroblasts, Basophilic erythroblasts, Polychromatic erythroblasts, Orthochromatic erythroblasts and reticulocytes and mature red blood cells; gates as regions I, II, III, IV and V respectively in Figure 9.4), in the bone marrow and spleen, separated on the basis of their CD44 and forward scatter profiles (Chen et al., 2009). Erythroid precursors (R I – R III) from wild-type mice took up C_6-NBD-PS rapidly whereas orthochromatic erythroblasts and reticulocytes as well as mature erythrocytes (R IV and R V respectively) showed a significantly reduced overall C_6-NBD-PS uptake (Figure 9.12 and Figure 9.13A, B), indicating that flippase activity decreases with erythrocyte maturity. At all stages, C_6-NBD-PS uptake approached equilibrium by 30 min (Figure 9.12 and Figure 9.13A, B). In comparison, the uptake of C_6-NBD-PS by ATP11C mutant erythroid precursors (R I – R III) was significantly slower (Figure 9.12 and Figure 9.13A, B). The difference in C_6-NBD-PS internalisation between wild-type and ATP11C-deficient cells was less marked in the more mature forms (R IV – R V) (Figure 9.12 and Figure 9.13A, B). Similarly, there was a very low uptake of C_6-NBD-PS in erythrocytes from peripheral blood of wild-type and ATP11C-deficient mice with only a minimal reduction in mutant erythrocytes (Figure 9.13C).

9.8 Increased PS exposure on the surface of ATP11C-deficient erythrocytes

The appearance of PS in the exoplasmic leaflet of erythrocyte membranes serves as an "eat-me" signal for the recognition and clearance of erythrocytes by phagocytes (McEvoy et al., 1986, Connor et al., 1994). To test if the defective flippase activity in mutant animals results in increased surface accumulation of PS, erythrocytes from the peripheral blood were stained with Annexin-V, which binds to PS in the exoplasmic leaflet (Koopman et al., 1994). The percentage of Annexin-V^+ erythrocytes in the blood of ATP11C-deficient mice was 17-fold higher than in control littermates in which there were virtually no Annexin-V^+ erythrocytes (4.28 ± 0.50 % vs. 0.25 ± 0.05 %, $P < 0.0001$) (Figure 9.14A). I next determined the extent of Annexin-V binding as a function of erythrocyte age using *in vivo* CFSE-labelling.

At all ages tested (newly generated to 40 days of age) there was virtually no Annexin-V binding by wild-type erythrocytes (Figure 9.14B). However, as ATP11C-deficient erythrocytes aged, there was a gradual increase in the number of Annexin-V binding from 4.3% of newly formed erythrocytes ($CFSE^-$) to more than 20% of erythrocytes aged $\geq$ 39 days ($CFSE^+$) (Figure 9.14B). In agreement with the accumulation of PS on aged erythrocytes I also found a greater than a two-fold increase in the frequency of Annexin-V^+ erythrocytes in the spleen of mutant mice compared to their control littermates (31 ± 2 % vs. 14 ± 1 %, $P < 0.0001$) (Figure 9.14C). In contrast, no difference in Annexin-V staining was observed on erythroblasts in the bone marrow of wild-type and ATP11C-deficient mice (Figure 9.14D).

Taken together, these data suggest that ATP11C-deficient erythrocytes accumulate PS on their surface in the peripheral circulation due possibly to a defect in PS internalisation. Alternatively, it could also be due to reduced removal of PS-expressing RBCs because of overload of the system.

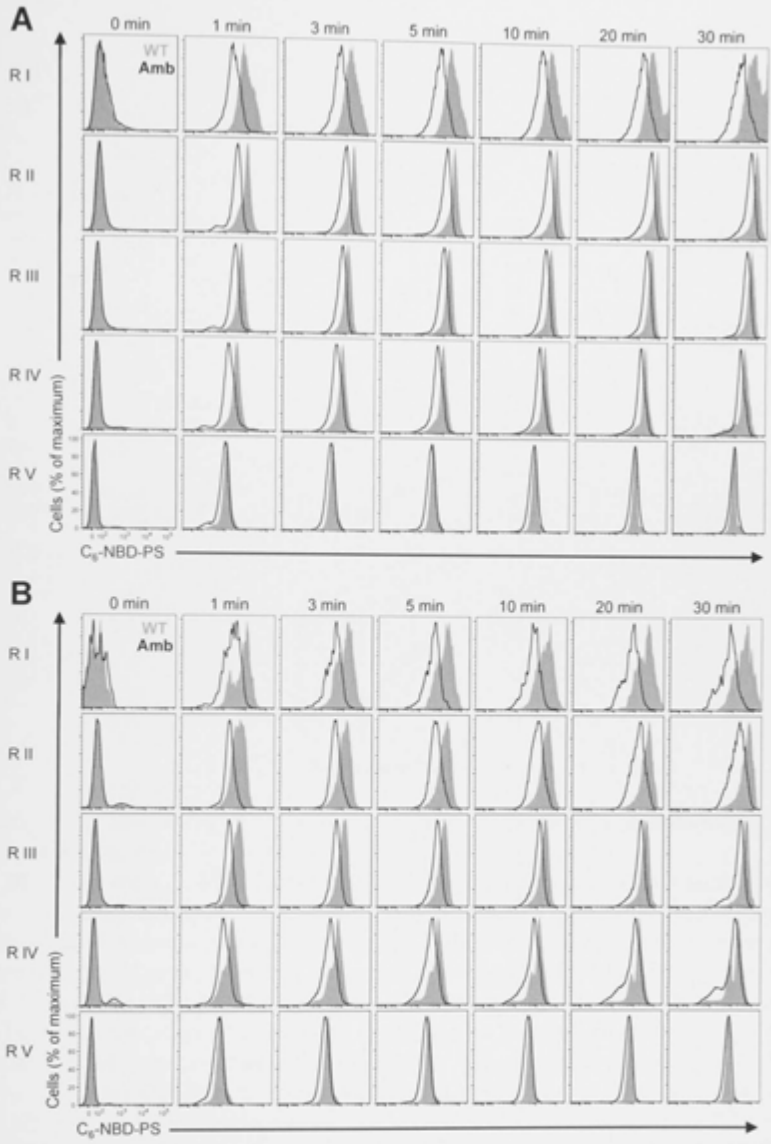

Figure 9.12 The ATP11C^{amb} mutation decreases C_6-NBD-PS translocation into erythroblasts

(A, B) Representative overlay histograms of C_6-NBD-PS fluorescence profiles after 0, 1, 3, 5, 10, 20 and 30 min incubation in Proerythroblasts, Basophilic erythroblasts, Polychromatic erythroblasts, Orthochromatic erythroblasts and reticulocytes and mature red blood cells (Regions I, II, III, IV and V, respectively, gated as in Figure 9.4) in the bone marrow (A) and spleen (B) of *Atp11c*$^{-/0}$ (WT, shaded grey) and *Atp11c*$^{amb/0}$ (Amb, black line) animals. Data are representative of at least five independent experiments with one mouse per genotype in each.

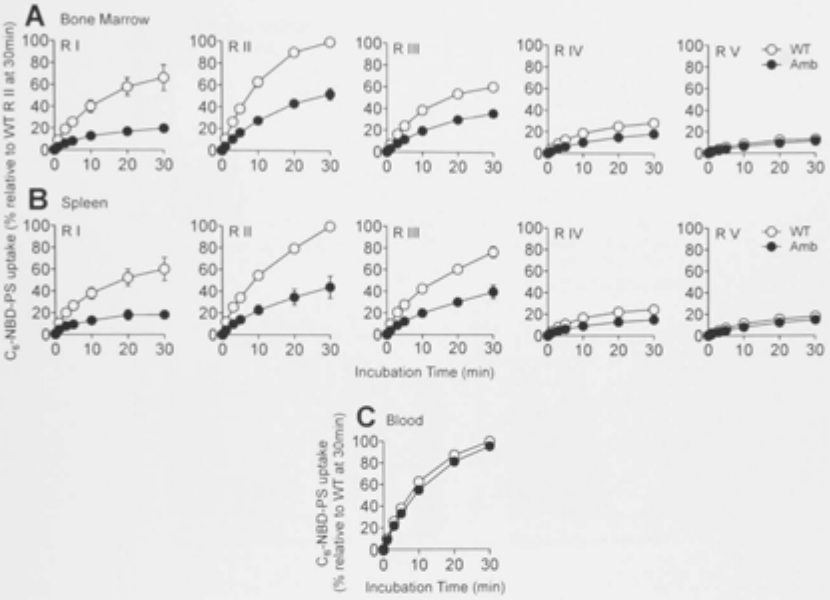

Figure 9.13 The ATP11C^{amb} mutation decreases C_6-NBD-PS translocation into erythroblasts *in vitro*

(A, B) Graphs show C_6-NBD-PS uptake after 0, 1, 3, 5, 10, 20 and 30 min incubation in Proerythroblasts, Basophilic erythroblasts, Polychromatic erythroblasts, Orthochromatic erythroblasts and reticulocytes and mature red blood cells (regions I, II, III, IV and V respectively, gated as in Figure 9.4) in the bone marrow (A) and spleen (B) from *Atp11c*$^{+/0}$ (WT, open circle) and *Atp11c*$^{amb/0}$ (Amb, black filled circle) mice. Graphs represent mean ± S.E.M. of the percentage of C_6-NBD-PS uptake relative to wild-type region II at 30 min. Data are pooled from five independent experiments with one mouse per genotype in each. **(C)** Graph shows C_6-NBD-PS uptake after 0, 1, 3, 5, 10, 20 and 30 min incubation in Ter119$^+$ erythrocytes in the blood from *Atp11c*$^{+/0}$ (WT, open circle) and *Atp11c*$^{amb/0}$ (Amb, black filled circle) mice. Graph represents mean ± S.E.M. of the percentage of C_6-NBD-PS uptake relative to wild-type erythrocytes at 30 min. Data are pooled from four independent experiments with one mouse per genotype in each.

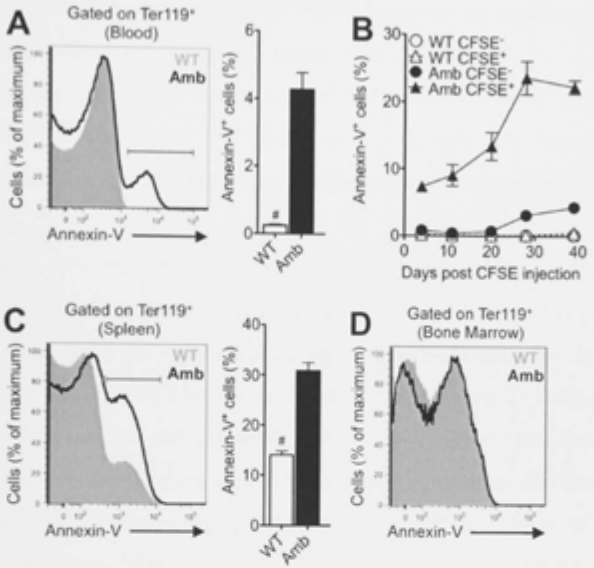

Figure 9.14 Mature erythrocytes from ATP11C-deficient mice demonstrate increased PS exposure on their surface

(A) Representative overlay histogram of Annexin-V staining in Ter119$^+$ erythrocytes in the blood of *Atp11c*$^{+/0}$ (WT, shaded grey) and *Atp11c*$^{amb/0}$ (Amb, black line) animals. Bar graphs represent mean ± S.E.M. of the percentage of Annexin-V$^+$ cells in Ter119$^+$ erythrocytes. Data are representative of at least three independent experiments with four to six mice per genotype in each. **(B)** Graph shows mean ± S.E.M. of the percentage of Annexin-V$^+$ cells among circulating CFSE$^-$ or CFSE$^+$ erythrocytes in the blood of *Atp11c*$^{+/0}$ (WT) and *Atp11c*$^{amb/0}$ (Amb) mice after *in vivo* labelling. **(C)** Representative overlay histogram of Annexin-V staining in Ter119$^+$ erythrocytes in the spleen of *Atp11c*$^{+/0}$ (WT, shaded grey) and *Atp11c*$^{amb/0}$ (Amb, black line) animals. Bar graphs represent mean ± S.E.M. of the percentage of Annexin-V$^+$ cells in Ter119$^+$ erythrocytes. Data are representative of at least three independent experiments with four to six mice per genotype in each. **(D)** Representative overlay histogram of Annexin-V staining in Ter119$^+$ erythrocytes in the bone marrow of *Atp11c*$^{+/0}$ (WT, shaded grey) and *Atp11c*$^{amb/0}$ (Amb, black line) animals. Statistical significance was calculated using the two-tailed Student's *t*-test. $^{\#}$, $P < 0.0001$.

9.9 Chapter summary and discussion

The first description of a phospholipid translocase activity was the characterisation of the erythrocyte membrane aminophospholipid translocase (Seigneuret and Devaux, 1984, Daleke and Huestis, 1985). Despite the extensive research over the ensuing 30 years to characterise this enzyme activity and its influence on membrane asymmetry and erythrocyte shape, the protein(s) responsible for this activity is still mostly unknown (Daleke, 2008). The data presented in this chapter revealed a significant role for the P4-type ATPase ATP11C in erythrocyte biology, and identified ATP11C as the main aminophospholipid translocase in developing erythrocytes.

The findings of this chapter demonstrated that erythrocytes in ATP11C-deficient mice have 1) reduced numbers in circulation, 2) increased exposure of PS in the outer leaflet, particularly for older erythrocytes, 3) a decreased lifetime in circulation, 4) a large percentage of stomatocytic cells, and 5) a significantly reduced NBD-PS translocase activity during development. Interestingly, erythrocytes from ATP11C mutant mice had normal development and maturation in the bone marrow and spleen. Previously ATP8A1 has been suggested to be expressed in erythrocyte membranes (Soupene and Kuypers, 2006), however *Atp8a1*$^{-/-}$ erythrocytes display none of the phenotypic changes seen in ATP11C-deficient mice (Levano et al., 2012). Therefore, this study identifies the first enzyme responsible for the flippase activity in erythrocytes.

In line with the role of ATP11C as a flippase (Sebastian et al., 2012, van der Mark et al., 2013, Segawa et al., 2014) and the expression of *Atp11c* in adult erythroblasts (Figure 9.15) (Kingsley et al., 2013), *in vitro* uptake of a PS analogue by mutant erythroblasts was severely reduced compared to erythroblasts from wild-type control mice. Moreover, mature erythrocytes from mutant mice showed increased PS-exposure. These data suggest that a defective translocation activity results in the accumulation of PS on the surface, and removal of PS-expressing erythrocytes from the circulation by phagocytes will eventually result in anaemia. Interestingly, PS-exposing erythrocytes in ATP11C-deficient mice continued to circulate, which suggests that overload of the phagocytic capacity of the reticuloendothelial macrophages or other extrinsic factors may also be involved. Future studies are

required to identify any cell extrinsic factors that influence the survival of ATP11C-deficient erythrocytes and also their relative importance compared to the cell-intrinsic flippase defect.

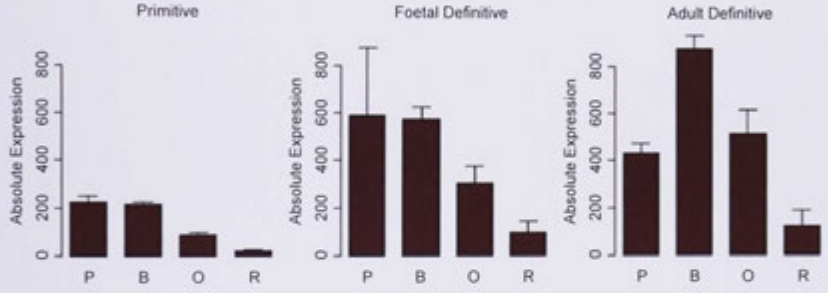

Figure 9.15 *Atp11c* expression in different erythroblast stages
Normalised expression for all probes associated with *Atp11c* in primitive, foetal definitive, and adult definitive erythroid cells. Proerythroblast (P), Basophilic Erythroblast (B), Polyorthochromatic Erythroblast (O), and Reticulocyte (R). Data from the Erythron Database (http://www.cbil.upenn.edu/ErythronDB), and methods of isolation and expression measurement are described on the paper (Kingsley et al., 2013).

CHAPTER 10: General Discussion

10.1 Unveiling complexities in the immune system through identification of novel genes by ENU mutagenesis

Phenotype-driven ENU mutagenesis screens in mice provide a powerful tool to shed light into understanding important biological processes including the immune system. Identification of the function of novel genes through ENU mutagenesis contributes to the understanding of the immune system and the molecular basis that controls lymphocyte differentiation, development of effector responses, immune tolerance and homeostasis. The mouse strains generated not only in our laboratory (Jun et al., 2003, Papathanasiou et al., 2003, Vinuesa et al., 2005, Siggs et al., 2007, Wu et al., 2008, Randall et al., 2009, Enders et al., 2012, Bergmann et al., 2013, Teh et al., 2013, Enders et al., 2014) but also in other laboratories around the world (Arnold et al., 2012) provide a good example of how ENU mutagenesis screens in a non-biased manner can help uncover important "checkpoints" in the immune system that are crucial for the development and/or function of lymphocyte subsets.

The *Ambrosius* strain was discovered in the mutagenesis program at the John Curtin School of Medical Research because of a selective reduction in B cell frequency in the peripheral blood. The observed block in B cell development in the bone marrow of *Ambrosius* mice helped to identify for the first time a role for a previously uncharacterised aminophospholipid translocase in the immune system.

It has been known for a long time that every eukaryotic cell is surrounded by a plasma membrane that is made of a lipid bilayer with an asymmetric distribution of the specific lipids between the two leaflets of the plasma membrane (Sebastian et al., 2012, van der Mark et al., 2013). A growing body of work suggests that specific lipid transporters found in the cellular membranes are crucial for the establishment and maintenance of the dynamic lipid asymmetry. Energy-dependent transporters known as flippases and floppases are responsible for the transport of phospholipids from the outer to the inner leaflet of the plasma membrane and vice versa, respectively (Sebastian et al., 2012, van der Mark et al., 2013). Beside their role in the internalisation of specific lipids such as PS and PE, flippases are also involved in vesicle-mediated protein transport (Sebastian et al., 2012).

Several flippases are highly expressed in cells of the immune system, which suggests a possible involvement of these enzymes in the development and/or function of immune cells (Heng and Painter, 2008). However, until the start of this project specific roles for flippases in the immune system remained completely unknown. Thus, the discovery of the *Ambrosius* strain and the results presented in this thesis have provided a novel entry point to understand the role of phospholipid flipping in the control of B cell development within the immune system. Moreover, in addition to its contribution to the immune system, this study also revealed the importance of lipid asymmetry in the survival of erythrocytes, and provides the leading candidate for the flippase activity in erythrocytes, which was shown about 30 years ago (Seigneuret and Devaux, 1984, Daleke and Huestis, 1985).

10.2 Insights into the role of ATP11C in B cell development

The development of B cells in the foetal liver and bone marrow is a complex process, and is critical for long-term health. Although studies over the last few decades have identified key signals that are needed for normal B cell development (Herzog et al., 2009, Clark et al., 2014, Reth and Nielsen, 2014), there is still much to uncover. In this thesis, the phospholipid transporter ATP11C has been shown, for the first time, to play a critical role in B lymphopoiesis. B cell development in the bone marrow of ATP11C-deficient animals is arrested at the pro-B cell stage of B lymphopoiesis. Since the transition from pro- to pre-B cell stage is dependent on two main receptor-signalling pathways, namely IL-7R and pre-BCR signalling (Herzog et al., 2009, Clark et al., 2014, Reth and Nielsen, 2014), the focus of the mechanistic studies in this thesis was on these two signalling pathways.

IL-7 is an important cytokine for the development of B cells in the bone marrow and signals through its receptor, IL-7R (Corfe and Paige, 2012). The importance of IL-7 in early B lymphopoiesis has been shown by studies where genetic ablation of IL-7 or IL-7R resulted in a developmental arrest at the pre/pro-B cells stage of B cell development (Peschon et al., 1994, von Freeden-Jeffry et al., 1995, Miller et al., 2002). The findings presented here that ATP11C diminishes effects of an *Il7* transgene *in vivo* suggest that ATP11C might have a role in IL-7R signalling during B cell development in the bone marrow. Consistently, as shown in Chapter 3,

ATP11C-deficient animals possess normal numbers of MZ B cells in the spleen, which resembles the phenotype seen in mice deficient for IL-7 or IL-7R (Carvalho et al., 2001, Hesslein et al., 2006). However, there are some crucial distinctions between ATP11C- and IL-7-deficient animals. In *Il7*$^{-/-}$ or *Il7ra*$^{-/-}$ mice with complete absence of IL-7R signalling (Kikuchi et al., 2005), B cells fail to develop into the pro-B cell stage. In contrast, B cells in *Atp11c* mutant mice develop into pro-B cells similar to *Il7ra*$^{-/-}$ *Vav-Bcl2* mice (Malin et al., 2010b). Furthermore, the presence of residual B lymphopoiesis in *Il7*$^{-/-}$ or *Il7r*$^{-/-}$ mice can be completely abrogated by the introduction of Flt3 deficiency (Sitnicka et al., 2003, Jensen et al., 2008), but Siggs et al. revealed that mice double deficient for ATP11C and Flt3 exhibit a similar B cell phenotype to those with a single deficiency in ATP11C (Siggs et al., 2011a). Moreover, high doses of IL-7 were able to induce normal proliferation of sorted pro-B cells from ATP11C-deficient animals. These observations suggest that ATP11C most likely has no direct influence on signalling through the IL-7R, but it may have a more indirect effect.

IL-7R signalling has been shown to upregulate the expression of EBF1 in B cells (Kikuchi et al., 2005), and this marks a key step in the commitment to the B cell lineage (Lin and Grosschedl, 1995). The findings that ectopic expression of EBF1 alone was sufficient to rescue B cell deficiency in mice deficient for IL-7, IL-7Rα, PU.1, Ikaros or E2A (Seet et al., 2004, Dias et al., 2005, Kikuchi et al., 2005, Medina et al., 2004, Reynaud et al., 2008) suggest a vital involvement of EBF1 in early B cell development in the bone marrow. Thus, another possibility for the phenotype observed in ATP11C mutant mice could be that the mutation may indirectly affect EBF1 expression through the IL-7R signalling. Consistent with this hypothesis, the microarray analysis presented in this thesis revealed that mRNA expression of *Ebf1* in pro-B cells from mutant mice was reduced. In keeping with this notion, Siggs et al. demonstrated that EBF1 expression was impaired in pre/pro-B cells from ATP11C-deficient animals (Siggs et al., 2011a). In contrast, both mRNA and protein expression of the SLC component λ5, which is a target of EBF1 (Lin and Grosschedl, 1995), has been found to be comparable between ATP11C mutant and control mice pre/pro-B cells (Siggs et al., 2011a). By contrast, I found here that mRNA expression of *Igll1*, which encodes λ5, is significantly reduced in mutant pro-B cells compared

to cells from control animals. The reduced expression of *Igll1* in pro-B cells but normal expression in pre/pro-B cells is consistent with the pro-B cell stage specific defect in ATP11C mutant animals. It would be interesting to test if ectopic expression of EBF1 can rescue B cell deficiency in ATP11C-deficient mice.

The bone marrow contains two distinct niches based on the availability of IL-7, namely IL-7^{hi} and IL-7^{lo} (Tokoyoda et al., 2004), and migration of B cell progenitors through the different niches is important in order for them to access IL-7 and undergo their normal proliferation and differentiation (Clark et al., 2014). Given the fact that IL-7 signalling appears normal in ATP11C mutant mice, a possibility to explain the *in vivo* unresponsiveness to IL-7 in these mice could be that there is a role of ATP11C in the determination and/or entry to the specific niches within the bone marrow. This hypothesis is currently speculative, and requires further examination to reveal how impaired flippase activity and a loss of lipid asymmetry by ATP11C-deficiency affects the movement of pro-B cells between the different niches.

Downstream of the IL-7R the signals bifurcate with the activation of not only JAK/STAT5 but also the PI3K/AKT/FOXO and MAPK-ERK pathways (Hofmeister et al., 1999). Although I was able to analyse the JAK/STAT portion of the pathway of IL-7R signalling in *Atp11c*^{enu10} pro-B cells there was insufficient time to analyse the activation of the PI3K/AKT/FOXO and MAPK-ERK pathways. Therefore, one of the clear aims for future research in this area is to focus on whether or not there is normal activation of the PI3K/AKT/FOXO and MAPK-ERK pathways in *Atp11c*^{enu10} pro-B cells upon IL-7 stimulation.

A synergistic cross talk between the IL-7R and pre-BCR signalling has been suggested to control early B cell development in the bone marrow (Fleming and Paige, 2002, Clark et al., 2014). The proper expression of pre-BCR is critical for the selection of a population within pro-B cells that can respond to the limiting concentration of IL-7 and that eventually differentiates into pre-B cells (Fleming and Paige, 2002). While pro-B cells from *Rag2*$^{-/-}$ animals, which lack a pre-BCR, have a normal proliferative capacity in response to high concentration of IL-7 compared to wild-type pro-B cells, their proliferation was reduced when IL-7 level was limiting

(Marshall et al., 1998, Fleming and Paige, 2001). These studies suggest an important checkpoint in early B cell development in which pre-BCR expression controls the ability of pro-B cells to respond to low concentration of IL-7 (Fleming and Paige, 2002). Interestingly, pro-B cells from ATP11C mutant mice exhibited an *in vitro* proliferative capacity comparable to *Rag2*$^{-/-}$-deficient pro-B cells. These results suggest that the lack of *in vivo* response to elevated IL-7 in ATP11C-deficient mice may be due to a lack of pre-BCR signalling. In keeping with this notion, ATP11C-deficient mice had a developmental arrest at the pro-B cell stage, which is similar to that observed in animals deficient for pre-BCR signalling (Kitamura et al., 1991, Kitamura et al., 1992, Torres et al., 1996, Gong and Nussenzweig, 1996, Mundt et al., 2001, Pelanda et al., 2002). Further support for impaired pre-BCR signalling in ATP11C-deficient pro-B cells comes from experiments where pre-BCR signalling was mimicked by treating cells with an antibody against Igβ, which is a key component of the pre-BCR. Similarly, Igβ-stimulation induced Ca^{2+} mobilisation was also compromised in mutant pro-B cells. In addition, ATP11C-deficient pro-B cells exhibited reduced transcript expression of most of the genes encoding the key molecules that are involved in the expression and signalling through the pre-BCR. These results collectively indicate a critical involvement of ATP11C in the expression and/or signalling of the pre-BCR.

The observation that transgenic expression of BCL-2 in ATP11C mutant mice failed to activate the pre-B cell transition is similar to what was observed in mice deficient in Igβ (Gong et al., 1996). Thus, one possibility to explain the failure of mutant pro-B cells to respond *in vivo* and *in vitro* to anti-Igβ-stimulation could simply be due to reduced Igβ expression on the surface of pro-B cells in mutant mice. Reduced Igβ expression would also explain why transgenic expression of functional heavy and light chains failed to correct B cell development fully in ATP11C mutant mice. In support of this hypothesis, I observed that mRNA expression of *Cd79b* in mutant pro-B cells was reduced compared to cells from control animals. In agreement with published results (Nagata et al., 1997), I found that the expression of Igβ on pro-B cells is too low to be quantitatively detected by flow cytometry. It needs to be tested by further experiments, for example western blotting, if protein expression of Igβ is

reduced in ATP11C-deficient pro-B cells. Moreover, future experiments are also needed to validate the microarray results.

How can ATP11C deficiency disrupt the pre-BCR signalling besides a possibly reduced expression of Igβ? As mentioned earlier, one of the fundamental differences between the pre-BCR and mature BCR signalling is the way that activation cascade is initiated. While an antigen is absolutely required for signalling through the mature BCR, activation of the pre-BCR signalling remains controversial (Herzog et al., 2009, Clark et al., 2014, Reth and Nielsen, 2014). Although different stimuli such as Heparin and Galectin 1 have been shown to be required for the activation of pre-BCR signalling (Bradl and Jack, 2001, Gauthier et al., 2002), autoaggregation of pre-BCRs has also been suggested to be critical for the activation (Ohnishi and Melchers, 2003). In the case of latter hypothesis, it is possible that normal lipid asymmetry in the plasma membrane of pro-B cells is required for aggregation and initiation of signalling through the pre-BCRs. Thus, the possibility that loss of ATP11C activity may disrupt the asymmetric lipid distribution, leading to impaired autoaggregation of pre-BCRs for their activation cannot be disregarded. Another possibility is that expression of pre-BCR leads to a lipid raft-dependent Ca^{2+} flux, which activates scramblase activity. This could result in a transient PS exposure in these cells, and a consequent requirement of flippases for the reestablishment of the asymmetric phospholipid distribution in the plasma membrane. It is plausible that in the absence of ATP11C activity, cells cannot reestablish the lipid asymmetry, which may lead to rapid uptake of PS-expressing B cells in mutant mice by macrophages. This possibility could be tested by genetic ablation of PS receptor Tim 4 (Miyanishi et al., 2007) or the membrane tyrosine kinase c-mer (Cohen et al., 2002) in ATP11C mutant mice, followed by the analysis of resulting B cell phenotype in double deficient animals.

Both the *in vivo* and *in vitro* defects could all reflect some critical qualitative element of IL-7 signalling, or could be secondary since there is a complex feed-forward loop between IL-7 signalling, B cell transcription factors, and pre-BCR signalling (Malin et al., 2010a, Ye and Graf, 2007, Mandel and Grosschedl, 2010, Nutt and Kee, 2007). The elevated expression of the IL-7R on the surface of mutant pro-B cells may reflect less signalling through the IL-7 receptor, because binding of IL-7 to the IL-7R

normally leads to rapid endocytosis of the receptor via clathrin-coated pits and this internalization is necessary for efficient signal transduction (Henriques et al., 2010). A further reduction of IL-7R expression is achieved through a feedback loop where IL-7R signalling normally diminishes IL-7R mRNA transcription (Alves et al., 2008, Park et al., 2004). The biophysics of antigen receptor or IL-7R signalling is not well understood, but several independent observations provide possible connections with PS concentrations in the cytoplasmic membrane leaflet and in lipid rafts. PS is most concentrated on the inner leaflet of the plasma membrane at endocytic cups and early endosomes (Leventis and Grinstein, 2010) and in lipid rafts associated with the T cell receptor (Zech et al., 2009), where it serves as a binding site and regulatory factor for proteins with cationic or C2-domains, such as Src, Ras, Rho and PKC family proteins (Leventis and Grinstein, 2010), and for binding the cationic stretch preceding ITAMs in CD3 subunits (Xu et al., 2008, Aivazian and Stern, 2000). The efficiency of IL-7R signalling has also recently been linked to its association with lipid rafts (Cho et al., 2010, Rose et al., 2010). PS has also been found to be externalised and co-capped with the BCR during BCR or pre-BCR signalling (Dillon et al., 2000). Thus, it will be important in future studies to test the consequences of *Atp11c* mutation for accumulation of PS and signal-transducing proteins at subcellular patches where IL-7, pre-BCR or BCR signalling has been initiated.

As mentioned above, PS in the cytoplasmic leaflet of the plasma membrane provides docking sites for important intracellular signalling molecules including Src, Ras, Rho and PKC family proteins (Leventis and Grinstein, 2010). Among those, activation of endogenous Ras has been suggested to play a critical role in pre-BCR signalling as constitutive activation of Ras in RAG-deficient animals rescued the developmental arrest at the pro-B cells stage and led to accumulation of B cells in the bone marrow and periphery (Shaw et al., 1999). Therefore, one possibility to explain the defect in the differentiation of pre-B cells in mutant mice could be that PS is important for the localisation, recruitment and/or activation of Ras in the cytoplasmic leaflet of the plasma membrane. Accordingly, in the presence of an impaired flippase activity in ATP11C mutant mice, Ras cannot be activated, which leads to a block at the pro-B cells stage of B lymphopoiesis. Further studies including testing if the constitutive expression of Ras in ATP11C-deficient mice can rescue B cell deficiency are warranted to explore this important possibility.

With respect to the biochemical function of ATP11C, the simplest interpretation of the data is that ATP11C is an essential aminophospholipid flippase in the plasma membrane of pro-B cells. Other members of this protein family have been shown to be PS flippases in biochemical reconstitution and yeast genetic studies (Tang et al., 1996, van der Velden et al., 2010, Paulusma and Elferink, 2010, Muthusamy et al., 2009). The finding that ATP11C functions as a flippase has been confirmed by a recent paper, which showed that ATP11C functions as a flippase in human cells (Segawa et al., 2014). In addition to the PS flippase activity this paper has also reported some activity of ATP11C for PE, but not for PC (Segawa et al., 2014). The observation that PS flippase activity was slower but by not completely abolished in ATP11C mutant cells implies that other aminophospholipid flippases also act in B cells, consistent with the relatively ubiquitous mRNA expression of many other P4 ATPase family members (Heng and Painter, 2008). However, analysis of yeast mutants in P4 ATPases have underscored the potential for effects on protein or organelle trafficking and cell metabolism that could indirectly affect PS flippase activity (Muthusamy et al., 2009, Gall et al., 2002, Hua et al., 2002, Alder-Baerens et al., 2006). This possibility has so far not been tested, and further studies are required to determine if ATP11C has also some of these indirect effects.

Why are B cells profoundly compromised by the *Atp11c* mutation while T cells and most other tissues appear normal? Microarray profiling of *Atp11c* mRNA shows that it is equally expressed in B and T lymphocytes (Figure 1.9 in Chapter 1) (Heng and Painter, 2008) and most other tissues with highest expression in liver (Figure 1.10 in Chapter 1) (Wu et al., 2009). In agreement with the broad expression profile, PS flippase activity was reduced in all cells of the immune system, yet the mutation selectively compromised differentiation of pro-B cells. One explanation for the pro-B cell specific defect would be that these cells rely more on flippase activity in comparison to other cells. Indeed, pro-B cells from wild-type mice exhibited the highest flippase activity. Therefore, the absence of ATP11C thereby impaired flippase activity may explain the developmental arrest at the pro-B cell stage. Consistent with this notion, viable pro- and pre-B cells were shown to express PS on their surface (Dillon et al., 2000, Dillon et al., 2001), thus pro-B and pre-B cells may exhibit an increased need for flippase activity. Alternatively, post-translational regulatory changes in phospholipid flippase, floppase and scramblase activity, and

unique membrane events required in bone marrow pro-B and pre-B cells, may explain the stage- and lineage-specific dependence upon ATP11C.

10.3 Insights into the role of ATP11C in erythrocyte biology

In the course of their journey through the blood capillaries erythrocytes undergo dramatic, transient changes in shape. The asymmetric distribution of phospholipids in the erythrocyte membrane plays a role in erythrocyte deformability and is essential for the development, survival and function of red blood cells (Daleke, 2008, Mohandas and Gallagher, 2008). Similar to other cells, members of the P4-type ATPase family contribute to the generation and maintenance of membrane lipid assymetry in erythrocytes by mediating the inward movement of PS and PE (Daleke, 2008, Sebastian et al., 2012), but their functions in red cell biology remains to be fully eluciated (van der Mark et al., 2013). Several P4-type ATPases are expressed during erythropoiesis with ATP8A1, ATP11B and ATP11C being particularly prominent in primitive, fetal and adult erythroblasts (Kingsley et al., 2013). The high expression of several flippases suggests a potential role for them in erythrocyte biology. So far only ATP8A1, a homologue of which has a PS flippase activity in yeast (Soupene et al., 2008), has been shown to be expressed in erythroblasts and to be present in the plasma membrane of mature erythrocytes (Soupene and Kuypers, 2006). However, erythrocytes from *Atp8a1*$^{-/-}$ animals exhibit no increased PS exposure on their surface, and this is explained by the compensatory expression of ATP8A2 in erythrocytes from *Atp8a1*$^{-/-}$ animals (Levano et al., 2012).

The results of this thesis demonstrated that erythrocytes from ATP11C-deficient animals have an apparently normal development in the bone marrow but show stomatocytic morphology in the peripheral blood as well as having a shortened lifespan. Furthermore, erythrocyte precursors lacking the putative PS transporter ATP11C display a lower rate of C_6-NBD-PS internalisation than their wild-type counterparts. Thus, this study reveals ATP11C as an essential flippase in red blood cells and highlights the important role of phospholipid transport in maintaining the normal shape and survival of erythrocytes. Multiple attempts have been made to isolate and identify the major aminophospholipid flippases from red blood cells and other membranes (Moriyama and Nelson, 1988, Morrot et al., 1990, Daleke et al.,

1992, Auland et al., 1994b, Auland et al., 1994a). The biochemical characterisation suggests that the erythrocyte flippase is a Mg^{2+}-dependent, vanadate-sensitive ATPase (Moriyama and Nelson, 1988). Our finding of ATP11C being involved in the maintenance of lipid asymmetry in erythrocytes is consistent with those biochemical findings and proposes a molecular candidate for this function.

Exposure of PS on the outer leaflet of the erythrocyte membrane is believed to be one of the key signals for removal of old or damaged cells from the circulation (McEvoy et al., 1986, Connor et al., 1994). In ATP11C-deficient animals there is increased PS-exposure at the surface of aged mature erythrocytes in the blood and spleen, but not of erythroblasts in the bone marrow. As shown by *in vivo* CFSE labelling, newly formed ATP11C-deficient erythrocytes do not show increased binding of Annexin-V to the surface; however, over time, there is an increased proportion of erythrocytes that expose PS, and hence increased Annexin-V binding. In line with these findings, development of erythrocytes in the bone marrow of ATP11C-deficient animals is normal. Similarly, the increased forward scatter of ATP11C-deficient erythrocytes, indicative of increased cell size, is only observed in mature red blood cells, and not in reticulocytes or earlier developmental stages in the bone marrow and periphery.

As cells of the immune system from ATP11C-deficient mice demonstrated a slower internalisation of a fluorescently labelled PS analogue, a likely explanation of the ATP11C-deficient erythrocyte phenotype observed in this thesis is a reduced internalisation of PS. Indeed, *in vitro* uptake of the PS analogue C_6-NBD-PS by mutant erythroblasts is significantly reduced; however, there was no major difference observed in mature erythrocytes. While this result is consistent with the fact that the protein is expressed predominantly during erythropoiesis (Figure 9.15) (Kingsley et al., 2013), it contrasts with the slow increase of PS exposure on older, but not newly formed, mature red cells in ATP11C mutant mice. One possible explanation for this apparent inconsistency is a small defect in PS internalisation in mature erythrocytes that is below the detection limit of 30 min *in vitro* assay becomes physiologically relevant over the lifespan of the erythrocyte. Alternatively, in ATP11C deficient erythrocytes the reduced rate of PS flipping during the early developmental stages may have a lasting change on the membrane composition, resulting in reduced

erythrocyte deformability, increased intravascular damage and hence PS exposure. Elevated levels of bilirubin in ATP11C mutant mice suggest that significant haemolysis does occur in these mice. Irrespective of the precise mechanism, it is clear from the results that ATP11C deficiency results in impaired flippase activity in erythroblasts, increased accumulation of PS on the surface of erythrocytes, with the shortened lifespan of these cells leading to anaemia in ATP11C-deficient mice.

Maintenance of the normal discoid shape of erythrocytes is essential for their function and a range of haematological disorders, arising from mutations in genes encoding globin, membrane or associated skeletal proteins, are characterised by altered erythrocyte shape (Mohandas and Gallagher, 2008, Da Costa et al., 2013). One of the disease-associated shape changes is stomatocytosis. In at least some cases, erythrocytes from patients suffering from stomatocytosis have an increased leak of cations across the plasma membrane, and patients have been found to carry mutations in the mechanosensitive ion channel protein PIEZO1 (Zarychanski et al., 2012, Bae et al., 2013, Andolfo et al., 2013, Albuisson et al., 2013), or in the transporter proteins SLC4A1 (Bruce et al., 2005), RHAG (Bruce et al., 2009), or SLC2A1 (Flatt et al., 2011). By contrast, stomatocytosis arising from mutations in either the ABCG5 protein or the ABCG8 protein is not associated with increased cation leakage (Rees et al., 2005). Interestingly, erythrocytes from ATP11C-deficient mice had a normal osmotic fragility curve, no abnormality in the erythrocyte Na^+/K^+ ratio, and no apparent temperature-sensitive K^+ leak. Furthermore, the mice had normal iron parameters. These observations indicate that stomatocyte formation in ATP11C mutant erythrocytes is independent of cation leaks or hydration status, and suggest that an alternative mechanism is responsible for the stomatocytosis in these mice. One possibility is a mechanism similar to that responsible for Mediterranean stomatocytosis (Ducrou and Kimber, 1969), in which a lack of control over sterol absorption and excretion leads to changes in the plasma lipid composition and presumably the membrane lipid composition of circulating cells. Alterations in the relative lipid composition of the erythrocyte membrane can lead to an expansion or contraction of either the inner or outer leaflet, resulting in altered erythrocyte shape (Sheetz and Singer, 1974, Seigneuret and Devaux, 1984, Daleke and Huestis, 1985). In addition, reduced accumulation of PS at the cytofacial leaflet is predicted to interfere with the interaction between skeletal proteins and the membrane (An et al.,

2004, Manno et al., 2002). It is plausible, therefore, that a disturbance in these interactions underlies the observed formation of stomatocytes in the ATP11C mutant mice. However, future studies are needed for investigation of this theory.

10.4 Conclusion

The asymmetrical distribution of specific lipids between the two leaflets of cellular membranes is generated and maintained by transporters, but few genetic tools are available to test their function within the immune system. I revealed in this thesis a critical role for the phospholipid transporter ATP11C in B cell development in the bone marrow. Loss of ATP11C blocked B cell development in a cell-autonomous manner at the pro-B cell to pre-B cell transition. In order to identify the molecular mechanisms underlying the observed phenotype in mutant animals, the further analysis focused on the two crucial signaling pathways that each are necessary for normal pre-B cell development in mice, namely signaling through the IL-7R and pre-BCR. I found that while IL-7R signaling appears intact in isolated pro-B cells from ATP11C mutant mice, the mutation leads to a defect in the assembly and/or signaling through the pre-BCR. Functional analysis of B cells revealed that while mutant animals showed a variably reduced primary and secondary response to T-dependent antigens, the response to an antigen, which requires GC formation, was severely reduced. Surprisingly, B cells from BCR transgenic ATP11C-deficient BCR transgenic mice were able to mount a normal GC response upon transfer into wild-type recipients indicating that the absent GC response in ATP11C-deficient mice is caused by a B cell extrinsic effect.

Consistent with the predicted function of ATP11C, biochemical analysis revealed a critical role for ATP11C in PS internalisation in multiple cells. The defective flippase activity in other cells of the immune system did not cause an obvious phenotype. However, the ATP11C^{amb} mutation had an impact on erythrocyte survival, shape and flippase activity.

Taken together, the results presented in this thesis reveal an important functional role for ATP11C in the immune system and erythrocyte biology, and raise the question of

whether mutations in ATP11C serve as a previously unclassified cause of B cell deficiency and anaemia in humans.

CHAPTER 11: References

ADAMS, B., DORFLER, P., AGUZZI, A., KOZMIK, Z., URBANEK, P., MAURER-FOGY, I. & BUSSLINGER, M. 1992. Pax-5 encodes the transcription factor BSAP and is expressed in B lymphocytes, the developing CNS, and adult testis. *Genes Dev,* 6, 1589-607.

AIVAZIAN, D. & STERN, L. J. 2000. Phosphorylation of T cell receptor zeta is regulated by a lipid dependent folding transition. *Nat Struct Biol,* 7, 1023-6.

ALBUISSON, J., MURTHY, S. E., BANDELL, M., COSTE, B., LOUIS-DIT-PICARD, H., MATHUR, J., FENEANT-THIBAULT, M., TERTIAN, G., DE JAUREGUIBERRY, J. P., SYFUSS, P. Y., CAHALAN, S., GARCON, L., TOUTAIN, F., SIMON ROHRLICH, P., DELAUNAY, J., PICARD, V., JEUNEMAITRE, X. & PATAPOUTIAN, A. 2013. Dehydrated hereditary stomatocytosis linked to gain-of-function mutations in mechanically activated PIEZO1 ion channels. *Nat Commun,* 4, 1884.

ALDER-BAERENS, N., LISMAN, Q., LUONG, L., POMORSKI, T. & HOLTHUIS, J. C. M. 2006. Loss of P4 ATPases Drs2p and Dnf3p disrupts aminophospholipid transport and asymmetry in yeast post-Golgi secretory vesicles. *Mol Biol Cell,* 17, 1632-42.

ALLMAN, D., LINDSLEY, R. C., DEMUTH, W., RUDD, K., SHINTON, S. A. & HARDY, R. R. 2001. Resolution of three nonproliferative immature splenic B cell subsets reveals multiple selection points during peripheral B cell maturation. *J Immunol,* 167, 6834-40.

ALLMAN, D. & PILLAI, S. 2008. Peripheral B cell subsets. *Curr Opin Immunol,* 20, 149-57.

ALLMAN, D. M., FERGUSON, S. E., LENTZ, V. M. & CANCRO, M. P. 1993. Peripheral B cell maturation. II. Heat-stable antigen(hi) splenic B cells are an immature developmental intermediate in the production of long-lived marrow-derived B cells. *J Immunol,* 151, 4431-44.

ALVES, N. L., AROSA, F. A. & VAN LIER, R. A. W. 2007. Common [gamma] chain cytokines: dissidence in the details. *Immunol Lett.,* 108, 113-120.

ALVES, N. L., VAN LEEUWEN, E. M. M., DERKS, I. A. M. & VAN LIER, R. A. W. 2008. Differential regulation of human IL-7 receptor alpha expression by IL-7 and TCR signaling. *J Immunol,* 180, 5201-10.

AMIN, R. H. & SCHLISSEL, M. S. 2008. Foxo1 directly regulates the transcription of recombination-activating genes during B cell development. *Nat Immunol,* 9, 613-22.

AN, X., GUO, X., SUM, H., MORROW, J., GRATZER, W. & MOHANDAS, N. 2004. Phosphatidylserine binding sites in erythroid spectrin: location and implications for membrane stability. *Biochemistry,* 43, 310-5.

ANDOLFO, I., ALPER, S. L., DE FRANCESCHI, L., AURIEMMA, C., RUSSO, R., DE FALCO, L., VALLEFUOCO, F., ESPOSITO, M. R., VANDORPE, D. H., SHMUKLER, B. E., NARAYAN, R., MONTANARO, D.,

D'ARMIENTO, M., VETRO, A., LIMONGELLI, I., ZUFFARDI, O., GLADER, B. E., SCHRIER, S. L., BRUGNARA, C., STEWART, G. W., DELAUNAY, J. & IOLASCON, A. 2013. Multiple clinical forms of dehydrated hereditary stomatocytosis arise from mutations in PIEZO1. *Blood,* 121, 3925-35, S1-12.

ANDREWS, T. D., SJOLLEMA, G. & GOODNOW, C. C. 2013. Understanding the immunological impact of the human mutation explosion. *Trends Immunol,* 34, 99-106.

ANDREWS, T. D., WHITTLE, B., FIELD, M. A., BALAKISHNAN, B., ZHANG, Y., SHAO, Y., CHO, V., KIRK, M., SINGH, M., XIA, Y., HAGER, J., WINSLADE, S., SJOLLEMA, G., BEUTLER, B., ENDERS, A. & GOODNOW, C. C. 2012. Massively parallel sequencing of the mouse exome to accurately identify rare, induced mutations: an immediate source for thousands of new mouse models. *Open Biol,* 2, 120061.

ANSEL, K. M., HARRIS, R. B. & CYSTER, J. G. 2002. CXCL13 is required for B1 cell homing, natural antibody production, and body cavity immunity. *Immunity,* 16, 67-76.

ARINOBU, Y., MIZUNO, S., CHONG, Y., SHIGEMATSU, H., IINO, T., IWASAKI, H., GRAF, T., MAYFIELD, R., CHAN, S., KASTNER, P. & AKASHI, K. 2007. Reciprocal activation of GATA-1 and PU.1 marks initial specification of hematopoietic stem cells into myeloerythroid and myelolymphoid lineages. *Cell Stem Cell,* 1, 416-27.

ARNOLD, C. N., BARNES, M. J., BERGER, M., BLASIUS, A. L., BRANDL, K., CROKER, B., CROZAT, K., DU, X., EIDENSCHENK, C., GEORGEL, P., HOEBE, K., HUANG, H., JIANG, Z., KREBS, P., LA VINE, D., LI, X., LYON, S., MORESCO, E. M., MURRAY, A. R., POPKIN, D. L., RUTSCHMANN, S., SIGGS, O. M., SMART, N. G., SUN, L., TABETA, K., WEBSTER, V., TOMISATO, W., WON, S., XIA, Y., XIAO, N. & BEUTLER, B. 2012. ENU-induced phenovariance in mice: inferences from 587 mutations. *BMC Res Notes,* 5, 577.

ATTANAVANICH, K. & KEARNEY, J. F. 2004. Marginal zone, but not follicular B cells, are potent activators of naive CD4 T cells. *J Immunol,* 172, 803-11.

AU-YEUNG, B. B., DEINDL, S., HSU, L. Y., PALACIOS, E. H., LEVIN, S. E., KURIYAN, J. & WEISS, A. 2009. The structure, regulation, and function of ZAP-70. *Immunol Rev,* 228, 41-57.

AULAND, M. E., MORRIS, M. B. & ROUFOGALIS, B. D. 1994a. Separation and characterization of two Mg(2+)-ATPase activities from the human erythrocyte membrane. *Arch Biochem Biophys,* 312, 272-7.

AULAND, M. E., ROUFOGALIS, B. D., DEVAUX, P. F. & ZACHOWSKI, A. 1994b. Reconstitution of ATP-dependent aminophospholipid translocation in proteoliposomes. *Proc Natl Acad Sci U S A,* 91, 10938-42.

BACK, J., ALLMAN, D., CHAN, S. & KASTNER, P. 2005. Visualizing PU.1 activity during hematopoiesis. *Exp Hematol,* 33, 395-402.

BAE, C., GNANASAMBANDAM, R., NICOLAI, C., SACHS, F. & GOTTLIEB, P. A. 2013. Xerocytosis is caused by mutations that alter the kinetics of the mechanosensitive channel PIEZO1. *Proc Natl Acad Sci U S A,* 110, E1162-8.

BAIN, G., MAANDAG, E. C., IZON, D. J., AMSEN, D., KRUISBEEK, A. M., WEINTRAUB, B. C., KROP, I., SCHLISSEL, M. S., FEENEY, A. J., VAN ROON, M. & ET AL. 1994. E2A proteins are required for proper B cell development and initiation of immunoglobulin gene rearrangements. *Cell,* 79, 885-92.

BAIN, G., ROBANUS MAANDAG, E. C., TE RIELE, H. P., FEENEY, A. J., SHEEHY, A., SCHLISSEL, M., SHINTON, S. A., HARDY, R. R. & MURRE, C. 1997. Both E12 and E47 allow commitment to the B cell lineage. *Immunity,* 6, 145-54.

BALDRIDGE, R. D. & GRAHAM, T. R. 2012. Identification of residues defining phospholipid flippase substrate specificity of type IV P-type ATPases. *Proc Natl Acad Sci U S A,* 109, E290-8.

BARBERIS, A., WIDENHORN, K., VITELLI, L. & BUSSLINGER, M. 1990. A novel B-cell lineage-specific transcription factor present at early but not late stages of differentiation. *Genes Dev,* 4, 849-59.

BASSE, F., STOUT, J. G., SIMS, P. J. & WIEDMER, T. 1996. Isolation of an erythrocyte membrane protein that mediates Ca2+-dependent transbilayer movement of phospholipid. *J Biol Chem,* 271, 17205-10.

BATTEN, M., GROOM, J., CACHERO, T. G., QIAN, F., SCHNEIDER, P., TSCHOPP, J., BROWNING, J. L. & MACKAY, F. 2000. BAFF mediates survival of peripheral immature B lymphocytes. *J Exp Med,* 192, 1453-66.

BAUMGARTH, N. 2011. The double life of a B-1 cell: self-reactivity selects for protective effector functions. *Nat Rev Immunol,* 11, 34-46.

BECK, K., PEAK, M. M., OTA, T., NEMAZEE, D. & MURRE, C. 2009. Distinct roles for E12 and E47 in B cell specification and the sequential rearrangement of immunoglobulin light chain loci. *J Exp Med,* 206, 2271-84.

BENDELAC, A., SAVAGE, P. B. & TEYTON, L. 2007. The biology of NKT cells. *Annu Rev Immunol,* 25, 297-336.

BEREK, C., BERGER, A. & APEL, M. 1991. Maturation of the immune response in germinal centers. *Cell,* 67, 1121-9.

BERGE, K. E., TIAN, H., GRAF, G. A., YU, L., GRISHIN, N. V., SCHULTZ, J., KWITEROVICH, P., SHAN, B., BARNES, R. & HOBBS, H. H. 2000. Accumulation of dietary cholesterol in sitosterolemia caused by mutations in adjacent ABC transporters. *Science,* 290, 1771-5.

BERGMANN, H., YABAS, M., SHORT, A., MIOSGE, L., BARTHEL, N., TEH, C. E., ROOTS, C. M., BULL, K. R., JEELALL, Y., HORIKAWA, K., WHITTLE, B., BALAKISHNAN, B., SJOLLEMA, G., BERTRAM, E. M., MACKAY, F., RIMMER, A. J., CORNALL, R. J., FIELD, M. A., ANDREWS, T. D., GOODNOW, C. C. & ENDERS, A. 2013. B cell survival, surface BCR and BAFFR expression, CD74 metabolism, and CD8- dendritic cells require the intramembrane endopeptidase SPPL2A. *J Exp Med,* 210, 31-40.

BERLAND, R. & WORTIS, H. H. 2002. Origins and functions of B-1 cells with notes on the role of CD5. *Annu Rev Immunol,* 20, 253-300.

BEVERS, E. M., COMFURIUS, P. & ZWAAL, R. F. 1983. Changes in membrane phospholipid distribution during platelet activation. *Biochim Biophys Acta,* 736, 57-66.

BEVERS, E. M., WIEDMER, T., COMFURIUS, P., SHATTIL, S. J., WEISS, H. J., ZWAAL, R. F. & SIMS, P. J. 1992. Defective Ca(2+)-induced microvesiculation and deficient expression of procoagulant activity in erythrocytes from a patient with a bleeding disorder: a study of the red blood cells of Scott syndrome. *Blood,* 79, 380-8.

BEVERS, E. M. & WILLIAMSON, P. L. 2010. Phospholipid scramblase: an update. *FEBS Lett,* 584, 2724-30.

BITBOL, M. & DEVAUX, P. F. 1988. Measurement of outward translocation of phospholipids across human erythrocyte membrane. *Proc Natl Acad Sci U S A,* 85, 6783-7.

BORGHESI, L., AITES, J., NELSON, S., LEFTEROV, P., JAMES, P. & GERSTEIN, R. 2005. E47 is required for V(D)J recombinase activity in common lymphoid progenitors. *J Exp Med,* 202, 1669-77.

BRADL, H. & JACK, H. M. 2001. Surrogate light chain-mediated interaction of a soluble pre-B cell receptor with adherent cell lines. *J Immunol,* 167, 6403-11.

BRATTON, D. L., FADOK, V. A., RICHTER, D. A., KAILEY, J. M., GUTHRIE, L. A. & HENSON, P. M. 1997. Appearance of phosphatidylserine on apoptotic cells requires calcium-mediated nonspecific flip-flop and is enhanced by loss of the aminophospholipid translocase. *J Biol Chem,* 272, 26159-65.

BRETSCHER, M. S. 1972. Asymmetrical lipid bilayer structure for biological membranes. *Nat New Biol,* 236, 11-2.

BRINK, R., PHAN, T. G., PAUS, D. & CHAN, T. D. 2008. Visualizing the effects of antigen affinity on T-dependent B-cell differentiation. *Immunol Cell Biol,* 86, 31-9.

BRUCE, L. J. 2009. Hereditary stomatocytosis and cation-leaky red cells--recent developments. *Blood Cells Mol Dis,* 42, 216-22.

BRUCE, L. J., GUIZOUARN, H., BURTON, N. M., GABILLAT, N., POOLE, J., FLATT, J. F., BRADY, R. L., BORGESE, F., DELAUNAY, J. & STEWART, G. W. 2009. The monovalent cation leak in overhydrated stomatocytic red blood cells results from amino acid substitutions in the Rh-associated glycoprotein. *Blood,* 113, 1350-7.

BRUCE, L. J., ROBINSON, H. C., GUIZOUARN, H., BORGESE, F., HARRISON, P., KING, M. J., GOEDE, J. S., COLES, S. E., GORE, D. M., LUTZ, H. U., FICARELLA, R., LAYTON, D. M., IOLASCON, A., ELLORY, J. C. & STEWART, G. W. 2005. Monovalent cation leaks in human red cells caused by single amino-acid substitutions in the transport domain of the band 3 chloride-bicarbonate exchanger, AE1. *Nat Genet,* 37, 1258-63.

BULL, K. R., RIMMER, A. J., SIGGS, O. M., MIOSGE, L. A., ROOTS, C. M., ENDERS, A., BERTRAM, E. M., CROCKFORD, T. L., WHITTLE, B., POTTER, P. K., SIMON, M. M., MALLON, A. M., BROWN, S. D., BEUTLER, B., GOODNOW, C. C., LUNTER, G. & CORNALL, R. J. 2013. Unlocking the bottleneck in forward genetics using whole-genome sequencing and identity by descent to isolate causative mutations. *PLoS Genet,* 9, e1003219.

BULL, L. N., VAN EIJK, M. J., PAWLIKOWSKA, L., DEYOUNG, J. A., JUIJN, J. A., LIAO, M., KLOMP, L. W., LOMRI, N., BERGER, R., SCHARSCHMIDT, B. F., KNISELY, A. S., HOUWEN, R. H. & FREIMER, N. B. 1998. A gene encoding a P-type ATPase mutated in two forms of hereditary cholestasis. *Nat Genet,* 18, 219-24.

BUTIKOFER, P., LIN, Z. W., CHIU, D. T., LUBIN, B. & KUYPERS, F. A. 1990. Transbilayer distribution and mobility of phosphatidylinositol in human red blood cells. *J Biol Chem,* 265, 16035-8.

CACCIAGLI, P., HADDAD, M. R., MIGNON-RAVIX, C., EL-WALY, B., MONCLA, A., MISSIRIAN, C., CHABROL, B. & VILLARD, L. 2010. Disruption of the ATP8A2 gene in a patient with a t(10;13) de novo balanced translocation and a severe neurological phenotype. *Eur J Hum Genet,* 18, 1360-3.

CAI, S. Y., GAUTAM, S., NGUYEN, T., SOROKA, C. J., RAHNER, C. & BOYER, J. L. 2009. ATP8B1 deficiency disrupts the bile canalicular membrane bilayer structure in hepatocytes, but FXR expression and activity are maintained. *Gastroenterology,* 136, 1060-9.

CAO, X., SHORES, E. W., HU-LI, J., ANVER, M. R., KELSALL, B. L., RUSSELL, S. M., DRAGO, J., NOGUCHI, M., GRINBERG, A., BLOOM, E. T. & ET AL. 1995. Defective lymphoid development in mice lacking expression of the common cytokine receptor gamma chain. *Immunity,* 2, 223-38.

CARSETTI, R., KOHLER, G. & LAMERS, M. C. 1995. Transitional B cells are the target of negative selection in the B cell compartment. *J Exp Med,* 181, 2129-40.

CARVALHO, T. L., MOTA-SANTOS, T., CUMANO, A., DEMENGEOT, J. & VIEIRA, P. 2001. Arrested B lymphopoiesis and persistence of activated B cells in adult interleukin 7(-/)- mice. *J Exp Med,* 194, 1141-50.

CASTOLDI, E., COLLINS, P. W., WILLIAMSON, P. L. & BEVERS, E. M. 2011. Compound heterozygosity for 2 novel TMEM16F mutations in a patient with Scott syndrome. *Blood,* 117, 4399-400.

CHEN, B., JIANG, Y., ZENG, S., YAN, J., LI, X., ZHANG, Y., ZOU, W. & WANG, X. 2010. Endocytic sorting and recycling require membrane phosphatidylserine asymmetry maintained by TAT-1/CHAT-1. *PLoS Genet,* 6, e1001235.

CHEN, C. Y., INGRAM, M. F., ROSAL, P. H. & GRAHAM, T. R. 1999. Role for Drs2p, a P-type ATPase and potential aminophospholipid translocase, in yeast late Golgi function. *J Cell Biol,* 147, 1223-36.

CHEN, K., LIU, J., HECK, S., CHASIS, J. A., AN, X. & MOHANDAS, N. 2009. Resolving the distinct stages in erythroid differentiation based on dynamic changes in membrane protein expression during erythropoiesis. *Proc Natl Acad Sci U S A,* 106, 17413-8.

CHENG, A. M., ROWLEY, B., PAO, W., HAYDAY, A., BOLEN, J. B. & PAWSON, T. 1995. Syk tyrosine kinase required for mouse viability and B-cell development. *Nature,* 378, 303-6.

CHO, J.-H., KIM, H.-O., SURH, C. D. & SPRENT, J. 2010. T Cell Receptor-Dependent Regulation of Lipid Rafts Controls Naive CD8+ T Cell Homeostasis. *Immunity,* 32, 214-226.

CINAMON, G., ZACHARIAH, M. A., LAM, O. M., FOSS, F. W., JR. & CYSTER, J. G. 2008. Follicular shuttling of marginal zone B cells facilitates antigen transport. *Nat Immunol,* 9, 54-62.

CLARK, M. R., MANDAL, M., OCHIAI, K. & SINGH, H. 2014. Orchestrating B cell lymphopoiesis through interplay of IL-7 receptor and pre-B cell receptor signalling. *Nat Rev Immunol,* 14, 69-80.

COBALEDA, C., JOCHUM, W. & BUSSLINGER, M. 2007. Conversion of mature B cells into T cells by dedifferentiation to uncommitted progenitors. *Nature,* 449, 473-7.

COHEN, P. L., CARICCHIO, R., ABRAHAM, V., CAMENISCH, T. D., JENNETTE, J. C., ROUBEY, R. A., EARP, H. S., MATSUSHIMA, G. & REAP, E. A. 2002. Delayed apoptotic cell clearance and lupus-like autoimmunity in mice lacking the c-mer membrane tyrosine kinase. *J Exp Med,* 196, 135-40.

COLEMAN, J. A., KWOK, M. C. & MOLDAY, R. S. 2009. Localization, purification, and functional reconstitution of the P4-ATPase Atp8a2, a phosphatidylserine flippase in photoreceptor disc membranes. *J Biol Chem,* 284, 32670-9.

COLEMAN, J. A., ZHU, X., DJAJADI, H. R., MOLDAY, L. L., SMITH, R. S., LIBBY, R. T., JOHN, S. W. & MOLDAY, R. S. 2014. Phospholipid flippase ATP8A2 is required for normal visual and auditory function and photoreceptor and spiral ganglion cell survival. *J Cell Sci,* 127, 1138-49.

COMFURIUS, P., SENDEN, J. M., TILLY, R. H., SCHROIT, A. J., BEVERS, E. M. & ZWAAL, R. F. 1990. Loss of membrane phospholipid asymmetry in platelets and red cells may be associated with calcium-induced shedding of plasma membrane and inhibition of aminophospholipid translocase. *Biochim Biophys Acta,* 1026, 153-60.

COMFURIUS, P., WILLIAMSON, P., SMEETS, E. F., SCHLEGEL, R. A., BEVERS, E. M. & ZWAAL, R. F. 1996. Reconstitution of phospholipid scramblase activity from human blood platelets. *Biochemistry,* 35, 7631-4.

CONG, L., RAN, F. A., COX, D., LIN, S., BARRETTO, R., HABIB, N., HSU, P. D., WU, X., JIANG, W., MARRAFFINI, L. A. & ZHANG, F. 2013. Multiplex genome engineering using CRISPR/Cas systems. *Science,* 339, 819-23.

CONNOR, J., PAK, C. C. & SCHROIT, A. J. 1994. Exposure of phosphatidylserine in the outer leaflet of human red blood cells. Relationship to cell density, cell age, and clearance by mononuclear cells. *J Biol Chem,* 269, 2399-404.

CONNOR, J., PAK, C. H., ZWAAL, R. F. & SCHROIT, A. J. 1992. Bidirectional transbilayer movement of phospholipid analogs in human red blood cells. Evidence for an ATP-dependent and protein-mediated process. *J Biol Chem,* 267, 19412-7.

COOPER, A. B., SAWAI, C. M., SICINSKA, E., POWERS, S. E., SICINSKI, P., CLARK, M. R. & AIFANTIS, I. 2006. A unique function for cyclin D3 in early B cell development. *Nat Immunol,* 7, 489-97.

CORCORAN, A. E., SMART, F. M., COWLING, R. J., CROMPTON, T., OWEN, M. J. & VENKITARAMAN, A. R. 1996. The interleukin-7 receptor alpha chain transmits distinct signals for proliferation and differentiation during B lymphopoiesis. *EMBO J,* 15, 1924-32.

CORFE, S. A. & PAIGE, C. J. 2012. The many roles of IL-7 in B cell development; mediator of survival, proliferation and differentiation. *Semin Immunol,* 24, 198-208.

COUPLAND, L. A., CROMER, D., DAVENPORT, M. P. & PARISH, C. R. 2010. A novel fluorescent-based assay reveals that thrombopoietin signaling and Bcl-X(L) influence, respectively, platelet and erythrocyte lifespans. *Exp Hematol,* 38, 453-461 e1.

CROTTY, S. 2011. Follicular helper CD4 T cells (TFH). *Annu Rev Immunol,* 29, 621-63.

DA COSTA, L., GALIMAND, J., FENNETEAU, O. & MOHANDAS, N. 2013. Hereditary spherocytosis, elliptocytosis, and other red cell membrane disorders. *Blood Rev,* 27, 167-78.

DAKIC, A., METCALF, D., DI RAGO, L., MIFSUD, S., WU, L. & NUTT, S. L. 2005. PU.1 regulates the commitment of adult hematopoietic progenitors and restricts granulopoiesis. *J Exp Med,* 201, 1487-502.

DALEKE, D. L. 2003. Regulation of transbilayer plasma membrane phospholipid asymmetry. *J Lipid Res,* 44, 233-42.

DALEKE, D. L. 2007. Phospholipid flippases. *J Biol Chem,* 282, 821-5.

DALEKE, D. L. 2008. Regulation of phospholipid asymmetry in the erythrocyte membrane. *Curr Opin Hematol,* 15, 191-5.

DALEKE, D. L., CORNELY-MOSS, K., LYLES, J., SMITH, C. M. & ZIMMERMAN, M. 1992. Identification and characterization of a candidate phosphatidylserine-transporting ATPase. *Ann N Y Acad Sci,* 671, 468-70.

DALEKE, D. L. & HUESTIS, W. H. 1985. Incorporation and translocation of aminophospholipids in human erythrocytes. *Biochemistry,* 24, 5406-16.

DARLAND-RANSOM, M., WANG, X., SUN, C. L., MAPES, J., GENGYO-ANDO, K., MITANI, S. & XUE, D. 2008. Role of C. elegans TAT-1 protein in maintaining plasma membrane phosphatidylserine asymmetry. *Science,* 320, 528-31.

DE JONG, K., EMERSON, R. K., BUTLER, J., BASTACKY, J., MOHANDAS, N. & KUYPERS, F. A. 2001. Short survival of phosphatidylserine-exposing red blood cells in murine sickle cell anemia. *Blood,* 98, 1577-84.

DECKER, T., PASCA DI MAGLIANO, M., MCMANUS, S., SUN, Q., BONIFER, C., TAGOH, H. & BUSSLINGER, M. 2009. Stepwise activation of enhancer and promoter regions of the B cell commitment gene Pax5 in early lymphopoiesis. *Immunity,* 30, 508-20.

DEKOTER, R. P., LEE, H. J. & SINGH, H. 2002. PU.1 regulates expression of the interleukin-7 receptor in lymphoid progenitors. *Immunity,* 16, 297-309.

DELOGU, A., SCHEBESTA, A., SUN, Q., ASCHENBRENNER, K., PERLOT, T. & BUSSLINGER, M. 2006. Gene repression by Pax5 in B cells is essential for blood cell homeostasis and is reversed in plasma cells. *Immunity,* 24, 269-81.

DHAR, M. S., SOMMARDAHL, C. S., KIRKLAND, T., NELSON, S., DONNELL, R., JOHNSON, D. K. & CASTELLANI, L. W. 2004. Mice heterozygous for Atp10c, a putative amphipath, represent a novel model of obesity and type 2 diabetes. *J Nutr,* 134, 799-805.

DHAR, M. S., YUAN, J. S., ELLIOTT, S. B. & SOMMARDAHL, C. 2006. A type IV P-type ATPase affects insulin-mediated glucose uptake in adipose tissue and skeletal muscle in mice. *J Nutr Biochem,* 17, 811-20.

DIAO, J., WINTER, E., CHEN, W., CANTIN, C. & CATTRAL, M. S. 2004. Characterization of distinct conventional and plasmacytoid dendritic cell-committed precursors in murine bone marrow. *J Immunol,* 173, 1826-33.

DIAS, S., MANSSON, R., GURBUXANI, S., SIGVARDSSON, M. & KEE, B. L. 2008. E2A proteins promote development of lymphoid-primed multipotent progenitors. *Immunity,* 29, 217-27.

DIAS, S., SILVA, H., JR., CUMANO, A. & VIEIRA, P. 2005. Interleukin-7 is necessary to maintain the B cell potential in common lymphoid progenitors. *J Exp Med,* 201, 971-9.

DILLON, S. R., CONSTANTINESCU, A. & SCHLISSEL, M. S. 2001. Annexin V binds to positively selected B cells. *J Immunol,* 166, 58-71.

DILLON, S. R., MANCINI, M., ROSEN, A. & SCHLISSEL, M. S. 2000. Annexin V binds to viable B cells and colocalizes with a marker of lipid rafts upon B cell receptor activation. *J Immunol,* 164, 1322-32.

DISANTO, J. P., MULLER, W., GUY-GRAND, D., FISCHER, A. & RAJEWSKY, K. 1995. Lymphoid development in mice with a targeted deletion of the interleukin 2 receptor gamma chain. *Proc Natl Acad Sci U S A,* 92, 377-81.

DORSHKIND, K. & MONTECINO-RODRIGUEZ, E. 2007. Fetal B-cell lymphopoiesis and the emergence of B-1-cell potential. *Nat Rev Immunol,* 7, 213-9.

DUCROU, W. & KIMBER, R. J. 1969. Stomatocytes, haemolytic anaemia and abdominal pain in Mediterranean migrants. Some examples of a new syndrome? *Med J Aust,* 2, 1087-91.

ELGUETA, R., BENSON, M. J., DE VRIES, V. C., WASIUK, A., GUO, Y. & NOELLE, R. J. 2009. Molecular mechanism and function of CD40/CD40L engagement in the immune system. *Immunol Rev,* 229, 152-72.

ENDERS, A., SHORT, A., MIOSGE, L. A., BERGMANN, H., SONTANI, Y., BERTRAM, E. M., WHITTLE, B., BALAKISHNAN, B., YOSHIDA, K., SJOLLEMA, G., FIELD, M. A., ANDREWS, T. D., HAGIWARA, H. & GOODNOW, C. C. 2014. Zinc-finger protein ZFP318 is essential for expression of IgD, the alternatively spliced Igh product made by mature B lymphocytes. *Proc Natl Acad Sci U S A,* 111, 4513-8.

ENDERS, A., STANKOVIC, S., TEH, C., ULDRICH, A. P., YABAS, M., JUELICH, T., ALTIN, J. A., FRANKENREITER, S., BERGMANN, H., ROOTS, C. M., KYPARISSOUDIS, K., GOODNOW, C. C. & GODFREY, D. I. 2012. ZBTB7B (Th-POK) regulates the development of IL-17-producing CD1d-restricted mouse NKT cells. *J Immunol,* 189, 5240-9.

ERLANDSSON, L., LICENCE, S., GASPAL, F., LANE, P., CORCORAN, A. E. & MARTENSSON, I. L. 2005. Both the pre-BCR and the IL-7Ralpha are essential for expansion at the pre-BII cell stage in vivo. *Eur J Immunol,* 35, 1969-76.

ERNEST, S. & BELLO-REUSS, E. 1999. Secretion of platelet-activating factor is mediated by MDR1 P-glycoprotein in cultured human mesangial cells. *J Am Soc Nephrol,* 10, 2306-13.

ESPLIN, B. L., WELNER, R. S., ZHANG, Q., BORGHESI, L. A. & KINCADE, P. W. 2009. A differentiation pathway for B1 cells in adult bone marrow. *Proc Natl Acad Sci U S A,* 106, 5773-8.

FADOK, V. A., VOELKER, D. R., CAMPBELL, P. A., COHEN, J. J., BRATTON, D. L. & HENSON, P. M. 1992. Exposure of phosphatidylserine on the surface of apoptotic lymphocytes triggers specific recognition and removal by macrophages. *J Immunol,* 148, 2207-16.

FAGARASAN, S. & HONJO, T. 2000. T-Independent immune response: new aspects of B cell biology. *Science,* 290, 89-92.

FELDHAUS, A. L., MBANGKOLLO, D., ARVIN, K. L., KLUG, C. A. & SINGH, H. 1992. BLyF, a novel cell-type- and stage-specific regulator of the B-lymphocyte gene mb-1. *Mol Cell Biol,* 12, 1126-33.

FERGUSON, A. R., YOUD, M. E. & CORLEY, R. B. 2004. Marginal zone B cells transport and deposit IgM-containing immune complexes onto follicular dendritic cells. *Int Immunol,* 16, 1411-22.

FLAMANT, S., PESCHER, P., LEMERCIER, B., CLEMENT-ZIZA, M., KEPES, F., FELLOUS, M., MILON, G., MARCHAL, G. & BESMOND, C. 2003. Characterization of a putative type IV aminophospholipid transporter P-type ATPase. *Mamm Genome,* 14, 21-30.

FLASWINKEL, H. & RETH, M. 1994. Dual role of the tyrosine activation motif of the Ig-alpha protein during signal transduction via the B cell antigen receptor. *EMBO J,* 13, 83-9.

FLATT, J. F., GUIZOUARN, H., BURTON, N. M., BORGESE, F., TOMLINSON, R. J., FORSYTH, R. J., BALDWIN, S. A., LEVINSON, B. E., QUITTET, P., AGUILAR-MARTINEZ, P., DELAUNAY, J., STEWART, G. W. & BRUCE, L. J. 2011. Stomatin-deficient cryohydrocytosis results from mutations in SLC2A1: a novel form of GLUT1 deficiency syndrome. *Blood,* 118, 5267-77.

FLEMING, H. E. & PAIGE, C. J. 2001. Pre-B cell receptor signaling mediates selective response to IL-7 at the pro-B to pre-B cell transition via an ERK/MAP kinase-dependent pathway. *Immunity,* 15, 521-31.

FLEMING, H. E. & PAIGE, C. J. 2002. Cooperation between IL-7 and the pre-B cell receptor: a key to B cell selection. *Semin Immunol,* 14, 423-30.

FLEMMING, A., BRUMMER, T., RETH, M. & JUMAA, H. 2003. The adaptor protein SLP-65 acts as a tumor suppressor that limits pre-B cell expansion. *Nat Immunol,* 4, 38-43.

FUJIKAWA, K., MILETIC, A. V., ALT, F. W., FACCIO, R., BROWN, T., HOOG, J., FREDERICKS, J., NISHI, S., MILDINER, S., MOORES, S. L., BRUGGE, J., ROSEN, F. S. & SWAT, W. 2003. Vav1/2/3-null mice define an essential role for Vav family proteins in lymphocyte development and activation but a differential requirement in MAPK signaling in T and B cells. *J Exp Med,* 198, 1595-608.

FUXA, M. & BUSSLINGER, M. 2007. Reporter gene insertions reveal a strictly B lymphoid-specific expression pattern of Pax5 in support of its B cell identity function. *J Immunol,* 178, 3031-7.

GALL, W. E., GEETHING, N. C., HUA, Z., INGRAM, M. F., LIU, K., CHEN, S. I. & GRAHAM, T. R. 2002. Drs2p-dependent formation of exocytic clathrin-coated vesicles in vivo. *Curr Biol,* 12, 1623-7.

GARDAM, S. & BRINK, R. 2014. Non-Canonical NF-kappaB Signaling Initiated by BAFF Influences B Cell Biology at Multiple Junctures. *Front Immunol,* 4, 509.

GASCARD, P., TRAN, D., SAUVAGE, M., SULPICE, J. C., FUKAMI, K., TAKENAWA, T., CLARET, M. & GIRAUD, F. 1991. Asymmetric distribution of phosphoinositides and phosphatidic acid in the human erythrocyte membrane. *Biochim Biophys Acta,* 1069, 27-36.

GAUTHIER, L., ROSSI, B., ROUX, F., TERMINE, E. & SCHIFF, C. 2002. Galectin-1 is a stromal cell ligand of the pre-B cell receptor (BCR) implicated in synapse formation between pre-B and stromal cells and in pre-BCR triggering. *Proc Natl Acad Sci U S A,* 99, 13014-9.

GAY, D., SAUNDERS, T., CAMPER, S. & WEIGERT, M. 1993. Receptor editing: an approach by autoreactive B cells to escape tolerance. *J Exp Med,* 177, 999-1008.

GEORGOPOULOS, K., BIGBY, M., WANG, J. H., MOLNAR, A., WU, P., WINANDY, S. & SHARPE, A. 1994. The Ikaros gene is required for the development of all lymphoid lineages. *Cell,* 79, 143-56.

GEORGOPOULOS, K., MOORE, D. D. & DERFLER, B. 1992. Ikaros, an early lymphoid-specific transcription factor and a putative mediator for T cell commitment. *Science,* 258, 808-12.

GODIN, I. E., GARCIA-PORRERO, J. A., COUTINHO, A., DIETERLEN-LIEVRE, F. & MARCOS, M. A. 1993. Para-aortic splanchnopleura from early mouse embryos contains B1a cell progenitors. *Nature,* 364, 67-70.

GOETZ, C. A., HARMON, I. R., O'NEIL, J. J., BURCHILL, M. A. & FARRAR, M. A. 2004. STAT5 activation underlies IL7 receptor-dependent B cell development. *J Immunol,* 172, 4770-8.

GOMES, E., JAKOBSEN, M. K., AXELSEN, K. B., GEISLER, M. & PALMGREN, M. G. 2000. Chilling tolerance in Arabidopsis involves ALA1, a member of a

new family of putative aminophospholipid translocases. *Plant Cell,* 12, 2441-2454.

GONDO, Y. 2008. Trends in large-scale mouse mutagenesis: from genetics to functional genomics. *Nat Rev Genet,* 9, 803-10.

GONG, E. Y., PARK, E., LEE, H. J. & LEE, K. 2009. Expression of Atp8b3 in murine testis and its characterization as a testis specific P-type ATPase. *Reproduction,* 137, 345-51.

GONG, S. & NUSSENZWEIG, M. C. 1996. Regulation of an early developmental checkpoint in the B cell pathway by Ig beta. *Science,* 272, 411-4.

GONG, S., SANCHEZ, M. & NUSSENZWEIG, M. C. 1996. Counterselection against D mu is mediated through immunoglobulin (Ig)alpha-Igbeta. *J Exp Med,* 184, 2079-84.

GOODNOW, C. C., CROSBIE, J., ADELSTEIN, S., LAVOIE, T. B., SMITH-GILL, S. J., BRINK, R. A., PRITCHARD-BRISCOE, H., WOTHERSPOON, J. S., LOBLAY, R. H., RAPHAEL, K. & ET AL. 1988. Altered immunoglobulin expression and functional silencing of self-reactive B lymphocytes in transgenic mice. *Nature,* 334, 676-82.

GOODNOW, C. C., VINUESA, C. G., RANDALL, K. L., MACKAY, F. & BRINK, R. 2010. Control systems and decision making for antibody production. *Nat Immunol,* 11, 681-8.

GORDESKY, S. E. & MARINETTI, G. V. 1973. The asymetric arrangement of phospholipids in the human erythrocyte membrane. *Biochem Biophys Res Commun,* 50, 1027-31.

GORTER, E. & GRENDEL, F. 1925. On Bimolecular Layers of Lipoids on the Chromocytes of the Blood. *J Exp Med,* 41, 439-43.

GRAHAM, T. R. 2004. Flippases and vesicle-mediated protein transport. *Trends Cell Biol,* 14, 670-7.

GRAWUNDER, U., LEU, T. M., SCHATZ, D. G., WERNER, A., ROLINK, A. G., MELCHERS, F. & WINKLER, T. H. 1995. Down-regulation of RAG1 and RAG2 gene expression in preB cells after functional immunoglobulin heavy chain rearrangement. *Immunity,* 3, 601-8.

GROOM, J., KALLED, S. L., CUTLER, A. H., OLSON, C., WOODCOCK, S. A., SCHNEIDER, P., TSCHOPP, J., CACHERO, T. G., BATTEN, M., WHEWAY, J., MAURI, D., CAVILL, D., GORDON, T. P., MACKAY, C. R. & MACKAY, F. 2002. Association of BAFF/BLyS overexpression and altered B cell differentiation with Sjogren's syndrome. *J Clin Invest,* 109, 59-68.

GROSS, J. A., DILLON, S. R., MUDRI, S., JOHNSTON, J., LITTAU, A., ROQUE, R., RIXON, M., SCHOU, O., FOLEY, K. P., HAUGEN, H., MCMILLEN, S., WAGGIE, K., SCHRECKHISE, R. W., SHOEMAKER, K., VU, T.,

MOORE, M., GROSSMAN, A. & CLEGG, C. H. 2001. TACI-Ig neutralizes molecules critical for B cell development and autoimmune disease. impaired B cell maturation in mice lacking BLyS. *Immunity,* 15, 289-302.

GYORY, I., BOLLER, S., NECHANITZKY, R., MANDEL, E., POTT, S., LIU, E. & GROSSCHEDL, R. 2012. Transcription factor Ebf1 regulates differentiation stage-specific signaling, proliferation, and survival of B cells. *Genes Dev,* 26, 668-82.

HAGMAN, J., BELANGER, C., TRAVIS, A., TURCK, C. W. & GROSSCHEDL, R. 1993. Cloning and functional characterization of early B-cell factor, a regulator of lymphocyte-specific gene expression. *Genes Dev,* 7, 760-73.

HAGMAN, J., TRAVIS, A. & GROSSCHEDL, R. 1991. A novel lineage-specific nuclear factor regulates mb-1 gene transcription at the early stages of B cell differentiation. *EMBO J,* 10, 3409-17.

HALVERSON, R., TORRES, R. M. & PELANDA, R. 2004. Receptor editing is the main mechanism of B cell tolerance toward membrane antigens. *Nat Immunol,* 5, 645-50.

HAMEL, K. M., LIARSKI, V. M. & CLARK, M. R. 2012. Germinal center B-cells. *Autoimmunity,* 45, 333-47.

HANADA, K. & PAGANO, R. E. 1995. A Chinese hamster ovary cell mutant defective in the non-endocytic uptake of fluorescent analogs of phosphatidylserine: isolation using a cytosol acidification protocol. *J Cell Biol,* 128, 793-804.

HANDE, S., NOTIDIS, E. & MANSER, T. 1998. Bcl-2 obstructs negative selection of autoreactive, hypermutated antibody V regions during memory B cell development. *Immunity,* 8, 189-98.

HARDY, R. R., CARMACK, C. E., SHINTON, S. A., KEMP, J. D. & HAYAKAWA, K. 1991. Resolution and characterization of pro-B and pre-pro-B cell stages in normal mouse bone marrow. *J Exp Med,* 173, 1213-25.

HARDY, R. R. & HAYAKAWA, K. 2001. B cell development pathways. *Annu Rev Immunol,* 19, 595-621.

HASHIMOTO, A., TAKEDA, K., INABA, M., SEKIMATA, M., KAISHO, T., IKEHARA, S., HOMMA, Y., AKIRA, S. & KUROSAKI, T. 2000. Cutting edge: essential role of phospholipase C-gamma 2 in B cell development and function. *J immunol,* 165, 1738-42.

HAYAKAWA, K., HARDY, R. R., PARKS, D. R. & HERZENBERG, L. A. 1983. The "Ly-1 B" cell subpopulation in normal immunodefective, and autoimmune mice. *J Exp Med,* 157, 202-18.

HAYDAY, A. C. & PENNINGTON, D. J. 2007. Key factors in the organized chaos of early T cell development. *Nat Immunol,* 8, 137-44.

HEIZMANN, B., KASTNER, P. & CHAN, S. 2013. Ikaros is absolutely required for pre-B cell differentiation by attenuating IL-7 signals. *J Exp Med,* 210, 2823-32.

HELTEMES-HARRIS, L. M. & FARRAR, M. A. 2012. The role of STAT5 in lymphocyte development and transformation. *Curr Opin Immunol,* 24, 146-52.

HENDRIKS, R. W. & MIDDENDORP, S. 2004. The pre-BCR checkpoint as a cell-autonomous proliferation switch. *Trends Immunol,* 25, 249-56.

HENG, T. S. & PAINTER, M. W. 2008. The Immunological Genome Project: networks of gene expression in immune cells. *Nat Immunol,* 9, 1091-4.

HENRIQUES, C. M., RINO, J., NIBBS, R. J., GRAHAM, G. J. & BARATA, J. T. 2010. IL-7 induces rapid clathrin-mediated internalization and JAK3-dependent degradation of IL-7Ralpha in T cells. *Blood,* 115, 3269-77.

HENSELEIT, U., PLASA, G. & HAEST, C. 1990. Effects of divalent cations on lipid flip-flop in the human erythrocyte membrane. *Biochim Biophys Acta,* 1029, 127-35.

HERZENBERG, L. A. 2000. B-1 cells: the lineage question revisited. *Immunol Rev,* 175, 9-22.

HERZOG, S., HUG, E., MEIXLSPERGER, S., PAIK, J. H., DEPINHO, R. A., RETH, M. & JUMAA, H. 2008. SLP-65 regulates immunoglobulin light chain gene recombination through the PI(3)K-PKB-Foxo pathway. *Nat Immunol,* 9, 623-31.

HERZOG, S., RETH, M. & JUMAA, H. 2009. Regulation of B-cell proliferation and differentiation by pre-B-cell receptor signalling. *Nat Rev Immunol,* 9, 195-205.

HESSLEIN, D. G., YANG, S. Y. & SCHATZ, D. G. 2006. Origins of peripheral B cells in IL-7 receptor-deficient mice. *Mol Immunol,* 43, 326-34.

HIBBS, M. L., TARLINTON, D. M., ARMES, J., GRAIL, D., HODGSON, G., MAGLITTO, R., STACKER, S. A. & DUNN, A. R. 1995. Multiple defects in the immune system of Lyn-deficient mice, culminating in autoimmune disease. *Cell,* 83, 301-11.

HITOTSUMACHI, S., CARPENTER, D. A. & RUSSELL, W. L. 1985. Dose-repetition increases the mutagenic effectiveness of N-ethyl-N-nitrosourea in mouse spermatogonia. *Proc Natl Acad Sci U S A,* 82, 6619-21.

HOCKENBERY, D., NUNEZ, G., MILLIMAN, C., SCHREIBER, R. D. & KORSMEYER, S. J. 1990. Bcl-2 is an inner mitochondrial membrane protein that blocks programmed cell death. *Nature,* 348, 334-6.

HOFMEISTER, R., KHALED, A. R., BENBERNOU, N., RAJNAVOLGYI, E., MUEGGE, K. & DURUM, S. K. 1999. Interleukin-7: physiological roles and mechanisms of action. *Cytokine Growth Factor Rev.*, 10, 41-60.

HORNE, M. C., ROTH, P. E. & DEFRANCO, A. L. 1996. Assembly of the truncated immunoglobulin heavy chain D mu into antigen receptor-like complexes in pre-B cells but not in B cells. *Immunity*, 4, 145-58.

HORVATH, P. & BARRANGOU, R. 2010. CRISPR/Cas, the immune system of bacteria and archaea. *Science*, 327, 167-70.

HOYNE, G. F. & GOODNOW, C. C. 2006. The use of genomewide ENU mutagenesis screens to unravel complex mammalian traits: identifying genes that regulate organ-specific and systemic autoimmunity. *Immunol Rev*, 210, 27-39.

HU, Y. L., METZ, D. P., CHUNG, J., SIU, G. & ZHANG, M. 2009. B7RP-1 blockade ameliorates autoimmunity through regulation of follicular helper T cells. *J Immunol*, 182, 1421-8.

HUA, Z., FATHEDDIN, P. & GRAHAM, T. R. 2002. An essential subfamily of Drs2p-related P-type ATPases is required for protein trafficking between Golgi complex and endosomal/vacuolar system. *Mol Biol Cell*, 13, 3162-77.

INLAY, M. A., BHATTACHARYA, D., SAHOO, D., SERWOLD, T., SEITA, J., KARSUNKY, H., PLEVRITIS, S. K., DILL, D. L. & WEISSMAN, I. L. 2009. Ly6d marks the earliest stage of B-cell specification and identifies the branchpoint between B-cell and T-cell development. *Genes Dev*, 23, 2376-81.

IWASAKI, H., SOMOZA, C., SHIGEMATSU, H., DUPREZ, E. A., IWASAKI-ARAI, J., MIZUNO, S., ARINOBU, Y., GEARY, K., ZHANG, P., DAYARAM, T., FENYUS, M. L., ELF, S., CHAN, S., KASTNER, P., HUETTNER, C. S., MURRAY, R., TENEN, D. G. & AKASHI, K. 2005. Distinctive and indispensable roles of PU.1 in maintenance of hematopoietic stem cells and their differentiation. *Blood*, 106, 1590-600.

JACOB, J., KELSOE, G., RAJEWSKY, K. & WEISS, U. 1991. Intraclonal generation of antibody mutants in germinal centres. *Nature*, 354, 389-92.

JAMSAI, D. & O'BRYAN, M. K. 2010. Genome-wide ENU mutagenesis for the discovery of novel male fertility regulators. *Syst Biol Reprod Med*, 56, 246-59.

JANEWAY, C. A. 2001. How the immune system works to protect the host from infection: a personal view. *Proc Natl Acad Sci. USA*, 98, 7461-7468.

JENSEN, C. T., KHARAZI, S., BOIERS, C., CHENG, M., LUBKING, A., SITNICKA, E. & JACOBSEN, S. E. 2008. FLT3 ligand and not TSLP is the key regulator of IL-7-independent B-1 and B-2 B lymphopoiesis. *Blood*, 112, 2297-304.

JIANG, Q., LI, W. Q., AIELLO, F. B., MAZZUCCHELLI, R., ASEFA, B., KHALED, A. R. & DURUM, S. K. 2005. Cell biology of IL-7, a key lymphotrophin. *Cytokine Growth Factor Rev.*, 16, 513-533.

JOHNSON, K., HASHIMSHONY, T., SAWAI, C. M., PONGUBALA, J. M., SKOK, J. A., AIFANTIS, I. & SINGH, H. 2008. Regulation of immunoglobulin light-chain recombination by the transcription factor IRF-4 and the attenuation of interleukin-7 signaling. *Immunity*, 28, 335-45.

JOHNSTON, R. J., POHOLEK, A. C., DITORO, D., YUSUF, I., ETO, D., BARNETT, B., DENT, A. L., CRAFT, J. & CROTTY, S. 2009. Bcl6 and Blimp-1 are reciprocal and antagonistic regulators of T follicular helper cell differentiation. *Science*, 325, 1006-10.

JOSHI, I., YOSHIDA, T., JENA, N., QI, X., ZHANG, J., VAN ETTEN, R. A. & GEORGOPOULOS, K. 2014. Loss of Ikaros DNA-binding function confers integrin-dependent survival on pre-B cells and progression to acute lymphoblastic leukemia. *Nat Immunol*, 15, 294-304.

JUN, J. E., WILSON, L. E., VINUESA, C. G., LESAGE, S., BLERY, M., MIOSGE, L. A., COOK, M. C., KUCHARSKA, E. M., HARA, H., PENNINGER, J. M., DOMASHENZ, H., HONG, N. A., GLYNNE, R. J., NELMS, K. A. & GOODNOW, C. C. 2003. Identifying the MAGUK protein Carma-1 as a central regulator of humoral immune responses and atopy by genome-wide mouse mutagenesis. *Immunity*, 18, 751-62.

KANTOR, A. B., STALL, A. M., ADAMS, S. & HERZENBERG, L. A. 1992. Differential development of progenitor activity for three B-cell lineages. *Proc Natl Acad Sci U S A*, 89, 3320-4.

KARASUYAMA, H., ROLINK, A. & MELCHERS, F. 1996. Surrogate light chain in B cell development. *Adv Immunol*, 63, 1-41.

KATOH, Y. & KATOH, M. 2004. Identification and characterization of CDC50A, CDC50B and CDC50C genes in silico. *Oncol Rep*, 12, 939-43.

KEAN, L. S., BROWN, L. E., NICHOLS, J. W., MOHANDAS, N., ARCHER, D. R. & HSU, L. L. 2002. Comparison of mechanisms of anemia in mice with sickle cell disease and beta-thalassemia: peripheral destruction, ineffective erythropoiesis, and phospholipid scramblase-mediated phosphatidylserine exposure. *Exp Hematol*, 30, 394-402.

KELLEY, C. M., IKEDA, T., KOIPALLY, J., AVITAHL, N., WU, L., GEORGOPOULOS, K. & MORGAN, B. A. 1998. Helios, a novel dimerization partner of Ikaros expressed in the earliest hematopoietic progenitors. *Curr Biol*, 8, 508-15.

KHAN, W. N., ALT, F. W., GERSTEIN, R. M., MALYNN, B. A., LARSSON, I., RATHBUN, G., DAVIDSON, L., MULLER, S., KANTOR, A. B., HERZENBERG, L. A. & ET AL. 1995. Defective B cell development and function in Btk-deficient mice. *Immunity*, 3, 283-99.

KIKUCHI, K., LAI, A. Y., HSU, C. L. & KONDO, M. 2005. IL-7 receptor signaling is necessary for stage transition in adult B cell development through up-regulation of EBF. *J Exp Med,* 201, 1197-203.

KINGSLEY, P. D., GREENFEST-ALLEN, E., FRAME, J. M., BUSHNELL, T. P., MALIK, J., MCGRATH, K. E., STOECKERT, C. J. & PALIS, J. 2013. Ontogeny of erythroid gene expression. *Blood,* 121, e5-e13.

KIRSTETTER, P., THOMAS, M., DIERICH, A., KASTNER, P. & CHAN, S. 2002. Ikaros is critical for B cell differentiation and function. *Eur J Immunol,* 32, 720-30.

KITAMURA, D., KUDO, A., SCHAAL, S., MULLER, W., MELCHERS, F. & RAJEWSKY, K. 1992. A critical role of lambda 5 protein in B cell development. *Cell,* 69, 823-31.

KITAMURA, D., ROES, J., KUHN, R. & RAJEWSKY, K. 1991. A B cell-deficient mouse by targeted disruption of the membrane exon of the immunoglobulin mu chain gene. *Nature,* 350, 423-6.

KLEIN, U. & DALLA-FAVERA, R. 2008. Germinal centres: role in B-cell physiology and malignancy. *Nat Rev Immunol,* 8, 22-33.

KLOMP, L. W., VARGAS, J. C., VAN MIL, S. W., PAWLIKOWSKA, L., STRAUTNIEKS, S. S., VAN EIJK, M. J., JUIJN, J. A., PABON-PENA, C., SMITH, L. B., DEYOUNG, J. A., BYRNE, J. A., GOMBERT, J., VAN DER BRUGGE, G., BERGER, R., JANKOWSKA, I., PAWLOWSKA, J., VILLA, E., KNISELY, A. S., THOMPSON, R. J., FREIMER, N. B., HOUWEN, R. H. & BULL, L. N. 2004. Characterization of mutations in ATP8B1 associated with hereditary cholestasis. *Hepatology,* 40, 27-38.

KLUG, C. A., MORRISON, S. J., MASEK, M., HAHM, K., SMALE, S. T. & WEISSMAN, I. L. 1998. Hematopoietic stem cells and lymphoid progenitors express different Ikaros isoforms, and Ikaros is localized to heterochromatin in immature lymphocytes. *Proc Natl Acad Sci U S A,* 95, 657-62.

KOOPMAN, G., REUTELINGSPERGER, C. P., KUIJTEN, G. A., KEEHNEN, R. M., PALS, S. T. & VAN OERS, M. H. 1994. Annexin V for flow cytometric detection of phosphatidylserine expression on B cells undergoing apoptosis. *Blood,* 84, 1415-20.

KOYAMA, M., ISHIHARA, K., KARASUYAMA, H., CORDELL, J. L., IWAMOTO, A. & NAKAMURA, T. 1997. CD79 alpha/CD79 beta heterodimers are expressed on pro-B cell surfaces without associated mu heavy chain. *Int Immunol,* 9, 1767-72.

KOZMIK, Z., WANG, S., DORFLER, P., ADAMS, B. & BUSSLINGER, M. 1992. The promoter of the CD19 gene is a target for the B-cell-specific transcription factor BSAP. *Mol Cell Biol,* 12, 2662-72.

KRAUS, M., ALIMZHANOV, M. B., RAJEWSKY, N. & RAJEWSKY, K. 2004. Survival of resting mature B lymphocytes depends on BCR signaling via the Igalpha/beta heterodimer. *Cell,* 117, 787-800.

KUDO, A. & MELCHERS, F. 1987. A second gene, VpreB in the lambda 5 locus of the mouse, which appears to be selectively expressed in pre-B lymphocytes. *EMBO J,* 6, 2267-72.

KUROSAKI, T., SHINOHARA, H. & BABA, Y. 2010. B cell signaling and fate decision. *Annu Rev Immunol,* 28, 21-55.

KUYPERS, F. A., YUAN, J., LEWIS, R. A., SNYDER, L. M., KIEFER, C. R., BUNYARATVEJ, A., FUCHAROEN, S., MA, L., STYLES, L., DE JONG, K. & SCHRIER, S. L. 1998. Membrane phospholipid asymmetry in human thalassemia. *Blood,* 91, 3044-51.

KWON, K., HUTTER, C., SUN, Q., BILIC, I., COBALEDA, C., MALIN, S. & BUSSLINGER, M. 2008. Instructive role of the transcription factor E2A in early B lymphopoiesis and germinal center B cell development. *Immunity,* 28, 751-62.

LEVANO, K., PUNIA, V., RAGHUNATH, M., DEBATA, P. R., CURCIO, G. M., MOGHA, A., PURKAYASTHA, S., MCCLOSKEY, D., FATA, J. & BANERJEE, P. 2012. Atp8a1 deficiency is associated with phosphatidylserine externalization in hippocampus and delayed hippocampus-dependent learning. *J Neurochem,* 120, 302-13.

LEVENTIS, P. A. & GRINSTEIN, S. 2010. The distribution and function of phosphatidylserine in cellular membranes. *Annu Rev Biophys,* 39, 407-27.

LI, Y. S., HAYAKAWA, K. & HARDY, R. R. 1993. The regulated expression of B lineage associated genes during B cell differentiation in bone marrow and fetal liver. *J Exp Med,* 178, 951-60.

LI, Y. S., WASSERMAN, R., HAYAKAWA, K. & HARDY, R. R. 1996. Identification of the earliest B lineage stage in mouse bone marrow. *Immunity,* 5, 527-35.

LIN, H. & GROSSCHEDL, R. 1995. Failure of B-cell differentiation in mice lacking the transcription factor EBF. *Nature,* 376, 263-7.

LINGWOOD, D. & SIMONS, K. 2010. Lipid rafts as a membrane-organizing principle. *Science,* 327, 46-50.

LINTERMAN, M. A., RIGBY, R. J., WONG, R. K., YU, D., BRINK, R., CANNONS, J. L., SCHWARTZBERG, P. L., COOK, M. C., WALTERS, G. D. & VINUESA, C. G. 2009. Follicular helper T cells are required for systemic autoimmunity. *J Exp Med,* 206, 561-76.

LIU, X., DOBBIE, M., TUNNINGLEY, R., WHITTLE, B., ZHANG, Y., ITTNER, L. M. & GOTZ, J. 2011. ENU mutagenesis screen to establish motor

phenotypes in wild-type mice and modifiers of a pre-existing motor phenotype in tau mutant mice. *J Biomed Biotechnol,* 2011, 130947.

LIU, Y. J., MALISAN, F., DE BOUTEILLER, O., GURET, C., LEBECQUE, S., BANCHEREAU, J., MILLS, F. C., MAX, E. E. & MARTINEZ-VALDEZ, H. 1996. Within germinal centers, isotype switching of immunoglobulin genes occurs after the onset of somatic mutation. *Immunity,* 4, 241-50.

LIUBCHENKO, G. A., APPLEBERRY, H. C., HOLERS, V. M., BANDA, N. K., WILLIS, V. C. & LYUBCHENKO, T. 2012. Potentially autoreactive naturally occurring transitional T3 B lymphocytes exhibit a unique signaling profile. *J Autoimmun,* 38, 293-303.

LODER, F., MUTSCHLER, B., RAY, R. J., PAIGE, C. J., SIDERAS, P., TORRES, R., LAMERS, M. C. & CARSETTI, R. 1999. B cell development in the spleen takes place in discrete steps and is determined by the quality of B cell receptor-derived signals. *J Exp Med,* 190, 75-89.

LOPEZ-MARQUES, R. L., POULSEN, L. R., HANISCH, S., MEFFERT, K., BUCH-PEDERSEN, M. J., JAKOBSEN, M. K., POMORSKI, T. G. & PALMGREN, M. G. 2010. Intracellular targeting signals and lipid specificity determinants of the ALA/ALIS P4-ATPase complex reside in the catalytic ALA alpha-subunit. *Mol Biol Cell,* 21, 791-801.

LOPEZ-MARQUES, R. L., THEORIN, L., PALMGREN, M. G. & POMORSKI, T. G. 2013. P4-ATPases: lipid flippases in cell membranes. *Pflugers Arch.*

LU, R., MEDINA, K. L., LANCKI, D. W. & SINGH, H. 2003. IRF-4,8 orchestrate the pre-B-to-B transition in lymphocyte development. *Genes Dev,* 17, 1703-8.

LUKIN, K., FIELDS, S., GUERRETTAZ, L., STRAIGN, D., RODRIGUEZ, V., ZANDI, S., MANSSON, R., CAMBIER, J. C., SIGVARDSSON, M. & HAGMAN, J. 2011. A dose-dependent role for EBF1 in repressing non-B-cell-specific genes. *Eur J Immunol,* 41, 1787-93.

LUND, F. E. 2008. Cytokine-producing B lymphocytes-key regulators of immunity. *Curr Opin Immunol,* 20, 332-8.

MA, S., PATHAK, S., TRINH, L. & LU, R. 2008. Interferon regulatory factors 4 and 8 induce the expression of Ikaros and Aiolos to down-regulate pre-B-cell receptor and promote cell-cycle withdrawal in pre-B-cell development. *Blood,* 111, 1396-403.

MA, S., TURETSKY, A., TRINH, L. & LU, R. 2006. IFN regulatory factor 4 and 8 promote Ig light chain kappa locus activation in pre-B cell development. *J Immunol,* 177, 7898-904.

MACKAY, F., FIGGETT, W. A., SAULEP, D., LEPAGE, M. & HIBBS, M. L. 2010. B-cell stage and context-dependent requirements for survival signals from BAFF and the B-cell receptor. *Immunol Rev,* 237, 205-25.

MACKAY, F., WOODCOCK, S. A., LAWTON, P., AMBROSE, C., BAETSCHER, M., SCHNEIDER, P., TSCHOPP, J. & BROWNING, J. L. 1999. Mice transgenic for BAFF develop lymphocytic disorders along with autoimmune manifestations. *J Exp Med,* 190, 1697-710.

MALI, P., YANG, L., ESVELT, K. M., AACH, J., GUELL, M., DICARLO, J. E., NORVILLE, J. E. & CHURCH, G. M. 2013. RNA-guided human genome engineering via Cas9. *Science,* 339, 823-6.

MALIN, S., MCMANUS, S. & BUSSLINGER, M. 2010a. STAT5 in B cell development and leukemia. *Curr Opin Immunol,* 22, 168-76.

MALIN, S., MCMANUS, S., COBALEDA, C., NOVATCHKOVA, M., DELOGU, A., BOUILLET, P., STRASSER, A. & BUSSLINGER, M. 2010b. Role of STAT5 in controlling cell survival and immunoglobulin gene recombination during pro-B cell development. *Nat Immunol,* 11, 171-9.

MALYNN, B. A., SHAW, A. C., YOUNG, F., STEWART, V. & ALT, F. W. 2002. Truncated immunoglobulin Dmu causes incomplete developmental progression of RAG-deficient pro-B cells. *Mol Immunol,* 38, 547-56.

MANDAL, M., POWERS, S. E., OCHIAI, K., GEORGOPOULOS, K., KEE, B. L., SINGH, H. & CLARK, M. R. 2009. Ras orchestrates exit from the cell cycle and light-chain recombination during early B cell development. *Nat Immunol,* 10, 1110-7.

MANDEL, E. M. & GROSSCHEDL, R. 2010. Transcription control of early B cell differentiation. *Curr Opin Immunol,* 22, 161-7.

MANNO, S., TAKAKUWA, Y. & MOHANDAS, N. 2002. Identification of a functional role for lipid asymmetry in biological membranes: Phosphatidylserine-skeletal protein interactions modulate membrane stability. *Proc Natl Acad Sci U S A,* 99, 1943-8.

MANSSON, R., WELINDER, E., AHSBERG, J., LIN, Y. C., BENNER, C., GLASS, C. K., LUCAS, J. S., SIGVARDSSON, M. & MURRE, C. 2012. Positive intergenic feedback circuitry, involving EBF1 and FOXO1, orchestrates B-cell fate. *Proc Natl Acad Sci U S A,* 109, 21028-33.

MARDIS, E. R. 2011. A decade's perspective on DNA sequencing technology. *Nature,* 470, 198-203.

MARSHALL, A. J., FLEMING, H. E., WU, G. E. & PAIGE, C. J. 1998. Modulation of the IL-7 dose-response threshold during pro-B cell differentiation is dependent on pre-B cell receptor expression. *J Immunol,* 161, 6038-45.

MARTIN, F., OLIVER, A. M. & KEARNEY, J. F. 2001. Marginal zone and B1 B cells unite in the early response against T-independent blood-borne particulate antigens. *Immunity,* 14, 617-29.

MATSUMOTO, M., LO, S. F., CARRUTHERS, C. J., MIN, J., MARIATHASAN, S., HUANG, G., PLAS, D. R., MARTIN, S. M., GEHA, R. S., NAHM, M. H.

& CHAPLIN, D. D. 1996. Affinity maturation without germinal centres in lymphotoxin-alpha-deficient mice. *Nature,* 382, 462-6.

MCEVOY, L., WILLIAMSON, P. & SCHLEGEL, R. A. 1986. Membrane phospholipid asymmetry as a determinant of erythrocyte recognition by macrophages. *Proc Natl Acad Sci U S A,* 83, 3311-5.

MCKERCHER, S. R., TORBETT, B. E., ANDERSON, K. L., HENKEL, G. W., VESTAL, D. J., BARIBAULT, H., KLEMSZ, M., FEENEY, A. J., WU, G. E., PAIGE, C. J. & MAKI, R. A. 1996. Targeted disruption of the PU.1 gene results in multiple hematopoietic abnormalities. *EMBO J,* 15, 5647-58.

MEDINA, K. L., PONGUBALA, J. M., REDDY, K. L., LANCKI, D. W., DEKOTER, R., KIESLINGER, M., GROSSCHEDL, R. & SINGH, H. 2004. Assembling a gene regulatory network for specification of the B cell fate. *Dev Cell,* 7, 607-17.

MEFFRE, E., CASELLAS, R. & NUSSENZWEIG, M. C. 2000. Antibody regulation of B cell development. *Nat Immunol,* 1, 379-85.

MERRELL, K. T., BENSCHOP, R. J., GAULD, S. B., AVISZUS, K., DECOTE-RICARDO, D., WYSOCKI, L. J. & CAMBIER, J. C. 2006. Identification of anergic B cells within a wild-type repertoire. *Immunity,* 25, 953-62.

MERTSCHING, E., GRAWUNDER, U., MEYER, V., ROLINK, T. & CEREDIG, R. 1996. Phenotypic and functional analysis of B lymphopoiesis in interleukin-7-transgenic mice: expansion of pro/pre-B cell number and persistence of B lymphocyte development in lymph nodes and spleen. *Eur J Immunol,* 26, 28-33.

MIDDENDORP, S., DINGJAN, G. M. & HENDRIKS, R. W. 2002. Impaired precursor B cell differentiation in Bruton's tyrosine kinase-deficient mice. *J Immunol,* 168, 2695-703.

MIKKOLA, I., HEAVEY, B., HORCHER, M. & BUSSLINGER, M. 2002. Reversion of B cell commitment upon loss of Pax5 expression. *Science,* 297, 110-3.

MILLER, J. P., IZON, D., DEMUTH, W., GERSTEIN, R., BHANDOOLA, A. & ALLMAN, D. 2002. The earliest step in B lineage differentiation from common lymphoid progenitors is critically dependent upon interleukin 7. *J Exp Med,* 196, 705-11.

MINEGISHI, Y., COUSTAN-SMITH, E., WANG, Y. H., COOPER, M. D., CAMPANA, D. & CONLEY, M. E. 1998. Mutations in the human lambda5/14.1 gene result in B cell deficiency and agammaglobulinemia. *J Exp Med,* 187, 71-7.

MIYANISHI, M., TADA, K., KOIKE, M., UCHIYAMA, Y., KITAMURA, T. & NAGATA, S. 2007. Identification of Tim4 as a phosphatidylserine receptor. *Nature,* 450, 435-9.

MOHANDAS, N. & GALLAGHER, P. G. 2008. Red cell membrane: past, present, and future. *Blood,* 112, 3939-48.

MOMBAERTS, P., IACOMINI, J., JOHNSON, R. S., HERRUP, K., TONEGAWA, S. & PAPAIOANNOU, V. E. 1992. RAG-1-deficient mice have no mature B and T lymphocytes. *Cell,* 68, 869-77.

MONTECINO-RODRIGUEZ, E., LEATHERS, H. & DORSHKIND, K. 2006. Identification of a B-1 B cell-specified progenitor. *Nat Immunol,* 7, 293-301.

MORESCO, E. M., LI, X. & BEUTLER, B. 2013. Going forward with genetics: recent technological advances and forward genetics in mice. *Am J Pathol,* 182, 1462-73.

MORGAN, B., SUN, L., AVITAHL, N., ANDRIKOPOULOS, K., IKEDA, T., GONZALES, E., WU, P., NEBEN, S. & GEORGOPOULOS, K. 1997. Aiolos, a lymphoid restricted transcription factor that interacts with Ikaros to regulate lymphocyte differentiation. *EMBO J,* 16, 2004-13.

MORITA, S. Y., KOBAYASHI, A., TAKANEZAWA, Y., KIOKA, N., HANDA, T., ARAI, H., MATSUO, M. & UEDA, K. 2007. Bile salt-dependent efflux of cellular phospholipids mediated by ATP binding cassette protein B4. *Hepatology,* 46, 188-99.

MORIYAMA, Y. & NELSON, N. 1988. Purification and properties of a vanadate- and N-ethylmaleimide-sensitive ATPase from chromaffin granule membranes. *J Biol Chem,* 263, 8521-7.

MORROT, G., ZACHOWSKI, A. & DEVAUX, P. F. 1990. Partial purification and characterization of the human erythrocyte Mg2(+)-ATPase. A candidate aminophospholipid translocase. *FEBS Lett,* 266, 29-32.

MULJO, S. A. & SCHLISSEL, M. S. 2003. A small molecule Abl kinase inhibitor induces differentiation of Abelson virus-transformed pre-B cell lines. *Nat Immunol,* 4, 31-7.

MUNDT, C., LICENCE, S., SHIMIZU, T., MELCHERS, F. & MARTENSSON, I. L. 2001. Loss of precursor B cell expansion but not allelic exclusion in VpreB1/VpreB2 double-deficient mice. *J Exp Med,* 193, 435-45.

MURALI-KRISHNA, K., ALTMAN, J. D., SURESH, M., SOURDIVE, D. J. D., ZAJAC, A. J., MILLER, J. D., SLANSKY, J. & AHMED, R. 1998. Counting antigen-specific CD8 T cells: a reevaluation of bystander activation during viral infection. *Immunity,* 8, 177-187.

MURPHY, K. M. 2012. *Janeway's immunobiology,* New York, NY, Garland Science, Taylor & Francis Group.

MUTHUSAMY, B.-P., NATARAJAN, P., ZHOU, X. & GRAHAM, T. R. 2009. Linking phospholipid flippases to vesicle-mediated protein transport. *Biochim Biophys Acta,* 1791, 612-9.

MYERS, C. D. 1991. Role of B cell antigen processing and presentation in the humoral immune response. *FASEB J,* 5, 2547-53.

NAGAO, K., KIMURA, Y., MASTUO, M. & UEDA, K. 2010. Lipid outward translocation by ABC proteins. *FEBS Lett,* 584, 2717-23.

NAGATA, K., NAKAMURA, T., KITAMURA, F., KURAMOCHI, S., TAKI, S., CAMPBELL, K. S. & KARASUYAMA, H. 1997. The Ig alpha/Igbeta heterodimer on mu-negative proB cells is competent for transducing signals to induce early B cell differentiation. *Immunity,* 7, 559-70.

NECHANITZKY, R., AKBAS, D., SCHERER, S., GYORY, I., HOYLER, T., RAMAMOORTHY, S., DIEFENBACH, A. & GROSSCHEDL, R. 2013. Transcription factor EBF1 is essential for the maintenance of B cell identity and prevention of alternative fates in committed cells. *Nat Immunol,* 14, 867-75.

NELMS, K. A. & GOODNOW, C. C. 2001. Genome-wide ENU mutagenesis to reveal immune regulators. *Immunity,* 15, 409-18.

NEMAZEE, D. A. & BURKI, K. 1989. Clonal deletion of B lymphocytes in a transgenic mouse bearing anti-MHC class I antibody genes. *Nature,* 337, 562-6.

NG, L. G., SUTHERLAND, A. P., NEWTON, R., QIAN, F., CACHERO, T. G., SCOTT, M. L., THOMPSON, J. S., WHEWAY, J., CHTANOVA, T., GROOM, J., SUTTON, I. J., XIN, C., TANGYE, S. G., KALLED, S. L., MACKAY, F. & MACKAY, C. R. 2004. B cell-activating factor belonging to the TNF family (BAFF)-R is the principal BAFF receptor facilitating BAFF costimulation of circulating T and B cells. *J Immunol,* 173, 807-17.

NICHOGIANNOPOULOU, A., TREVISAN, M., NEBEN, S., FRIEDRICH, C. & GEORGOPOULOS, K. 1999. Defects in hemopoietic stem cell activity in Ikaros mutant mice. *J Exp Med,* 190, 1201-14.

NISHIMOTO, N., KUBAGAWA, H., OHNO, T., GARTLAND, G. L., STANKOVIC, A. K. & COOPER, M. D. 1991. Normal pre-B cells express a receptor complex of mu heavy chains and surrogate light-chain proteins. *Proc Natl Acad Sci U S A,* 88, 6284-8.

NISHIZUMI, H., TANIUCHI, I., YAMANASHI, Y., KITAMURA, D., ILIC, D., MORI, S., WATANABE, T. & YAMAMOTO, T. 1995. Impaired proliferation of peripheral B cells and indication of autoimmune disease in lyn-deficient mice. *Immunity,* 3, 549-60.

NOSAKA, T., VAN DEURSEN, J. M., TRIPP, R. A., THIERFELDER, W. E., WITTHUHN, B. A., MCMICKLE, A. P., DOHERTY, P. C., GROSVELD, G. C. & IHLE, J. N. 1995. Defective lymphoid development in mice lacking Jak3. *Science,* 270, 800-2.

NURIEVA, R. I., CHUNG, Y., MARTINEZ, G. J., YANG, X. O., TANAKA, S., MATSKEVITCH, T. D., WANG, Y. H. & DONG, C. 2009. Bcl6 mediates the development of T follicular helper cells. *Science,* 325, 1001-5.

NUTT, S. L., HEAVEY, B., ROLINK, A. G. & BUSSLINGER, M. 1999. Commitment to the B-lymphoid lineage depends on the transcription factor Pax5. *Nature,* 401, 556-62.

NUTT, S. L. & KEE, B. L. 2007. The transcriptional regulation of B cell lineage commitment. *Immunity,* 26, 715-25.

NUTT, S. L., METCALF, D., D'AMICO, A., POLLI, M. & WU, L. 2005. Dynamic regulation of PU.1 expression in multipotent hematopoietic progenitors. *J Exp Med,* 201, 221-31.

NUTT, S. L., THEVENIN, C. & BUSSLINGER, M. 1997a. Essential functions of Pax-5 (BSAP) in pro-B cell development. *Immunobiology,* 198, 227-35.

NUTT, S. L., URBANEK, P., ROLINK, A. & BUSSLINGER, M. 1997b. Essential functions of Pax5 (BSAP) in pro-B cell development: difference between fetal and adult B lymphopoiesis and reduced V-to-DJ recombination at the IgH locus. *Genes Dev,* 11, 476-91.

O'RIORDAN, M. & GROSSCHEDL, R. 1999. Coordinate regulation of B cell differentiation by the transcription factors EBF and E2A. *Immunity,* 11, 21-31.

OCHIAI, K., MAIENSCHEIN-CLINE, M., MANDAL, M., TRIGGS, J. R., BERTOLINO, E., SCIAMMAS, R., DINNER, A. R., CLARK, M. R. & SINGH, H. 2012. A self-reinforcing regulatory network triggered by limiting IL-7 activates pre-BCR signaling and differentiation. *Nat Immunol.*

OGILVY, S., METCALF, D., PRINT, C. G., BATH, M. L., HARRIS, A. W. & ADAMS, J. M. 1999. Constitutive Bcl-2 expression throughout the hematopoietic compartment affects multiple lineages and enhances progenitor cell survival. *Proc Natl Acad Sci USA,* 96, 14943-8.

OHNISHI, K. & MELCHERS, F. 2003. The nonimmunoglobulin portion of lambda5 mediates cell-autonomous pre-B cell receptor signaling. *Nat Immunol,* 4, 849-56.

OLIVER, A. M., MARTIN, F. & KEARNEY, J. F. 1999. IgMhighCD21high lymphocytes enriched in the splenic marginal zone generate effector cells more rapidly than the bulk of follicular B cells. *J Immunol,* 162, 7198-207.

OLIVER, P. L. & DAVIES, K. E. 2012. New insights into behaviour using mouse ENU mutagenesis. *Hum Mol Genet,* 21, R72-81.

ONAT, O. E., GULSUNER, S., BILGUVAR, K., NAZLI BASAK, A., TOPALOGLU, H., TAN, M., TAN, U., GUNEL, M. & OZCELIK, T. 2013. Missense mutation in the ATPase, aminophospholipid transporter protein ATP8A2 is associated with cerebellar atrophy and quadrupedal locomotion. *Eur J Hum Genet,* 21, 281-5.

OPFERMAN, J. T., LETAI, A., BEARD, C., SORCINELLI, M. D., ONG, C. C. & KORSMEYER, S. J. 2003. Development and maintenance of B and T lymphocytes requires antiapoptotic MCL-1. *Nature,* 426, 671-6.

OSMOND, D. G., ROLINK, A. & MELCHERS, F. 1998. Murine B lymphopoiesis: towards a unified model. *Immunol Today,* 19, 65-8.

PANCER, Z. & COOPER, M. D. 2006. The evolution of adaptive immunity. *Annu Rev Immunol,* 24, 497-518.

PAPATHANASIOU, P., ATTEMA, J. L., KARSUNKY, H., HOSEN, N., SONTANI, Y., HOYNE, G. F., TUNNINGLEY, R., SMALE, S. T. & WEISSMAN, I. L. 2009. Self-renewal of the long-term reconstituting subset of hematopoietic stem cells is regulated by Ikaros. *Stem Cells,* 27, 3082-92.

PAPATHANASIOU, P., PERKINS, A. C., COBB, B. S., FERRINI, R., SRIDHARAN, R., HOYNE, G. F., NELMS, K. A., SMALE, S. T. & GOODNOW, C. C. 2003. Widespread failure of hematolymphoid differentiation caused by a recessive niche-filling allele of the Ikaros transcription factor. *Immunity,* 19, 131-44.

PAPPU, R., CHENG, A. M., LI, B., GONG, Q., CHIU, C., GRIFFIN, N., WHITE, M., SLECKMAN, B. P. & CHAN, A. C. 1999. Requirement for B cell linker protein (BLNK) in B cell development. *Science,* 286, 1949-54.

PARK, J.-H., YU, Q., ERMAN, B., APPELBAUM, J. S., MONTOYA-DURANGO, D., GRIMES, H. L. & SINGER, A. 2004. Suppression of IL7Ralpha transcription by IL-7 and other prosurvival cytokines: a novel mechanism for maximizing IL-7-dependent T cell survival. *Immunity,* 21, 289-302.

PARK, S. Y., SAIJO, K., TAKAHASHI, T., OSAWA, M., ARASE, H., HIRAYAMA, N., MIYAKE, K., NAKAUCHI, H., SHIRASAWA, T. & SAITO, T. 1995. Developmental defects of lymphoid cells in Jak3 kinase-deficient mice. *Immunity,* 3, 771-82.

PARKER, M. J., LICENCE, S., ERLANDSSON, L., GALLER, G. R., CHAKALOVA, L., OSBORNE, C. S., MORGAN, G., FRASER, P., JUMAA, H., WINKLER, T. H., SKOK, J. & MARTENSSON, I. L. 2005. The pre-B-cell receptor induces silencing of VpreB and lambda5 transcription. *EMBO J,* 24, 3895-905.

PATHAK, S., MA, S., TRINH, L. & LU, R. 2008. A role for interferon regulatory factor 4 in receptor editing. *Mol Cell Biol,* 28, 2815-24.

PAULUSMA, C. C. & ELFERINK, R. P. J. O. 2010. P4 ATPases--the physiological relevance of lipid flipping transporters. *FEBS Lett,* 584, 2708-16.

PAULUSMA, C. C., GROEN, A., KUNNE, C., HO-MOK, K. S., SPIJKERBOER, A. L., RUDI DE WAART, D., HOEK, F. J., VREELING, H., HOEBEN, K. A., VAN MARLE, J., PAWLIKOWSKA, L., BULL, L. N., HOFMANN, A. F., KNISELY, A. S. & OUDE ELFERINK, R. P. 2006. Atp8b1 deficiency in

mice reduces resistance of the canalicular membrane to hydrophobic bile salts and impairs bile salt transport. *Hepatology,* 44, 195-204.

PAUS, D., PHAN, T. G., CHAN, T. D., GARDAM, S., BASTEN, A. & BRINK, R. 2006. Antigen recognition strength regulates the choice between extrafollicular plasma cell and germinal center B cell differentiation. *J Exp Med,* 203, 1081-91.

PELANDA, R., BRAUN, U., HOBEIKA, E., NUSSENZWEIG, M. C. & RETH, M. 2002. B cell progenitors are arrested in maturation but have intact VDJ recombination in the absence of Ig-alpha and Ig-beta. *J Immunol,* 169, 865-72.

PELANDA, R., SCHAAL, S., TORRES, R. M. & RAJEWSKY, K. 1996. A prematurely expressed Ig(kappa) transgene, but not V(kappa)J(kappa) gene segment targeted into the Ig(kappa) locus, can rescue B cell development in lambda5-deficient mice. *Immunity,* 5, 229-39.

PELAYO, R., HIROSE, J., HUANG, J., GARRETT, K. P., DELOGU, A., BUSSLINGER, M. & KINCADE, P. W. 2005. Derivation of 2 categories of plasmacytoid dendritic cells in murine bone marrow. *Blood,* 105, 4407-15.

PESCHON, J. J., MORRISSEY, P. J., GRABSTEIN, K. H., RAMSDELL, F. J., MARASKOVSKY, E., GLINIAK, B. C., PARK, L. S., ZIEGLER, S. F., WILLIAMS, D. E., WARE, C. B., MEYER, J. D. & DAVISON, B. L. 1994. Early lymphocyte expansion is severely impaired in interleukin 7 receptor-deficient mice. *J Exp Med,* 180, 1955-60.

PETRO, J. B., GERSTEIN, R. M., LOWE, J., CARTER, R. S., SHINNERS, N. & KHAN, W. N. 2002. Transitional type 1 and 2 B lymphocyte subsets are differentially responsive to antigen receptor signaling. *J Biol Chem,* 277, 48009-19.

PHAN, T. G., AMESBURY, M., GARDAM, S., CROSBIE, J., HASBOLD, J., HODGKIN, P. D., BASTEN, A. & BRINK, R. 2003. B cell receptor-independent stimuli trigger immunoglobulin (Ig) class switch recombination and production of IgG autoantibodies by anergic self-reactive B cells. *J Exp Med,* 197, 845-60.

PHAN, T. G., GARDAM, S., BASTEN, A. & BRINK, R. 2005. Altered migration, recruitment, and somatic hypermutation in the early response of marginal zone B cells to T cell-dependent antigen. *J Immunol,* 174, 4567-78.

PHAN, T. G., PAUS, D., CHAN, T. D., TURNER, M. L., NUTT, S. L., BASTEN, A. & BRINK, R. 2006. High affinity germinal center B cells are actively selected into the plasma cell compartment. *J Exp Med,* 203, 2419-24.

PILLAI, S. & CARIAPPA, A. 2009. The follicular versus marginal zone B lymphocyte cell fate decision. *Nat Rev Immunol,* 9, 767-77.

PISTOIA, V. 1997. Production of cytokines by human B cells in health and disease. *Immunol Today,* 18, 343-50.

POLLI, M., DAKIC, A., LIGHT, A., WU, L., TARLINTON, D. M. & NUTT, S. L. 2005. The development of functional B lymphocytes in conditional PU.1 knock-out mice. *Blood,* 106, 2083-90.

POMORSKI, T., LOMBARDI, R., RIEZMAN, H., DEVAUX, P. F., VAN MEER, G. & HOLTHUIS, J. C. 2003. Drs2p-related P-type ATPases Dnf1p and Dnf2p are required for phospholipid translocation across the yeast plasma membrane and serve a role in endocytosis. *Mol Biol Cell,* 14, 1240-54.

POMORSKI, T. & MENON, A. K. 2006. Lipid flippases and their biological functions. *Cell Mol Life Sci,* 63, 2908-21.

PONGUBALA, J. M., NORTHRUP, D. L., LANCKI, D. W., MEDINA, K. L., TREIBER, T., BERTOLINO, E., THOMAS, M., GROSSCHEDL, R., ALLMAN, D. & SINGH, H. 2008. Transcription factor EBF restricts alternative lineage options and promotes B cell fate commitment independently of Pax5. *Nat Immunol,* 9, 203-15.

POULSEN, L. R., LOPEZ-MARQUES, R. L., MCDOWELL, S. C., OKKERI, J., LICHT, D., SCHULZ, A., POMORSKI, T., HARPER, J. F. & PALMGREN, M. G. 2008. The Arabidopsis P4-ATPase ALA3 localizes to the golgi and requires a beta-subunit to function in lipid translocation and secretory vesicle formation. *Plant Cell,* 20, 658-76.

POWERS, S. E., MANDAL, M., MATSUDA, S., MILETIC, A. V., CATO, M. H., TANAKA, A., RICKERT, R. C., KOYASU, S. & CLARK, M. R. 2012. Subnuclear cyclin D3 compartments and the coordinated regulation of proliferation and immunoglobulin variable gene repression. *J Exp Med,* 209, 2199-213.

PUEL, A., ZIEGLER, S. F., BUCKLEY, R. H. & LEONARD, W. J. 1998. Defective IL7R expression in T(-)B(+)NK(+) severe combined immunodeficiency. *Nat Genet,* 20, 394-7.

QUAH, B. J. & PARISH, C. R. 2012. New and improved methods for measuring lymphocyte proliferation in vitro and in vivo using CFSE-like fluorescent dyes. *J Immunol Methods,* 379, 1-14.

RADIC, M. Z., ERIKSON, J., LITWIN, S. & WEIGERT, M. 1993. B lymphocytes may escape tolerance by revising their antigen receptors. *J Exp Med,* 177, 1165-73.

RAGGERS, R. J., VOGELS, I. & VAN MEER, G. 2001. Multidrug-resistance P-glycoprotein (MDR1) secretes platelet-activating factor. *Biochem J,* 357, 859-65.

RAMADANI, F., BOLLAND, D. J., GARCON, F., EMERY, J. L., VANHAESEBROECK, B., CORCORAN, A. E. & OKKENHAUG, K. 2010. The PI3K isoforms p110alpha and p110delta are essential for pre-B cell receptor signaling and B cell development. *Sci Signal,* 3, ra60.

RAMIREZ, J., LUKIN, K. & HAGMAN, J. 2010. From hematopoietic progenitors to B cells: mechanisms of lineage restriction and commitment. *Curr Opin Immunol,* 22, 177-84.

RANDALL, K. L., LAMBE, T., JOHNSON, A. L., TREANOR, B., KUCHARSKA, E., DOMASCHENZ, H., WHITTLE, B., TZE, L. E., ENDERS, A., CROCKFORD, T. L., BOURIEZ-JONES, T., ALSTON, D., CYSTER, J. G., LENARDO, M. J., MACKAY, F., DEENICK, E. K., TANGYE, S. G., CHAN, T. D., CAMIDGE, T., BRINK, R., VINUESA, C. G., BATISTA, F. D., CORNALL, R. J. & GOODNOW, C. C. 2009. Dock8 mutations cripple B cell immunological synapses, germinal centers and long-lived antibody production. *Nat Immunol,* 10, 1283-91.

REBUFFE-SCRIVE, M., SURWIT, R., FEINGLOS, M., KUHN, C. & RODIN, J. 1993. Regional fat distribution and metabolism in a new mouse model (C57BL/6J) of non-insulin-dependent diabetes mellitus. *Metabolism,* 42, 1405-9.

REES, D. C., IOLASCON, A., CARELLA, M., O'MARCAIGH A, S., KENDRA, J. R., JOWITT, S. N., WALES, J. K., VORA, A., MAKRIS, M., MANNING, N., NICOLAOU, A., FISHER, J., MANN, A., MACHIN, S. J., CLAYTON, P. T., GASPARINI, P. & STEWART, G. W. 2005. Stomatocytic haemolysis and macrothrombocytopenia (Mediterranean stomatocytosis/macrothrombocytopenia) is the haematological presentation of phytosterolaemia. *Br J Haematol,* 130, 297-309.

RETH, M. & NIELSEN, P. 2014. Signaling circuits in early B-cell development. *Adv Immunol,* 122, 129-75.

RETH, M. G. & ALT, F. W. 1984. Novel immunoglobulin heavy chains are produced from DJH gene segment rearrangements in lymphoid cells. *Nature,* 312, 418-23.

REYNAUD, D., DEMARCO, I. A., REDDY, K. L., SCHJERVEN, H., BERTOLINO, E., CHEN, Z., SMALE, S. T., WINANDY, S. & SINGH, H. 2008. Regulation of B cell fate commitment and immunoglobulin heavy-chain gene rearrangements by Ikaros. *Nat Immunol,* 9, 927-36.

RODRIGUEZ-PINTO, D. 2005. B cells as antigen presenting cells. *Cell Immunol,* 238, 67-75.

ROESSLER, S., GYORY, I., IMHOF, S., SPIVAKOV, M., WILLIAMS, R. R., BUSSLINGER, M., FISHER, A. G. & GROSSCHEDL, R. 2007. Distinct promoters mediate the regulation of Ebf1 gene expression by interleukin-7 and Pax5. *Mol Cell Biol,* 27, 579-94.

ROLINK, A., TEN BOEKEL, E., MELCHERS, F., FEARON, D. T., KROP, I. & ANDERSSON, J. 1996. A subpopulation of B220+ cells in murine bone marrow does not express CD19 and contains natural killer cell progenitors. *J Exp Med,* 183, 187-94.

ROLINK, A. G., ANDERSSON, J. & MELCHERS, F. 1998. Characterization of immature B cells by a novel monoclonal antibody, by turnover and by mitogen reactivity. *Eur J Immunol,* 28, 3738-48.

ROLINK, A. G., WINKLER, T., MELCHERS, F. & ANDERSSON, J. 2000. Precursor B cell receptor-dependent B cell proliferation and differentiation does not require the bone marrow or fetal liver environment. *J Exp Med,* 191, 23-32.

ROSE, T., PILLET, A.-H., LAVERGNE, V., TAMARIT, B., LENORMAND, P., ROUSSELLE, J.-C., NAMANE, A. & THÈZE, J. 2010. Interleukin-7 compartmentalizes its receptor signaling complex to initiate CD4 T lymphocyte response. *J Biol Chem,* 285, 14898-908.

ROSING, J., BEVERS, E. M., COMFURIUS, P., HEMKER, H. C., VAN DIEIJEN, G., WEISS, H. J. & ZWAAL, R. F. 1985. Impaired factor X and prothrombin activation associated with decreased phospholipid exposure in platelets from a patient with a bleeding disorder. *Blood,* 65, 1557-61.

RUAUD, A. F., NILSSON, L., RICHARD, F., LARSEN, M. K., BESSEREAU, J. L. & TUCK, S. 2009. The C. elegans P4-ATPase TAT-1 regulates lysosome biogenesis and endocytosis. *Traffic,* 10, 88-100.

RUMFELT, L. L., ZHOU, Y., ROWLEY, B. M., SHINTON, S. A. & HARDY, R. R. 2006. Lineage specification and plasticity in CD19- early B cell precursors. *J Exp Med,* 203, 675-87.

RUSSELL, W. L., KELLY, E. M., HUNSICKER, P. R., BANGHAM, J. W., MADDUX, S. C. & PHIPPS, E. L. 1979. Specific-locus test shows ethylnitrosourea to be the most potent mutagen in the mouse. *Proc Natl Acad Sci U S A,* 76, 5818-9.

SAIJO, K., SCHMEDT, C., SU, I. H., KARASUYAMA, H., LOWELL, C. A., RETH, M., ADACHI, T., PATKE, A., SANTANA, A. & TARAKHOVSKY, A. 2003. Essential role of Src-family protein tyrosine kinases in NF-kappaB activation during B cell development. *Nat Immunol,* 4, 274-9.

SAITO, K., FUJIMURA-KAMADA, K., FURUTA, N., KATO, U., UMEDA, M. & TANAKA, K. 2004. Cdc50p, a protein required for polarized growth, associates with the Drs2p P-type ATPase implicated in phospholipid translocation in Saccharomyces cerevisiae. *Mol Biol Cell,* 15, 3418-32.

SAKAGUCHI, N. & MELCHERS, F. 1986. Lambda 5, a new light-chain-related locus selectively expressed in pre-B lymphocytes. *Nature,* 324, 579-82.

SAMITAS, K., LOTVALL, J. & BOSSIOS, A. 2010. B cells: from early development to regulating allergic diseases. *Arch Immunol Ther Exp (Warsz),* 58, 209-25.

SANCHEZ, M., MISULOVIN, Z., BURKHARDT, A. L., MAHAJAN, S., COSTA, T., FRANKE, R., BOLEN, J. B. & NUSSENZWEIG, M. 1993. Signal

transduction by immunoglobulin is mediated through Ig alpha and Ig beta. *J Exp Med,* 178, 1049-55.

SCHEBESTA, A., MCMANUS, S., SALVAGIOTTO, G., DELOGU, A., BUSSLINGER, G. A. & BUSSLINGER, M. 2007. Transcription factor Pax5 activates the chromatin of key genes involved in B cell signaling, adhesion, migration, and immune function. *Immunity,* 27, 49-63.

SCHEBESTA, M., PFEFFER, P. L. & BUSSLINGER, M. 2002. Control of pre-BCR signaling by Pax5-dependent activation of the BLNK gene. *Immunity,* 17, 473-85.

SCHIEMANN, B., GOMMERMAN, J. L., VORA, K., CACHERO, T. G., SHULGA-MORSKAYA, S., DOBLES, M., FREW, E. & SCOTT, M. L. 2001. An essential role for BAFF in the normal development of B cells through a BCMA-independent pathway. *Science,* 293, 2111-4.

SCHWEIGHOFFER, E., VANES, L., MATHIOT, A., NAKAMURA, T. & TYBULEWICZ, V. L. 2003. Unexpected requirement for ZAP-70 in pre-B cell development and allelic exclusion. *Immunity,* 18, 523-33.

SCHWICKERT, T. A., TAGOH, H., GULTEKIN, S., DAKIC, A., AXELSSON, E., MINNICH, M., EBERT, A., WERNER, B., ROTH, M., CIMMINO, L., DICKINS, R. A., ZUBER, J., JARITZ, M. & BUSSLINGER, M. 2014. Stage-specific control of early B cell development by the transcription factor Ikaros. *Nat Immunol,* 15, 283-93.

SCOTT, E. W., FISHER, R. C., OLSON, M. C., KEHRLI, E. W., SIMON, M. C. & SINGH, H. 1997. PU.1 functions in a cell-autonomous manner to control the differentiation of multipotential lymphoid-myeloid progenitors. *Immunity,* 6, 437-47.

SCOTT, E. W., SIMON, M. C., ANASTASI, J. & SINGH, H. 1994. Requirement of transcription factor PU.1 in the development of multiple hematopoietic lineages. *Science,* 265, 1573-7.

SEBASTIAN, T. T., BALDRIDGE, R. D., XU, P. & GRAHAM, T. R. 2012. Phospholipid flippases: building asymmetric membranes and transport vesicles. *Biochim Biophys Acta,* 1821, 1068-77.

SEET, C. S., BRUMBAUGH, R. L. & KEE, B. L. 2004. Early B cell factor promotes B lymphopoiesis with reduced interleukin 7 responsiveness in the absence of E2A. *J Exp Med,* 199, 1689-700.

SEGAWA, K., KURATA, S., YANAGIHASHI, Y., BRUMMELKAMP, T. R., MATSUDA, F. & NAGATA, S. 2014. Caspase-mediated cleavage of phospholipid flippase for apoptotic phosphatidylserine exposure. *Science,* 344, 1164-8.

SEIGNEURET, M. & DEVAUX, P. F. 1984. ATP-dependent asymmetric distribution of spin-labeled phospholipids in the erythrocyte membrane: relation to shape changes. *Proc Natl Acad Sci U S A,* 81, 3751-5.

SEMERAD, C. L., MERCER, E. M., INLAY, M. A., WEISSMAN, I. L. & MURRE, C. 2009. E2A proteins maintain the hematopoietic stem cell pool and promote the maturation of myelolymphoid and myeloerythroid progenitors. *Proc Natl Acad Sci U S A,* 106, 1930-5.

SHAW, A. C., SWAT, W., FERRINI, R., DAVIDSON, L. & ALT, F. W. 1999. Activated Ras signals developmental progression of recombinase-activating gene (RAG)-deficient pro-B lymphocytes. *J Exp Med,* 189, 123-9.

SHEETZ, M. P. & SINGER, S. J. 1974. Biological membranes as bilayer couples. A molecular mechanism of drug-erythrocyte interactions. *Proc Natl Acad Sci U S A,* 71, 4457-61.

SHINKAI, Y., RATHBUN, G., LAM, K. P., OLTZ, E. M., STEWART, V., MENDELSOHN, M., CHARRON, J., DATTA, M., YOUNG, F., STALL, A. M. & ET AL. 1992. RAG-2-deficient mice lack mature lymphocytes owing to inability to initiate V(D)J rearrangement. *Cell,* 68, 855-67.

SHORTMAN, K. & WU, L. 1996. Early T lymphocyte progenitors. *Annu Rev Immunol.,* 14, 29-47.

SHULGA-MORSKAYA, S., DOBLES, M., WALSH, M. E., NG, L. G., MACKAY, F., RAO, S. P., KALLED, S. L. & SCOTT, M. L. 2004. B cell-activating factor belonging to the TNF family acts through separate receptors to support B cell survival and T cell-independent antibody formation. *J Immunol,* 173, 2331-41.

SIGGS, O. M., ARNOLD, C. N., HUBER, C., PIRIE, E., XIA, Y., LIN, P., NEMAZEE, D. & BEUTLER, B. 2011a. The P4-type ATPase ATP11C is essential for B lymphopoiesis in adult bone marrow. *Nat Immunol,* 12, 434-40.

SIGGS, O. M., MIOSGE, L. A., YATES, A. L., KUCHARSKA, E. M., SHEAHAN, D., BRDICKA, T., WEISS, A., LISTON, A. & GOODNOW, C. C. 2007. Opposing functions of the T cell receptor kinase ZAP-70 in immunity and tolerance differentially titrate in response to nucleotide substitutions. *Immunity,* 27, 912-26.

SIGGS, O. M., SCHNABL, B., WEBB, B. & BEUTLER, B. 2011b. X-linked cholestasis in mouse due to mutations of the P4-ATPase ATP11C. *Proc Natl Acad Sci U S A,* 108, 7890-5.

SITNICKA, E., BRAKEBUSCH, C., MARTENSSON, I. L., SVENSSON, M., AGACE, W. W., SIGVARDSSON, M., BUZA-VIDAS, N., BRYDER, D., CILIO, C. M., AHLENIUS, H., MARASKOVSKY, E., PESCHON, J. J. & JACOBSEN, S. E. 2003. Complementary signaling through flt3 and interleukin-7 receptor alpha is indispensable for fetal and adult B cell genesis. *J Exp Med,* 198, 1495-506.

SMIT, J. J., SCHINKEL, A. H., OUDE ELFERINK, R. P., GROEN, A. K., WAGENAAR, E., VAN DEEMTER, L., MOL, C. A., OTTENHOFF, R., VAN DER LUGT, N. M., VAN ROON, M. A. & ET AL. 1993. Homozygous

disruption of the murine mdr2 P-glycoprotein gene leads to a complete absence of phospholipid from bile and to liver disease. *Cell,* 75, 451-62.

SMITH, E. M., GISLER, R. & SIGVARDSSON, M. 2002. Cloning and characterization of a promoter flanking the early B cell factor (EBF) gene indicates roles for E-proteins and autoregulation in the control of EBF expression. *J Immunol,* 169, 261-70.

SOCOLOVSKY, M., NAM, H., FLEMING, M. D., HAASE, V. H., BRUGNARA, C. & LODISH, H. F. 2001. Ineffective erythropoiesis in Stat5a(-/-)5b(-/-) mice due to decreased survival of early erythroblasts. *Blood,* 98, 3261-73.

SOUABNI, A., COBALEDA, C., SCHEBESTA, M. & BUSSLINGER, M. 2002. Pax5 promotes B lymphopoiesis and blocks T cell development by repressing Notch1. *Immunity,* 17, 781-93.

SOUPENE, E., KEMALADEWI, D. U. & KUYPERS, F. A. 2008. ATP8A1 activity and phosphatidylserine transbilayer movement. *J Receptor Ligand Channel Res,* 1, 1-10.

SOUPENE, E. & KUYPERS, F. A. 2006. Identification of an erythroid ATP-dependent aminophospholipid transporter. *Br J Haematol,* 133, 436-8.

SPANOPOULOU, E., ROMAN, C. A., CORCORAN, L. M., SCHLISSEL, M. S., SILVER, D. P., NEMAZEE, D., NUSSENZWEIG, M. C., SHINTON, S. A., HARDY, R. R. & BALTIMORE, D. 1994. Functional immunoglobulin transgenes guide ordered B-cell differentiation in Rag-1-deficient mice. *Genes Dev,* 8, 1030-42.

SRIVASTAVA, B., QUINN, W. J., 3RD, HAZARD, K., ERIKSON, J. & ALLMAN, D. 2005. Characterization of marginal zone B cell precursors. *J Exp Med,* 202, 1225-34.

STEIN, P. L., LEE, H. M., RICH, S. & SORIANO, P. 1992. pp59fyn mutant mice display differential signaling in thymocytes and peripheral T cells. *Cell,* 70, 741-50.

STEWART, G. W. 2004. Hemolytic disease due to membrane ion channel disorders. *Curr Opin Hematol,* 11, 244-50.

SU, T. T. & RAWLINGS, D. J. 2002. Transitional B lymphocyte subsets operate as distinct checkpoints in murine splenic B cell development. *J Immunol,* 168, 2101-10.

SURWIT, R. S., KUHN, C. M., COCHRANE, C., MCCUBBIN, J. A. & FEINGLOS, M. N. 1988. Diet-induced type II diabetes in C57BL/6J mice. *Diabetes,* 37, 1163-7.

SURWIT, R. S., SELDIN, M. F., KUHN, C. M., COCHRANE, C. & FEINGLOS, M. N. 1991. Control of expression of insulin resistance and hyperglycemia by different genetic factors in diabetic C57BL/6J mice. *Diabetes,* 40, 82-7.

SUZUKI, H., TERAUCHI, Y., FUJIWARA, M., AIZAWA, S., YAZAKI, Y., KADOWAKI, T. & KOYASU, S. 1999. Xid-like immunodeficiency in mice with disruption of the p85alpha subunit of phosphoinositide 3-kinase. *Science,* 283, 390-2.

SUZUKI, J., UMEDA, M., SIMS, P. J. & NAGATA, S. 2010. Calcium-dependent phospholipid scrambling by TMEM16F. *Nature,* 468, 834-8.

TANG, X., HALLECK, M. S., SCHLEGEL, R. A. & WILLIAMSON, P. 1996. A subfamily of P-type ATPases with aminophospholipid transporting activity. *Science,* 272, 1495-7.

TEAGUE, B. N., PAN, Y., MUDD, P. A., NAKKEN, B., ZHANG, Q., SZODORAY, P., KIM-HOWARD, X., WILSON, P. C. & FARRIS, A. D. 2007. Cutting edge: Transitional T3 B cells do not give rise to mature B cells, have undergone selection, and are reduced in murine lupus. *J Immunol,* 178, 7511-5.

TEH, C. E., HORIKAWA, K., ARNOLD, C. N., BEUTLER, B., KUCHARSKA, E. M., VINUESA, C. G., BERTRAM, E. M., GOODNOW, C. C. & ENDERS, A. 2013. Heterozygous mis-sense mutations in Prkcb as a critical determinant of anti-polysaccharide antibody formation. *Genes Immun,* 14, 223-33.

TEOH, N. C., ITO, Y., FIELD, J., BETHEA, N. W., AMR, D., MCCUSKEY, M. K., MCCUSKEY, R. S., FARRELL, G. C. & ALLISON, A. C. 2007. Diannexin, a novel annexin V homodimer, provides prolonged protection against hepatic ischemia-reperfusion injury in mice. *Gastroenterology,* 133, 632-46.

TEXIDO, G., SU, I. H., MECKLENBRAUKER, I., SAIJO, K., MALEK, S. N., DESIDERIO, S., RAJEWSKY, K. & TARAKHOVSKY, A. 2000. The B-cell-specific Src-family kinase Blk is dispensable for B-cell development and activation. *Mol Cell Biol,* 20, 1227-33.

THAL, M. A., CARVALHO, T. L., HE, T., KIM, H. G., GAO, H., HAGMAN, J. & KLUG, C. A. 2009. Ebf1-mediated down-regulation of Id2 and Id3 is essential for specification of the B cell lineage. *Proc Natl Acad Sci U S A,* 106, 552-7.

THOMAS, K. R. & CAPECCHI, M. R. 1987. Site-directed mutagenesis by gene targeting in mouse embryo-derived stem cells. *Cell,* 51, 503-12.

THOMIS, D. C., GURNIAK, C. B., TIVOL, E., SHARPE, A. H. & BERG, L. J. 1995. Defects in B lymphocyte maturation and T lymphocyte activation in mice lacking Jak3. *Science,* 270, 794-7.

TIEGS, S. L., RUSSELL, D. M. & NEMAZEE, D. 1993. Receptor editing in self-reactive bone marrow B cells. *J Exp Med,* 177, 1009-20.

TOKOYODA, K., EGAWA, T., SUGIYAMA, T., CHOI, B. I. & NAGASAWA, T. 2004. Cellular niches controlling B lymphocyte behavior within bone marrow during development. *Immunity,* 20, 707-18.

TORNBERG, U. C., BERGQVIST, I., HAURY, M. & HOLMBERG, D. 1998. Regulation of B lymphocyte development by the truncated immunoglobulin heavy chain protein Dmu. *J Exp Med,* 187, 703-9.

TORRES, R. M., FLASWINKEL, H., RETH, M. & RAJEWSKY, K. 1996. Aberrant B cell development and immune response in mice with a compromised BCR complex. *Science,* 272, 1804-8.

TREIBER, T., MANDEL, E. M., POTT, S., GYORY, I., FIRNER, S., LIU, E. T. & GROSSCHEDL, R. 2010. Early B cell factor 1 regulates B cell gene networks by activation, repression, and transcription- independent poising of chromatin. *Immunity,* 32, 714-25.

TUNG, J. W., MRAZEK, M. D., YANG, Y. & HERZENBERG, L. A. 2006. Phenotypically distinct B cell development pathways map to the three B cell lineages in the mouse. *Proc Natl Acad Sci U S A,* 103, 6293-8.

TURNER, M., MEE, P. J., COSTELLO, P. S., WILLIAMS, O., PRICE, A. A., DUDDY, L. P., FURLONG, M. T., GEAHLEN, R. L. & TYBULEWICZ, V. L. 1995. Perinatal lethality and blocked B-cell development in mice lacking the tyrosine kinase Syk. *Nature,* 378, 298-302.

URBANEK, P., WANG, Z. Q., FETKA, I., WAGNER, E. F. & BUSSLINGER, M. 1994. Complete block of early B cell differentiation and altered patterning of the posterior midbrain in mice lacking Pax5/BSAP. *Cell,* 79, 901-12.

VAN DER MARK, V. A., ELFERINK, R. P. & PAULUSMA, C. C. 2013. P4 ATPases: Flippases in Health and Disease. *Int J Mol Sci,* 14, 7897-922.

VAN DER VELDEN, L. M., VAN DE GRAAF, S. F. J. & KLOMP, L. W. J. 2010. Biochemical and cellular functions of P4 ATPases. *Biochem J,* 431, 1-11.

VAN GENDEREN, I. & VAN MEER, G. 1995. Differential targeting of glucosylceramide and galactosylceramide analogues after synthesis but not during transcytosis in Madin-Darby canine kidney cells. *J Cell Biol,* 131, 645-54.

VAN HELVOORT, A., SMITH, A. J., SPRONG, H., FRITZSCHE, I., SCHINKEL, A. H., BORST, P. & VAN MEER, G. 1996. MDR1 P-glycoprotein is a lipid translocase of broad specificity, while MDR3 P-glycoprotein specifically translocates phosphatidylcholine. *Cell,* 87, 507-17.

VAN LOO, P. F., DINGJAN, G. M., MAAS, A. & HENDRIKS, R. W. 2007. Surrogate-light-chain silencing is not critical for the limitation of pre-B cell expansion but is for the termination of constitutive signaling. *Immunity,* 27, 468-80.

VAUX, D. L., CORY, S. & ADAMS, J. M. 1988. Bcl-2 gene promotes haemopoietic cell survival and cooperates with c-myc to immortalize pre-B cells. *Nature,* 335, 440-2.

VENKITARAMAN, A. R. & COWLING, R. J. 1994. Interleukin-7 induces the association of phosphatidylinositol 3-kinase with the alpha chain of the interleukin-7 receptor. *Eur J Immunol,* 24, 2168-74.

VERHOVEN, B., SCHLEGEL, R. A. & WILLIAMSON, P. 1992. Rapid loss and restoration of lipid asymmetry by different pathways in resealed erythrocyte ghosts. *Biochim Biophys Acta,* 1104, 15-23.

VERHOVEN, B., SCHLEGEL, R. A. & WILLIAMSON, P. 1995. Mechanisms of phosphatidylserine exposure, a phagocyte recognition signal, on apoptotic T lymphocytes. *J Exp Med,* 182, 1597-601.

VIGORITO, E., GAMBARDELLA, L., COLUCCI, F., MCADAM, S. & TURNER, M. 2005. Vav proteins regulate peripheral B-cell survival. *Blood,* 106, 2391-8.

VILAGOS, B., HOFFMANN, M., SOUABNI, A., SUN, Q., WERNER, B., MEDVEDOVIC, J., BILIC, I., MINNICH, M., AXELSSON, E., JARITZ, M. & BUSSLINGER, M. 2012. Essential role of EBF1 in the generation and function of distinct mature B cell types. *J Exp Med,* 209, 775-92.

VINUESA, C. G., COOK, M. C., ANGELUCCI, C., ATHANASOPOULOS, V., RUI, L., HILL, K. M., YU, D., DOMASCHENZ, H., WHITTLE, B., LAMBE, T., ROBERTS, I. S., COPLEY, R. R., BELL, J. I., CORNALL, R. J. & GOODNOW, C. C. 2005. A RING-type ubiquitin ligase family member required to repress follicular helper T cells and autoimmunity. *Nature,* 435, 452-8.

VINUESA, C. G. & CYSTER, J. G. 2011. How T cells earn the follicular rite of passage. *Immunity,* 35, 671-80.

VINUESA, C. G., SANZ, I. & COOK, M. C. 2009. Dysregulation of germinal centres in autoimmune disease. *Nat Rev Immunol,* 9, 845-57.

VON FREEDEN-JEFFRY, U., VIEIRA, P., LUCIAN, L. A., MCNEIL, T., BURDACH, S. E. & MURRAY, R. 1995. Lymphopenia in interleukin (IL)-7 gene-deleted mice identifies IL-7 as a nonredundant cytokine. *J Exp Med,* 181, 1519-26.

VOSSHENRICH, C. A., CUMANO, A., MULLER, W., DI SANTO, J. P. & VIEIRA, P. 2003. Thymic stromal-derived lymphopoietin distinguishes fetal from adult B cell development. *Nat Immunol,* 4, 773-9.

VOSSHENRICH, C. A., CUMANO, A., MULLER, W., DI SANTO, J. P. & VIEIRA, P. 2004. Pre-B cell receptor expression is necessary for thymic stromal lymphopoietin responsiveness in the bone marrow but not in the liver environment. *Proc Natl Acad Sci U S A,* 101, 11070-5.

WANG, H., LEE, C. H., QI, C., TAILOR, P., FENG, J., ABBASI, S., ATSUMI, T. & MORSE, H. C., 3RD 2008. IRF8 regulates B-cell lineage specification, commitment, and differentiation. *Blood,* 112, 4028-38.

WANG, H., YANG, H., SHIVALILA, C. S., DAWLATY, M. M., CHENG, A. W., ZHANG, F. & JAENISCH, R. 2013. One-step generation of mice carrying mutations in multiple genes by CRISPR/Cas-mediated genome engineering. *Cell,* 153, 910-8.

WANG, J. H., NICHOGIANNOPOULOU, A., WU, L., SUN, L., SHARPE, A. H., BIGBY, M. & GEORGOPOULOS, K. 1996. Selective defects in the development of the fetal and adult lymphoid system in mice with an Ikaros null mutation. *Immunity,* 5, 537-49.

WANG, L., BESERRA, C. & GARBERS, D. L. 2004. A novel aminophospholipid transporter exclusively expressed in spermatozoa is required for membrane lipid asymmetry and normal fertilization. *Dev Biol,* 267, 203-15.

WANG, R., SALEM, M., YOUSEF, I. M., TUCHWEBER, B., LAM, P., CHILDS, S. J., HELGASON, C. D., ACKERLEY, C., PHILLIPS, M. J. & LING, V. 2001. Targeted inactivation of sister of P-glycoprotein gene (spgp) in mice results in nonprogressive but persistent intrahepatic cholestasis. *Proc Natl Acad Sci U S A,* 98, 2011-6.

WARDEMANN, H., YURASOV, S., SCHAEFER, A., YOUNG, J. W., MEFFRE, E. & NUSSENZWEIG, M. C. 2003. Predominant autoantibody production by early human B cell precursors. *Science,* 301, 1374-7.

WATERSTON, R. H., LINDBLAD-TOH, K., BIRNEY, E., ROGERS, J., ABRIL, J. F., AGARWAL, P., AGARWALA, R., AINSCOUGH, R., ALEXANDERSSON, M., AN, P., ANTONARAKIS, S. E., ATTWOOD, J., BAERTSCH, R., BAILEY, J., BARLOW, K., BECK, S., BERRY, E., BIRREN, B., BLOOM, T., BORK, P., BOTCHERBY, M., BRAY, N., BRENT, M. R., BROWN, D. G., BROWN, S. D., BULT, C., BURTON, J., BUTLER, J., CAMPBELL, R. D., CARNINCI, P., CAWLEY, S., CHIAROMONTE, F., CHINWALLA, A. T., CHURCH, D. M., CLAMP, M., CLEE, C., COLLINS, F. S., COOK, L. L., COPLEY, R. R., COULSON, A., COURONNE, O., CUFF, J., CURWEN, V., CUTTS, T., DALY, M., DAVID, R., DAVIES, J., DELEHAUNTY, K. D., DERI, J., DERMITZAKIS, E. T., DEWEY, C., DICKENS, N. J., DIEKHANS, M., DODGE, S., DUBCHAK, I., DUNN, D. M., EDDY, S. R., ELNITSKI, L., EMES, R. D., ESWARA, P., EYRAS, E., FELSENFELD, A., FEWELL, G. A., FLICEK, P., FOLEY, K., FRANKEL, W. N., FULTON, L. A., FULTON, R. S., FUREY, T. S., GAGE, D., GIBBS, R. A., GLUSMAN, G., GNERRE, S., GOLDMAN, N., GOODSTADT, L., GRAFHAM, D., GRAVES, T. A., GREEN, E. D., GREGORY, S., GUIGO, R., GUYER, M., HARDISON, R. C., HAUSSLER, D., HAYASHIZAKI, Y., HILLIER, L. W., HINRICHS, A., HLAVINA, W., HOLZER, T., HSU, F., HUA, A., HUBBARD, T., HUNT, A., JACKSON, I., JAFFE, D. B., JOHNSON, L. S., JONES, M., JONES, T. A., JOY, A., KAMAL, M., KARLSSON, E. K., et al. 2002. Initial sequencing and comparative analysis of the mouse genome. *Nature,* 420, 520-62.

WEBB, S. R., HUTCHINSON, J., HAYDEN, K. & SPRENT, J. 1994. Expansion/deletion of mature T cells exposed to endogenous superantigens in vivo. *J Immunol.,* 152, 586-597.

WEISS, H. J., VICIC, W. J., LAGES, B. A. & ROGERS, J. 1979. Isolated deficiency of platelet procoagulant activity. *Am J Med,* 67, 206-13.

WELINDER, E., MANSSON, R., MERCER, E. M., BRYDER, D., SIGVARDSSON, M. & MURRE, C. 2011. The transcription factors E2A and HEB act in concert to induce the expression of FOXO1 in the common lymphoid progenitor. *Proc Natl Acad Sci U S A,* 108, 17402-7.

WIEDMER, T., ZHOU, Q., KWOH, D. Y. & SIMS, P. J. 2000. Identification of three new members of the phospholipid scramblase gene family. *Biochim Biophys Acta,* 1467, 244-53.

WIKSTROM, I., BERGQVIST, I., HOLMBERG, D. & FORSSELL, J. 2006. Dmu expression causes enrichment of MZ B cells, but is non permissive for B cell maturation in Rag2-/- mice even if combined with Bcl-2. *Mol Immunol,* 43, 1316-24.

WILLIAMSON, P., CHRISTIE, A., KOHLIN, T., SCHLEGEL, R. A., COMFURIUS, P., HARMSMA, M., ZWAAL, R. F. & BEVERS, E. M. 2001. Phospholipid scramblase activation pathways in lymphocytes. *Biochemistry,* 40, 8065-72.

WILLIAMSON, P., KULICK, A., ZACHOWSKI, A., SCHLEGEL, R. A. & DEVAUX, P. F. 1992. Ca2+ induces transbilayer redistribution of all major phospholipids in human erythrocytes. *Biochemistry,* 31, 6355-60.

WINTERBERG, M., RAJENDRAN, E., BAUMEISTER, S., BIETZ, S., KIRK, K. & LINGELBACH, K. 2012. Chemical activation of a high-affinity glutamate transporter in human erythrocytes and its implications for malaria-parasite-induced glutamate uptake. *Blood,* 119, 3604-12.

WOOD, B. L., GIBSON, D. F. & TAIT, J. F. 1996. Increased erythrocyte phosphatidylserine exposure in sickle cell disease: flow-cytometric measurement and clinical associations. *Blood,* 88, 1873-80.

WU, C., OROZCO, C., BOYER, J., LEGLISE, M., GOODALE, J., BATALOV, S., HODGE, C. L., HAASE, J., JANES, J., HUSS, J. W., 3RD & SU, A. I. 2009. BioGPS: an extensible and customizable portal for querying and organizing gene annotation resources. *Genome Biol,* 10, R130.

WU, Z., JIA, X., DE LA CRUZ, L., SU, X. C., MARZOLF, B., TROISCH, P., ZAK, D., HAMILTON, A., WHITTLE, B., YU, D., SHEAHAN, D., BERTRAM, E., ADEREM, A., OTTING, G., GOODNOW, C. C. & HOYNE, G. F. 2008. Memory T cell RNA rearrangement programmed by heterogeneous nuclear ribonucleoprotein hnRNPLL. *Immunity,* 29, 863-75.

XU, C., GAGNON, E., CALL, M. E., SCHNELL, J. R., SCHWIETERS, C. D., CARMAN, C. V., CHOU, J. J. & WUCHERPFENNIG, K. W. 2008. Regulation of T cell receptor activation by dynamic membrane binding of the CD3epsilon cytoplasmic tyrosine-based motif. *Cell,* 135, 702-13.

XU, P., OKKERI, J., HANISCH, S., HU, R. Y., XU, Q., POMORSKI, T. G. & DING, X. Y. 2009. Identification of a novel mouse P4-ATPase family member highly expressed during spermatogenesis. *J Cell Sci,* 122, 2866-76.

YABAS, M., TEH, C. E., FRANKENREITER, S., LAL, D., ROOTS, C. M., WHITTLE, B., ANDREWS, D. T., ZHANG, Y., TEOH, N. C., SPRENT, J., TZE, L. E., KUCHARSKA, E. M., KOFLER, J., FARELL, G. C., BROER, S., GOODNOW, C. C. & ENDERS, A. 2011. ATP11C is critical for the internalization of phosphatidylserine and differentiation of B lymphocytes. *Nat Immunol,* 12, 441-9.

YAMAZAKI, T., TAKEDA, K., GOTOH, K., TAKESHIMA, H., AKIRA, S. & KUROSAKI, T. 2002. Essential immunoregulatory role for BCAP in B cell development and function. *J Exp Med,* 195, 535-45.

YANG, H., KIM, A., DAVID, T., PALMER, D., JIN, T., TIEN, J., HUANG, F., CHENG, T., COUGHLIN, S. R., JAN, Y. N. & JAN, L. Y. 2012. TMEM16F forms a Ca2+-activated cation channel required for lipid scrambling in platelets during blood coagulation. *Cell,* 151, 111-22.

YANG, H., WANG, H., SHIVALILA, C. S., CHENG, A. W., SHI, L. & JAENISCH, R. 2013. One-step generation of mice carrying reporter and conditional alleles by CRISPR/Cas-mediated genome engineering. *Cell,* 154, 1370-9.

YAO, Z., CUI, Y., WATFORD, W. T., BREAM, J. H., YAMAOKA, K., HISSONG, B. D., LI, D., DURUM, S. K., JIANG, Q., BHANDOOLA, A., HENNIGHAUSEN, L. & O'SHEA, J. J. 2006. Stat5a/b are essential for normal lymphoid development and differentiation. *Proc Natl Acad Sci U S A,* 103, 1000-5.

YASIN, Z., WITTING, S., PALASCAK, M. B., JOINER, C. H., RUCKNAGEL, D. L. & FRANCO, R. S. 2003. Phosphatidylserine externalization in sickle red blood cells: associations with cell age, density, and hemoglobin F. *Blood,* 102, 365-70.

YASUDA, T., SANJO, H., PAGES, G., KAWANO, Y., KARASUYAMA, H., POUYSSEGUR, J., OGATA, M. & KUROSAKI, T. 2008. Erk kinases link pre-B cell receptor signaling to transcriptional events required for early B cell expansion. *Immunity,* 28, 499-508.

YATES, L., MCMURRAY, F., ZHANG, Y., GREENFIELD, A., MOFFATT, M., COOKSON, W. & DEAN, C. 2009. ENU mutagenesis as a tool for understanding lung development and disease. *Biochem Soc Trans,* 37, 838-42.

YE, M., ERMAKOVA, O. & GRAF, T. 2005. PU.1 is not strictly required for B cell development and its absence induces a B-2 to B-1 cell switch. *J Exp Med,* 202, 1411-22.

YE, M. & GRAF, T. 2007. Early decisions in lymphoid development. *Curr Opin Immunol,* 19, 123-8.

YOKOYAMA, W. M., KIM, S. & FRENCH, A. R. 2004. The dynamic life of natural killer cells. *Annu Rev Immunol,* 22, 405-29.

YOSHIDA, T., NG, S. Y., ZUNIGA-PFLUCKER, J. C. & GEORGOPOULOS, K. 2006. Early hematopoietic lineage restrictions directed by Ikaros. *Nat Immunol,* 7, 382-91.

YOULE, R. J. & STRASSER, A. 2008. The BCL-2 protein family: opposing activities that mediate cell death. *Nat Rev Mol Cell Biol,* 9, 47-59.

YU, D., RAO, S., TSAI, L. M., LEE, S. K., HE, Y., SUTCLIFFE, E. L., SRIVASTAVA, M., LINTERMAN, M., ZHENG, L., SIMPSON, N., ELLYARD, J. I., PARISH, I. A., MA, C. S., LI, Q. J., PARISH, C. R., MACKAY, C. R. & VINUESA, C. G. 2009. The transcriptional repressor Bcl-6 directs T follicular helper cell lineage commitment. *Immunity,* 31, 457-68.

ZARYCHANSKI, R., SCHULZ, V. P., HOUSTON, B. L., MAKSIMOVA, Y., HOUSTON, D. S., SMITH, B., RINEHART, J. & GALLAGHER, P. G. 2012. Mutations in the mechanotransduction protein PIEZO1 are associated with hereditary xerocytosis. *Blood,* 120, 1908-15.

ZECH, T., EJSING, C. S., GAUS, K., DE WET, B., SHEVCHENKO, A., SIMONS, K. & HARDER, T. 2009. Accumulation of raft lipids in T-cell plasma membrane domains engaged in TCR signalling. *EMBO J,* 28, 466-76.

ZHOU, Q., ZHAO, J., STOUT, J. G., LUHM, R. A., WIEDMER, T. & SIMS, P. J. 1997. Molecular cloning of human plasma membrane phospholipid scramblase. A protein mediating transbilayer movement of plasma membrane phospholipids. *J Biol Chem,* 272, 18240-4.

ZHOU, X. & GRAHAM, T. R. 2009. Reconstitution of phospholipid translocase activity with purified Drs2p, a type-IV P-type ATPase from budding yeast. *Proc Natl Acad Sci U S A,* 106, 16586-91.

ZHU, X., LIBBY, R. T., DE VRIES, W. N., SMITH, R. S., WRIGHT, D. L., BRONSON, R. T., SEBURN, K. L. & JOHN, S. W. 2012. Mutations in a P-type ATPase gene cause axonal degeneration. *PLoS Genet,* 8, e1002853.

ZHUANG, Y., SORIANO, P. & WEINTRAUB, H. 1994. The helix-loop-helix gene E2A is required for B cell formation. *Cell,* 79, 875-84.

ZÚÑIGA-PFLÜCKER, J. C. 2004. T-cell development made simple. *Nat Rev Immunol.,* 4, 67-72.